



MONASH University

Novel approaches for functionalisation of fibrous polymer surfaces for catalytic application

Priydarshani Amit Shinde

Master of Science

This thesis is submitted to the Faculty of Science

Monash University, in fulfilment of the

Requirements for the degree of

DOCTOR OF PHILOSOPHY

School of Chemistry

Monash University

Clayton, Australia

November 2018

I would like to dedicate this thesis to my son and husband.
I thank them for encouraging me to always achieve higher goals...

Copyright Notice

© Priydarshani Shinde (2018).

I certify that I have made all reasonable efforts to secure copyright permissions for third-party content included in this thesis and have not knowingly added copyright content to my work without the owner's permission.

Abstract

Enzymatic processes are widely implemented throughout a broad range of chemical industries. The employment of immobilised enzymes provides operational advantages including long-term operational stability, recycling opportunity and efficient product separation. Alcohol dehydrogenase (ADH) is an oxidoreductase which performs oxidation and reduction in the presence of nicotinamide-based cofactors. In this thesis, ADH has been used as a model system for enzyme immobilisation protocol and used to construct a biosensor and continuous flow reactor.

Chapter 2 presents several fibre and fabric surface modification strategies and immobilisation of ADH for the development of stable and supported ADH constructs. Fibrous surfaces such as cotton fabric, nylon fabric and polyacrylonitrile fibre, were chemically modified and explored as carrier supports for ADH immobilisation. ADH immobilised on these modified supports was characterised for activity and stability with respect to pH, temperature, storage time and recyclability. The modification of ADH with bifunctional groups, including nylon monomers (C3 and C6 monomer), BMPS and allyl glycidyl ether (AGE), to facilitate enzyme immobilisation was also investigated.

Chapter 3 focuses on the surface functionalisation of PVA fibre and knitted fabric supports. Modified PVA supports were characterized using IR spectroscopy and subsequently modified with ADH using various immobilisation protocols. Model reactions with 2,4-pentanediol were also performed to explore the inter and intra molecular reactions of PVA. The PVA-ADH construct with the highest activity was further characterised for pH, temperature, storage stability and assessed for recyclability.

Chapter 4 presents the surface modification of glass woven and non-woven fabric with trialkoxysilane reagents to generate a variety of surface modified functionality for attachment of ADH. Trialkoxysilane modified glass supports were investigated for immobilisation of ADH and the glass fabric-ADH construct with the highest activity was assessed for stability (pH, temperature and storage). The optimised glass non-woven fabric-ADH construct was then developed into a biosensor for detection of ethanol. In addition, the glass non-woven fabric ADH construct was used to design a flow reactor using flow injection analysis (FIA) for amperometric ethanol detection.

General Declaration

This thesis contains no material which has been accepted for the award of any other degree or diploma at any university or equivalent institution and that, to the best of my knowledge and belief, this thesis contains no material previously published or written by another person, except where due reference is made in the text of the thesis.

This thesis includes one original paper published in a peer reviewed journal and one manuscript which is drafted for publication. The core theme of the thesis centres on fibrous surface modification for biocatalysis applications.

The ideas, development and writing up of all the papers in the thesis were the principal responsibility of myself, the student, working within the School of Chemistry and the CSIRO Manufacturing Flagship under the supervision of Professor Andrea Robinson, Dr. Ilias Louis Kyratzis, Dr. Mustafa Musameh and Dr. Yuan Gao.

The inclusion of co-authors reflects the fact that the work came from active collaboration between researchers and acknowledges input into team-based research. In Chapter 3 contributions to the work have been apportioned as follows:

Thesis Chapter	Publication Title	Publication Status	Nature and % of Student Contribution	Co-author Name(s), Nature and % of Co-author's Contribution	Co-author(s), Monash Student Y/N
Chapter 3	Immobilization and stabilization of alcohol dehydrogenase on polyvinyl alcohol fibre	Published	80 %, Collected and analysed data and writing of the manuscript	1) A.J Robinson, supervisor, 5%	N
				2) Mustafa Musameh, supervisor, 5%	N
				3) Louis Kyrtzis, supervisor, 5%	N
				4) Yuan Gao, 5%	N

I have not renumbered sections of these drafted/submitted/published papers in order to maintain a consistent presentation within the thesis.

Student signature:



Date: 7/11/2018

The undersigned hereby certify that the above declaration correctly reflects the nature and extent of the student's and co-authors' contributions to this work.

Main Supervisor signature:



Date: Nov 11, 2018

Acknowledgements

I sincerely thank all those who have supported and encouraged me throughout this journey, I couldn't have done it without you.

My supervisors Andrea Robinson, Louis Kyrtziz, Mustafa Musameh and Yuan Gao have all been instrumental for the last four years. They have trusted and challenged my ways of thinking and inspired me to achieve higher limits. Their guidance and encouragement has been invaluable and has enabled me to reach the finish line. I feel very privileged to have had the opportunity to work for such talented, creative, enthusiastic and inspirational scientists

I would like to thank my group members, both past and present, that have helped make my time an enjoyable experience. These include, but not limited to Thomas, Alessia, Lauren, and Szabi.

I really feel privileged to have the opportunity to work at CSIRO and be a part of the team. Funding from CSIRO is gratefully acknowledged.

I would like to thank my sister Pallavi and brother Anup staying overseas who have supported me from afar, your emotional support is greatly appreciated. I always hold memories of my beloved parents who I think must be very proud of me.

A final word of thanks to my son Omkar and husband Amit, you both have been my rock for the last four years and have helped me throughout the hardest period of my life so far.

Table of Contents

Chapters.....	XIII
List of Figures.....	XVIII
List of Tables.....	XXIV
Chapter 1	1
1.1 Introduction	2
1.2 Methods for immobilisation	6
1.2.1 Adsorption	7
1.2.2 Entrapment	8
1.2.3 Covalent	9
1.3 Enzymes and cofactors	10
1.3.1 ADH enzyme	10
1.3.2 Enzyme cofactors	16
1.4 Choice of supports	17
1.4.1 Classical support materials for immobilisation	18
1.4.2 New materials for enzyme immobilisation	21
1.5 Immobilisation chemistry	24
1.6 Immobilised enzyme activity	26
1.7 Gaps and opportunity	27
1.7.1 Methods of fabrication	30
1.7.2 Enzyme immobilisation on fabrics	31
1.8 Project Objectives	34
1.9 Summary	36
1.10 References	37
Chapter 2	45
2.1 Introduction	46
2.2 Soluble ADH concentration and stability study	47

2.3 Surface modification and immobilisation	49
2.3.1 Cotton	49
2.3.2 Nylon	59
2.3.3 Polyacrylonitrile (PAN)	62
2.4 ADH modification	65
2.4.1 Modification with nylon monomers	66
2.4.2 Modification with BMPS	67
2.4.3 Modification with AGE	69
2.5 Conclusion	70
2.6 Experimental Section	71
2.6.1 Instrumentation	71
2.6.2 Solvents and reagents	71
2.6.3 Experimental Procedures	73
2.6.4 ADH modification	84
2.6.5 ADH immobilisation on fabric protocol	86
2.6.6 ADH activity assay	87
2.6.7 ADH concentration study	87
2.6.8 Soluble ADH pH stability	88
2.7 References	90
Chapter 3	95
3.1 Introduction	96
3.2 Surface modification of PVA fibre and fabric	100
3.2.1 Reactions with PVA fibre and fabric	100
3.3 ADH immobilisation	109
3.3.1 PVA-Cl immobilisation	111
3.3.2 PVA-COOH immobilisation	112
3.3.3 PVA-isocyanate immobilisation	113
3.3.4 PVA-chlorotriazine immobilisation	114
3.3.5 PVA-Cl-EDA immobilisation	115

3.4 Storage stability of PVA-Cl-EDA-GA immobilised ADH	125
3.5 Conclusion	126
3.6 Experimental Section	127
3.6.1 Solvents and reagents	127
3.6.2 Instrumentation	128
3.6.3 PVA Surface modification procedures	130
3.6.4 Model reaction	150
3.7 ADH immobilisation and assay protocol	151
3.7.1 Immobilisation protocol	151
3.7.2 ADH activity assay	152
3.7.3 Immobilised ADH pH stability	152
3.7.4 Immobilised ADH thermal stability	153
3.7.5 Immobilised ADH recyclability	154
3.8 References	156
Chapter 4	159
4.1 Introduction.....	160
4.2 Woven glass fabric.....	166
4.2.1 Surface modification and immobilisation.....	166
4.2.2 APTMS concentration effect on immobilised ADH activity.....	168
4.2.3 GA concentration effect on immobilised ADH activity	169
4.2.4 Characterisation of APTMS-GA modified woven glass fabric	171
4.2.5 Immobilised ADH stability studies	174
4.3 Non-woven glass fabric	178
4.3.1 Surface modification and ADH immobilisation.....	179
4.3.2 Characterisation of APTMS modified non-woven glass fabric.....	184
4.3.3 Immobilised ADH stability studies.....	187
4.4 Comparison of immobilised ADH activity.....	190
4.5 Non-woven glass fabric support use in the fabrication of a biosensor.....	192
4.5.1 Fabrication of the electrode.....	192

4.5.2 NADH oxidation	193
4.5.3 Ethanol detection	194
4.6 Non-woven glass fabric supports in flow reactors.....	196
4.6.1 Flow-injection system.....	196
4.6.2 Optimization of the flow-injection system	197
4.7 Conclusions.....	199
4.8 Experimental Section.....	201
4.8.1 Instrumentation.....	201
4.8.2 Solvents and reagent.....	202
4.8.3 ADH assay.....	204
4.8.4 Surface modification procedures woven and non-woven glass fabric.....	204
4.8.5 Immobilised ADH Stability Studies.....	215
4.8.6 Fabrication of glass fabric-APTMS-GA electrode	223
4.8.7 Flow-injection system.....	224
4.9 References.....	227
Chapter 5	231
5.1 Conclusion	232
5.2 Future Work.....	235
Appendix-I	237
1.0 Introduction.....	238
2.0 Experimental.....	240
2.1 Materials.....	240
2.2 Characterisation.....	240
2.3 Methods.....	241
2.3.1 Modification of Glass Fibre and Fabric.....	241
2.3.2 ADH Immobilisation and Assay.....	242

2.3.3 Stability Studies of Soluble and Immobilised ADH.....	243
2.3.4 Fabrication of Biosensor.....	244
2.3.5 Continuous Flow-Injection System.....	245
3.0 Results and Discussion.....	246
3.1 Characterisation.....	246
3.2 ADH Covalent Immobilisation and Characterisation.....	251
3.2.1 pH Study.....	253
3.2.2 Storage Stability.....	254
3.2.3 Thermal Stabilization.....	255
3.3 Electrochemical Detection of Ethanol.....	257
3.3.1 Detection with Glass fibre-APTMS-GA-MB-ADH electrode.....	257
3.3.2 Detection using a glass fibre-APTMS-GA-ADH support in a continuous flow reactor.....	258
3.3.3 Calibration Curve.....	259
4.0 Conclusions.....	261
5.0 Acknowledgement.....	262
6.0 References.....	263
Appendix-II.....	265

List of Figures

Chapter 1

Figure 1.1. Enzyme use in the industry based on the sale of the enzyme.....	3
Figure 1.2. Simplified schematic of enzyme immobilisation protocols or methods.....	7
Figure 1.3. ADH enzyme used in a whole cell biotransformation.....	11
Figure 1.4. A: Crystal structure of the ADH homodimer and energy minimised model. B: Model of the active site of yeast alcohol dehydrogenase.....	15
Figure 1.5. Oxidation of ethanol to acetaldehyde with ADH and NAD ⁺ cofactor.....	16
Figure 1.6. Structure of NAD ⁺ , NADP ⁺ , NADH and NADPH.....	17
Figure 1.7. Desirable properties in support materials used for enzyme immobilisation...	18
Figure 1.8. Examples of inorganic and organic supports used for enzyme immobilisation.....	18
Figure 1.9. New inorganic, organic and hybrid supports used for enzyme immobilisation.....	21
Figure 1.10. Enzyme (amine based) immobilisation on aldehydes, epoxides, acid and alcohols functionalised solid supports via covalent bonds.....	25
Figure 1.11. Ethanol oxidation with ADH in presence of NAD ⁺	27
Figure 1.12. Activation of agarose to glyoxyl support.....	28
Figure 1.13. Weave pattern.....	30
Figure 1.14. Different weft and wrap knitting patterns.....	31
Figure 1.15. Schematic representation of ADH immobilised on a fibrous carrier/support to perform ethanol oxidation with the addition of NAD ⁺ cofactor.....	34
Figure 1.16. General representation of covalent linkage of an enzyme to a functionalised support.....	35

Chapter 2

Figure 2.1. ADH concentration study 0.1 to 1.0 mg/mL in PBS buffer (pH 7.5) at RT. The ADH assay was performed on triplicate samples for each conc. and error bars represent standard deviations. To display the data, the highest activity was taken as 100% and subsequent activities were normalised accordingly.....	47
---	----

Figure 2.2. ADH activity at different pHs. The ADH assay was performed on triplicate samples for each pH value and error bars represent standard deviations. To display the data, the highest activity was taken as 100% and subsequent activities were normalised accordingly.....48

Figure 2.3. Cellulose chain showing the glucose units and the position of the hydroxyl groups.....49

Figure 2.4. FTIR spectra of cotton and cotton-citric fabric.....53

Figure 2.5. FTIR spectra of cotton fabric and cotton-silane amine fabric.....55

Figure 2.6. Effect of pH on the activity of free and immobilised ADH. The reactions for each pH measurement were performed in triplicate and error bars represent standard deviations. The highest activity was taken as 100% and subsequent % activity was normalised against this value.....56

Figure 2.7. Schematic illustration of the PDA-coated cellulose fabric.....58

Figure 2.8. Effect of AGE concentration on ADH activity. The ADH assay was performed on triplicate samples for each conc. and error bars represent standard deviations. To display the data, the highest activity was taken as 100% and subsequent activities were normalised accordingly.....70

Chapter 3

Figure 3.1. PVA various applications.....98

Figure 3.2. Storage stability of the immobilised ADH. The activity measurements were performed in triplicate and error bars present standard deviations. The highest activity was taken as 100 % and subsequent % activity was normalised against this value.....125

Chapter 4

Figure 4.1. Effect of concentration of 3-trimethoxysilylpropylamine (APTMS) on ADH activity. The assay was performed in triplicate and error bars represent standard deviations (S.D.).....169

Figure 4.2. A. Effect of glutaraldehyde (GA) concentration on immobilised ADH activity. B. Effect of glutaraldehyde (GA) activation time on immobilised ADH activity. The ADH assay was performed on triplicate samples and error bars represent standard deviations. To

display the data, the highest activity was taken as 100 % and subsequent activities were normalised accordingly.....170

Figure 4.3. a) SEM images showing the morphology of woven glass fabric as received; b) HCl activated and APTMS treated, c) GA crosslinked, and d) immobilised with ADH..... 172

Figure 4.4. High-resolution XPS spectra C1s (A) and N1s (B) for woven glass fabric (red line), 2.5% APTMS modified glass fabric (yellow line), GA activation (blue line) and ADH immobilised glass fabric (green line).....174

Figure 4.5. Effects of pH on the activities of the free and immobilised ADH. The ADH assay was performed on triplicate samples for each pH value and error bars represent standard deviations. To display the data, the highest activity was taken as 100 % and subsequent activities were normalised accordingly.....175

Figure 4.6. Effects of temperature on the activity of the soluble and immobilised ADH on woven glass fabric. The ADH assay was performed on triplicate samples for each temp value and error bars represent standard deviations. To display the data, the highest activity was taken as 100 % and subsequent activities were normalised accordingly.....176

Figure 4.7. Storage stability of ADH immobilised on woven glass fabric and soluble ADH in PBS (0.05 M) at 4 °C. The ADH assay was performed on triplicate samples and error bars represent standard deviations. To display the data, the highest activity was taken as 100 % and subsequent activities were normalised accordingly.....178

Figure 4.8. Effect of silane reagents on immobilised ADH activity. The ADH assay was performed on triplicate and error bars represent standard deviations. To display the data, the highest activity was taken as 100 % and subsequent activities were normalised accordingly180

Figure 4.9. Effect of concentration of 3-trimethoxysilylpropylamine (APTMS) on ADH activity on non-woven glass fabric. The ADH assay was performed on triplicate samples and error bars represent standard deviations. To display the data, the highest activity was taken as 100 % and subsequent activities were normalised accordingly.....181

Figure 4.10 A. Effect of glutaraldehyde (GA) concentration on immobilised ADH activity. B. Effect of glutaraldehyde (GA) activation time on immobilised ADH activity. The ADH assay was performed on triplicate samples and error bars represent standard deviations. To

display the data, the highest activity was taken as 100 % and subsequent activities were normalised accordingly.....183

Figure 4.11. SEM images showing the morphology of glass fabric: as received (A); HCl activated and APTMS treated (B); GA crosslinked (C); and immobilised with ADH (D).....184

Figure 4.12. High-resolution XPS spectra N1s (A) and C1s (B) for non-woven glass fabric (red line), 2.5% APTMS modified glass fabric (yellow line), GA activation (blue line) and ADH immobilised non-woven glass fabric (green line).....186

Figure 4.13. Effects of pH on the activities of the free and immobilised ADH. The ADH assay was performed on triplicate samples and error bars represent standard deviations. To display the data, the highest activity was taken as 100% and subsequent activities were normalised accordingly.....187

Figure 4.14. Effects of temperature on the activity of the soluble and immobilised ADH on glass fabric. The ADH assay was performed on triplicate samples and error bars represent standard deviations. To display the data, the highest activity was taken as 100% and subsequent activities were normalised accordingly.....188

Figure 4.15. Storage stability of ADH immobilised on non-woven glass fabric and soluble ADH in PBS (0.05 M) at 4 °C. The ADH assay was performed on triplicate samples and error bars represent standard deviations. To display the data, the highest activity was taken as 100 % and subsequent activities were normalised accordingly.....189

Figure 4.16. Mechanism of ethanol detection represented by the non-woven glass fabric-APTMS-GA-ADH biosensor. MB_{red} and MB_{oxi} represent the MB mediator reduced and oxidized, respectively.....193

Figure 4.17. Cyclic voltammograms obtained using a GC electrode with non-woven glass fabric modification: (a) GC-MP-glass fabric in absence of NADH; (b) GC-MP-glass fabric-APTMS-GA electrode in the absence of NADH, and (c) GC-MP-glass fabric-APTMS-GA electrode in the presence of NADH. Scan rate 100 mVs⁻¹ in PBS (0.05 M, pH 7.5) solution with 0.1 M KCl.....194

Figure 4.18. Amperometric response of the biosensor towards ethanol; 0.05 M PBS buffer (pH 7.5) and 1 mM NAD⁺; working potential 0.6 V, ethanol concentrations: 1 to 16 mM.

(Inset) Calibration plot illustrating the response obtained upon increasing ethanol concentrations in PBS (0.05 M, pH 7.5) containing 1 mM NAD⁺ using modified GC electrodes at 0.60 V versus Ag/AgCl.....195

Figure 4.19. Schematic representation of FIA showing all the different components.....197

Figure 4.20. Flow injection amperometric responses of the GC-MP to increasing concentrations of ethanol (1mM to 10 mM) using PBS (0.05 M, pH 7.5) containing 1 mM NAD⁺ (mobile phase) when passed through the immobilised ADH bioreactor, flow rate 1 mL/min, working potential + 0.6 V(A); Calibration plot (B).....198

Figure 4.21. Flow injection amperometric responses of the GC/MB electrode with immobilised ADH supports eleven successive injections of 1 mM ethanol and 1 mM NAD⁺. The operating potential was + 0.6 V, flow rate 1 mL/min with mobile phase PBS (0.05 M, PH 7.5).....199

Figure 4.22. The FIA used for electrochemical measurements.....202

Chapter 5

Figure 5.1. Proposed schematic of NAD⁺ regeneration by NADH oxidase with oxidation of alcohol when both enzymes immobilised on a fibrous support..... 236

Appendix I

Figure 1. Schematic representation of Glass fibre and fabric surface modification and immobilisation with ADH.....242

Figure 2. Mechanism of electrochemical detection for G fibre-APTMS-GA-MB-ADH biosensor. MB red and MB oxi represent the MB mediator reduced and oxidized, respectively.....244

Figure 3. Schematic representation of FIA.....246

Figure 4. SEM images showing the surface morphology of G fibres as received (A), HCl activated and 2.5% APTMS treated (B), GA treatment and immobilized with ADH (D)..247

Figure 5. XPS spectra of Glass fibre HCl activated (red line), Glass fibre APTMS modification (yellow line),Glass fibre-APTMS-GA (blue line) and Glass fibre-APTMS-GA-ADH (green line).....248

Figure 6. Comparison between glass fibre and fabric using various silane reagents effect on ADH activity. Activity assay was performed in triplicate and error bars represent standard deviations (S.D.).....	250
Figure 7. Effect various concentrations of APTMS on ADH activity. The assay was performed in triplicate and error bars represent standard deviations (S.D.).....	251
Figure 8. Effects of pH on the activities of the free and immobilized ADH (glass fibre and fabric). Reactions were performed in triplicate and error bars represent standard deviations (S.D.).....	253
Figure 9. Storage stability of ADH immobilized on glass fibres and fabric and soluble ADH in PBS (0.05M) at 4 °C.....	255
Figure 10. Effects of temperature on the activity of the soluble and immobilized ADH on glass fibre and fabric.....	256
Figure 11. (A) Amperometric response of the biosensor towards ethanol;0.5M phosphate buffer solution (pH 7.5) and 1 mM NAD ⁺ ; working potential: 0.6V, ethanol concentrations: 1 to 16 mM (B) Calibration plot illustrating the response obtained upon increasing ethanol concentrations in PBS containing 1 mM NAD ⁺ using modified GC electrodes at 0.60 V versus Ag/AgCl.....	258
Figure 12. (1) Flow injection amperometric responses of the GC-MP to increasing concentrations of ethanol (1 mM to 10 mM) in 0.05 M phosphate buffer (pH 7.5) and 1 mM NAD ⁺ (mobile phase), flow rate 1 mL/min, working potential +0.6V, Calibration plot (2) and (3).....	260
Figure 13. Flow injection amperometric responses of the Glass fibre-APTMS-GA-ADH electrode to 11 successive injections of 1 mM ethanol and 1 mM NAD ⁺ . Operating potential was +0.6V, flow rate 1 mL/min with 0.05 M phosphate buffer (pH 7.5) carrier.....	261

List of Tables

Chapter 1

Table 1.1 Advantages and disadvantages of enzyme immobilisation.....	4
Table 1.2 Large scale industrial processes utilising immobilised biocatalysts.....	5
Table 1.3 Factors influencing the performance of immobilised enzymes.....	6
Table 1.4 Summary of ADH immobilisation on various supports.....	12
Table 1.5 Summary and examples of inorganic and organic materials used for enzyme immobilisation.....	19
Table 1.6 Summary and examples of newer inorganic, organic and hybrid materials used for enzyme immobilisation.....	22
Table 1.7 Previous strategies of enzyme immobilisation on fabrics.....	32

Chapter 2

Table 2.1 Cellulose supports for enzyme immobilisation.....	49
Table 2.2 Nylon supports for enzyme immobilisation.....	59
Table 2.3 PAN supports for enzyme immobilisation.....	62
Table 2.4 Attempted PAN fibre surface modifications.....	63
Table 2.5 Activity data measured before and after Sephadex purification.....	68
Table 2.6 Effect of pH on soluble and immobilised ADH (silane cotton support) activity.....	76
Table. 2.7 ADH immobilised on nylon 6 fabric support ADH activity data.....	80
Table 2.8 Reaction details and activity data for Reaction A (45 min).....	86
Table 2.9 Reaction details and activity data for Reaction B (4 min).....	86
Table 2.10 ADH concentration study.....	88
Table 2.11 Effect of pH on soluble ADH activity.....	89

Chapter 3

Table 3.1 PVA support used for various enzyme immobilisations.....	98
--	----

Table 3.2 Reactions of polyvinyl alcohol classified according to functional group interconversion.....	100
Table 3.3 Detailed reaction conditions and TLC analysis of the model reaction.....	107
Table 3.4 Covalent attachment of ADH and modified PVA fabric.....	110
Table 3.5 Activity data for immobilised ADH on modified PVA supports.....	116
Table 3.6 Activity measurement: Effect of EDA concentration on immobilised ADH....	134
Table 3.7 Activity measurement: ADH immobilised on PVA acid support.....	142
Table 3.8 Activity measurement: ADH immobilised on PVA-isocyanate support.....	148
Table 3.9 Activity measurement: ADH immobilised on PVA chlorotriazine support.....	150
Table 3.10 Activity measurement: pH stability of soluble and immobilised ADH.....	153
Table 3.11 Activity measurement: Thermal stability of soluble and immobilised ADH...	154
Table 3.12 Activity measurement: ADH immobilised on PVA-Cl-EDA-GA disc reusability.....	155

Chapter 4

Table 4.1 Examples of the analytical parameters and performance of some recently reported ADH based ethanol biosensors.....	162
Table 4.2 Glass supports used for the immobilisation of enzymes.....	164
Table 4.3 Effect of various silane modifications on immobilised ADH activity.....	168
Table 4.4 Elemental compositions expressed as atomic ratios X/C, i.e. the atomic concentration of element X relative to that of C.....	172
Table 4.5 Effect of various silane reagents on immobilised ADH activity.....	179
Table 4.6 Elemental compositions expressed as atomic ratios X/C, i.e. the atomic concentration of element X relative to that of C. Listed are the mean values (± deviation) based on three analyses points.....	185
Table 4.7 ADH activity after immobilisation after each modification of non-woven glass fabric and woven glass fabric (ADH was immobilised on these supports under identical protocols).....	190

Table 4.8 Activity data measured for woven and non-woven glass fabric after various APTMS conc treatment.....	212
Table 4.9 Activity data measured for woven and non-woven glass fabric after varying GA concentrations.....	214
Table 4.10 Activity data for woven and non-woven glass fabric after various pH treatment.....	216
Table 4.11 Thermal stability data of soluble and immobilised ADH on both woven and non-woven glass fabric.....	218
Table 4.12 Storage stability data of soluble and immobilised ADH on both woven and non-woven glass fabric.....	220
Table 4.13 Current measured at various concentrations of ethanol.....	224
Table 4.14 Current measured at varying concentrations of ethanol.....	225

Appendix I

Table 1 Elemental compositions expressed as atomic ratios X/C, i.e atomic concentration of element X relative to that of C (mean value (+/- deviation) of two measurements at two different locations on each sample).....	247
Table 2 Effect of various silane reagents on immobilized ADH activity.....	249
Table 3 ADH activity after immobilisation after each modification of Glass fibre and fabric (ADH was immobilized on these supports under identical protocols).....	252

Acronyms/Abbreviations

APTMS	(3-Aminopropyl)-trimethoxysilane
ADH	Alcohol Dehydrogenase
Ag/AgCl	Silver/Silver Chloride Electrode
AuNP	Gold Nanoparticles
AGE	Allyl glycidyl ether
AOX	Alcohol oxidase
BSA	Bovine Serum Albumin
BMPS	3-Maleimidopropionic acid <i>N</i> -hydroxysuccinimide ester
DMF	Dimethylformamide
E°	Standard Potential
EDC	1-Ethyl-3-(3-Dimethylamino-Propyl) Carbodiimide Hydrochloride
ESI	Electron Spray Ionization
FAD	Flavin Adenine Dinucleotide
FIA	Flow Injection Analysis
GC	Glassy Carbon Electrode
GA	Glutaraldehyde
KLH	Keyhole Limpet Hemocyanin
Med	Mediator

MB	Meldola's blue
MS	Mass Spectroscopy
MWCNT	Multi-Walled Carbon Nanotubes
MES	2-(<i>N</i> -Morpholino) ethane sulfonic acid
NADH/NAD ⁺	β-Nicotinamide Adenine Dinucleotide
NADPH/NADP ⁺	Nicotinamide Adenine Dinucleotide Phosphate
NHS	<i>N</i> -Hydroxysuccinimide
NOX	NADH Oxidase
PBS	Phosphate-Buffered Saline
PVA	Polyvinyl alcohol
PAN	Polyacrylonitrile
PDA	Polydopamine
Red	Electrochemically Reduced
SEM	Scanning Electron Microscope
TEA	Triethylamine
TLC	Total Layer Chromatography
XPS	X-Ray Photoelectron Spectroscopy
YADH	Yeast Alcohol Dehydrogenase

Chapter 1

INTRODUCTION

1.1 Introduction

Virtually all bioprocesses that sustain life in organisms are catalyzed by enzymes. Enzymes can be used in the chemical reaction to enhance reaction rate without changing their composition or utilizing themselves.^{1, 2} They can enhance the reaction rate between the reactants and the products without changing the equilibrium. Enzymes are well known as biocatalysts and they are usually highly efficient, chemo, regio and stereoselective such as esterases, lipases and proteases.³⁻⁷ This feature makes them attractive for biotechnological use.⁶ The environmental benefits of enzymatic processes over conventional processes in various industries have been discussed in numerous books, articles and reports over the past decade.^{8, 9, 10}

Enzymes were known for the fermentation process since the start of twentieth century and later their structural and chemical composition were critically studied to make their use as biological catalysts in different industries like textile, pharma and chemical.¹¹ (Figure 1.1)

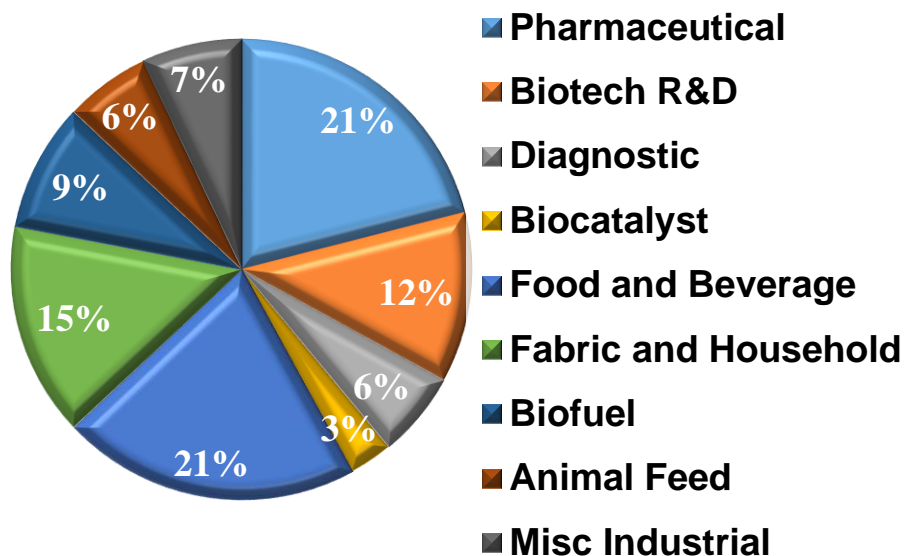


Figure 1.1. Enzyme use in industry based on the sale of the enzyme. Data from Freedonia Group Inc.¹²

Enzymatic processes have been implemented in a broad range of industries in recent decades and usage continues to expand.^{4, 7, 13} The world market for industrial enzymes in 2016 was US \$4.61 billion with a growth projection increase of 6.3% for 2017-2022.¹⁴

Industrial application of enzymes can be hindered due to low operational stability, recovery process, separation of product and recycling of the enzyme.¹⁵⁻¹⁷ Immobilisation of the enzyme on an insoluble, inert support is one way of overcoming some of these limitations.

Heterogeneous catalysts are insoluble forms of enzymes which facilitate long-term stability, reuse and recovery.^{2, 18} Table 1.1 summarises the advantages and disadvantages of enzyme immobilisation.

(the below table is reproduced from reference 24)

Table 1.1 Advantages and disadvantages of enzyme immobilisation¹⁹

Advantages	Disadvantages
Susceptible to continuous and batch process	Enzyme activity loss upon immobilisation
Reuse over multiple cycles	Contrary alterations in kinetic properties
Favourable variations in pH and temperature optima	Cost of the immobilisation process
Enhancement in stability compared to the soluble form of the enzyme	Cost of the carrier and fixing agents
Co-immobilisation with other enzymes possible	Subject to fouling

In addition to the advantages described above, enzyme immobilisation may also enhance enzyme activity and enzyme stabilization.²⁰ Before 1970s only single immobilised enzymes were used and in latter years more complex systems such as two-enzyme reactions with cofactor regeneration were developed.²¹ The major applications of immobilised enzymes are the industrial production of sugars, other amino acids and pharmaceutical intermediates are shown in Table 1.2 reproduced from literature. More recently, the technology of immobilised enzyme were used in different fields of research majorly for applications in sectors of clinical, environmental and industrial fields.²² The whole microbial cells are immobilisation which contain the desired enzymes are used as biocatalysts in some industrial processes.²³

Table 1.2 Large scale industrial processes utilising immobilised biocatalysts

Enzyme	Form	Process	Production (tons)	Ref.
Glucose isomerase	CWC, IME, CIE	High fructose corn syrup from corn syrup	10 ⁷	24, 25
Nitrile hydratase	CWC, CIE	Acrylamide from acrylonitrile	10 ⁵	26, 27
Lipase	IME	Transesterification of food oils	10 ⁵	28
Lactase	IME	Lactose hydrolysis, GOS synthesis	10 ⁵	29, 30
Lipase	IME	Biodiesel from triglycerides	10 ⁴	36, 39
Penicillin G acylase	CWC	Antibiotic modification	10 ⁴	31, 32
Lipase	IME, CIE	Chiral resolution of alcohols and amines	10 ³	33, 34
Aspartase	CWC, IME	Aspartic acid from fumaric acid	10 ⁴	35, 36
Thermolysin	IME	Aspartame synthesis	10 ⁴	37
<i>CWC = cross-linked whole cell; IME = immobilised enzyme; CIE = covalently immobilised enzyme</i>				

In addition to facilitating chemical reactions, immobilised enzymes are also finding widespread use in chromatography, bioreactors and biosensors.^{38,39} Although there are number of different immobilisation processes,⁴⁰⁻⁴³ the design of new protocols that permit improvement of enzyme activity after immobilisation is still an aspirational goal. The immobilisation process is ideal when it is simple, robust and should not use toxic or unstable reagents. Further the process should be suitable for continuous mode of operation and automated processes that will allow the easy recovery. However, commercialisation of immobilised enzymes has been retarded by their high cost, stability and storage drawbacks.⁴⁴ Therefore effort is being focused towards reducing or overcoming limitations related to the immobilisation process in order to expand their use. Table 1.3 summarises the main factors influencing the performance of immobilised enzymes.

Table 1.3 Factors influencing the performance of immobilised enzymes⁴⁵

Factors	Implications of immobilisation
Hydrophobic partition	Enhancement of reaction rate of hydrophobic substrate
Multipoint attachment of the support	Improvement of enzyme thermal stability
Various binding mode	Activity and stability can be influenced
Spacer of different types of immobilised enzymes	Hinder enzyme deactivation
Physical post-treatments	Enhancement of enzyme performance
Diffusion constraints	Stability enhancement and decrease in enzyme activity
Physical structure of the support such as pore size	Activity retention can be dependent on pore size
Physical nature of the support	Higher activity retention is observed due to large pore size support material reduction in diffusion limit

In enzyme immobilisation process selection of attachment protocol or method between the reactive groups on the support surface and enzyme amino acid residue is very important to preserve the catalytic activity of the enzyme.^{2, 46} Indeed, immobilised enzymes may be even less stable than the free enzyme if the immobilisation protocol is not well planned.⁴⁷ There are principal key points to be considered in the development of immobilised biocatalysts, such as the method of immobilisation, selection of the support and conditions to be used for immobilisation. In this thesis, the term solid-phase, solid support, support, or matrix are used synonymously to describe what the enzyme is immobilised onto.

1.2 Methods for immobilisation

The method of immobilising an enzyme can influence the enzyme's activity and stability.⁴⁸ Immobilisation methods are divided into two types namely, physical and chemical methods. Physical immobilisation method is mainly due to the hydrophobic interactions, hydrogen

bonding, van der Waals forces or ionic binding between support and enzyme. This method is always considered as weak interaction. Chemical methods involve the formation of strong bonds between the enzyme and a support material, namely covalent bonds through varying linkages such as ether, thioether, ester, amide or carbamate bonds between the enzyme and support material.⁴⁹ There are three main techniques for immobilisation of enzymes namely, adsorption, entrapment and covalent bonding/cross-linking (Figure 1.2).⁷

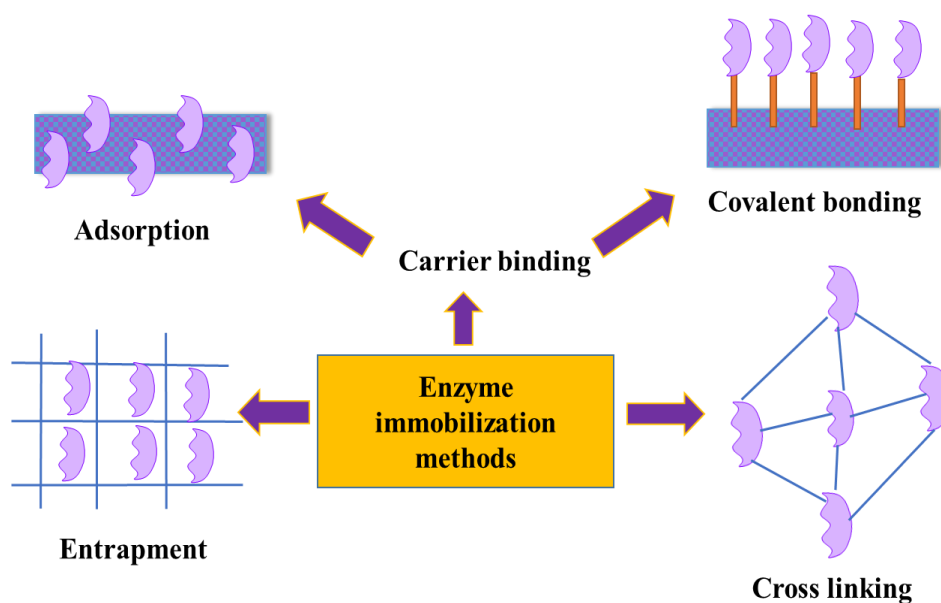


Figure 1.2. Simplified schematic of enzyme immobilisation protocols or methods

1.2.1 Adsorption

Adsorption is the simplest method of immobilisation and is mainly based on the adsorption and formation of weak bonds through hydrogen bonding, electrostatic forces and hydrophobic effects.⁵⁰ Physical adsorption can be obtained by immersing of the support into a solution of enzyme. The affinity binding, is one of the physical methods for the immobilisation of enzymes which can be achieved either by pre-coupling the support to an affinity ligand for the target enzyme, or the enzyme can be conjugated to an entity that develops an affinity towards the support.⁵¹ The adsorption binding results in a high retention of activity for the immobilised

enzyme. In general, enzyme immobilisation through physical adsorption is simple and is commercially attractive, as it is simple, available in low cost, and high enzyme activity.^{52, 53} However, a disadvantage of the technique is that physical bonding in most cases is too weak to keep the enzyme attached to the support and hence the enzyme is prone to leaching.⁵⁴ Enzyme leaching is a major issue when the enzyme and support material complex is subjected to industrial conditions such as high ionic strength, high reactant and product concentrations.⁴⁴ Some of the supports used to immobilise enzymes by physical adsorption include: activated carbon, bentonite, kaoline, collagen, alumina, Amicon-AP10, diatomaceous earth, silanised alumina, silica gel, calcium carbonate, propyl agarose, nitrocellulose fibre, cheese cloth, DEAE-cellulose, TEAE-cellulose, DEAE-Sephadex, CM-Sephadex, CM-cellulose, Amberlite XE-9 polyamino polystyrene, DEAE-Sephadex A-50, Duloite S-761, and ion exchange resins such as Amberlite CG-50, Dowex 2-anion-exchange and Dowex 50-cation exchange.⁵⁵

1.2.2 Entrapment

The enzymes can be retained on the porous solid support by the method of entrapment. It improves mechanical stability, reduces enzyme leaching and it does not interact chemically with polymer.⁵⁶

In spite of this, the entrapment method is restricted to the practical use due to possibility of leakage from support matrix, low loading of enzyme and scraping of support material during its use.³ Further entrapment suffers from transfer of mass restrictions of substrate or analyte to the enzyme active site.⁵⁷

1.2.3 Covalent

The most popular method of immobilisation involves covalent attachment of an enzyme to its support material. The functional group that take part in the binding of the enzyme generally involve the side chains of the endogenous amino residues like cysteine, lysine and aspartic and glutamic acids,⁵⁸ imidazole and phenolic groups which are not essential for the catalytic activity of the enzyme. The activity of the covalently bonded enzyme depends on the method and protocol used during coupling, size, shape and composition of the support material. The amino acid residues that are important for the catalytic activity must not be involved in the covalent binding to the support so as to reach the high levels of activity.⁵⁹ Diverse reactions have been developed depending on the functional groups available for reaction on the support surface and the enzyme amino acid residues available.²⁵ Spacers can be included between the support and the enzyme to avoid unwanted spacer/support and spacer/enzyme interactions (steric effects). Covalent based coupling methods are mainly divided into two main classes:

- Activation of the support material's surface by addition of reactive functional groups, and
- Modification of the support material's surface backbone to produce an activated group.

The electrophilic groups on the support material can be generated by the activation processes which can further react with nucleophilic residues within the enzyme sequence in the coupling step.⁵⁹ Biocatalysts synthesized by covalent immobilisation can be used in aqueous, multiphase, and viscous media.⁶⁰ Silica gel,⁶¹ montmorillonite,⁶² polystyrene,⁶³ chitosan,⁶⁴ agarose,^{65, 66} gelatin,⁶⁷ and pectin⁶⁸ are common supports used for covalent immobilisation. The another irreversible method of enzyme immobilisation is cross-linking. It is performed by formation of intermolecular cross-linkages between the enzyme and support via bi- or multi-functional reagents such as glutaraldehyde (GA).⁶⁹ GA is known to react with various nucleophilic

functional groups of the enzyme, such as amine, thiol, phenol, and imidazole functional groups.⁷⁰ Cross-linking is pH dependent and involves both Schiff base formation and Michael-type 1,4-addition to α,β -unsaturated aldehyde moieties.⁶⁹ However, cross-linking, may result in reduced diffusion of reactants and products and can also cause significant changes to the active site; both of these can result in loss of enzyme activity.³³ Non-cross-linked covalent immobilisation, however, does not usually interfere with reagent and product mass transfer but allows an increase in enzyme stability (especially towards heat, pH, organic solvents, and storage). These stability parameters, in addition to minimised leakage, are crucial in industrial processes.⁷¹

1.3 Enzymes and cofactors

1.3.1 ADH enzyme

The six enzyme classes are: oxidoreductases, transferases, hydrolases, lyases, isomerases, and ligases⁷² are based on the type of reaction they catalyse which are used for catalysing the transfer of functional groups, electrons or atoms. Enzyme catalyzed oxidation reactions have gained increasing interest in biocatalysis. Oxidoreductases constitute an important group of biocatalysts as they facilitate not only the widely used stereoselective reduction of ketones but also the less well-exploited oxidation of alcohols and amines.⁷³ Oxidoreductases require a non-protein cofactor to facilitate catalysis. These cofactors act as an electron source or electron sink. Aldo- and keto-reductases and dehydrogenases, in particular, act on the substrate by the transfer of electrons from or to a cofactor, mostly by using cofactors such as nicotinamide-based nucleotides NAD(H) and NADP(H). There are a number of different naturally occurring

cofactors including NADH, FAD (flavin adenine dinucleotide), and ATP (adenosine 5'-triphosphate).

Alcohol dehydrogenase (ADH) from Baker's yeast has been widely used as a biocatalyst in organic synthesis, primarily because it is inexpensive, readily available and can be used in aqueous media.⁶⁵ The majority of reported literature on the biotransformation capability of yeast involve reductions of carbonyl groups and carbon-carbon double bonds. Reactions involving carbon-carbon bond formation are of great interest in chemical synthesis. The ADH enzyme are known for selective oxidations and reductions varying from kinetic resolution to asymmetric reduction.^{74-75, 76} For example, ADH can be used to generate asymmetric centres to allow the synthesis of high-value chiral drugs such as thalidomide and verapamil.^{77, 78}

In this thesis, ADH is chosen as the model enzyme as it catalyses the oxidation of alcohols and the reduction of aldehydes and ketones, and therefore has many prospective applications in the pharmaceutical, food and chemical industries.⁷⁹ Additionally, ADH is available in quantity and the reaction is well characterised.⁸⁰ The conversion of benzaldehyde and pyruvate to L-phenyl acetyl carbinol (a precursor of ephedrine) was one of the first commercial processes to utilize ADH, where yeast was used in a whole cell form instead of the isolated form of ADH (Figure 1.3).⁸¹

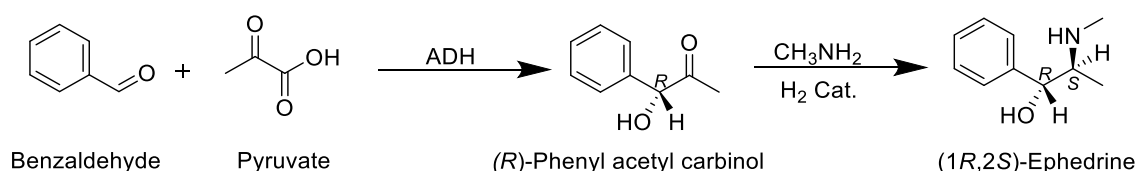


Figure 1.3. ADH enzyme used in a whole cell biotransformation

In the literature many examples can be found describing the use of soluble^{5, 82, 83} and immobilised^{75, 84-90} ADH. Reactions involving immobilised ADH are affected by the

hydrophobicity, the hydrophilicity and the physical structure of the support.⁸¹ Further, the nature of substrate attachment can also result in altered enzyme activity after immobilisation.⁶⁵ Many literature examples of ADH immobilisation have been described and include physical adsorption, covalent attachment and aggregation. The resultant activity is generally adequate, however operational stabilisation of the immobilised enzyme under biotransformation conditions is rarely achieved.⁹¹

Table 1.4 Summary of ADH immobilisation on various supports

Support	Source of ADH enzyme	Immobilisation method	Thermal stability of immobilised ADH	Storage stability of immobilised ADH	Reusability of immobilised ADH	Ref.
Polyaniline coated silver nanoparticles	Yeast alcohol dehydrogenase	Covalent	At 70 °C, immobilised ADH retained 78% activity as compared to 26% for soluble enzyme	90% activity over 30 days	90% after 15 cycles	92
Gelatine beads	Yeast alcohol dehydrogenase	Encapsulation	At 60 °C, immobilised ADH retained 60% activity as compared to 12% for soluble enzyme	80% activity over 40 days	60% after 6 cycles	93
PVA powder	Alcohol dehydrogenase from Lactobacillus kefir	Entrapment	-	-	-	94
Porous glass tube	Horse liver Alcohol Dehydrogenase	Adsorption	At 60 °C, immobilised ADH retained 60% activity	-	-	95
Chitosan-coated magnetic nanoparticles	Yeast alcohol dehydrogenase	Covalent	At 70 °C, immobilised ADH retained 54% activity	--	32% after 6 cycles	96

Table 1.4 Continued...						
Support	Source of ADH enzyme	Immobilisation method	Thermal stability of immobilised ADH	Storage stability of immobilised ADH	Reusability of immobilised ADH	Ref.
Non-porous glass beads	Yeast alcohol dehydrogenase	Adsorption	At 60 °C, immobilised ADH retained 60% activity	-	-	97
Glyoxyl-agarose	Horse liver Alcohol Dehydrogenase	Covalent	At 78 °C, immobilised ADH retained 65% activity	-	-	113
Magnetic nanoparticles (Fe ₃ O ₄ @Au NPs)	Yeast Alcohol Dehydrogenase	Adsorption	-	-	-	98
Amino-epoxy support (amino epoxy Sepabeads)	Alcohol dehydrogenase from <i>Lactobacillus brevis</i>	Covalent	-	-	-	99
Glyoxyl-agarose	Horse liver Alcohol Dehydrogenase	Covalent	At 60 °C, immobilised ADH retained 54% activity	-	-	65
Graphene oxide nanoparticles	Yeast Alcohol Dehydrogenase	Covalent	-	35% over 20 days	20% after 10 cycles	100
Attapulgit Nanofibers	Yeast Alcohol Dehydrogenase	Covalent	At 60 °C, immobilised ADH retained 44% activity	-	48% after 8 cycles	101

1.3.1.1 Structure and mechanism of ADH

Yeast ADH is a member of the zinc-containing alcohol dehydrogenase family. ADH from *Saccharomyces cerevisiae* has three isoenzymes, YADH-1, YADH-2, and YADH-3. ADH is

a tetramer composed of four similar subunits; each subunit is made of a single polypeptide chain of 347 amino acids with 36 kDa molecular mass.⁸⁰ The yeast ADH subunits are divided into two domains; the catalytic domain and the coenzyme-binding domain. Each subunit has one coenzyme-binding site and one tightly bound zinc ion. The zinc ion plays an important role in the catalysis.¹⁰² The sequence and tertiary structure of liver (*Equus Caballus*) and yeast enzyme are closely related and hence both ADH sources display comparable activity.¹⁰³

Ligand to the active site of zinc

The catalytic domain is comprised of three residues, Cys-46, His-67 and Cys-174, coordinated to the catalytic zinc ion. The second zinc ion is ligated by four sulfur atoms from the cysteine residues 97, 100, 103 and 111 in a tetrahedral arrangement; further this zinc ion is important for its structural role.⁸⁰ The zinc ion is coordinated to the three amino acids via two thiolates from Cys-46 and Cys-174 and the imidazole nitrogen of His-67 (Figure 1.4) in the lower side of substrate binding pocket. The carboxylic group of Asp-49 and Glu-68 are also in close proximity to the active-site zinc ion and the same are conserved in all known zinc-dependent alcohol dehydrogenases. The polar groups present in the pocket close to the zinc ion are the zinc ligands, nicotinamide moiety of the coenzyme and the side chain of Thr-48. The nicotinamide ring interacts with Thr-178, Leu-203 and Met-294 while the other side faces to the active centre (Figure 1.4).

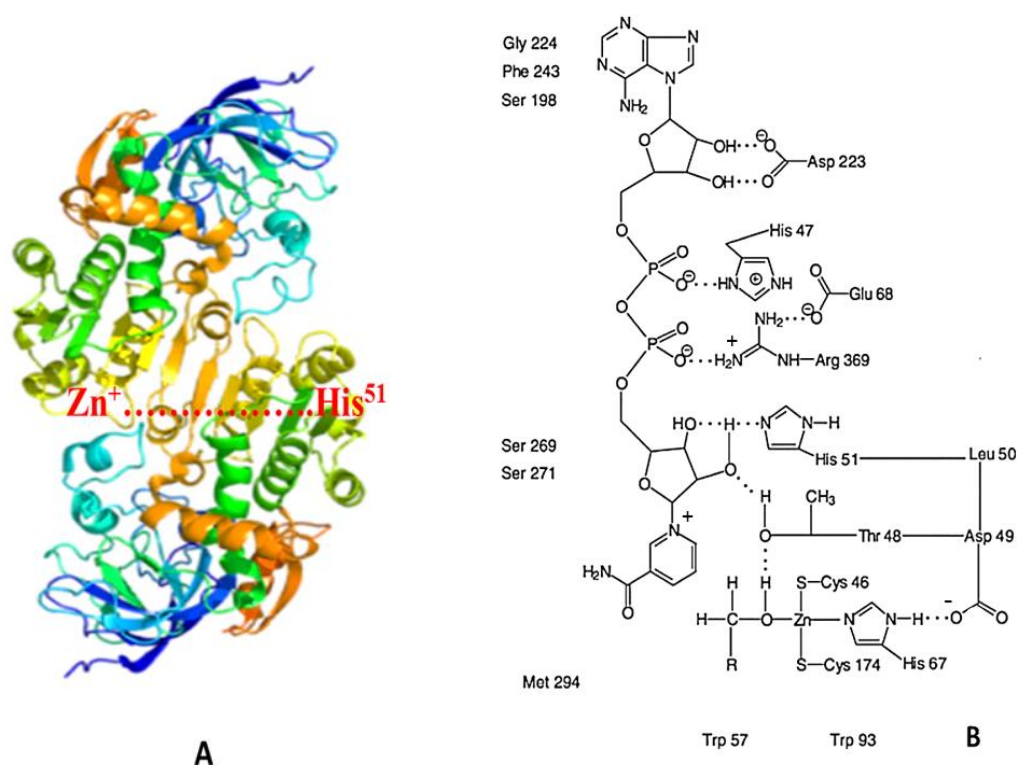


Figure 1.4. A: Crystal structure of the ADH homodimer and energy minimised model. B: Model of the active site of yeast alcohol dehydrogenase¹⁰⁴

ADH catalyses the oxidation of alcohols by reducing NAD^+ to NADH. During oxidation process, the alcohol oxygen from substrate molecule is electrostatically stabilised to increase the acidity of the hydroxyl proton by utilising zinc ion from ADH. In the mechanistic route, His-51 is activated by base catalysis such that the histidine can then accept a proton from the NAD^+ , which further take a proton from Thr-48, again representing general base catalysis (Figure 1.5). Simultaneously, there is a hydride transfer to the NAD^+ in its hydride accepting region. Thus, the whole mechanism sequence is essentially comprised of transfer of a hydride to the NAD^+ and the oxidation of an alcohol to an aldehyde (Figure 1.5). The orientation of the amino acid proton acceptors and donors is of critical importance, that are besides the position of the zinc ion in relation to the substrate such that it stabilizes a negative charge on the substrate thereby taking part in the stabilization of the transition state.

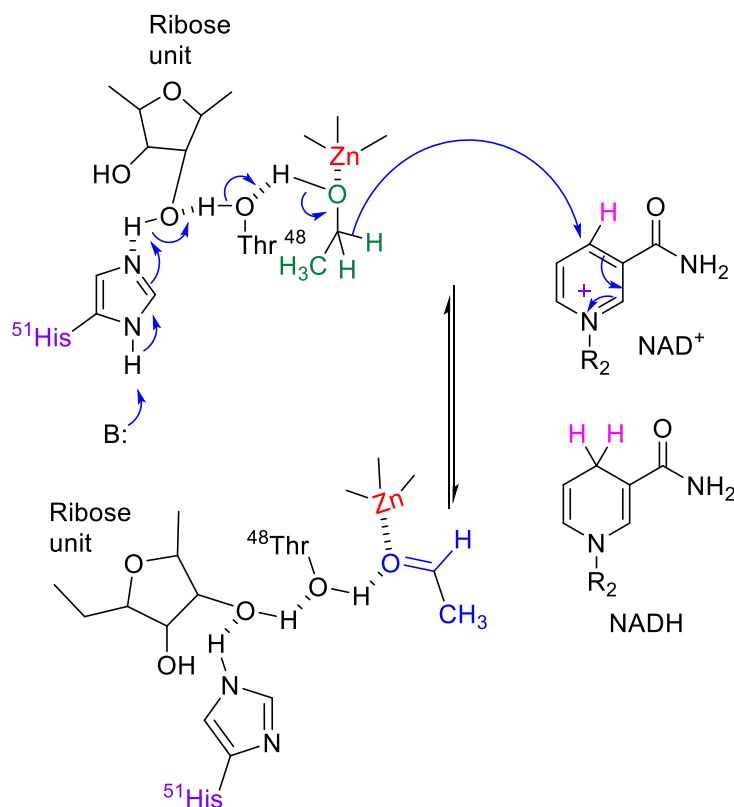


Figure 1.5. Oxidation of ethanol to acetaldehyde with ADH and NAD⁺ cofactor⁸⁰

1.3.2 Enzyme cofactors

Unlike enzymes, cofactors act as stoichiometric agents in biotransformation reactions and undergo chemical reactions along with the substrates.¹⁰⁵ These cofactors differ from each other in their redox potentials, binding constants and mode of regeneration.¹⁰⁶ NADH is the most common cofactor and is required by over 300 different dehydrogenases for catalysis. It exists in two forms, NADH and NADPH, with enzymes normally having a preference for only one form. The structure of NAD(H) is shown in Figure 1.6 with the 2-phosphate on the adenosine of NAD(H) being the only difference between NADP(H) and NAD(H).¹¹ The adenosine and pyrophosphate moieties are involved in binding the cofactor to the active site of the enzyme while the nicotinamide moiety is involved in electron transfer.⁷³

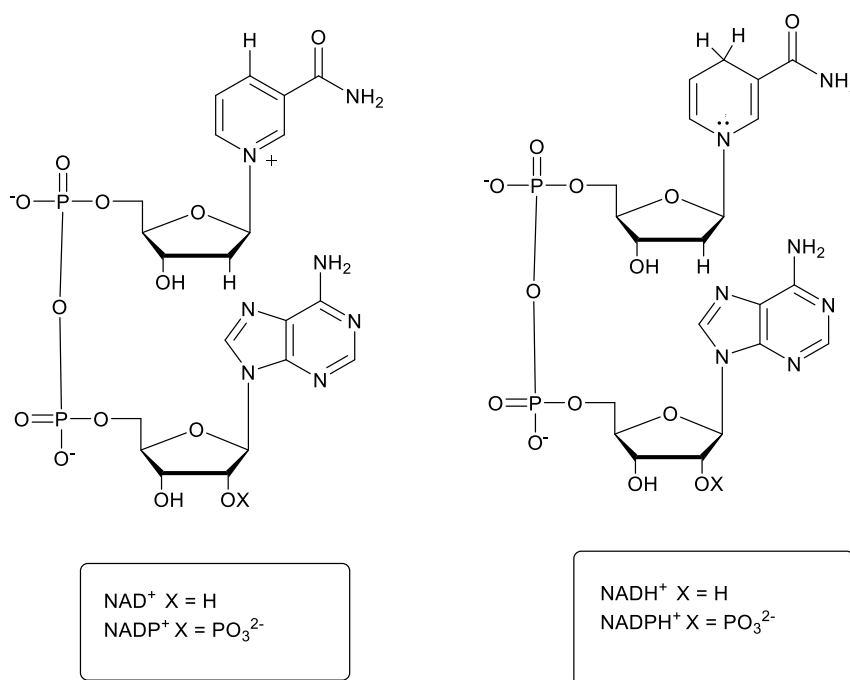


Figure 1.6. Structure of NAD⁺, NADP⁺, NADH and NADPH¹⁰⁷

1.4 Choice of supports

In the literature, numerous immobilisation methods with different supports such as inorganic, organic, hybrid and composite materials have been used to achieve stability and efficiency.¹⁰⁸ This section provides an review of the characteristics and properties of well established (Section 4.1) and new (Section 4.2) support materials used for enzyme immobilisation. Highly desired properties of support materials for operative enzyme immobilisation are shown in Figure 1.7. The support should protect the enzyme structure against harsh reaction conditions and facilitate high catalytic activity.¹⁸ Often bespoke and extensive optimisation of the attachment technique and support material needs to be performed to deliver a robust biocatalytic process.

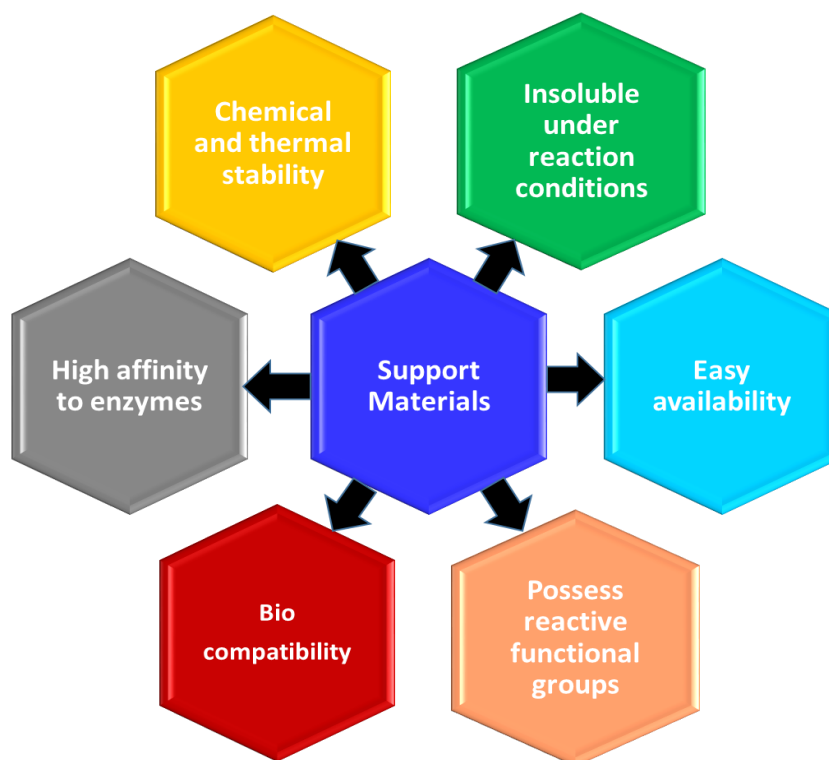


Figure 1.7. Desirable properties in support materials used for enzyme immobilisation¹⁰⁹

1.4.1 Classical support materials for immobilisation

Different inorganic and organic materials were used as supports for immobilisation (Figure 1.8)

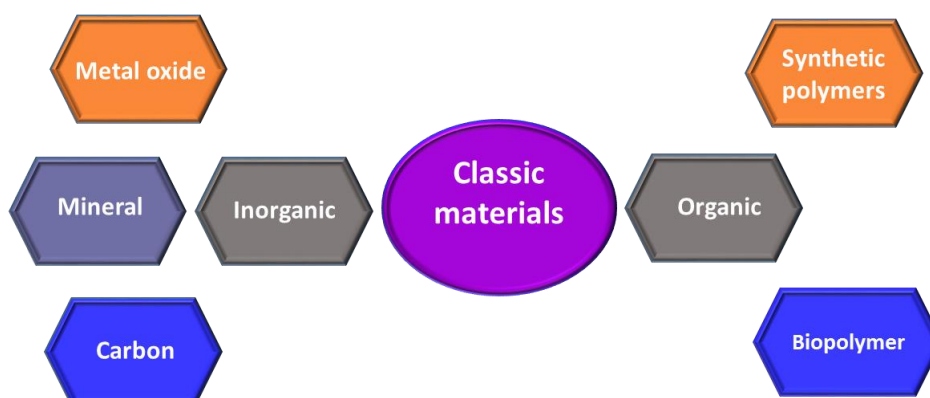


Figure 1.8. Examples of inorganic and organic supports used for enzyme immobilisation.¹⁰⁹

Inorganic oxides (e.g silica and various forms of silica such sol-gel, fumed, colloidal nanoparticles), minerals (bentonite, halloysite and kaolinite) and activated carbons are known for porous structure and the high surface area which is essential for effective enzyme immobilisation. Furthermore they possess good thermal, chemical stability along with mechanical resistance.^{110, 111}

Synthetic polymers (e.g. polyvinyl alcohol, nylon, polyaniline) and biopolymers (e.g. collagen, cellulose, keratins, carrageenan, chitin, chitosan and alginate) comprises of various functional groups that can participate in covalent linkage of enzymes without cross-linking agents.⁶⁰

Examples of immobilised enzymes are summarised in Table 1.5 reproduced from literature together with information about immobilisation type, cross-linking agents and binding group(s).

Table 1.5 Summary and examples of inorganic and organic materials used for enzyme immobilisation¹⁰⁹

Support Material	Binding Groups	Cross-linking agent	Immobilisation type	Immobilised enzyme	Ref.
Inorganic Materials					
Sol-gel silica	-OH	-	Adsorption	Lipase from <i>Aspergillus niger</i>	112
Silica gel	-OH, C=O	Glutaraldehyde	Covalent	Lipase	61
Al ₂ O ₃	-OH	-	Adsorption	Cysteine proteinases from <i>Solanum</i>	113
ZrO ₂	-OH	-	Adsorption	α -Amylase from <i>Bacillus subtilis</i>	114
Montmorillonite	-OH	3-Aminopropyl triethoxysilane	Covalent binding	Glucoamylase from <i>Aspergillus niger</i>	62
Hydroxyapatite	-OH	-	Adsorption	<i>Aspergillus niger</i>	115

Table 1.5 continued.....					
Support Material	Binding Groups	Cross-linking agent	Immobilisation type	Immobilised enzyme	Ref.
Bentonite	-OH, NH ₂	Tetramethyl ammonium hydroxide	Covalent binding	Glucose oxidase from <i>Aspergillus niger</i>	116
Commercial activated carbon	-OH, C=O	-	Adsorption	Cellulose from <i>Aspergillus niger</i>	117
Activated charcoal	-OH, C=O, COOH	-	Adsorption	Papain	118
Activated charcoal	-OH, C=O, COOH	-	Adsorption	Amino glucose	119
Organic Materials					
Polyaniline	-NH, C=O	Glutaraldehyde	Covalent binding	α -Amylase	108
Polystyrene	C=O, epoxy groups	Poly(glycidyl methacrylate)	Covalent binding	Lipase	63
Poly(vinyl alcohol)	-OH, C=O	Glutaraldehyde	Covalent binding	Laccase from <i>Trametes versicolor</i>	120
Polypropylene	-OH	Plasma activated	Covalent binding	Glucose oxidase	121
Cellulose nanocrystals	-OH	-	Adsorption	Lipase from <i>Candida rugosa</i>	122
<i>Luffa cylindrica</i> sponges	-OH, C=O, COOH	-	Adsorption	Lipase from <i>Aspergillus niger</i>	122
Chitosan	-OH, -NH ₂	-	Entrapment	Lipase from <i>Candida rugosa</i>	123
Agarose	-OH	-	Entrapment	α -Amylase	124

1.4.2 New materials for enzyme immobilisation

Classical support materials have relatively low efficiencies for catalytic conversions and continuous interest in immobilised enzymes has driven demand for new support materials.¹⁰⁹ Newer supports consist of organic (e.g. electrospun nanomaterials and polymeric membranes) and inorganic (e.g. magnetic nanoparticles, mesoporous silica, nano-gold and graphene) materials (Figure 1.9). Mostly, these materials possess good mechanical properties along with excellent thermal and chemical stability, and can be produced in various morphological shapes.¹²⁵ Furthermore, these materials also possess high functional group loading to facilitate enzyme binding.^{125, 126}

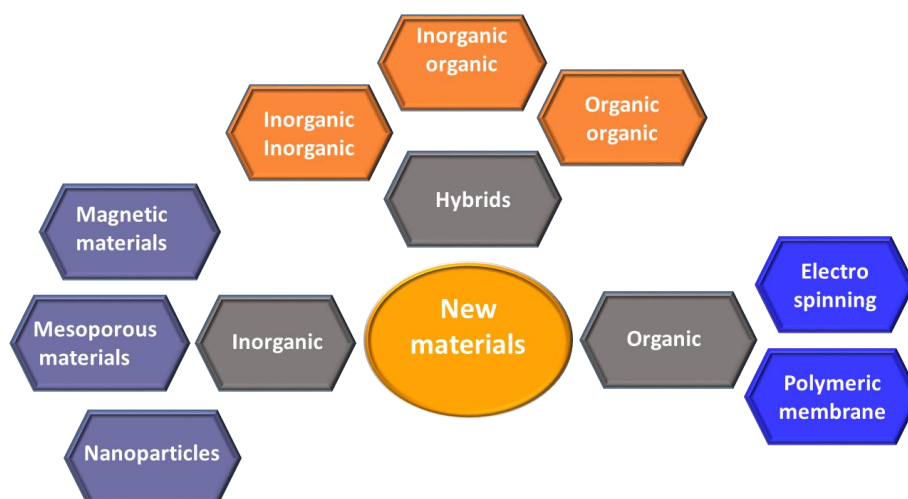


Figure 1.9. New inorganic, organic and hybrid supports used for enzyme immobilisation¹⁰⁹

The new materials allow separation of the biocatalyst from the reaction mixture (e.g. iron magnetic nanoparticles and an external magnetic field).¹²⁷ Other supports, such as graphene or graphene oxide, improve the transfer of electrons between the immobilised enzyme and the substrate which can result in increased catalytic activity of the enzyme.¹²⁸ Furthermore, bespoke mesoporous materials with hierarchic pore structure facilitate uniform distribution of biomolecules in the support pores and provide high catalytic activity. An additional advantage of organic based support materials is that they can be prepared in different geometrical shapes

including fibres and membranes. Along with nano, microfibre and other porous based membrane, they tend to reduce diffusion leading to the improvement of efficiency of biocatalytic process.¹²⁹ Hence there is a increasing interest in hybrid materials due to the ability to adapt the structure-activity relationship towards higher functioning biocatalysts.¹²⁹ Hybrid or composite materials can be obtained with the conjugation of (i) organic-organic, (ii) inorganic-inorganic, or (iii) organic-inorganic precursors (Figure 1.9). Table 1.6 describes key types of new materials together with the enzymes that have been immobilised on these supports are reproduced from literature.¹⁰⁹ Inclusive information presented about binding groups, immobilisation type and cross-linking agents.

Table 1.6 Summary and examples of newer inorganic, organic and hybrid materials used for enzyme immobilisation¹⁰⁹

Support material	Binding Groups	Cross-linking agent	Immobilisation type	Immobilised enzyme	Ref.
Inorganic Materials					
Magnetic nanoparticles	Epoxy groups	3-Glycidoxypropyl trimethoxysilane	Covalent binding	Lipase from <i>Candida</i>	149
Silica SBA-15	–OH	-	Adsorption	Alkaline protease	150
Mesoporous silica	–OH	-	Encapsulation	Catalase	151
Silica mesoporous nanoparticles	Epoxy groups	3-Glycidoxypropyl trimethoxysilane	Covalent binding	Lipase from <i>Rhizomucor miehei</i>	152
TiO ₂ nanoparticles	–OH	-	Adsorption	Carbonic anhydrase	153
Cordierite	–NH ₂	<i>N</i> -(2-Aminoethyl)-3-aminopropyl-trimethoxysilane	Covalent binding	Horseradish peroxidase	154
Multi-walled carbon nanotubes	–NH ₂	3-Aminopropyl triethoxysilane	Covalent binding	<i>α</i> -Glucosidase	155

Table 1.6 continued....

Support material	Binding Groups	Cross-linking agent	Immobilisation type	Immobilised enzyme	Ref.
Reduced graphene oxide	C=O	Glutaraldehyde	Covalent binding	Horseradish peroxidase	156
Organic Materials					
Electrospinning fibres of Polycaprolactone	C=O	-	Adsorption	Catalase	157
Electrospinning nanofibres of Polyvinyl alcohol	-OH	-	Encapsulation	Lipase from <i>Burkholderia cepacia</i>	158
Poly ether-sulphone membrane	-	-	Adsorption	Phosphotriesterase lactonase from <i>Sulfolobus</i>	159
Hybrid/Composite Materials					
Polyaniline Polyacrylonitrile	-NH	-	Encapsulation	Glucose oxidase	161
Cellulose Poly acrylic acid fibres	-OH, COOH	-	Covalent binding	Horseradish peroxidase	162
Chitosan-alginate beads	-NH ₂ , -OH	-	Entrapment	Amyloglucosidase	163
Graphene oxide-Fe ₃ O ₄	-OH, C=O	Cyanuric chloride	Covalent binding	Glucoamylase	164
Silica-lignin	-OH, C=O	-	Adsorption	Glucose oxidase form <i>Aspergillus niger</i>	165
Polyacrylonitrile multi-walled carbon nanotubes	-NH, C=O, -OH	<i>N</i> -Hydroxy succinimide	Covalent binding	Catalase	166
Silica-graphene oxide particles	-OH, C=O	<i>N</i> -Hydroxy succinimide	Covalent binding	Cholesterol oxidase	167
ZnO-SiO ₂ nanowires	-OH	-	Adsorption	Horseradish peroxidase	168
CaCO ₃ -gold nanoparticles	-OH, C=O	-	Adsorption	Horseradish peroxidase	169

Material supports (matrix) in fibre and fabric/textile that are durable, lightweight, easy to handle have been the point of attraction in many industrial fields. Porous fibres and textile carriers possess high surface area, which facilitates high enzyme loading, and also offer greater environmental resilience.¹³⁰ The advantages of fibres and fabrics as immobilisation supports are detailed further in Section 1.7.

1.5 Immobilisation chemistry

Functionalised supports enhance the binding efficacy and stability of enzyme immobilisation through multipoint attachment.^{71, 131} Solid supports bearing reactive functionality (e.g. amine-NH₂, alcoholic-OH, carboxyl-COOH, epoxy) can be further modified to enhance enzyme attachment *via* spacer groups (e.g. organic and inorganic halides, glutaraldehyde (GA), carbodiimides, various bi-functional agents).⁷¹

The immobilisation is usually accomplished *via* a reaction of enzyme side chains with the solid support.¹³² The enzyme can be attached to the solid support using different methods of immobilisation (e.g. adsorption, covalent binding, and entrapment).^{2, 133, 134} There are twenty major amino acids involved in enzyme/protein composition however, only one-third of them possess functionality suitable for immobilisation.¹³² The use of primary amine groups for enzyme bioconjugation is widely used. There are two main types of amine groups : the α -amino group (situated in *N*-terminus proteins chains) and the ϵ -amino groups (of lysine residues). In the most of cases, these amino acids are protonated at physiological pH and hence present predominantly outside surfaces of the protein's/enzyme tertiary structure. Therefore, they are easily available to conjugation reagents and easily protonated into the aqueous medium. However protonation decrease their activity and hence even though they possess higher nucleophilicity cannot be used in conjugation at physiological pH

The majority of the amines are protonated and have no remarkable nucleophilicity compared to other side chains present in the enzyme/ protein at acidic pH. The functional groups from the support which can react with enzyme based amines include isocyanates,¹³⁵ activated carboxyl groups¹³⁶ epoxy and aldehydes.^{18, 69} Under mild and moderate conditions aliphatic and aromatic amines can react with aldehyde groups of support to form imines (Figure 1.10). This imine intermediate further can be reduced by sodium cyanoborohydride, to give a stable amine¹³²

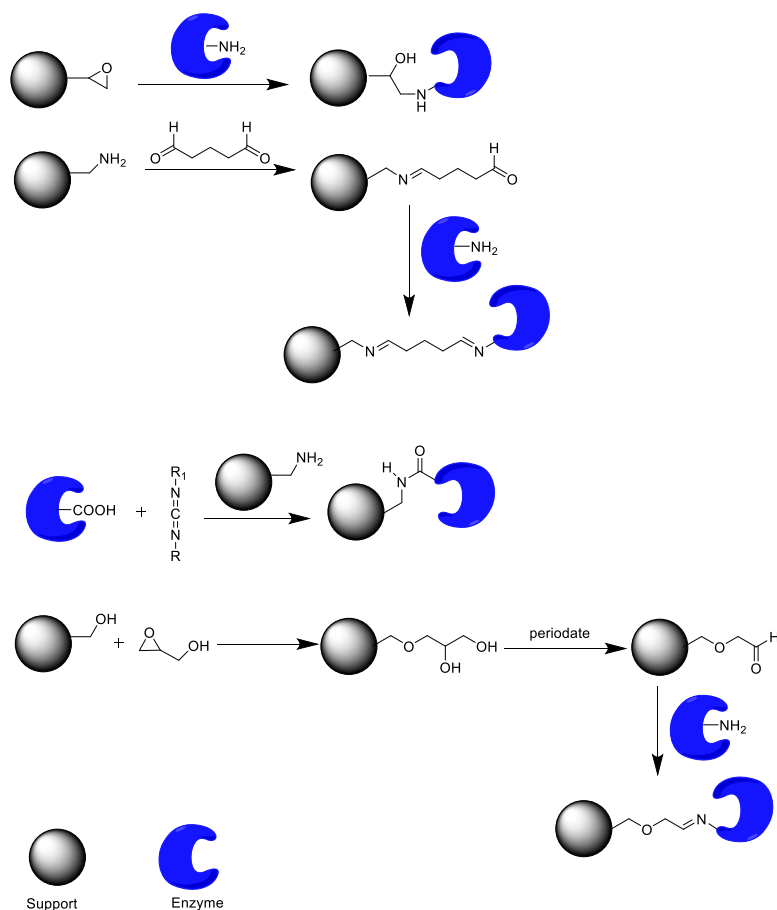


Figure 1.10. Enzyme (amine based) immobilisation on aldehydes, epoxides, acid and alcohols functionalised solid supports via covalent bonds

The hydroxyl groups of serine (Ser, S) and threonine (Thr, T) amino acid (pK_a values > 13), are less reactive (poor nucleophiles) at physiological pH. There are no examples of hydroxyl groups of serine and threonine involvement in conjugation at physiological pH. However, *N*-hydroxysuccinimide (NHS) esters modification on hydroxyl side chain of serine have been documented.^{137, 138}

Cysteine (Cys, C) possess high nucleophilicity due to its thiolate (RS^-) form. These amino residue are mainly found at the active site of the enzyme and present relatively low amount in the remainder of the enzyme (1–2%).¹³⁹ Next low abundance amino acid is Tryptophan (Trp, W). Almost major proteins, contains one Trp residue in their peptide sequence.^{132, 140} The pK_a for Histidine (His, H) is in the physiological range and hence present in active sites of enzymes where abstraction or donation of a proton is required (e.g. ADH as shown in Figure 1.5).¹⁴¹

The amino acid mainly found in its protonated form in acidic, neutral, and even in alkaline environments is Arginine (Arg, pK_a value 12.5). The delocalisation of a positive charge between nitrogen lone pairs and the double bond makes it easy to form the hydrogen bonds¹⁴² which makes the guanidinium side chain of arginine the least acidic cationic group among the rest of natural amino acids.¹⁴³

Aspartic and glutamic acids (Asp and Glu) contains carboxylic acid groups. These carboxylate groups present on the side chain of Asp and Glu possess low reactivity in water. These carboxylate can be converted into reactive moieties by generating reactive ester.¹⁴²

1.6 Immobilised enzyme activity

The three key criteria for immobilised enzymes are activity, stability and reusability. The activity of ADH and immobilised ADH can be assayed similar to the assay used for all NAD^+ dependent oxidoreductases where reduction of NAD^+ to NADH is observed. This reduction of NAD^+ is followed by a change in absorption of the NAD^+ molecule which can be followed spectrophotometrically at 340 nm in real time (Figure 1.11).¹⁴⁴ Lambert-Beer law, states the extinction of NAD^+ is proportional to its concentration [$A = \epsilon \times c \times l$, where A is the absorbance, ϵ is the extinction coefficient ($6220 \text{ M}^{-1} \text{ cm}^{-1}$), c is the concentration (mM) and l is the path length (cm)].¹⁴⁴ The change in concentration of NAD^+ can be used to calculate the activity of alcohol dehydrogenase in the solution in real time. Therefore, one unit of alcohol dehydrogenase can also convert $1.0 \mu\text{mole}$ of NAD^+ to NADH per minute.

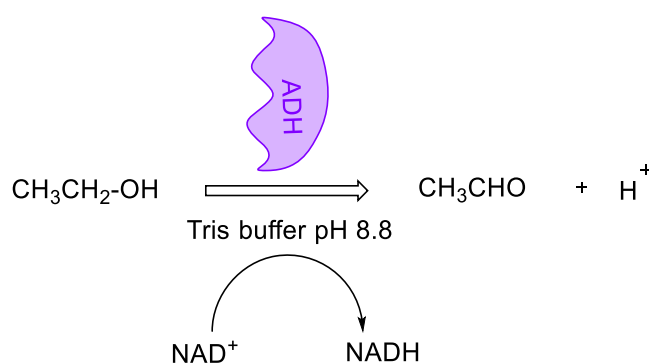


Figure 1.11. Ethanol oxidation with ADH in presence of NAD^+

1.7 Gaps and opportunity

In recent studies, various agarose-activated supports like MANAE-agarose, PEI-agarose and glyoxyl agarose have been used for immobilisation.⁶⁵ Glyoxyl agarose plays an important role

because it offers the most effective multipoint covalent attachment and can direct immobilisation to areas that are richest in the reactive groups.^{66, 145-147}

Furthermore, glyoxyl functionalised agarose possesses desirable properties such as:

- Very high reactivity of the glyoxyl groups with amino groups
- Very low steric hindrance in the reaction between enzyme/protein amine groups and glyoxyl groups of the support
- Good geometric consistency between the support surface and protein/enzyme
- High stability of the glyoxyl groups, which accommodates long reaction times and long storage times.

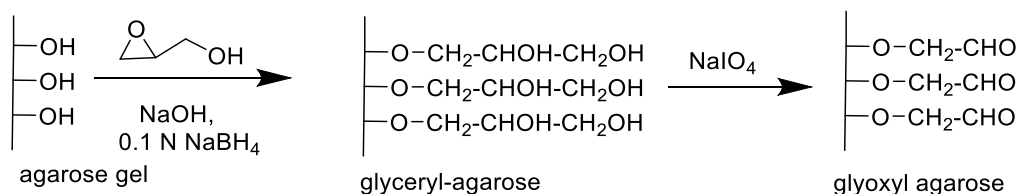


Figure 1.12. Activation of agarose to glyoxyl support¹⁷

However, although glyoxyl agarose has good properties, its industrial implementation is marred by several factors:

- The immobilisation of glyoxyl agarose involves the use of sodium borohydride and sodium periodate and where the first compound is considered a contaminant (as it is difficult to remove from the reaction) and combustible, while the second reagent is explosive (Figure 1.12).^{17, 66}
- The need for alkaline pH during immobilisation; pH parameters must be closely controlled to avoid enzyme inactivation and ensure high immobilisation.
- The fragility of the agarose resulting in slow decantation times.¹⁸⁹

The main large-scale application areas of immobilised enzymes are in the food and pharmaceutical industries. Enzymes used in the pharmaceutical industry are amino acylase (for resolving racemic mixtures of amino acids), penicillin amidase (used for selective hydrolysis in the preparation of antibiotics), pepsin (for the breakdown of dietary proteins into their constituent amino acid residues), amylase (for glucose extractions from starch) and glucoamylase (for hydrolysis of α -D-1,4-glycosidic linkages and α -D-1,6-glycosidic branch in starch) in batch processes.⁵

However, batch processing has some intrinsic disadvantages. These include:

- High operating costs of batch reactors due to reactor charging
- Difficult separation of reactant, product, enzyme and cofactors after the reaction
- Batch-to-batch variation and transfer to large scale

On the other hand, continuous flow reactors offer an alternative strategy to conventional batch-based regimes.^{70, 148, 149} Continuous flow processes are commonly found in chemical and biotechnological industrial production environments.¹⁵⁰ There are several main differences between batch and flow processes with respect to production, time and yield. Continuous flow reactors can provide greater productivity from a fixed amount of enzyme and constant reaction conditions can be achieved resulting in purer and more reproducible products.²³ In continuous flow reactors the catalyst can be introduced in two ways either by the addition of a homogeneous catalyst directly into the reaction mixture or *via* immobilisation of the catalyst on a solid support. The drawbacks to homogeneous catalysts are the cost of the catalyst and the need for its removal from the products. The combination of immobilised catalysts and flow chemistry is a promising way to avoid these problems.¹⁵¹ Packed-bed reactors have been used with immobilised catalytic systems since decades in industrial applications. Sparingly cross-

linked organic and inorganic supports are not suitable in microreactors because they can block the device, create high back-pressures and cause irreproducibility.¹⁵²⁻¹⁵⁴

To address this issue fibres and fabrics made of different polymers can be used as inert solid supports for enzyme immobilisation in flow based systems. Fibres and fabrics have large specific surface areas and possess excellent adjustable flow-through properties which facilitate their use in a continuous flow through process.^{155,156} Furthermore, with high enzyme load a high relative activity can be achieved with these supports.¹⁵⁶ Support with control porosity is crucial to avoid clogging of the reactor which ultimately resolves the back pressure issue in most flow reactor systems.¹⁵⁷ Fabric supports allow controlled porosity to be achieved *via* the fabrication process (i.e. method to convert fibre into the fabric such as knitting and weaving). Additionally, fibre and fabric supports exhibit good drapability and can be moulded to reactor geometry and easily removed without leaving any residue.^{157, 158}

1.7.1 Methods of fabrication

1.7.1.1 Weaving

Weaving forms a textile by interlacing two sets of yarns at right angles by means of a loom.¹⁵⁹ Simple woven fabric consists of one set of warp yarns (the length-wise yarn) and one set of weft yarns (the cross-wise yarn) and all equally contribute to the strength and appearance of the fabric. The closeness of the fibres is expressed as a number of ends per centimetre and determines the fabric porosity, i.e. porosity can be controlled by the changing the number of ends per centimetre (Figure 1.13).

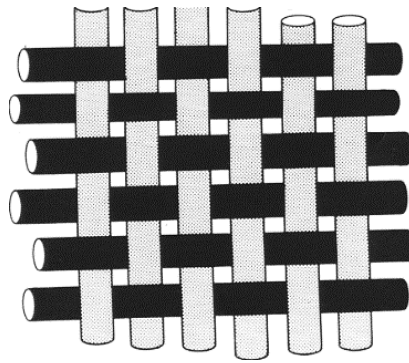
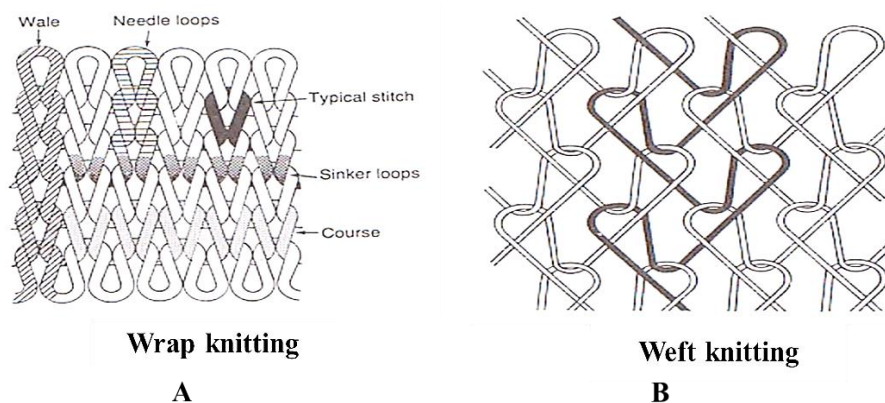


Figure 1.13. Weave pattern¹⁶⁰

1.7.1.2 Knitting

Knitted structures are produced from a series of interlocked loops.¹⁶¹ They are therefore elastic compared to woven structures. There are two types of knitting structures: weft and warp knits. In weft knitted fabrics (Figure 1.14B), the fibres run horizontally across the fabric (weft direction) and the rows or courses of the knitted textile are built up sequentially one above the other.¹⁶² Fabrics manufactured by the warp knitting process, on the other hand, are constructed of fibres running in a vertical axis (warp direction) of the fabric (Figure 1.14A). The porosity of a knitted structure is altered by changing the loop length.¹⁵⁹



Wrap knitting

A

Weft knitting

B

Figure 1.14. Different weft and wrap knitting patterns¹⁶²

Knitting has advantages over weaving such as low preparation time and the use of a single yarn to produce a structure (weft knit). Knitting can also be used to produce three dimensional structures.^{158, 163}

1.7.2 Enzyme immobilisation on fabrics

Fabrics are drawing attention as support matrix for enzyme immobilisation and can be used to create support materials with bespoke properties (e.g. anti-microbial activity and control of packaging volatiles) (Table 1.6).¹⁶⁴ For example, non-woven polyester fabrics was immobilised with horseradish peroxidase (HRP) using glutaraldehyde and showed 85% retention of its activity after 4 weeks of storage at 4 °C against 90% activity loss of the soluble HRP under the same conditions.¹⁶⁵ Beside from various inorganic carrier materials fabrics have been used for catalase immobilisation. Catalase was photochemically immobilised on polyester (PET) and polyamide 6.6 and the immobilised catalase possessed high stability with 3.5 times higher activity after 20 cycles when compared with the free enzyme.¹⁶⁶ Further more catalase immobilisation on the cotton fabric was performed with sodium periodate followed by covalent attachment of the enzyme.¹⁶⁷

Table 1.7 Previous strategies of enzyme immobilisation on fabrics¹⁶⁸

Support martial	Binding Groups	Immobilised enzyme
Polyester (PET) Polyethylene	Glutaraldehyde Plasma	Peroxidase (HRP)
Polyester (PET) Polyamide 6,6	1) Photochemical 2) Diallylphthalate or cyclohexane-1,4-dimethanol divinyl ether	Catalase

Table 1.7 Continued...		
Cotton	Oxidation by sodium periodate	Catalase
Silk fibroin	-	Tyrosinase
Polyamide 6,6	Glutaraldehyde	-
Support martial	Binding Groups	Immobilised enzyme
Polyamide 6,6	1) Enzymatic hydrolysis 2) Glutaraldehyde and spacer	Laccase
Silk fibroin, Viscose rayon, PET, Polyamide 6, Polypropylene	Various activation strategies	Glucose oxidase
Silk fibroin	Low-temperature plasma	Alkaline phosphatase
Cotton	1) Esterification with glycine 2) Carbonyldiimidazole /glutaraldehyde	Lysozyme
Wool	Glutaraldehyde	
Cotton	1) Esterification with glycine 2) Carbonyldiimidazole/ glutaraldehyde	Organophosphate hydrolase
PET	1) Ethylenediamine 2) Glutaraldehyde	
Polyester (Dacron)	Ethylenediamine	Thrombin
Wool	1) Polyethyleneimine 2) Glutaraldehyde	Lipase

Tyrosinase has been immobilised on fibroin¹⁶⁹ and nylon 6,6^{170, 171} glutaraldehyde crosslinking agent. and immobilised by entrapment method in alginate, polyacrylamide and gelatin.¹⁷² Laccase has been immobilised onto inorganic carrier materials such as alumina pellets for various applications.¹⁷³ Glucose oxidase is extensively used in many applications including bleaching of textiles.¹⁷⁴ Fabric supports such as viscose rayon, polyethylene terephthalate, nylon-6, polypropylene and non-woven fabrics of silk fibroin were immobilised with glucose

oxidase.¹⁷⁵ Urease enzyme was immobilised on cellulose fibre by biotinylation and used in electro dialysis cell to remove urea.¹⁷⁶

1.8 Project Objectives

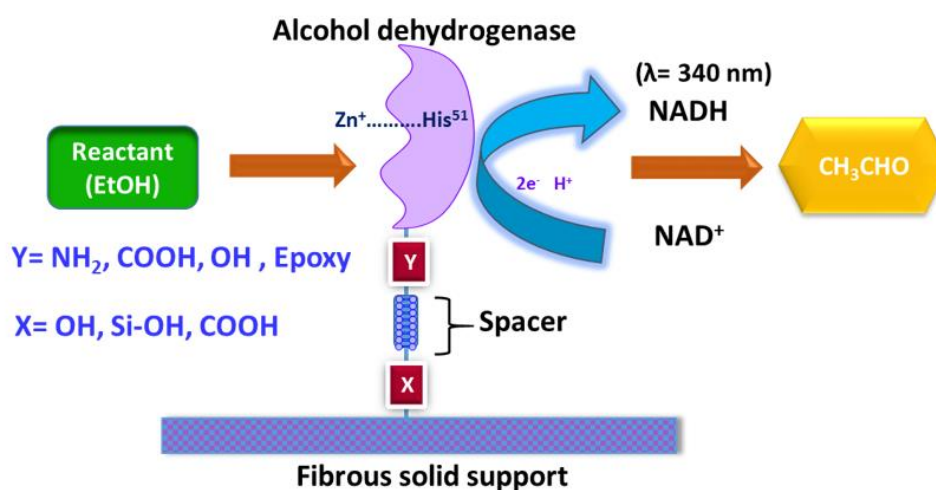


Figure 1.15. Schematic representation of ADH immobilised on a fibrous carrier/support to perform ethanol oxidation with the addition of NAD⁺ cofactor

This project aimed to:

- Fabricate novel flexible fibre based polymer supports which can be functionalised to allow covalent attachment of enzymes;
- Investigate the feasibility of using fibrous substrates comprised of cotton, nylon, polyacrylonitrile (PAN), polyvinyl alcohol (PVA) and glass fabric;
- Investigate novel methods to immobilise ADH (model enzyme) on a chemically modified fibre surface. The reaction to be studied involved the oxidation of ethanol to acetaldehyde using ADH along with its cofactor NAD⁺, which undergoes reduction to NADH;

- Develop a biosensor or flow reactor system for the catalysis of ethanol to acetaldehyde in a proof of concept format which incorporates a porous fabric support with immobilised ADH.
- Structurally characterise and assess the activity and stability of immobilised enzyme constructs using spectroscopy, mechanical analysis, microscopy and activity assays.

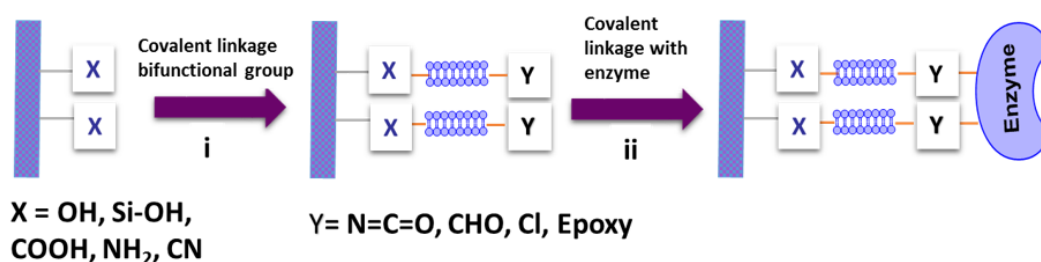


Figure 1.16. General representation of covalent linkage of an enzyme to a functionalised support

A schematic diagram for support modification and enzyme immobilisation is depicted in Figure 1.16. Highly active enzyme constructs on fibre/fabric were examined for bioreactor and biosensor applications. The functionalisation of supports and immobilisation study has been divided into several sections: The first section describes surface modification of fibre based supports (e.g. cotton, nylon, polyacrylonitrile (PAN), polyvinyl alcohol (PVA), glass fibre and glass fabric). A bifunctional spacer was appended to the support to facilitate the covalent linkage to ADH (i.e. *via* Y in Figure 1.16). The second section covers the covalent immobilisation of the enzyme to a range of supports.

1.9 Summary

The above written introduction chapter serves to review the field of enzyme immobilisation on solid supports and discussed various supports used in past literature. Gaps and opportunity section introduces the topic of this research thesis, the immobilisation and characterisation of ADH on chemically modified fibrous supports. Further immobilised enzyme constructs characterisation for stability under varying pH, temperature, time conditions, and ability to recycling experiments is useful for industrial application. There are main factors to be considered in the development of immobilised biocatalysts, such as the method of immobilisation and selection of the support matrix. To achieve high enzyme load and ultimately a high relative activity can be obtained with fibre and fabric support materials. Fibre and fabric support with control porosity can be used to avoid clogging of the reactor which ultimately resolves the back pressure issue in most flow reactor systems. There are several choices available for fibre based supports. Fibrous supports such as cellulose fibre (-OH), glass fibre (-Si-OH), polyvinyl alcohol (-OH), and polyacrylonitrile (-CN) possess functionalities which can be used for immobilisation after surface modification or spacer inclusion. In Chapter 2, cotton fabric, nylon fabric and polyacrylonitrile fibre explored as carrier supports for ADH immobilisation. Chapter 3 describes the surface functionalisation of polyvinyl alcohol (PVA) fibre and knitted fabric supports. In Chapter 4, surface modification of woven and non-woven glass fabric studied with various silane reagents. Finally, Chapter 5 describes future work for this project.

1.10 References

1. C. Spahn and S. D. Minter, *Recent Patents on Engineering*, 2008, **2**, 195-200.
2. S. Datta, L. R. Christena and Y. R. S. Rajaram, *Biotech*, 2013, **3**, 1-9.
3. N. R. Mohamad, N. H. C. Marzuki, N. A. Buang, F. Huyop and R. A. Wahab, *Biotechnology & Biotechnological Equipment*, 2015, **29**, 205-220.
4. K. Faber and M. C. R. Franssen, *Trends in Biotechnology*, 1993, **11**, 461-470.
5. S. Sanchez and A. L. Demain, *Organic Process Research & Development*, 2011, **15**, 224-230.
6. K. M. Koeller and C.H. Wong, *Nature*, 2001, **409**, 232-240.
7. H. E. Schoemaker, D. Mink and M. G. Wubbolts, *Science*, 2003, **299**, 1694-1697.
8. K. R. Jegannathan and P. H. Nielsen, *Journal of Cleaner Production*, 2013, **42**, 228-240.
9. C. Wandrey, A. Liese and D. Kihumbu, *Organic Process Research & Development*, 2000, **4**, 286-290.
10. E. B. Pereira, G. M. Zanin and H. F. Castro, *Brazilian Journal of Chemical Engineering*, 2003, **20**, 343-355.
11. T. E. Creighton, *The Journal of Physical Chemistry*, 1985, **89**, 2452-2459.
12. <https://www.freedoniagroup.com/industry-study/world-enzymes-2824.htm>, accessed on 1, Aug 2017
13. P. Tufvesson, W. Fu, J. S. Jensen and J. M. Woodley, *Food and Bioproducts Processing*, **88**, 3-11.
14. www.marketsandmarkets.com/PressReleases/industrial-enzymes.asp, accessed on 1, Aug 2017
15. B. Krajewska, *Acta Biotechnologica*, 1991, **11**, 269-277.
16. K. Hernandez and R. Fernandez-Lafuente, *Enzyme and Microbial Technology*, 2011, **48**, 107-122.
17. J. M. Guisan, J.M., Penzol, G., Armisen, P., Bastida, A., Blanco, R.M., FernándezLafuente, R. and Garcia-Junceda, E. (1997). Immobilization of enzymes acting on macromolecular substrates. In: Bickerstaff, G.F. (Ed.) Immobilization of enzymes and cells. Humana Press, Totowa, **21**, pp.261-275.
18. R. A. Sheldon and S. van Pelt, *Chemical Society Reviews*, 2013, **42**, 6223-6235.
19. R. DiCosimo, J. McAuliffe, A. J. Poulouse and G. Bohlmann, *Chemical Society Reviews*, 2013, **42**, 6437-6474.
20. C. Mateo, J. M. Palomo, G. Fernandez-Lorente, J. M. Guisan and R. Fernandez-Lafuente, *Enzyme and Microbial Technology*, 2007, **40**, 1451-1463.
21. M. Chiriac, I. Lupan, N. Bucurenci, O. Popescu and N. Palibroda, *Journal of Labelled Compounds and Radiopharmaceuticals*, 2008, **51**, 171-174.
22. A. M. A. Alzohairy, *Research Journal of Biological Sciences*, 2010, **5**, 565-575.

23. E. Katchalskikatzir, *Trends in Biotechnology*, 1993, **11**, 471-478.
24. L. W. Powell, *Biotechnology and Genetic Engineering Reviews*, 1984, **2**, 409-438.
25. S. Ravikumar, S. Shyamala, P. Muthuraman and K. Srikumar, *Preparative Biochemistry and Biotechnology*, 2011, **41**, 122-137.
26. Y. R. Zheng, *Acrylamide microbial production by nitrile hydratase*, in *Encyclopedia of Industrial Biotechnology*, 2010, **vol. 1**, 25–36.
27. J. Chen, R.C.Zheng, Y.G. Zheng and Y.C. Shen, in *Biotechnology in China I: From Bioreaction to Bioseparation and Bioremediation*, eds. J.J. Zhong, F.W. Bai and W. Zhang, Springer Berlin Heidelberg, Berlin, Heidelberg, 2009, DOI: 10.1007/10-2008-25, pp. 33-77.
28. H. C. Holm and D. Cowan, *European Journal of Lipid Science and Technology*, 2008, **110**, 679-691.
29. S.T. Yang and J. A. Bednarcik, in *Applied Biocatalysis in Specialty Chemicals and Pharmaceuticals*, American Chemical Society, 2001, vol. 776, ch. 9, pp. 131-154.
30. A. R. Park and D.-K. Oh, *Applied Microbiology and Biotechnology*, 2010, **85**, 1279-1286.
31. A. K. Chandel, L. V. Rao, M. L. Narasu and O. V. Singh, *Enzyme and Microbial Technology*, 2008, **42**, 199-207.
32. R. C. Giordano, M. P. A. Ribeiro and R. L. C. Giordano, *Biotechnology Advances*, 2006, **24**, 27-41.
33. R. C. Rodrigues and R. Fernandez-Lafuente, *Journal of Molecular Catalysis B: Enzymatic*, 2010, **64**, 1-22.
34. F. Hasan, A. A. Shah and A. Hameed, *Enzyme and Microbial Technology*, 2006, **39**, 235-251.
35. I. Chibata, T. Tosa and T. Sato, *Applied Microbiology*, 1974, **27**, 878-885.
36. M. C. Fusee, W. E. Swann and G. J. Calton, *Applied and Environmental Microbiology*, 1981, **42**, 672-676.
37. K. M. N. Ryuichi, *Annals of the New York Academy of Sciences*, 1990, **613**, 652-655.
38. J. M. K. G. G Guibault, *Protein Immobilization. Fundamentals and applications*, 1991, 209–262
39. A. M. Azevedo, D. M. F. Prazeres, J. M. S. Cabral and L. P. Fonseca, *Biosensors and Bioelectronics*, 2005, **21**, 235-247.
40. I. Chibata, T. Tosa and T. Sato, *Journal of Molecular Catalysis*, 1986, **37**, 1-24.
41. E. Katchalski-Katzir, *Trends in Biotechnology*, 1993, **11**, 471-478.
42. P. S. J. Cheetham, *Trends in Biotechnology*, 1993, **11**, 478-488.
43. W. Hampel, *Acta Biotechnologica*, 1997, **17**, 159-160.
44. R. A. Sheldon, *Advanced Synthesis & Catalysis*, 2007, **349**, 1289-1307.
45. L. Cao, *Carrier-bound immobilized enzymes: Principles, Application and Design*, 2006.

46. C. Garcia-Galan, A. Berenguer-Murcia, R. Fernandez-Lafuente and R. C. Rodrigues, *Advanced Synthesis & Catalysis*, 2011, **353**, 2885-2904.
47. O. Barbosa, R. Torres, C. Ortiz, A. Berenguer-Murcia, R. C. Rodrigues and R. Fernandez-Lafuente, *Biomacromolecules*, 2013, **14**, 2433-2462.
48. F. Secundo, *Chemical Society Reviews*, 2013, **42**, 6250-6261.
49. B. Brena, P. Gonzalez-Pombo and F. Batista-Viera, in *Immobilization of Enzymes and Cells: Third Edition*, ed. J. M. Guisan, Humana Press, Totowa, NJ, 2013, DOI: 10.1007/978-1-62703-550-7, 2, pp. 15-31.
50. K. R. Jegannathan, S. Abang, D. Poncelet, E. S. Chan and P. Ravindra, *Critical Reviews in Biotechnology*, 2008, **28**, 253-264.
51. B. M. Brena and F. Batista-Viera, in *Immobilization of Enzymes and Cells*, ed. J. M. Guisan, Humana Press, Totowa, NJ, 2006, DOI: 10.1007/978-1-59745-053-9_2, pp. 15-30.
52. L. Huang and Z.-M. Cheng, *Chemical Engineering Journal*, 2008, **144**, 103-109.
53. L. Chronopoulou, G. Kamel, C. Sparago, F. Bordi, S. Lupi, M. Diociaiuti and C. Palocci, *Soft Matter*, 2011, **7**, 2653-2662.
54. Pryakhin AN, Chukhrai ES, Poltorak OM. *Glucose 6- Phosphate Dehydrogenase Immobilized by Adsorption on Silica gel solid supports*. Vest Moskov Univ Ser 2 Khim.1977, **18** (1), 125 A.
55. D. Norouzian, *Iranian Journal of Biotechnology*, 2003, **1**, 197-206.
56. Q. Shen, R. Yang, X. Hua, F. Ye, W. Zhang and W. Zhao, *Process Biochemistry*, 2011, **46**, 1565-1571.
57. N. R. Mohamad, N. H. C. Marzuki, N. A. Buang, F. Huyop and R. A. Wahab, *Biotechnology, Biotechnological Equipment*, 2015, **29**, 205-220.
58. B. Singh, *Journal of Molecular Catalysis B*, 2009, **74**, 101-105.
59. L. B. Wingard, E. Katchalski-Katzir and L. Goldstein, *Immobilized Enzyme Principles: Applied Biochemistry and Bioengineering*, Elsevier, 2014.
60. S. Cantone, V. Ferrario, L. Corici, C. Ebert, D. Fattor, P. Spizzo and L. Gardossi, *Chemical Society Reviews*, 2013, **42**, 6262-6276.
61. S. K. Narwal, N. K. Saun and R. Gupta, *Journal of Oleo Science*, 2014, **63**, 599-605.
62. G. Sanjay and S. Sugunan, *Journal of Porous Materials*, 2008, **15**, 359-367.
63. W. Wang, W. Zhou, J. Li, D. Hao, Z. Su and G. Ma, *Bioprocess and Biosystems Engineering*, 2015, **38**, 2107-2115.
64. B. Krajewska, *Enzyme and Microbial Technology*, 2004, **35**, 126-139.
65. J. M. Bolivar, L. Wilson, S. A. Ferrarotti, J. M. Guisan, R. Fernandez-Lafuente and C. Mateo, *Journal of Biotechnology*, 2006, **125**, 85-94.
66. C. Mateo, J. M. Palomo, M. Fuentes, L. Betancor, V. Grazu, F. Lopez-Gallego, B. C. C. Pessela, A. Hidalgo, G. Fernandez-Lorente, R. Fernandez-Lafuente and J. M. Guisan, *Enzyme and Microbial Technology*, 2006, **39**, 274-280.

67. J. Kennedy, B. Kalogerakis and J. Cabral, *Enzyme and Microbial Technology*, 1984, **6**, 127-131.
68. J. C. S. d. Santos, O. Barbosa, C. Ortiz, A. Berenguer. Murcia, R. C. Rodrigues and R. Fernandez-Lafuente, *ChemCatChem*, 2015, **7**, 2413-2432.
69. I. Migneault, C. Dartiguenave, M. J. Bertrand and K. C. Waldron, *Biotechniques*, 2004, **37**, 790-802.
70. J. W. Payne, *Biochemical Journal*, 1973, **135**, 867-873.
71. P. Zucca and E. Sanjust, *Molecules*, 2014, **19**, 14139.
72. S. Martinez Cuesta, Syed A. Rahman, N. Furnham and Janet M. Thornton, *Biophysical Journal*, 2015, **109**, 1082-1086.
73. B. Petschacher, N. Staunig, M. Muller, M. Schürmann, D. Mink, S. De Wildeman, K. Gruber and A. Glieder, *Computational and Structural Biotechnology Journal*, 2014, **9**, e201402005.
74. T. Matsuda, R. Yamanaka and K. Nakamura, *Tetrahedron-Asymmetry*, 2009, **20**, 513-557.
75. J. C. Moore, D. J. Pollard, B. Kosjek and P. N. Devine, *Accounts of Chemical Research*, 2007, **40**, 1412-1419.
76. S. M. A. De Wildeman, T. Sonke, H. E. Schoemaker and O. May, *Accounts of Chemical Research*, 2007, **40**, 1260-1266.
77. Y. Huang, N. Liu, X. R. Wu and Y. J. Chen, *Current Organic Chemistry*, 2010, **14**, 1447-1460.
78. M. Breuer, K. Ditrich, T. Habicher, B. Hauer, M. Kessler, R. Sturmer and T. Zelinski, *Angewandte Chemie-International Edition*, 2004, **43**, 788-824.
79. R. d. S. Pereira, *Critical Reviews in Biotechnology*, 1998, **18**, 25-64.
80. O. De Smidt, J. C. Du Preez and J. Albertyn, *FEMS Yeast Research*, 2008, **8**, 967-978.
81. O. P. Ward, *Canadian Journal of Botany*, 1995, **73**, 1043-1048.
82. A. Berenguer-Murcia and R. Fernandez Lafuente, *Current Organic Chemistry*, 2010, **14**, 1000-1021.
83. R. D. Pereira, *Critical Reviews in Biotechnology*, 1998, **18**, 25-83.
84. S. Soni, J. D. Desai and S. Devi, *Journal of Applied Polymer Science*, 2001, **82**, 1299-1305.
85. M.-H. Liao and D.-H. Chen, *Biotechnology Letters*, 2001, **23**, 1723-1727.
86. C. S. Yu and B. Li, *Polymer Composites*, 2008, **29**, 998-1005.
87. G. Y. Li, Z. D. Zhou, Y. J. Li, K. L. Huang and M. Zhong, *Journal of Magnetism and Magnetic Materials*, 2010, **322**, 3862-3868.
88. U. T. Bhalerao, L. Dasaradhi, C. Muralikrishna and N. W. Fadnavis, *Tetrahedron Letters*, 1993, **34**, 2359-2360.
89. P. Nikolova and O. P. Ward, *Biotechnology Techniques*, 1993, **7**, 897-902.
90. P. Nikolova and O. P. Ward, *Journal of Industrial Microbiology*, 1994, **13**, 172-176.
91. J. M. Bolivar, J. Rocha-Martin, C. Mateo and J. M. Guisan, *Process Biochemistry*, 2012, **47**, 679-686.

92. M. F. Alam, A. A. Laskar, M. Zubair, U. Baig and H. Younus, *Journal of Molecular Catalysis B-Enzymatic*, 2015, **119**, 78-84.
93. X. K. Song, H. Wu, J. F. Shi, X. L. Wang, W. Y. Zhang, Q. H. Ai and Z. Y. Jiang, *Journal of Molecular Catalysis B-Enzymatic*, 2014, **100**, 49-58.
94. C. W. Bradshaw, W. Hummel and C. H. Wong, *The Journal of Organic Chemistry*, 1992, **57**, 1532-1536.
95. G. R. Mark, S. P. S., K. Pascale and C. D. S., *Biotechnology and Bioengineering*, 1991, **37**, 303-308.
96. M. Hiroyuki, H. Kazuya, S. Aki, T. Yuki, K. Akihiko, U. Mitsuyoshi, O. Hiroshi, T. Taro and A. Masayuki, *Yeast*, 2014, **31**, 67-76.
97. A. Trivedi, M. Heinemann, A. C. Spiess, T. Dausmann and J. Büchs, *Journal of Bioscience and Bioengineering*, 2005, **99**, 340-347.
98. A. Samphao, K. Kunpatee, S. Prayoonpokarach, J. Wittayakun, L. Svorc, D. M. Stankovic, K. Zagar, M. Ceh and K. Kalcher, *Electroanalysis*, 2015, **27**, 2829-2837.
99. F. Hildebrand and S. Lutz, *Tetrahedron-Asymmetry*, 2006, **17**, 3219-3225.
100. L. L. Liu, J. G. Yu and X. Q. Chen, *Journal of Nanoscience and Nanotechnology*, 2015, **15**, 1213-1220.
101. Q. Zhao, Y. Hou, G. H. Gong, M. A. Yu, L. Jiang and F. Liao, *Applied Biochemistry and Biotechnology*, 2010, **160**, 2287-2299.
102. Y. Yang, R. Chen and H. M. Zhou, *Biochemistry and Molecular Biology International*, 1998, **45**, 475-487.
103. V. Leskovac, S. Trivic and D. Pericin, *FEMS Yeast Research*, 2002, **2**, 481-494.
104. S. B. Raj, S. Ramaswamy and B. V. Plapp, *Biochemistry*, 2014, **53**, 5791-5803.
105. J. Rocha-Martin, D. Vega, J. M. Bolivar, C. A. Godoy, A. Hidalgo, J. Berenguer, J. M. Guisan and F. Lopez-Gallego, *Bmc Biotechnology*, 2011, **11**.
106. A. Radoi and D. Compagnone, *Bioelectrochemistry (Amsterdam, Netherlands)*, 2009, **76**, 126-134.
107. T. E. Creighton, N. J. Darby and J. Kemmink, *The Federation of American Societies For Experimental Biology*, 1996, **10**, 110-118.
108. L. Cao, *Carrier-bound Immobilized Enzymes: Principles, Applications and Design*, Wiley-VCH Verlag GmbH & Co, KGaA, 2005. DOI: 10.1002/3527607668, pp. 1-55
109. J. Zdarta, A. S. Meyer, T. Jesionowski and M. Pinelo, *Catalysts*, 2018, **8**.
110. T. Jesionowski, *Colloids and Surfaces A: Physicochemical and Engineering Aspects*, 2001, **190**, 153-165.
111. T. Jesionowski and A. Krysztalkiewicz, *Colloids and Surfaces A: Physicochemical and Engineering Aspects*, 2002, **207**, 49-58.

112. J. Zdarta, M. Wysokowski, M. Norman, A. Kołodziejczak-Radzimska, D. Moszynski, H. Maciejewski, H. Ehrlich and T. Jesionowski, *International Journal of Molecular Sciences*, 2016, **17**, 1581.
113. D. Valles, S. Furtado, C. Villadoniga and A. M. B. Cantera, *Process Biochemistry*, 2011, **46**, 592-598.
114. R. Reshmi, G. Sanjay and S. Sugunan, *Catalysis Communications*, 2007, **8**, 393-399.
115. S. Salman, S. Soundararajan, G. Safina, I. Satoh and B. Danielsson, *Talanta*, 2008, **77**, 490-493.
116. R. Chrisnasari, Z. G. Wuisan, A. Budhyantoro and R. K. Widi, 2015, 2015, **15**, 7.
117. F. B. O. Daoud, S. Kaddour and T. Sadoun, *Colloids and Surfaces B: Biointerfaces*, 2010, **75**, 93-99.
118. S. Dutta, A. Bhattacharyya, P. De, P. Ray and S. Basu, *Journal of Hazardous Materials*, 2009, **172**, 888-896.
119. A. S. Rani, M. L. M. Das and S. Satyanarayana, *Journal of Molecular Catalysis B: Enzymatic*, 2000, **10**, 471-476.
120. X. Bai, H. Gu, W. Chen, H. Shi, B. Yang, X. Huang and Q. Zhang, *Applied Biochemistry and Biotechnology*, 2014, **173**, 1097-1107.
121. V. Jari, R. Marjaana and P. Sabine, *Packaging Technology and Science*, 2005, **18**, 243-251.
122. H. J. Kim, S. Park, S. H. Kim, J. H. Kim, H. Yu, H. J. Kim, Y. H. Yang, E. Kan, Y. H. Kim and S. H. Lee, *Journal of Molecular Catalysis B: Enzymatic*, 2015, **122**, 170-178.
123. S. S. Betigeri and S. H. Neau, *Biomaterials*, 2002, **23**, 3627-3636.
124. O. J. Prakash, N. , *World Applied I. Science. J*, 2011, **12**, 572-577.
125. V. Singh, P. Srivastava, A. Singh, D. Singh and T. Malviya, *Polymer Reviews*, 2016, **56**, 113-136.
126. A. G. Grigoros, *Biochemical Engineering Journal*, 2017, **117**, 1-20.
127. C. G. C. M. Netto, H. E. Toma and L. H. Andrade, *Journal of Molecular Catalysis B: Enzymatic*, 2013, **85-86**, 71-92.
128. K. H. Lee, B. Lee, S.-J. Hwang, J.U. Lee, H. Cheong, O.S. Kwon, K. Shin and N. H. Hur, *Carbon*, 2014, **69**, 327-335.
129. J. Anu Bhushani and C. Anandharamkrishnan, *Trends in Food Science & Technology*, 2014, **38**, 21-33.
130. T. Mayer-Gall, J.W. Lee, K. Opwis, B. List and J. S. Gutmann, *ChemCatChem*, 2016, **8**, 1428-1436.
131. D. Brady and J. Jordaan, *Biotechnology Letters*, 2009, **31**, 1639.
132. O. Koniev and A. Wagner, *Chemical Society Reviews*, 2015, **44**, 5495-5551.
133. B. Brena, P. Gonzalez-Pombo and F. Batista-Viera, in *Immobilization of Enzymes and Cells*, ed. J. M. Guisan, Humana Press, 2013, vol. 1051, ch. 2, pp. 15-31.

134. F. H. Isgrove, R. J. H. Williams, G. W. Niven and A. T. Andrews, *Enzyme and Microbial Technology*, 2001, **28**, 225-232.
135. A. Todrick and E. Walker, *Biochemical Journal*, 1937, **31**, 297-298.
136. G. P. Smith, *Bioconjugate Chemistry*, 2006, **17**, 501-506.
137. C. L. Swaim, J. B. Smith and D. L. Smith, *Journal of the American Society for Mass Spectrometry*, 2004, **15**, 736-749.
138. S. Kalkhof and A. Sinz, *Analytical and Bioanalytical Chemistry*, 2008, **392**, 305-312.
139. D. Gilis, N. J. Cerf and M. Rooman, *Genome Biology*, 2001, **49**, 1- 49.
140. K. Gevaert, P. V. Damme, L. Martens and J. Vandekerckhove, *Analytical Biochemistry*, 2005, **345**, 18-29.
141. M. Fodje and S. Al Karadaghi, *Protein engineering*, 2002, **15**, 353-358.
142. C. L. Borders, J. A. Broadwater, P. A. Bekeny, J. E. Salmon, A. S. Lee, A. M. Eldridge and V. B. Pett, *Protein Science : A Publication of the Protein Society*, 1994, **3**, 541-548.
143. L. Shimoni and J. P. Glusker, *Protein Science : A Publication of the Protein Society*, 1995, **4**, 65-74.
144. J. R. L. Walker, *Biochemical Education*, 1992, **20**, 42-43.
145. F. Lopez-Gallego, G. Fernandez-Lorente, J. Rocha-Martin, J. M. Bolivar, C. Mateo and J. M. Guisan, in *Immobilization of Enzymes and Cells, 3rd Edition*, ed. J. M. Guisan, 2013, vol. 1051, pp. 59-71.
146. J. M. Bolivar, F. Lopez-Gallego, C. Godoy, D. S. Rodrigues, R. C. Rodrigues, P. Batalla, J. Rocha-Martin, C. Mateo, R. L. C. Giordano and J. M. Guisan, *Enzyme and Microbial Technology*, 2009, **45**, 477-483.
147. C. Mateo, O. Abian, M. B. Ernedo, E. Cuenca, M. Fuentes, G. Fernandez-Lorente, J. M. Palomo, V. Grazu, B. C. C. Pessela, C. Giacomini, G. Irazoqui, A. Villarino, K. Ovsejevi, F. Batista-Viera, R. Fernandez-Lafuente and J. M. Guisan, *Enzyme and Microbial Technology*, 2005, **37**, 456-462.
148. M. Fernandez, M. Sanroman, D. Moldes, *Biotechnology Advance*, 2013, **31**, 1808-1825.
149. P. Dayaram and D. Dasgupta, *Journal of Environmental Biology*, 2008, **29**, 831-836.
150. A. S. Rathore, H. Agarwal, A. K. Sharma, M. Pathak and S. Muthukumar, *Preparative Biochemistry and Biotechnology*, 2015, **45**, 836-849.
151. J. Cao, G. Xu, P. Y. Li, M. L. Tao and W. Q. Zhang, *Acs Sustainable Chemistry & Engineering*, 2017, **5**, 3438-3447.
152. N. T. S. Phan, D. H. Brown and P. Styring, *Green Chemistry*, 2004, **6**, 526-532.
153. M. Cerreti, K. Markosova, M. Esti, M. Rosenberg and M. Rebros, *International Journal of Food Science and Technology*, 2017, **52**, 531-539.
154. M. Rebros, M. Rosenberg, Z. Mlichova and E. Krisofikova, *Food Chemistry*, 2007, **102**, 784-787.

155. T. Debeche, C. Marmet, L. Kiwi-Minsker, A. Renken and M. A. Juillerat, *Enzyme and Microbial Technology*, 2005, **36**, 911-916.
156. K. Kiehl, T. Straube, K. Opwis and J. S. Gutmann, *Engineering in Life Sciences*, 2015, **15**, 622-626.
157. X. D. Feng, D. A. Patterson, M. Balaban and E. A. C. Emanuelsson, *Colloids and Surfaces B-Biointerfaces*, 2013, **102**, 526-533.
158. D. F. P. Warp Knitting Technology, Harlequin Press, 1952.
159. S. J. Kadolph and A. Langford, *Textiles*, Pearson Prentice Hall Upper Saddle River, 2007.
160. C. Reichman and A. National Knitted Outerwear, *Principles of knitting outerwear fabrics and garments: a manual on basic stitch formations and machine types*, National Knitted Outerwear Association, New York, 1963.
161. B. V. Sankar and R. V. Marrey, *Composites Science and Technology*, 1997, **57**, 703-713.
162. D. F. Paling, *Warp knitting technology*, Harlequin Press, Manchester, 1952.
163. E. J. W. Barber, *Prehistoric textiles: the development of cloth in the Neolithic and Bronze Ages with special reference to the Aegean*, Princeton University Press, 1991.
164. P. S.I., D. M.A. and Z. Y., *Journal of Food Science*, 2004, **69**, M215-M221.
165. S. A. Mohamed, A. S. Aly, T. M. Mohamed and H. A. Salah, *Applied Biochemistry and Biotechnology*, 2008, **144**, 169-179.
166. K. Opwis, D. Knittel and E. Schollmeyer, *Analytical and Bioanalytical Chemistry*, 2004, **380**, 937-941.
167. Q. Wang, C. X. Li, X. Fan, P. Wang and L. Cui, *Biocatalysis and Biotransformation*, 2008, **26**, 437-443.
168. E. Wehrschutz-Sigl, A. Hasmann and G. M. Guebitz, in *Advances in Textile Biotechnology*, Woodhead Publishing, 2010, DOI: <https://doi.org/10.1533/9780857090232.1.56>, pp. 56-74.
169. A. Chitragada, K. Veerendra, S. Ramkrishna and K. S. C., *Biotechnology Journal*, 2008, **3**, 226-233.
170. P. Pialis and B. A. Saville, *Enzyme and Microbial Technology*, 1998, **22**, 261-268.
171. P. Peter, J. H. M. C. and S. B. A., *Biotechnology and Bioengineering*, 1996, **51**, 141-147.
172. N. Munjal and S. K. Sawhney, *Enzyme and Microbial Technology*, 2002, **30**, 613-619.
173. E. Abadulla, T. Tzanov, S. Costa, K. H. Robra, A. Cavaco-Paulo and G. M. Guebitz, *Applied and Environmental Microbiology*, 2000, **66**, 3357-3362.
174. T. Tzanov, M. Calafell, G. M. Guebitz and A. Cavaco-Paulo, *Enzyme and Microbial Technology*, 2001, **29**, 357-362.
175. A. Tetsuo, K. Motohiro, D. Makoto, S. Harutoshi and K. Keiichi, *Journal of Applied Polymer Science*, 1992, **46**, 49-53.
176. E. Magnan, I. Catarino, D. Paolucci Jeanjean, L. Preziosi-Belloy and M. P. Belleville, *Journal of Membrane Science*, 2004, **241**, 161-166.

Chapter 2

Surface modification of fibrous supports and ADH immobilisation

This chapter presents i) surface modification of fibrous supports to facilitate immobilisation of the ADH enzyme, and ii) structural modification of the ADH enzyme to facilitate the same goal.

2.1 Introduction

In this chapter, the focus is centred on the surface modification of cotton and two synthetic polymer fibres, nylon and polyacrylonitrile (PAN), to facilitate immobilisation of the ADH enzyme. The chemistry used for the surface modification of these polymers was adapted from solution chemistry and solid liquid chemistry. Although each of these supports have been used to immobilise enzymes, to our knowledge they have not been used to immobilise the ADH enzyme.

Two different approaches to achieve ADH immobilisation were investigated:

- 1) Surface modification of the cotton, nylon and PAN fabric fibrous supports (fibre and/or fabric) followed by immobilisation of ADH *via* covalent ligation. The functionalisation of the fibrous supports was assessed by infrared spectroscopy.
- 2) ADH was modified using bifunctional reagents, e.g. nylon 3-maleimidopropionic acid, NHS ester (BMPS) and allyl glycidyl ether (AGE). The fibrous supports were then reacted with the modified enzyme.

After ADH immobilisation onto the modified surfaces, the activity of the enzyme was measured. Fibre and fabric supports without any surface modification were also exposed to ADH under similar conditions and used as controls. The fibre and fabric ADH constructs with the highest activity were then assessed for stability under varying temperature, pH, and storage time parameters.

2.2 Soluble ADH concentration and stability study

ADH concentration and pH stability studies were performed prior to the ADH immobilisation reactions to determine optimal concentration and ADH stability across a wide pH range. The ADH concentration study was performed using 0.1 mg/mL to 1.0 mg/mL ADH in 0.05 M PBS and coupled with an activity assay using NAD^+ and ethanol in tris buffer (Chapter 1, Figure 1.11). The detailed experimental and activity data for this study is described in Section 2.6.7 and the results are reported as an average of triplicate runs in Figure 2.1. The rate of an enzyme-catalysed reaction depends on the enzyme and substrate concentration.¹ As the concentration of either is increased the rate of reaction increases and eventually plateaus with no further increase in concentration. A calibration curve was performed to determine the maximum usable concentration for conversion of NAD^+ to NADH. An ADH concentration above 0.5 mg/mL did not provide an increase in enzyme activity. Hence, further studies were performed using ADH at a concentration of 0.5 mg/mL.

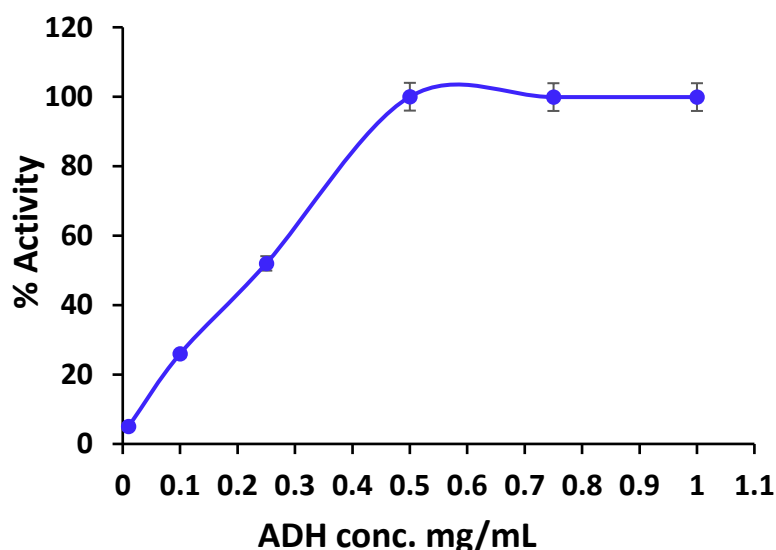


Figure 2.1. ADH concentration study 0.1 to 1.0 mg/mL in PBS buffer (pH 7.5) at RT. The ADH assay was performed on triplicate samples for each conc. and error bars represent standard deviations. To display the data, the highest activity was taken as 100% and subsequent activities were normalised accordingly

Enzyme structure can be affected by changes in pH and hence result in changes in activity. The optimal pH is the most favourable pH value where the enzyme possesses high activity. Change in pH such as very high or low pH values can result in complete loss of activity for most enzymes.² The effect of pH on ADH activity is shown in Figure 2.2. The ADH enzyme was incubated across a pH range, pH 6.5 to 10.55, at 40 °C in buffered solutions. The pH ranges and buffer solutions used were: pH 6.5 to 8.0 used Na₂HPO₄/NaH₂PO₄ PBS (0.05 M) and pH 8.5-10.55 used Na₂CO₃/NaHCO₃ (0.1 M). All solutions were made according to standard protocol and the final pH was adjusted as required.³ The ADH assay conditions were analogous to those described in Chapter 1 (Section 1.6).

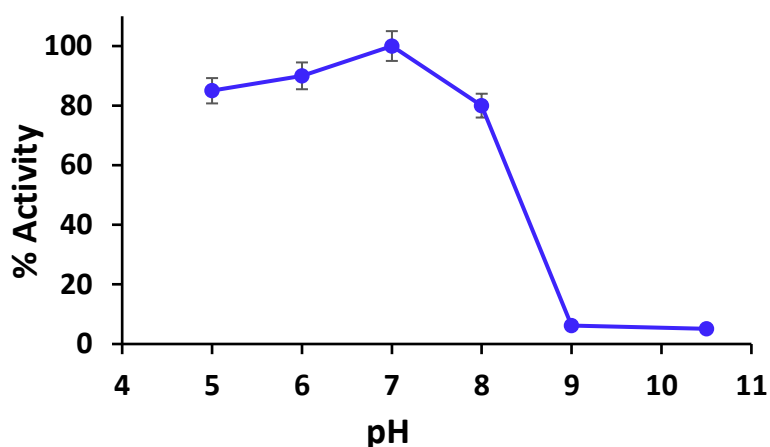


Figure 2.2. ADH activity at different pHs. The ADH assay was performed on triplicate samples for each pH value and error bars represent standard deviations. To display the data, the highest activity was taken as 100% and subsequent activities were normalised accordingly

At pH 5 and 6, the activity of ADH was > 80% however, optimal pH activity was observed at pH 7.0. At values above pH 9, ADH activity was negligible. ADH is a multimeric structured enzyme which under strongly acidic conditions dissociates into its subunits, while under alkaline conditions the gross tertiary structure distorts resulting in loss of activity.⁴ Analogous behaviour was reported by Goto and Fink who investigated the effect of ADH salt-induced inactivation in acidic and alkaline media.^{5, 12}

2.3 Surface modification and immobilisation

2.3.1 Cotton

Cotton is an abundant natural and biodegradable polymer. It is composed of cellulose consisting of glucose units linked together *via* glycoside linkages between the C-1 of one pyranose ring and the C-4 of the next ring.⁶ The reactivity of the hydroxyl groups at positions 2, 3 and 6 of the glucosyl units offers a variety of possibilities for making useful derivatives (Figure 2.3).^{7, 8}

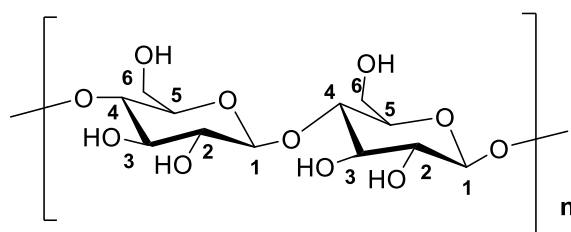


Figure 2.3. Cellulose chain showing the glucose units and the position of the hydroxyl groups

Below table (Table 2.1) summarised methods used for immobilizing enzymes onto cellulose matrixes/supports.

Table 2.1 Cellulose supports for enzyme immobilisation

Support	Enzyme	Method	Application	Ref.
Cellulose microfiber	Laccase, urease	Adsorption	Biocatalyst	9
Tissue	Lipase	Covalent binding	Biocatalyst	10
Cellulose membrane	Glucose oxidase	Entrapment	Biosensor	11
Electrospun cellulose nanofiber membrane	<i>C. rugose</i> lipase	Covalent binding	Biocatalyst	12
Cellulose hydrogel	Peroxidase	Covalent binding	Biocatalyst	13
Cellulose macro porous beads	Galactose oxidase	Covalent binding	Biocatalyst	14

Table 2.1 Continued...				
Support	Enzyme	Method	Application	Ref.
Cotton yarn	Trypsin	Covalent binding	Biomedicine	15
Non-woven cotton fabric	Lysozyme	Covalent binding	Biomedicine	15
Cotton gauze bandage	Trypsin	Covalent binding	Biomedicine	16
Make-up remover pads	<i>C. rugose</i> lipase	Covalent binding	Biocatalyst	15
Cotton nanocrystal	Lysozyme	Covalent binding	Biomedicine	17
Nano fibrillated cellulose	Alkaline	Covalent binding	Biocatalyst	18
Cellulose acetate beads	Catalase	Covalent binding	Biosensor	19
Cellulose acetate films	Lipase	Adsorption	Biocatalyst	20
Carboxy methyl cellulose beads	Polyphenol oxidase	Covalent binding	-	21
Carboxy methyl cellulose film	Carboxy methyl cellulose film Avidin	Adsorption	-	22
Cellulose–chitosan beads	Penicillin G, acylase	Covalent binding	Biocatalyst	23
Carboxy methyl cellulose silver nanoparticles–silica hybrid	Amylase	Adsorption	Biocatalyst	24
Cellulose acetate–TiO ₂ gel	Glucose oxidase	Entrapment	–	25
Cellulose acetate–TiO ₂ gel fiber	Urease, lipase	Entrapment	Biocatalyst	26
Cellulose acetate–ZrO gel	β -Galactosidase	Entrapment	Biocatalyst	27
Cellulose-coated magnetite nanoparticles	α -Amylase	Covalent binding	Biocatalyst	27
Cellulose	Urease	Entrapment	Biomedicine	28

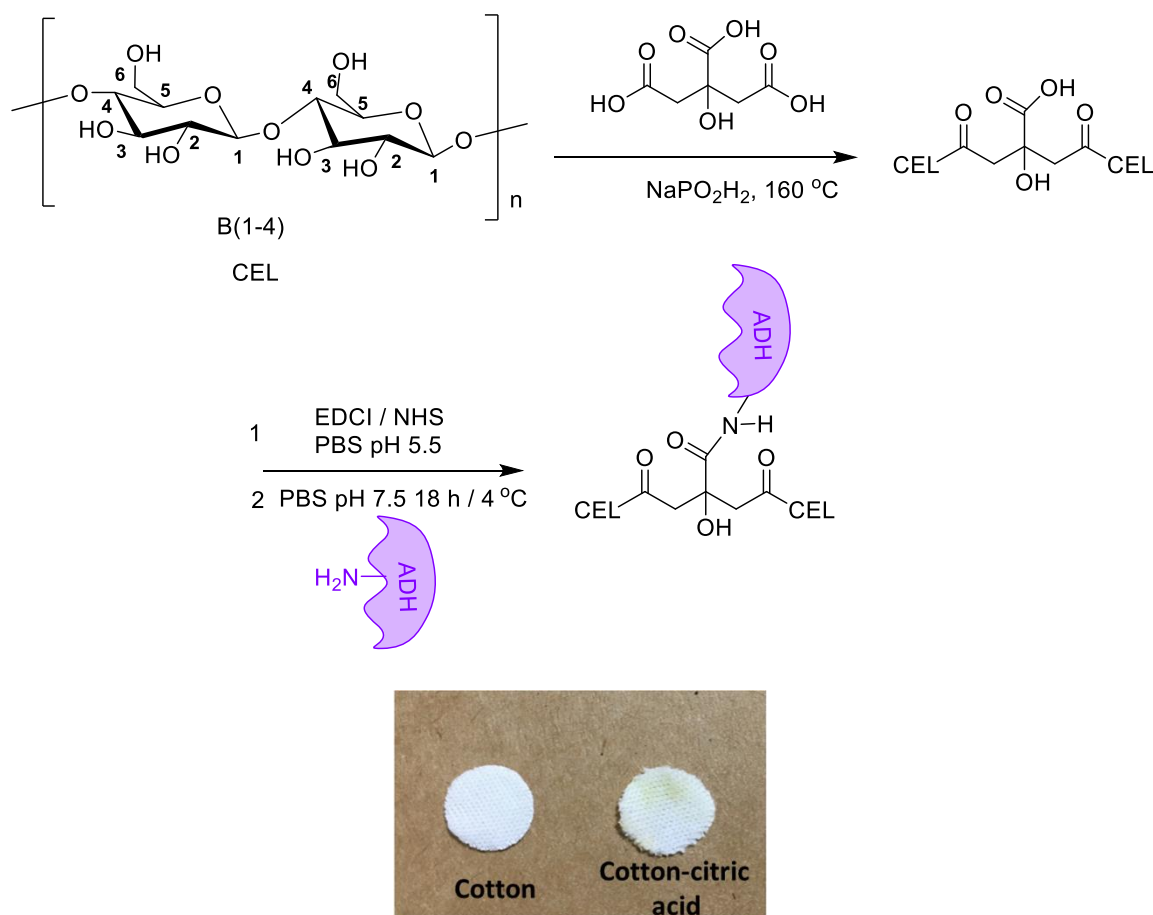
Functionalisation of cotton proceeds mainly through esterification and etherification reactions involving the primary hydroxyl groups and then can be used for covalent attachment of an enzyme.²⁹ The covalent attachment involves binding the enzyme amino acid residues ($-\text{NH}_2$, $-\text{COOH}$, $-\text{SH}$) to the support matrices. The cotton/cellulosic fabric support use in

covalent immobilisation is of interest in general, however it is the loss of enzyme activity over time that needs to be decreased.^{7, 30}

Herein cotton fabric was used in knitted form (knitting was done on yarn (15 tex) with a 30 inch diameter 22 gauge Bentley 9RJ/36 double jersey knitting machine) and cut into discs (13 mm disc) (13 mm disc) prior to the modification. The cotton fabric discs were modified with citric acid and (3-aminopropyl)triethoxysilane amino propyl silane using a modified procedure described by Edward *et al.*³¹ and reacted with ADH. Immobilisation of ADH *via* dopamine pre-treatment of the support was also investigated.

2.3.1.1 Citric acid (CA) modification

Citric acid is a tricarboxylic acid which can be used to esterify cotton (cellulose, CEL). Sodium hypophosphite (NaPO_2H_2) is used as a catalyst for this process. Teramoto *et al.* report that the reaction of cellulose with citric acid is very pH-dependant (optimal pH 2) with curing temperatures between 120-160 °C.³² After surface modification with CA, the cotton fabric turned yellow.³³ This colour was postulated to arise from the formation of α,β -unsaturated carboxylic acid moieties.³²



Scheme 2.1. Citric acid pre-treatment of cotton followed by ADH immobilisation

A comparison of IR spectra for untreated cotton and citric acid modified cotton are shown in Figure 2.4. The appearance of a new absorbance peak at 1721 cm^{-1} is consistent with ester formation.³¹ This stretching frequency peak was accompanied by a broad absorption at $3330\text{--}3332\text{ cm}^{-1}$ arising from the hydroxyl groups of the cellulose and linker structure.

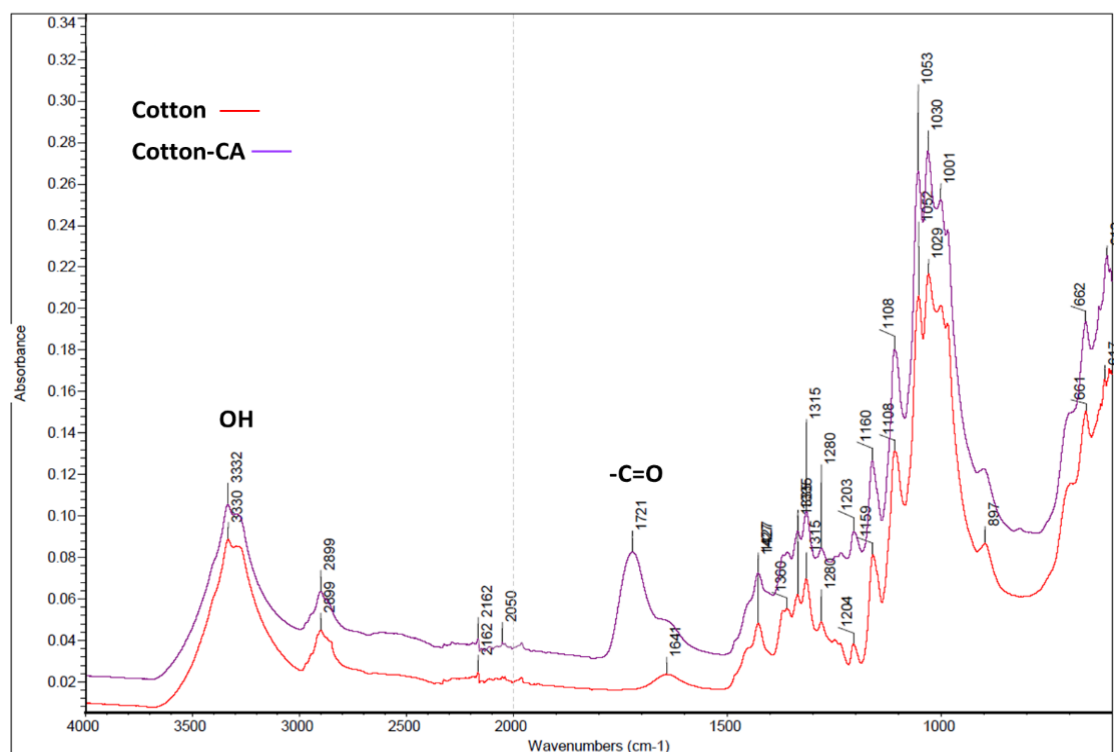
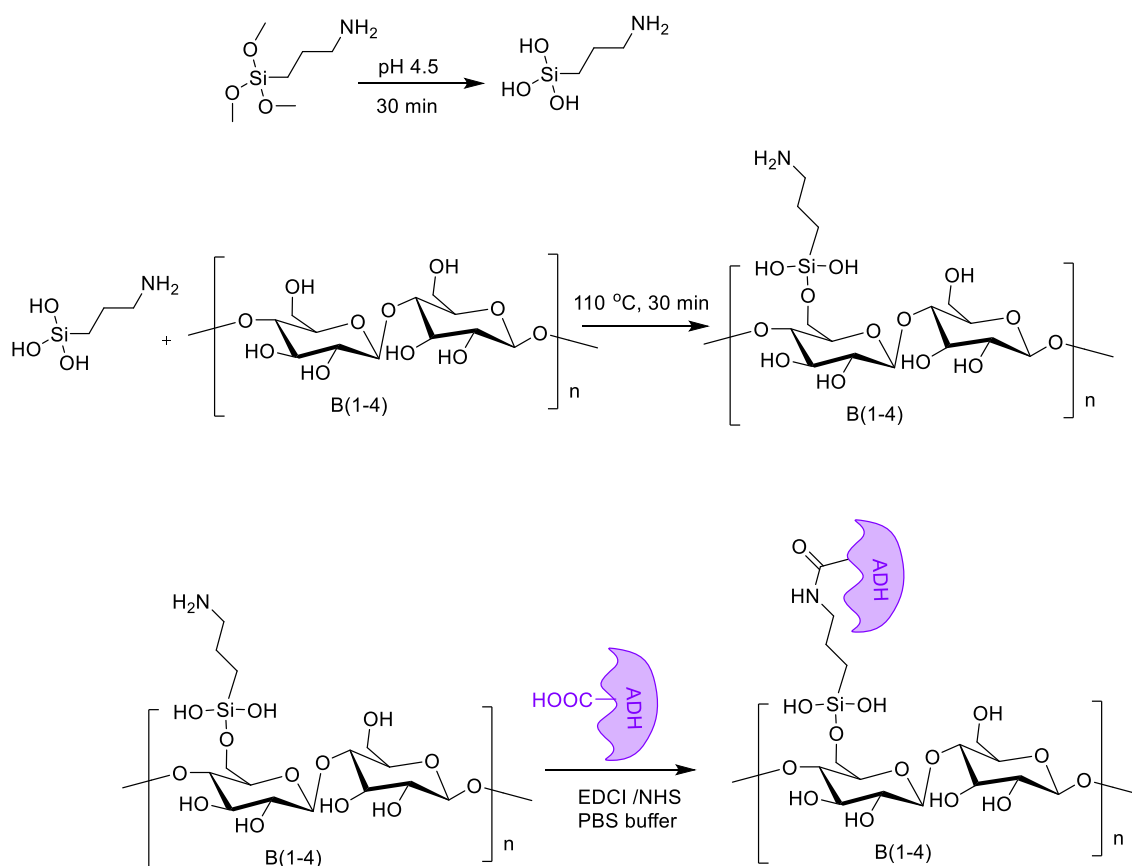


Figure 2.4. FTIR spectra of cotton and cotton-citric fabric

The pendant carboxylic acid groups of the citric acid treated cotton were activated *in situ* with EDC/NHS in PBS and the resultant activated ester was then exposed to ADH to form the immobilised ADH-cotton complex. The ADH activity recorded for the control fabric discs (i.e. cotton discs exposed to ADH without citric acid modification) was 0.521 ± 0.010 mmol/min/g fabric. The activity recorded for ADH immobilised on the citric acid-cotton was 0.881 ± 0.08 mmol/min/g fabric. Since there was only a 1.6 fold increase in activity compared to the control cotton fabric the observed activity is largely due to nonspecific binding *via* physical adsorption (i.e. electrostatic/hydrogen bonding) between the charged enzyme and unmodified cotton surface.³⁴

2.3.1.2 Silane modification

A silane derivative, (3-aminopropyl)trimethoxysilane (APTMS), was also used to modify the cotton fabric. This approach used mild reaction conditions and offered a facile way to introduce an aminosilane functionality onto the cotton fabric surface. The methoxyl groups on APTMS are easily hydrolyzed to form silanol which can readily react with the cellulose hydroxyl groups.³⁵



Scheme 2.2. Cotton activation with APTMS reaction to form ADH-cotton constructs

IR analysis of cotton fabric and cotton silane amine fabric is shown in Figure 2.5. The spectrum of the silyl amine-modified cotton fabric showed a peak at 1559 cm^{-1} which corresponds to N-H bending ($1640\text{--}1560\text{ cm}^{-1}$) consistent with a primary amine functionality. The N-H and O-H stretching bands are overlapped and observed at $3500\text{--}3300\text{ cm}^{-1}$.

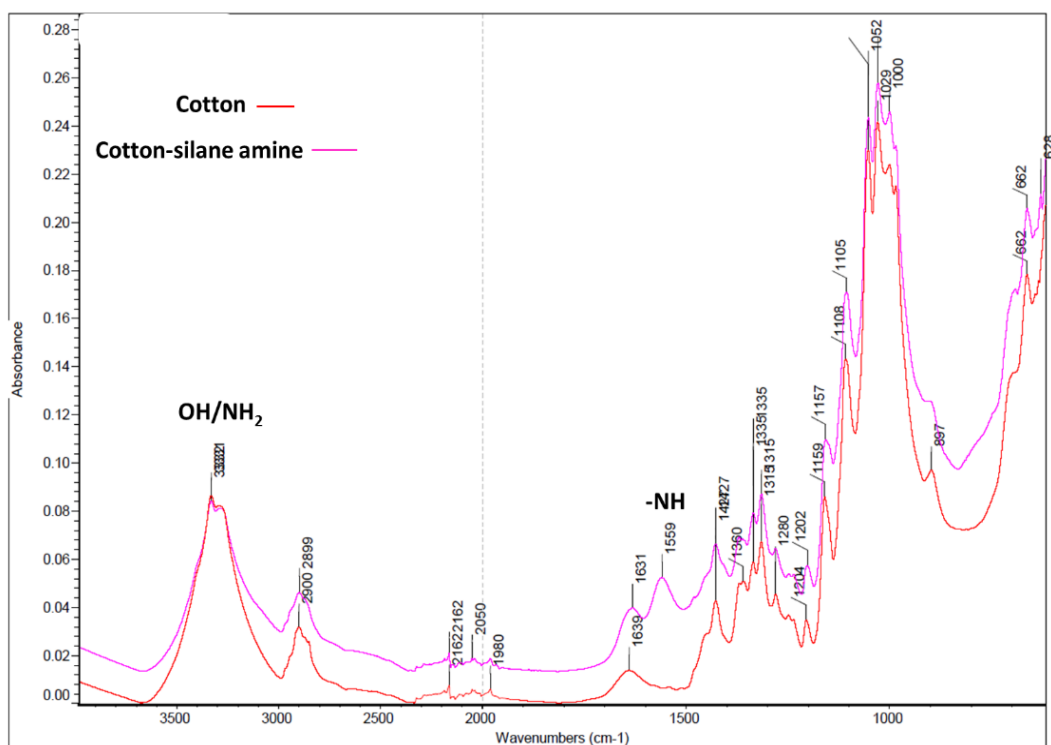


Figure 2.5. FTIR spectra of cotton fabric and cotton-silane amine fabric

Following cotton functionalisation, the ADH enzyme can be activated with EDC/NHS to form an activated ester and subsequently reacted with aminosilane functionalised cotton fabric (Scheme 2.2). The activity of the ADH immobilised on the control cotton fabric was measured to be 0.737 ± 0.018 mmol/min/g fabric while the activity on the silane amine modified cotton fabric was measured at 1.985 ± 0.0210 mmol/min/g fabric, an approximate three fold increase in activity compared to the control. ADH immobilised on silane amine cotton support was studied for pH stability across a pH range of 5 to 10.5 and residual activity was measured (Figure 2.6).

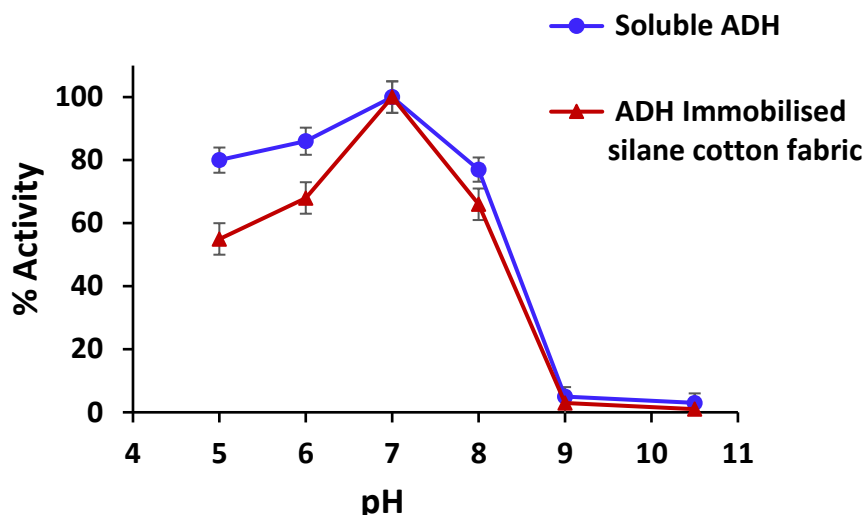
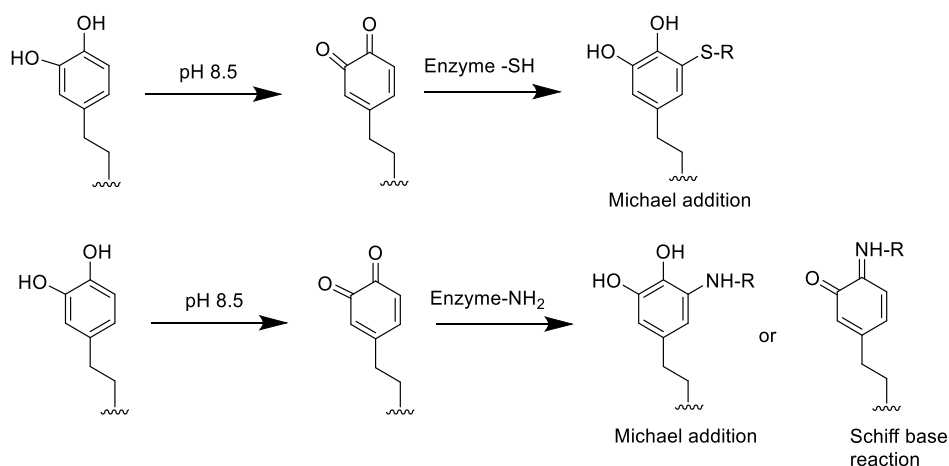


Figure 2.6. Effect of pH on the activity of free and immobilised ADH. The reactions for each pH measurement were performed in triplicate and error bars represent standard deviations. The highest activity was taken as 100% and subsequent % activity was normalised against this value

Figure 2.6 shows the effect of pH on the activities of soluble ADH and immobilised ADH on silane cotton support; the detailed experimental procedure and activity data are described in the Experimental Section 2.6.3.1.2 (Table 2.6). The optimal pH for both the soluble and the immobilised ADH was 7.0. In this case, the optimal pH and activity profile across the pH range did not significantly change after immobilisation. However, the immobilised ADH enzyme showed decreased activity in the pH range 5 to 6 (55% and 66% respectively) compared to soluble ADH at the same pH (77% and 86%). No shift of the enzymatic optimum pH value was observed which suggests that the microenvironment of the support did not change and an improved method for enzyme immobilisation was required. While this was encouraging we hoped to see high activity over a broader pH ranges. Hence further different modification and ADH immobilisation studies were continued.

2.3.1.3 Polydopamine modification

Polydopamine (PDA) is a biocompatible component of melanin (eumelanin). Under weak alkaline conditions (approximately pH 8-8.5), the catechol functional groups present on dopamine are oxidized to quinone, which can then react with other catechols and/or quinones to form polymerized dopamine (PDA).³⁶ The most widely investigated reactions involving PDA involve cross-linking with amine and/or thiol containing enzyme or ligands *via* Michael addition and/or Schiff base reactions (Scheme 2.3).^{37, 38} Due to the simplicity and versatility of the method, this approach has been widely exploited for substrate functionalisation since its discovery in 2007.³⁷ For example, trypsin has been immobilised on cellulose paper,³⁸ bivalirudin peptide on stainless steel,³⁹ and polylysine on neuronal interface materials (e.g. gold, glass, platinum, indium tin oxide and liquid crystal polymer).⁴⁰ While dopamine polymerised fibrous surfaces have not been used for ADH immobilisation, it was hypothesized that cotton-PDA fibrous supports could be used to form stable ADH enzyme constructs.



Scheme 2.3. Pathway for the reaction of dopamine with thiol and amine containing nucleophiles³⁶

The fabrication process of PDA-coated cellulose fabric is schematically illustrated in Figure 2.7. The cotton fabric discs were immersed in an aqueous solution of dopamine. After 24 h, the aqueous solution became black-brown, indicative of self-polymerization of dopamine.⁴¹

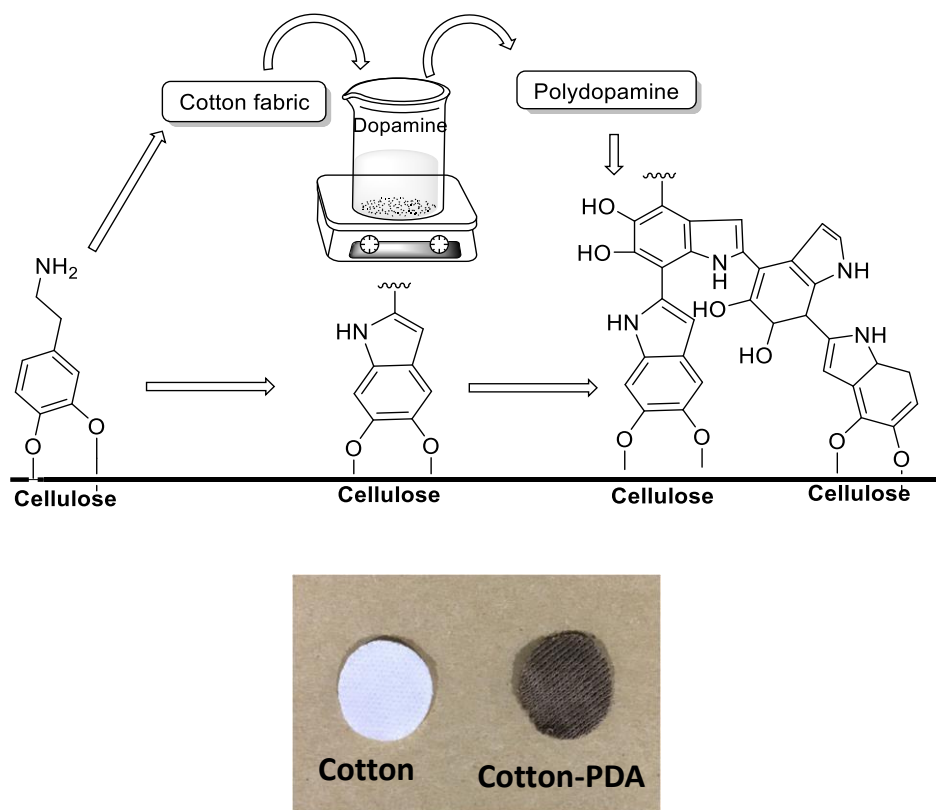


Figure 2.7. Schematic illustration of the PDA-coated cellulose fabric

The cotton-PDA fabric discs were then treated with ADH and the activity was measured. The immobilised ADH showed an activity of 2.271 ± 0.28 mmol/min/g fabric on dopamine modified cotton support where control cotton fabric activity (i.e. non-modified cotton) was 0.871 ± 0.19 mmol/min/g fabric. The observed activity represents only a 2.5 fold increase which again is indicative of a sub-optimal immobilisation process. Additionally, the observed decreased ADH activity could potentially arise from an undesirable reaction of active site amino acid residues (e.g. cysteine and lysine) with dopamine which are involved in the catalysis mechanism.

2.3.2 Nylon

Nylon was one of the first commercialised synthetic fibres.⁴² Nylon possess good chemical resistance, low toxicity and are available in a number of forms such as film and fibre. Several processes have been reported for the functionalisation of nylon surfaces using chemical and physical methods.⁴² In the literature, nylon has been used as a carrier for enzyme immobilisation in various forms such as membranes,⁴³ film⁴⁴ and non-woven fabric.⁴⁵ The existing techniques used for immobilizing enzymes onto nylon matrices are summarised in Table 2.2.

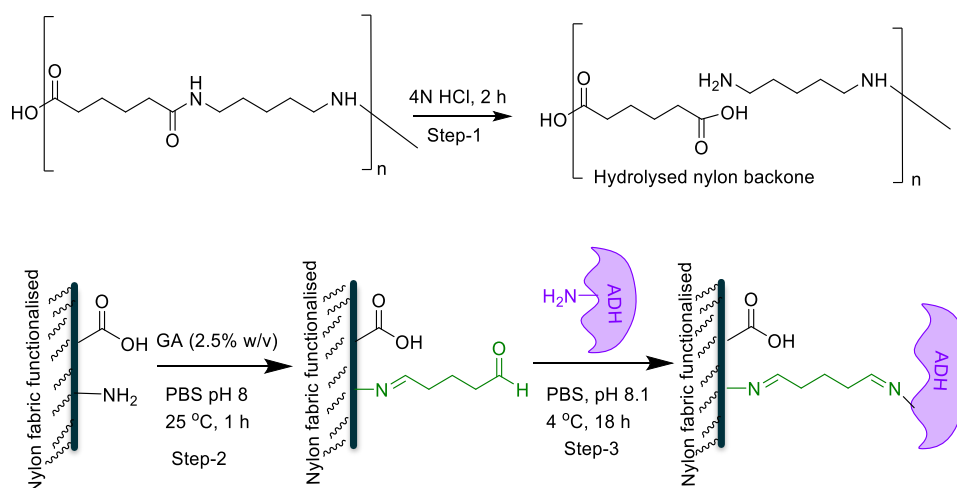
Table 2.2 Nylon supports for enzyme immobilisation

Support	Enzyme	Method of Immobilisation	Application	Ref.
Nylon film	Laccase	Covalent	Biocatalyst	46
Nylon membrane				
Nylon membrane	Invertase	Covalent	Biocatalyst	47
Nylon 6,6 non-woven	Laccase	Covalent	Biocatalyst	48
Nylon-6 microbeads	Invertase	Covalent	Biocatalyst	49
Nylon membrane	Urease	Covalent	Biosensor	50
Nylon powder	Beta-xylosidase	Covalent	Bioreactor	51
Nylon-6	Pectin lyase	Covalent	Bioreactor	52
Nylon mesh	Acetylcholinesterase	Crosslinking	Biosensor	53
Nylon-6 beads	Trypsin	Covalent	Biocatalyst	54
Nylon-6 non-woven	Glucose oxidase	Covalent	Biosensor	55
Nylon-6 non-woven	Thermolysin	Covalent	Biocatalyst	56
Nylon tubes	Invertase	Covalent	Biocatalyst	57

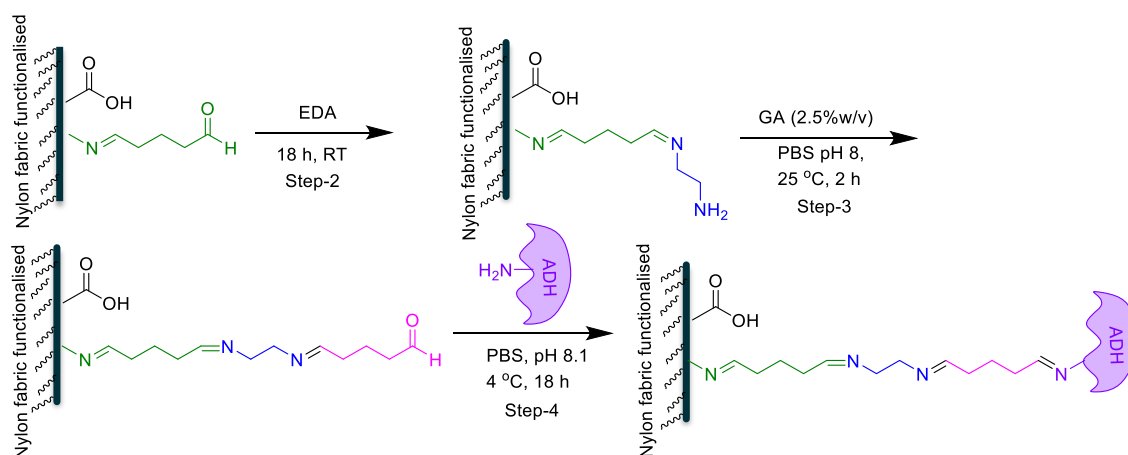
In the subsequent section, nylon 6 fabric in knitted form was used for surface modification. The surface modification involved activation *via* partial acid hydrolysis (using HCl) of the amide bond to liberate reactive amino and carboxyl groups. The amino groups can then be reacted with glutaraldehyde (GA) to immobilise ADH.⁵⁸

Nylon knitted fabric was stamped out in discs (13 mm diameter) and hydrolyzed with HCl. The hydrolysis process was optimized by changing the HCl concentration (2 N to 8 N) and reaction temperature (RT to 70°C). The treated fabric was characterised with infrared spectroscopy. Exposure of the fabric to the high concentration of HCl (e.g. 8 N HCl) resulted in fabric disintegration. Exposure to 4 N HCl, however, provided sufficient hydrolysis without decomposition of the fabric. The hydrolyzed discs were then activated with 2.5% GA (w/w) and i) reacted directly with ADH (Scheme 2.4, Process A), or ii) pre-treated with ethylene diamine to install a linker prior to reaction with ADH (Scheme 2.4, Process B). The modified nylon discs from processes A and B were then assessed in activity assays.

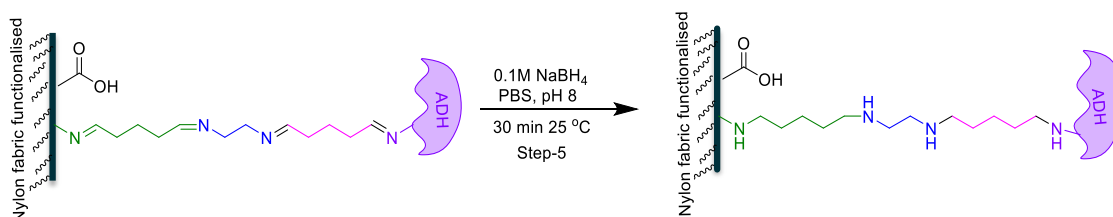
Process A



Process B



Process C



Scheme 2.4. Nylon polymer backbone modification (Processes A and B) and ADH immobilisation. Sodium borohydride reduction of imine (Process C)

The activity observed from direct ADH immobilisation on the GA functionalised nylon (Process A) was 1.64 ± 0.16 mmol/min/g fabric; Process B, utilising an EDA spacer, gave lower activity, 1.143 ± 0.25 mmol/min/g fabric. ADH immobilised on control nylon fabric showed an activity of 1.037 ± 0.25 mmol/min/g fabric. There was little overall difference in activity recorded between processes A, B and the control fabric which is indicative that considerable activity is arising from the non-covalent attachment of the ADH to the nylon (Scheme 2.4). One of the reasons for the low activity could be due to the hydrolytically unstable imine functional group.

As a result of the low activity difference, an additional approach was investigated involving the reduction of the imine with 0.1 M sodium borohydride (in PBS pH 8.1) as shown in Scheme 2.4 (Process C). Unfortunately, after borohydride reduction a significant loss of activity (0.015 ± 0.05 mmol/min/g fabric) was observed. A possible reason for this could be due to the denaturation of the enzyme from the modification of key amino residues (lysine and arginine) in the ADH enzyme. A similar observation was reported by Macro *et al.* when ADH from horse liver was reduced with borohydride.⁵⁹ The amino acid sequence and tertiary structure of horse liver and yeast ADH are highly similar.^{60, 61} Due to the disappointing activities shown by the nylon-enzyme constructs further exploration with nylon fabric was discontinued.

2.3.3 Polyacrylonitrile (PAN)

Polyacrylonitrile (PAN) has attracted great attention due to its thermal stability, tolerance to most solvents and high strength.⁶² For effective enzyme immobilisation, reactive functional groups have to be introduced into the PAN backbone in order to surmount the chemical inertness and the hydrophobicity of the polyacrylonitrile chain.⁶³ PAN possesses nitrile groups which can be modified to enable enzyme immobilisation by plasma and photo-induced graft copolymerisation,⁶⁴ enzymatic⁶⁵ and chemical modification (Table 2.3).^{66, 67}

Table 2.3 PAN supports for enzyme immobilisation

Support	Enzyme	Method of immobilisation	Application	Ref.
PAN nanofibre	Cellulase	Covalent	Bioreactor	68
Polyacrylonitrile membranes	Acetylcholinesterase	Adsorption	Biocatalyst	69

Table 2.3. Continued...				
Support	Enzyme	Method of immobilisation	Application	Ref.
Polyacrylonitrile nanofibres	Laccase	Covalent	Bioremediation	70
Polyacrylonitrile nanofibres	Glucose oxidase	Covalent	Biocatalyst	71
Polyacrylonitrile nanofibres	Cellulase	Covalent	Biocatalyst	68
Polyacrylonitrile fibres	Penicillin acylase	Covalent	Biocatalyst	72
Polyacrylonitrile nanofibers	Catalases	Covalent	Biocatalyst	73
Polyacrylonitrile powder	Urease	Covalent	Bioreactor	74
Polyacrylonitrile membranes	Amyloglucosidase	Covalent	Biocatalyst	75

In this section, PAN in fibre (yarn) form was surface modified to generate amino functionality to facilitate ADH enzyme immobilisation. A number of different modification reactions were investigated using ethylenediamine, diethylenetriamine and polyamine to generate aminated PAN fibre surfaces prior to ADH immobilisation. Reaction conditions are summarised below in Table 2.4

Table 2.4 Attempted PAN fibre surface modifications

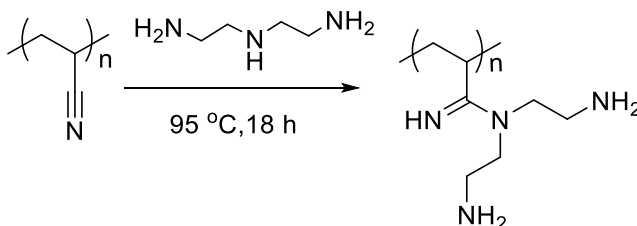
No	Reaction
1	

Table 2.4. Continued...	
No	Reaction
2	
3	
4	
5	

Table 2.4 summarises several unsuccessful attempts to generate aminated PAN fibres. Unfortunately, each attempt was unsuccessful (as revealed by infrared spectroscopy). This may have been due to deleterious inter and intra molecular reactions of the PAN homopolymer.⁴⁹ Further attempts to achieve ADH immobilisation on this fibrous support were not made. The lack of success in achieving stable and high activity fabric-ADH constructs on cotton, nylon and PAN fibrous supports therefore forced us to consider other ways to achieve this end.

2.4 ADH modification

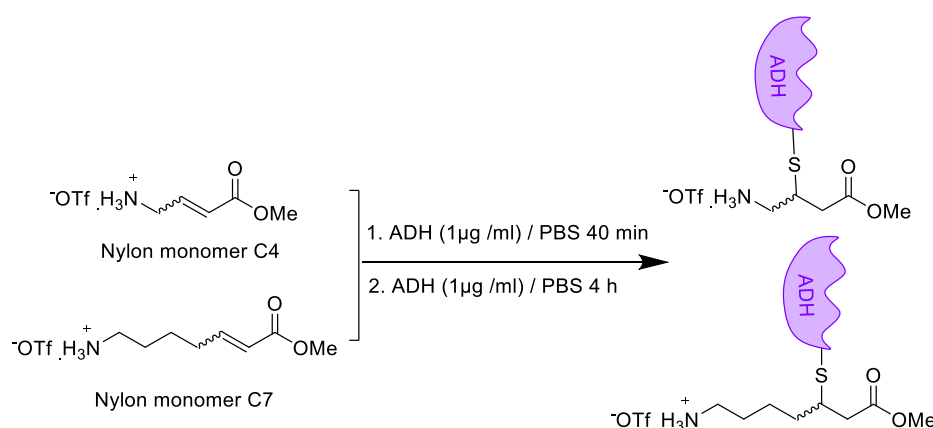
An alternative approach to surface functionalisation of the fibre support is *via* the modification of the enzyme.^{86,76} The chemical modification of an enzyme can be made site-directed by using chemistries directed to specific groups introduced into a protein/enzyme structure (e.g. Diels-Alder cycloaddition).⁷⁷ Chemical activation of an enzyme with glutaraldehyde can be used to achieve immobilisation onto polyethylenimine (PEI) or chitosan support.⁷⁸ The chemical modification of enzyme suffers from distinct drawbacks such as various range of chemical groups can be introduced into the enzyme structure,⁷⁹ does not require detailed enzyme structure knowledge and it is such rapid (contrast with genetic modification) that it can't be controlled.⁷⁹

In this section, ADH enzyme was chemically modified with small bifunctional reagents to achieve stable ADH-fabric/fibre constructs. This was undertaken by either modifying key functional groups or cross-linking the enzyme with bifunctional reagents such as nylon monomers (C3 and C6), allyl glycidyl ether (AGA) and BMPS. The subsequent functionalised ADH could then be immobilised on a suitable modified fibrous support through SH, OH or NH₂ functional groups.

The disadvantage of this approach includes the risk of covalent enzyme aggregation (using bifunctional reagents) and changes in the enzyme surface properties. The length of the cross linking reagent should be shorter or equal to the distance between the reactive groups that are in the enzyme.

2.4.1 Modification with Nylon monomers

α,β -Unsaturated esters are known to undergo rapid addition of alkyl and aryl thiols. Hence a novel approach to ADH immobilisation was explored using unsaturated variants of C4 nylon monomer (methyl 4-ammonium but-2-enoate triflate) and C7 nylon monomers (methyl 6-ammonium hex-2-enoate triflate) (Scheme 2.5). We hypothesised that surface active cysteine residues could be used to achieve covalent ligation of the enzyme to the monomer unit,⁸⁰ and later upon success, translate the chemistry into an unsaturated nylon polymer.



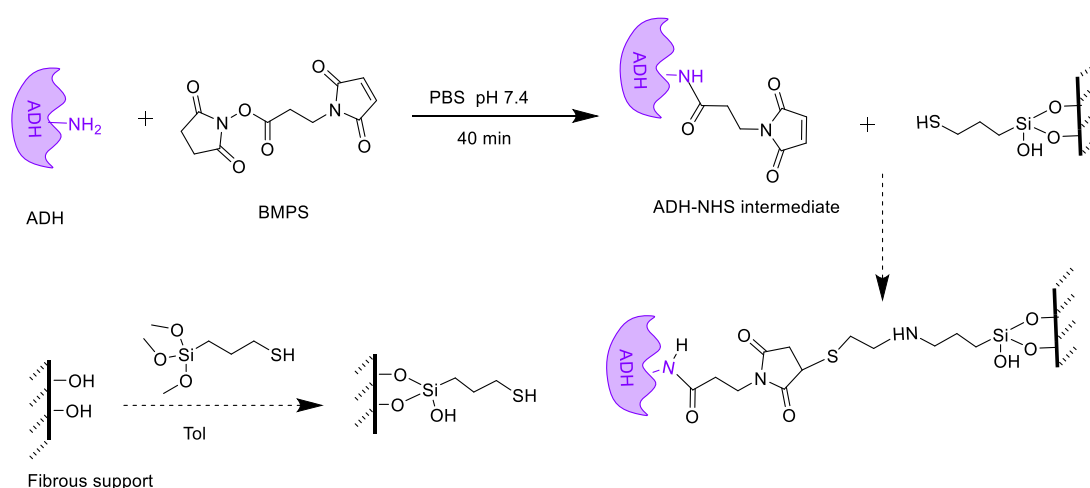
Scheme 2.5. Proposed ADH modification using unsaturated nylon monomers

ADH was reacted with unsaturated nylon monomers and assessed by LCMS and an ADH activity assay. Despite the LCMS showing only the molecular ion of the starting enzyme (m/z 8911.11), the activity of the enzyme was significantly affected. ADH exposed to C4 unsaturated nylon monomer has an activity of 0.921 mmol/min/g activity whereas C7 unsaturated nylon modified ADH showed an activity of 0.972 mmol/min/g activity. Soluble ADH on the other hand, showed a significantly higher activity at 2220.16 mmol/min/g. Apparent ADH inactivation may have resulted from a catalytic thiol being involved in the conjugate addition reaction instead of a surface thiol. The employment of a regioselective

reaction could be employed to avoid destruction of the catalytic domain but this was not investigated in this project.

2.4.2 Modification with BMPS

3-Maleimidopropionic acid *N*-hydroxysuccinimide ester (BMPS) is well known cross-linker which consists of succinimidyl ester (SE) which is an amine-reactive functional group and a sulfhydryl-reactive maleimide group. Primary amines at pH 7 to 9 can react with NHS esters to form stable amide bonds and at pH 6.5 to 7.5 maleimides react with sulfhydryl groups to form stable thioester bonds. Bui and co-workers have employed BMPS to conjugate Clenbuterol, a small molecule, to BSA and Keyhole Limpet Hemocyanin (KLH) proteins and this construct was successfully used to raise antibodies.⁸¹ Hence, BMPS was allowed to react with ADH to form an ADH-NHS intermediate according to the literature procedure. On this basis, it was postulated that the NHS ester of the ADH-NHS intermediate could be utilised to achieve immobilisation on a thio-silane modified fibrous support (Scheme 2.6).



Scheme 2.6. Proposed schematic for ADH immobilisation using BMPS

Upon reaction with BMS, the ADH-NHS intermediate was purified with Sephadex (G-25 desalting column) to remove excess low molecular weight BMS reagent. The activity of the ADH-NHS adduct was measured after column purification and compared with soluble ADH (both at RT and after 40 min of incubation) and the results are represented in Table 2.5.

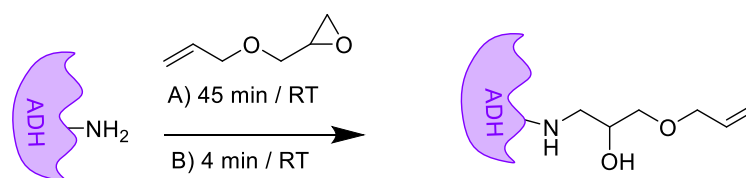
Table 2.5 Activity data measured before and after Sephadex purification

Description	Activity (mmol/min/g)
ADH at RT	2200.01 ± 0.23
ADH 40 min incubation at RT and Sephadex	2100.31 ± 0.07
ADH + BMPS after reaction at RT	8.034 ± 0.06
ADH-NHS intermediate and Sephadex (i.e. ADH + BMPS 40 min incubation)	5.601 ± 0.02

Reacting BMPS with ADH had a detrimental effect on ADH activity, with activity reducing from 2200.01 to 8.034 mmol/min/g. The unexplainable activity loss was recorded upon incubation with BMPS and column purification (5.601 ± 0.25 mmol/min/g). The soluble ADH after incubation and Sephadex purification showed an insignificant loss in activity (2100.312 ± 0.75 mmol/min/g) compared to ADH at RT. The ADH activity data herein described revealed that soluble ADH is stable at RT and exposure to the Sephadex solid phase. This result was disappointing and necessitated the exploration of other immobilisation strategies.

2.4.3 Modification with AGE

Finally a strategy for the immobilisation of ADH enzyme was investigated using bifunctional AGE. The AGE reagent provides a reactive epoxide group which is able to react spontaneously at room temperature with an amino functionality within an enzyme, and the pendant allyl groups can be used to effect photochemical fixation to the fibrous support material (Scheme 2.7). Opwis *et al.* successfully immobilised allyl-derivatised catalase to a fibre support *via* photochemical immobilisation.⁸² Similarly, we proposed that the ADH enzyme could be functionalised with AGE and fixed to a fibrous support *via* photochemical grafting.



Scheme 2.7. Proposed ADH modification with allyl glycidyl ether

AGE modification of ADH was carried out for 45 min (A) and 4 min (B) to observe the effect of reaction time on ADH activity. For both time trials, the ADH concentration (1mg/mL) was kept constant and AGE concentration was varied. Detailed experimental data can be found in Section 2.6.4.3 and Table 2.8. Soluble ADH was treated analogously and subsequently assessed for activity and used as a control for these reactions. Figure 2.8 represents the effect of varying AGE concentration on ADH activity over 45 min.

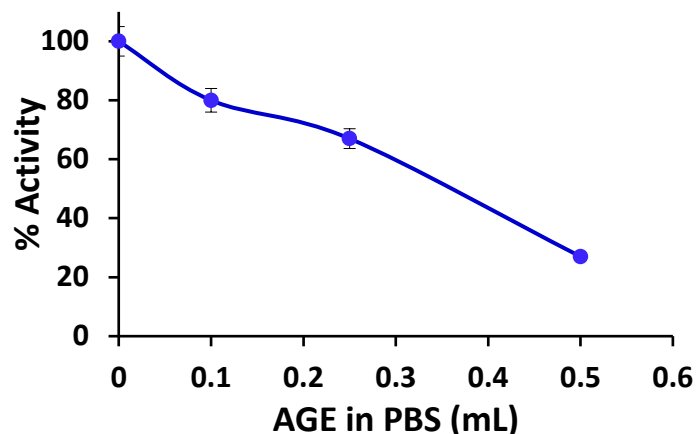


Figure 2.8. Effect of AGE concentration on ADH activity. The ADH assay was performed on triplicate samples for each conc. and error bars represent standard deviations. To display the data, the highest activity was taken as 100% and subsequent activities were normalised accordingly

ADH activity was found to decrease as AGE concentration increased and may arise from non-site specific alkylation at key active site residues (Figure 2.8). Enzyme activity arising from shorter time trails, regardless of AGE concentration, remained high. The details of reaction conditions used and measured activity data are described in Experimental Section 2.6.4.3 (Table 2.8 and Table 2.9). Here we hypothesised that the higher activity may be due to free ADH oxidation at low reaction time and not due to the AGE modified ADH.

2.5 Conclusion

In conclusion, all attempts at ADH modification, with nylon monomer, BMPS and AGE, resulted in the loss of enzyme activity suggesting that site-specific modification of the enzyme is required for a high activity construct.⁸³ Such protein engineering, however, was outside the scope of this project. Effective surface modification of fibrous nylon and PAN was also unsuccessful. Subsequently, in Chapter 3, it was decided to investigate surface modification of polyvinyl alcohol (PVA). The PVA fibres were also knitted into fabric structures and employed in surface modification experiments.

2.6 Experimental Section

2.6.1 Instrumentation

Infrared spectroscopy (IR) was carried out using a Nicolet 6700 ATR-FTIR (Thermo Scientific) in absorbance mode. IR absorptions are reported in wavenumbers (cm^{-1}) with the relative intensities expressed as s (strong), m (medium), w (weak) or prefixed b (broad).

Enzyme assays were carried out using a Cary 300 Bio-UV visible spectrophotometer at 340nm. The textiles or fabrics were knitted either on a circular 3.5 inch FAK fibre analysis knitting machine using a 35 gauge (35 needles per inch) needle bed or flatbed Shima Seiki WG 24 gauge bed machine.

2.6.2 Solvents and reagents

Acetone, hydrochloric acid (concentrated HCl), dichloromethane (DCM), ethanol (EtOH), methanol (MeOH), tetrahydrofuran (THF), triethylamine (TEA), acetic acid (glacial 100%, AR) were purchased from Merck and used without further purification.

3-Aminopropyl trimethoxysilane (APTMS), tris buffer, β -nicotinamide adenine dinucleotide (NAD^+), sodium bicarbonate (NaHCO_3), sodium carbonate (Na_2CO_3), sodium hydroxide (NaOH), citric acid, glutaraldehyde (25% solution in water), 1-Ethyl-3-(3-dimethylaminopropyl)carbodiimide (EDC), 2-(*N*-morpholino)ethane sulfonic acid, ethylenediamine (EDA), 2,2'-diaminodiethylamine, allyl glycidyl ether (AGE), sodium borohydride (NaBH_4), 2-(3,4-dihydroxyphenyl)ethylamine hydrochloride and alcohol dehydrogenase (ADH) from yeast (300 units/mg) was purchased from the Aldrich, Australia. β -Nicotinamide adenine dinucleotide, reduced disodium salt hydrate (NADH) was purchased from Alfa Aesar, Australia.

Methyl 4-ammonium but-2-enoate triflate and Methyl 6-ammonium hex-2-enoate triflate were gifts from Monash University, Australia.

The bleached cotton yarn (15 tex) was purchased from Leading Textiles Pty Ltd, Tullamarine, Australia.

The nylon multifilament (34 filaments) yarn (48 Denier) was a gift from Leading Textiles Pty Ltd., Tullamarine, Australia.

Polyacrylonitrile multifilament (count 2/18K, 64Tex) yarn (Acrilan™) was a gift from Bradmill Pty Ltd., Bendigo, Australia.

ADH Activity

Surface modification reactions were performed on fabric discs in bulk total mass (1-2 g) and enzyme immobilisation activity was measured on a single disc of known mass (8-10 mg) in triplicate according to the procedure described in Experimental Section 2.6.6. The activity was calculated from absorbance (Abs) using the following formula:

$$A = \epsilon \times c \times l,$$

$$c = A / \epsilon \times l$$

where A is the absorbance, ϵ is the extinction coefficient ($6220 \text{ M}^{-1} \text{ cm}^{-1}$), c is the concentration (M) and l is the path length (cm).

$$\text{Conc. mmol} = \text{Conc (mM)} / \text{Assay volume}$$

$$\text{Total activity} = \text{Conc. mmol} / \text{Time (i.e. assay time in min)}$$

$$\text{Activity (Specific activity) of immobilised ADH} = \text{Conc. mmol} / \text{Time (min)} / \text{Weight of fabric disc (g)}$$

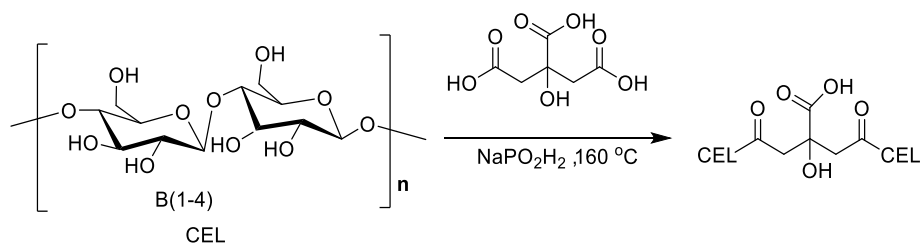
$$\text{Activity (Specific activity) of soluble ADH} = \text{Conc. mmol} / \text{Time (min)} / \text{Weight of ADH (g)}$$

2.6.3 Experimental Procedures

2.6.3.1 Cotton

Cotton fabric was knitted from yarn (15 tex) with a 30 inch diameter 22 gauge Bentley 9RJ/36 double jersey knitting machine set to interlock. The fabric was cut into 13 mm discs and washed with deionised water prior to chemical surface modification

2.6.3.1.1 Citric acid (CA) modification



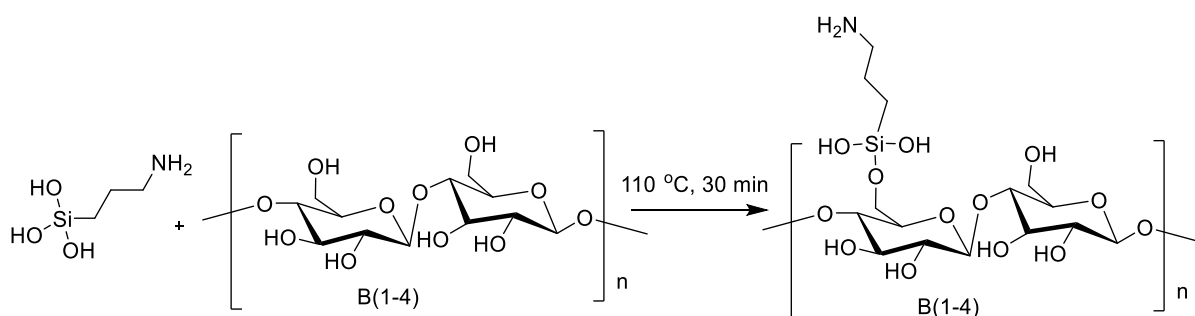
The cotton fabric citric acid modification was performed according to a procedure described by Edwards.³¹ Cotton discs (13 mm diameter, 0.50 g) were immersed in aqueous solution of 7% citric acid and 4.8% sodium hypophosphite monohydrate (10 mL) for 1 h. The cotton discs were dried at 85 °C for 25 min and cured at 160 °C for 10 min, then washed with water (10 ml; 3 x 10 min) and dried at 60 °C for 1 h. IR: 3330-3332bs, 2899bs, 2162w, 1721bs, 1427w, 1315w, 1103m, 1030m, 662m, 612m cm^{-1} .

1) ADH immobilisation

The above citric acid-cotton fabrics were placed in the EDC/NHS mixture (10 mmol/20 mmol, in 0.2 M PBS, pH 5.5). The samples were allowed to shake for 1 h, before being filtered and washed with PBS (0.05 M, pH 7.5). The EDC/NHS activated fabrics were then added to the

ADH solution (5 mL, 0.5 mg/mL) in PBS (0.05 M, pH 7.5) and incubated at 4 to 8 °C for 19 h. The cotton fabric without CA treatment was immobilised with ADH as per the above protocol and used as a control. Both immobilised discs were washed with PBS buffer (0.05 M, pH 7.5) to remove unbound enzyme and individually assayed for activity according to the procedure described under the ADH assay (Section 2.6.6).

2.6.3.1.2 Silane amine modification



Cotton fabric silane amine modification was performed according to a procedure described by Edwards.³¹ A solution of APTES (5%, 8 mL) in ethanol: distilled water (3:1) was prepared and the pH of the solution was adjusted to 4.5 with acetic acid. Cotton fabric discs (0.8 g) were immersed in the above solution and stirred for 1 h at RT. Further silane treated cotton discs were dried and placed in a convection oven at $110\text{ }^\circ\text{C}$ for 1 h to cure. The fabric samples were then rinsed with 60 mL of 3:1 ethanol/ distilled water to remove physio-absorbed silane reagent and dried overnight at RT. IR: 3550-3300bs, 2900bs, 2162w, 1627w, 1559bs, 1427w, 1315w, 1103m, 1030m, 662m, 628m cm^{-1} .

1) ADH immobilisation

ADH immobilisation was performed according to the procedure outlined in Section 2.6.3.1.1 under the following conditions: ADH (2 mL, 0.5 mg/mL), EDC (10 mg, 10 mmol) and NHS (160 mg, 35 mmole) were added to the above ADH solution and the mixture was stirred for 45 min at RT. The silane modified cotton fabrics were placed in the ADH/EDC/NHS solution and incubated at 4 to 8 °C for 19 h. The cotton fabric discs without silane modification were immobilised with ADH in an analogous fashion and were used as controls. The discs were then washed with PBS (0.05 M, pH 7.5, 10 mL; 3 x 5 min) to remove any unbound enzyme and individually assayed as per the procedure described for the ADH assay (Section 2.6.6).

2) Soluble and immobilised ADH pH stability

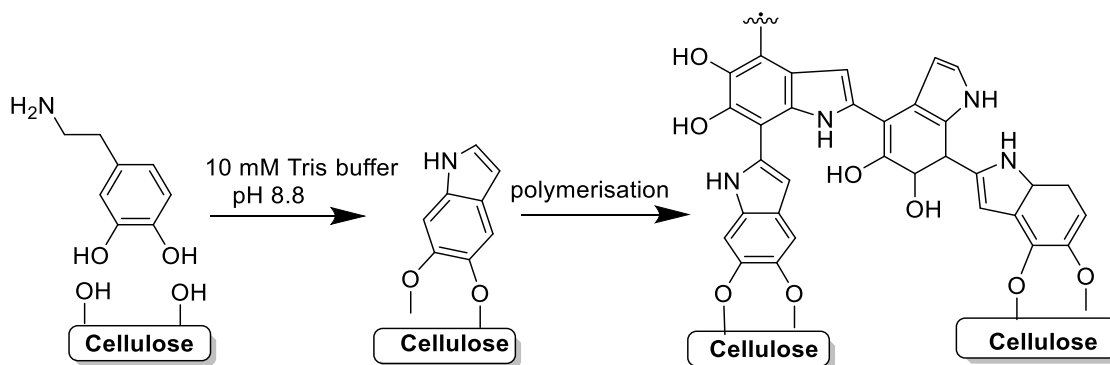
The effect of pH on enzyme stability was measured in different buffer systems incubating the soluble and immobilised ADH at 40 °C for 2 h (Figure 2.6). Sodium phosphate buffer (0.05 M) was used for the pH 6.5 to 8.0 region and sodium carbonate/bicarbonate buffer (0.1 M) was used for the pH 8.5 to 10.5 region. The enzyme was then slowly brought to RT and activity was determined as per the ADH activity assay (Section 2.6.6). Detailed activity data is presented below in Table 2.6.

Table 2.6 Effect of pH on soluble and immobilised ADH (silane cotton support) activity

pH	Abs	NADH coefficient	Conc (mM)	Conc (mmol)	Total activity mmol/min	Activity mmol/min/g	Average activity
Effect of pH on the activity of soluble ADH							
5	1.581	6200	0.255	0.255	0.064	1275.00	1276.667
	1.570	6200	0.253	0.253	0.063	1265.00	
	1.601	6200	0.258	0.258	0.065	1290.00	
6	1.820	6200	0.294	0.294	0.073	1470.00	1465.000
	1.810	6200	0.292	0.292	0.073	1460.00	
	1.818	6200	0.293	0.293	0.073	1465.00	
7	2.096	6200	0.338	0.338	0.085	1690.00	1698.333
	2.120	6200	0.342	0.342	0.085	1710.00	
	2.100	6200	0.339	0.339	0.085	1695.00	
8	1.635	6200	0.264	0.264	0.066	1320.00	1315.000
	1.610	6200	0.260	0.260	0.065	1300.00	
	1.640	6200	0.265	0.265	0.066	1325.00	
9	0.087	6200	0.014	0.014	0.003	70.00	73.830
	0.095	6200	0.015	0.015	0.004	76.00	
	0.090	6200	0.015	0.015	0.004	75.00	
10.5	0.066	6200	0.011	0.011	0.003	55.00	56.670
	0.076	6200	0.012	0.012	0.003	60.00	
	0.068	6200	0.011	0.011	0.003	55.00	

pH	Abs	NADH coefficient	Conc (mM)	Conc (mmol)	Total activity mmol/min	Activity mmol/min/g	Average activity
Effect of pH on activity of immobilised ADH							
5	0.244	6200	0.039	0.039	0.010	0.984	0.997
	0.250	6200	0.04	0.040	0.010	1.008	
	0.248	6200	0.04	0.040	0.010	1.000	
6	0.351	6200	0.057	0.057	0.014	1.415	1.434
	0.356	6200	0.057	0.057	0.014	1.435	
	0.360	6200	0.058	0.058	0.015	1.452	
7	0.436	6200	0.070	0.070	0.018	1.758	1.776
	0.443	6200	0.071	0.071	0.018	1.786	
	0.442	6200	0.071	0.071	0.018	1.782	
8	0.404	6200	0.065	0.065	0.016	1.629	1.641
	0.409	6200	0.066	0.066	0.016	1.649	
	0.408	6200	0.066	0.066	0.016	1.645	
9	0.380	6200	0.061	0.061	0.015	1.532	1.532
	0.380	6200	0.061	0.061	0.015	1.532	
	0.390	6200	0.063	0.063	0.016	1.573	
10.5	0.116	6200	0.019	0.019	0.005	0.468	0.485
	0.122	6200	0.020	0.020	0.005	0.492	
	0.123	6200	0.020	0.020	0.005	0.496	

2.6.3.1.3 Polydopamine modification



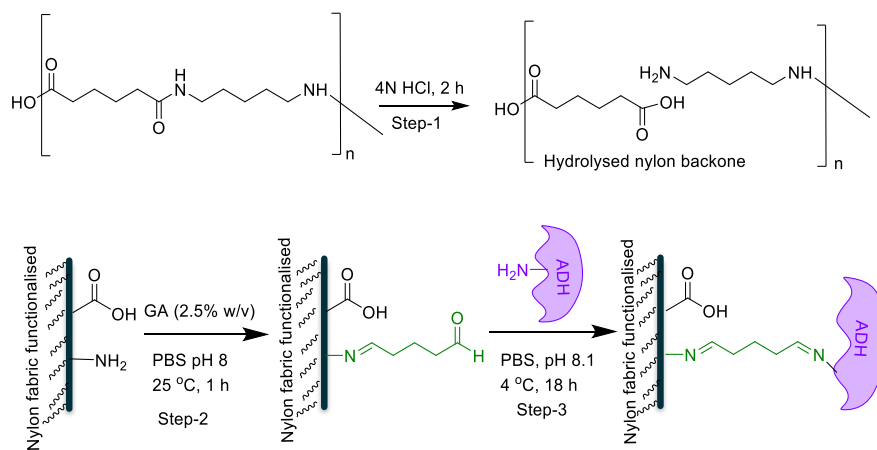
Polydopamine modification on cotton was carried out as per the procedure described by Q. Xu *et al.*⁴¹ Dopamine solution (10 mL, 0.2 mol/L) was prepared by dissolving dopamine in tris buffer (10 mM). The pH of the solution was adjusted to 8.8 by HCl to induce polymerization. The cotton discs (1.01 g) were immersed in the above prepared dopamine solution at RT and stirred for 24 h at 21 °C. The discs were rinsed with distilled water (10 mL; 3 x 5 min) and dried at 55 °C for 18 h.

1) ADH immobilisation

The above PDA modified cotton fabrics discs were placed into the ADH solution (4 mL, 0.5 mg/mL) in PBS (0.05 M, pH 8.1) and incubated at 4 °C to 8 °C for 19 h. ADH immobilised PDA discs were washed with PBS (0.05 M pH 8.1, 10 mL; 3 x 5 min) and individually assayed according to the procedure described under the ADH assay (Section 2.6.6). Cotton fabric discs without dopamine modification were immobilised with ADH in an analogous fashion and used as a control.

2.6.3.2 Nylon

2.6.3.2.1 Glutaraldehyde modification → Process (A)



Step-1 Hydrolysis

Nylon fabric discs (1.5 g) were immersed in aq. 4 N HCl (20 mL) for 2 h at RT, then washed with excess distilled water (50 mL; 10 x 10 min) until the pH of the washing solution reached neutral. The discs were dried at 85 °C for 3 h in an oven prior to IR analysis. IR: 3298bs, 3068bs, 2930bs, 2858bs 1749m, 1632bs, 1531bs 1474m, 1464m, 1370w 1272m, 1197m, 1139s, 934w, 905w cm^{-1} .

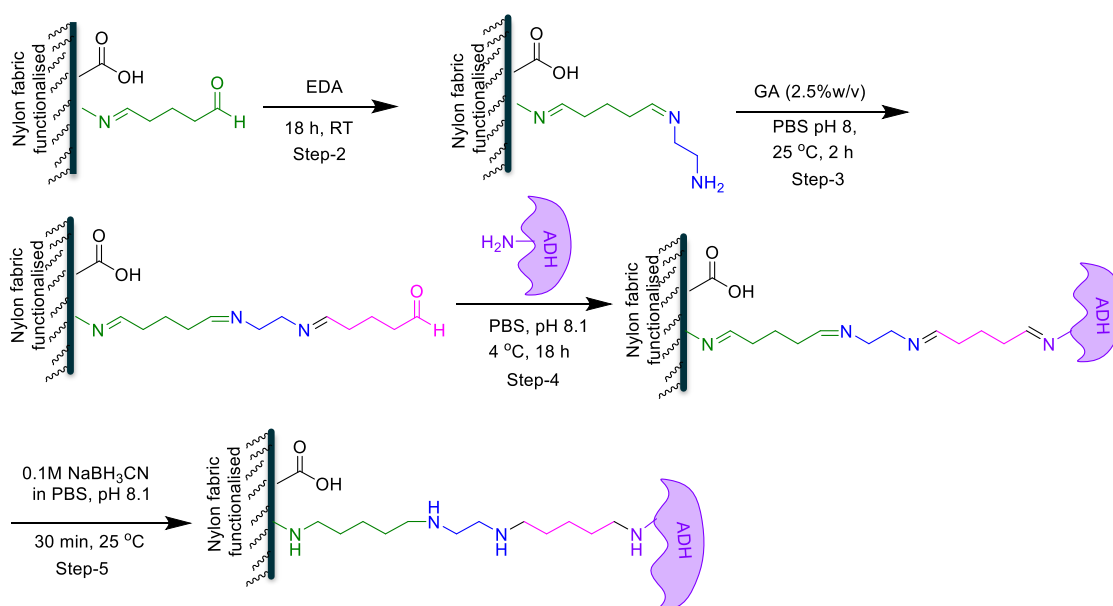
Step-2 GA activation

The GA activation was carried out according to the procedure described by S. Pahujani.⁵⁸ The acid treated nylon fabric discs (0.82 g) from Step-1 were added into 2.5% w/v GA solution (10 mL) in PBS (0.05 M, pH 8) and incubated for 1 h at RT. The GA activated discs were then washed with distilled water (20 mL; 5 x 5 min) and dried at 60 °C for 1 h.

Step-3 ADH immobilisation

The GA activated disc (0.5 g) from Step-2 were added to the ADH solution (5 mL, 0.5 mg/mL) in PBS (0.05 M, pH 8) and allowed to incubate at 4 °C for 18 h. The discs were then washed with excess PBS (0.05M, pH 8.0) and assayed individually to measure activity. Nylon fabric discs (0.05 g) were immobilised with ADH in an analogous fashion to measure activity and used as the control.

2.6.3.2.2 Ethylenediamine spacer → Process (B) & (C)



Step-2 EDA spacer (B)

GA activated nylon fabric disc (0.25 g) from Section 2.6.3.2.1 were incubated in 5 % v/v ethylenediamine (10 ml) in PBS (0.05M pH 8.0) for 18 h at RT. The discs were subsequently washed with distilled water and PBS (0.05M, pH 8.0) (25 mL; 4 x 5 min) respectively.

Step-3 & 4 GA activation and ADH immobilisation

The ethylenediamine activated nylon fabric discs (0.210 g) were subjected to 2.5 % v/v GA treatment (5 mL) in PBS (0.05 M, pH 8) and subsequently immobilised with ADH (5 mL, 0.5 mg/mL) in PBS (0.05 M, pH 8) according to the procedure described in Step 2 and Step 3 in Section 2.6.3.2.1.

Step- 5 Sodium borohydride reduction (C)

Reduction of the imine was carried out according to the procedure described by F. H. Isgrove.⁸⁴ Three ADH-nylon fabric discs (0.05 g) prepared in Step 4 (Section 2.6.3.2.2) were exposed to NaBH₄ (0.1 M, 2 mL) in PBS (0.05M, pH 8.0) solution for 30 min at RT. The fabric discs were removed from the solution and washed with distilled water (10 mL; 3 x 5 min), followed by brine solution (1 M NaCl in 0.05 M PBS, pH 8.0) containing 0.5% v/v Triton X-100 (10mL; 1 x 5 min) and finally washed with PBS (0.05M, pH 8.0, 10 mL; 3 x 3 min). Detailed activity measurements for process A, B and C are presented in Table 2.7.

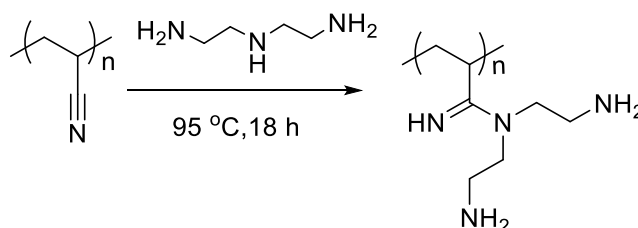
Table. 2.7 ADH immobilised on nylon 6 fabric support ADH activity data

Abs	NADH coefficient	Conc (mM)	Conc (mmol)	Total activity mmol/min	Activity mmol/min/g	Average activity
Treatment- Activity data for ADH immobilised on GA activated nylon fabric (A)						
0.285	6200	0.046	0.046	0.011	2.298	2.296
0.283	6200	0.046	0.046	0.011	2.280	
0.286	6200	0.046	0.046	0.012	2.310	
0.285	6200	0.046	0.046	0.011	2.296	
Control- Activity data for ADH immobilised on nylon fabric						
0.103	6200	0.017	0.017	0.004	0.830	0.790
0.095	6200	0.015	0.015	0.004	0.768	
0.096	6200	0.015	0.015	0.004	0.771	
0.098	6200	0.016	0.016	0.004	0.790	
Treatment –Activity data for ADH immobilised on nylon fabric via GA+ DEA + GA spacer(B)						
0.147	6200	0.024	0.024	0.006	1.187	1.603
0.226	6200	0.036	0.036	0.009	1.823	

Table 2.7 Continued...						
0.223	6200	0.036	0.036	0.009	1.798	
Control- Activity data for ADH immobilised on nylon fabric						
0.127	6200	0.020	0.020	0.005	1.024	1.014
0.126	6200	0.020	0.020	0.005	1.016	
0.124	6200	0.020	0.020	0.005	1.001	
Treatment-Immobilised ADH activity data after imine reduction (NaBH₄ treatment) (C)						
0.064	6200	0.010	0.010	0.003	0.516	0.649
0.093	6200	0.015	0.015	0.004	0.750	
0.081	6200	0.013	0.013	0.003	0.653	
0.084	6200	0.014	0.014	0.003	0.677	
Control-Activity data for ADH immobilised on nylon fabric						
0.120	6200	0.019	0.019	0.005	0.968	1.014
0.123	6200	0.020	0.020	0.005	0.992	
0.125	6200	0.020	0.020	0.005	1.008	
0.135	6200	0.022	0.022	0.005	1.089	

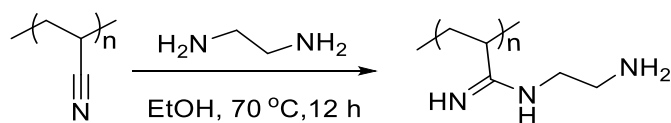
2.6.3.3 PAN

2.6.3.3.1 Surface modification with diethylenetriamine



Amination of PAN fibres was carried out according to a procedure described by P. K. Neghlani.⁸⁵ PAN fibres (1.09 g) were added to 33 % (v/v) diethylenetriamine solution (30 mL in ethanol) in a round bottom flask at RT. The mixture was stirred at 95 °C for 18 h. The fibres were then separated from the above reaction mixture and rinsed with distilled water (50 mL; 3 x 5 min) until pH of the washing reached neutral. The treated fibres were then dried at 50 °C for 18 h in an oven. IR data on the constructs was not consistent with the target structure.

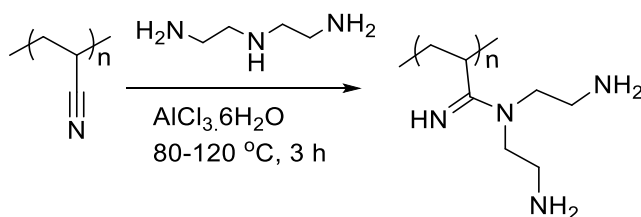
2.6.3.3.2 Surface modification by ethylenediamine



PAN fibre amination was carried out according to the procedure described by M.El-Newehy *et al.*⁸⁶ PAN fibre (1 g) was added to the ethylenediamine solution (20 mL, 10 % in ethanol) at 70 °C for 12 h. The reaction mixture was cooled and the fibres were separated from the mixture and washed with methanol (60 ml; 2 x 5 min) and dried in an oven for 18 h.

A model reaction of powderous PAN (0.5 g) using ethyldiamine (10 mL, 10 % in ethanol) was carried out according to the above procedure described for PAN fibres. IR data on the constructs was not consistent with the target structure.

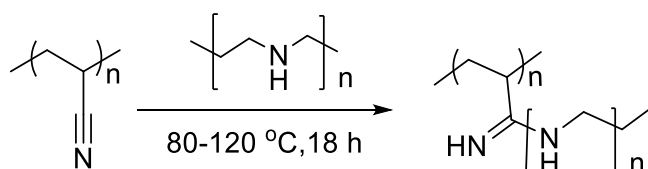
2.6.3.3.3 Surface modification with diethylenetriamine in presence of $\text{AlCl}_3/6\text{H}_2\text{O}$



Amination of the PAN fibres was carried out according to the procedure described by D. H. Shin.⁸⁷ PAN fibres (1.0 g) were added to a mixture of $\text{AlCl}_3 \cdot 6\text{H}_2\text{O}$ (0.5g) and diethyltriamine (25 mL) at RT. The reaction mixture was heated at 95 °C for 3 h. The reaction mixture was then allowed to cool to RT and the fibres were separated from the mixture and

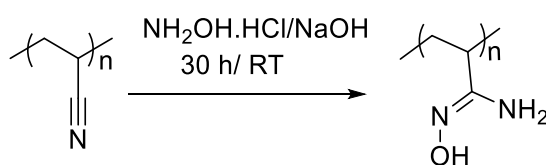
washed with distilled water (50 mL; 3x 5 min). The yellow fibres were then dried in an oven prior to IR analysis. IR data on the constructs was not consistent with the target structure.

2.6.3.3.4 Surface modification by polyethyleneimine



PAN fibres (1.02 g) were added to the polyethyleneimine solution (15 mL) in a round bottom flask. The mixture was stirred at 95 °C for 18 h. The fibres were separated from the solution, rinsed with distilled water (250 mL; 2 x 15 min) until the pH of the washings reached neutral pH and then dried in an oven for 18 h at 55 °C. IR data on the constructs was not consistent with the target structure.

2.6.3.3.5 Surface modification by hydroxylamine hydrochloride



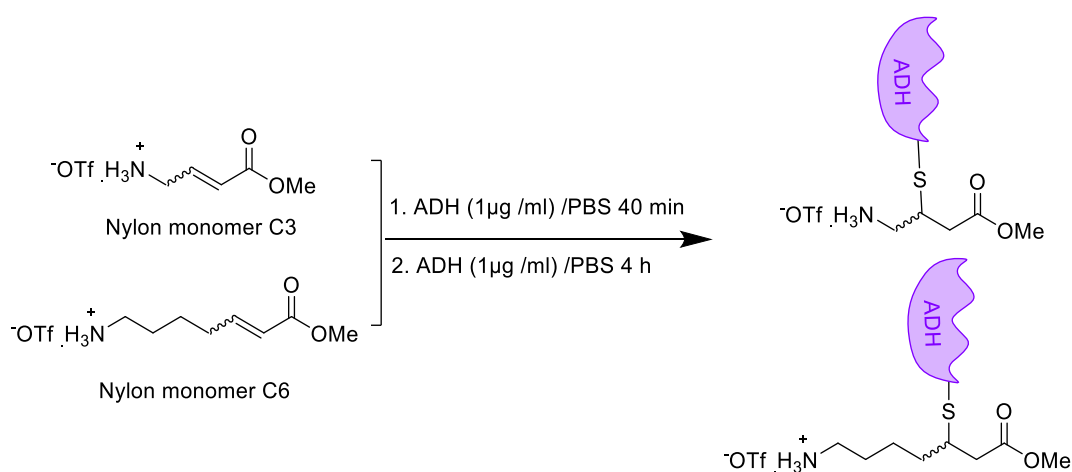
PAN surface modification with hydroxylamine hydrochloride was carried out according to a procedure described by N. Horzum.⁸⁸ PAN fibres (0.5 g) were added to the 20 mL mixture of hydroxylamine hydrochloride (3.75 g) and sodium hydroxide (3.75 g) in water. The reaction was stirred for 30 h at RT.⁸⁸ The fibres were then removed and washed with distilled water

(150 mL; 3 x 10 min) to remove the remaining salts and then dried in a vacuum oven at 60 °C.

IR data on the constructs was not consistent with the target structure.

2.6.4 ADH modification

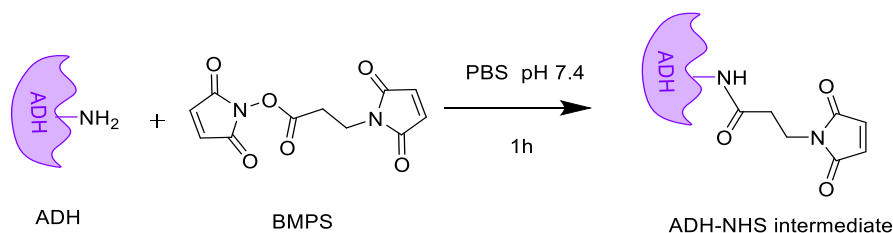
2.6.4.1 C3 and C6 Nylon monomer



Methyl 4-ammonium but-2-enoate triflate (10 µg/mL) in PBS (0.05M, pH 7.5) was incubated in ADH (1 mL, 1µg/ml) in PBS (0.05M, pH 7.5) for 40 min at RT. The activity of the modified ADH (10 µL) was assayed. ADH activity assay was carried out as per the procedure described for the ADH activity assay (Section 2.6.6).

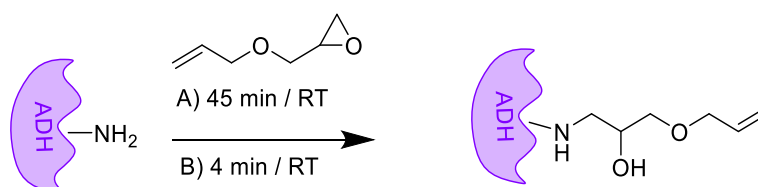
Methyl 6-ammonium hex-2-enoate triflate (10 µg/mL) in PBS (0.05M, pH 7.5) was reacted with ADH (1 mL, 1µg/ml) in PBS (0.05M, pH 7.5) according to the above procedure described for methyl 4-ammonium but-2-enoate triflate and assayed for ADH activity (Section 2.6.6).

2.6.4.2 BMPS modification



ADH (100 μL , 5 mg/mL) in PBS (0.05M, pH 7.5) was added to the BMPS solution (100 μL , 2 mg BMPS in 1ml distilled water) at RT. The reaction was incubated for 1 h at RT with periodic mixing. The maleimide-activated ADH was then purified by passing the reaction mixture through a Sephadex G-25 desalting column⁸¹ and fractions were collected. The ADH activity was performed on fractions according to the procedure described for the ADH activity assay (Section 2.6.6).

2.6.4.3 Allyl glycidyl ether modification



The ADH modification with AGE was carried out according to a procedure described by K. Opwis.⁸² AGE (20 % v/v) was dissolved in Triton-X (5 mL, 0.1% in distilled water) with vigorous stirring. ADH (1ml, 1mg/mL) in PBS (0.05 M, pH 8.01) was added to 0.0, 0.25, 0.5 and 1.0 mL AGE solution, which was made up to a final volume of 5.0 mL with PBS (0.05M, pH 7.5). The mixtures were stirred for 45 min at RT. Sample volumes (10 μL) were

removed from the mixture and ADH activity was assayed for different AGE concentrations. Activity data is represented in Table 2.8.

Table 2.8 Reaction details and activity data for Reaction A (45 min)

Reaction	ADH (1mg/mL in PBS)	Ethanol (0.2M)	AGE (20% in PBS)	PBS	Activity (mmol/min/g)
1	1 mL	1 mL	0.1 mL	3.70 mL	83.62
2	1 mL	1 mL	0.25 mL	2.75 mL	67.90
3	1 mL	1 mL	0.5 mL	2.50 mL	27.33
4 (Soluble ADH- Control)	1 mL	1 mL	0.0 mL	3 mL	1014.52
<i>From the above reactions, 10 μL of ADH was used for each activity assay</i>					

The AGE modification of ADH was carried out at a lower reaction time of 4 min instead of 45 min according to the procedure described above. The reaction conditions and measured activity presented in Table 2.9. The ADH activity was then assayed according to the procedure described in the ADH activity assay (Section 2.6.6).

Table 2.9 Reaction details and activity data for Reaction B (4 min)

Reaction	ADH (1mg/mL in PBS)	Ethanol (0.2M)	AGE (20% in PBS)	Tris Buffer	Activity (mmol/min/g)
1	1 mL	1 mL	0.1 mL	3.70 mL	1951.61
2	1 mL	1 mL	0.25 mL	2.75 mL	1806.45
3	1 mL	1 mL	0.5 mL	2.50 mL	1951.61
4 (Soluble ADH- Control)	1 mL	1 mL	0.0 mL	3 mL	1999.68
<i>From the above reactions, 10 μL of ADH was used for each activity assay</i>					

2.6.5 ADH immobilisation on fabric protocol

ADH (0.5 mg/mL) was dissolved in phosphate buffer (0.05 M, pH 7.5). The functionalised GA activated fabric discs (treatment) were placed in a 12 well plate containing 1 mL ADH solution.

The ADH fabrics were washed with PBS (0.05 M, pH 7.5) over a 30 min period (15 mL; 4 x 5 min) to remove any unbound enzyme. Fabric without any surface modification was immobilised with ADH in an similar way and subsequently used as controls. Treatment and control fabrics were generated in triplicate before the activities were measured and compared.

2.6.6 ADH activity assay

The activity of ADH immobilised on the support was assayed by submerging the support discs individually in tris buffer (0.1 M pH 8.8), ethanol (20 mM), and NAD⁺ (1 mM) at 25 °C in 12 well plates. After shaking for 4 min at 100 rpm on an orbital shaker, 1 mL of the solution was withdrawn for absorbance measurement. The activity measurement experiments were performed in triplicate and the results were presented as averages ± standard errors.

2.6.7 ADH concentration study

Crystalline ADH (300 units/mg) powder was dissolved in PBS buffer (0.05 M, pH 7.5) to make 10 mg/ml concentration and used as stock solution. Final ADH various concentrations (0.01 mg/mL, 0.1 mg/mL, 0.2 mg/mL, 0.5 mg/mL and 1mg/mL) were prepared by serial dilution of the stock solution with PBS buffer (0.05 M, pH 7.5). Each concentration of ADH was assayed according to the procedure described for the ADH activity assay (Section 2.6.6). Activity measurements are presented below (Table 2.10).

Table 2.10 ADH concentration study

ADH conc (mg/mL)	Abs	NADH coefficient	Conc (mM)	Conc (mmol)	Total activity mmol/min	Activity mmol / min/g	Average activity	% Activity
0.01	0.138	6200	0.022	0.022	0.006	111.20	108.53	5%
	0.136	6200	0.022	0.022	0.005	109.60		
	0.130	6200	0.021	0.021	0.005	104.80		
0.1	0.560	6201	0.090	0.090	0.023	451.60	454.13	26%
	0.590	6202	0.095	0.095	0.024	475.60		
	0.540	6203	0.087	0.087	0.022	435.20		
0.25	1.170	6204	0.189	0.189	0.047	943.00	910.60	52%
	1.100	6205	0.177	0.177	0.044	886.40		
	1.120	6206	0.181	0.181	0.045	902.40		
0.5	2.138	6207	0.344	0.344	0.086	1722.20	1736.46	100%
	2.150	6208	0.346	0.346	0.087	1731.60		
	2.180	6209	0.351	0.351	0.088	1755.60		
0.75	2.130	6210	0.343	0.343	0.086	1715.00	1732.93	99.9%
	2.150	6211	0.346	0.346	0.087	1730.80		
	2.178	6212	0.351	0.351	0.088	1753.00		
1.00	2.127	6213	0.342	0.342	0.086	1711.80	1731.86	99.9%
	2.150	6214	0.346	0.346	0.087	1730.00		
	2.180	6215	0.351	0.351	0.088	1753.80		

2.6.8 Soluble ADH pH stability

The effect of pH on enzyme stability was measured in different buffer systems incubating the soluble and immobilised ADH at 40 °C for 2 h. Sodium phosphate buffer (0.05 M) was used for the pH region 6.5 to 8.0 and sodium carbonate/bicarbonate buffer (0.1 M) was used for the pH 8.5 to 10.5 region. The enzyme was then slowly brought to RT and activity was assayed according to the procedure described for the ADH activity assay in Section 2.6.6. Detailed activity data is presented below (Table 2.11).

Table 2.11 Effect of pH on soluble ADH activity

pH	Abs	NADH coefficient	Conc (mM)	Conc (mmol)	Total activity mmol/min	Activity mmol/min/g	Average activity
5	1.581	6200	0.255	0.255	0.064	1280.00	1280.00
	1.570	6200	0.253	0.253	0.063	1260.00	
	1.601	6200	0.258	0.258	0.065	1300.00	
6	1.820	6200	0.294	0.294	0.073	1460.00	1460.00
	1.810	6200	0.292	0.292	0.073	1460.00	
	1.818	6200	0.293	0.293	0.073	1460.00	
7	2.096	6200	0.338	0.338	0.085	1700.00	1700.00
	2.120	6200	0.342	0.342	0.085	1700.00	
	2.100	6200	0.339	0.339	0.085	1700.00	
8	1.635	6200	0.264	0.264	0.066	1320.00	1313.33
	1.610	6200	0.26	0.260	0.065	1300.00	
	1.640	6200	0.265	0.265	0.066	1320.00	
9	0.087	6200	0.014	0.014	0.003	60.00	73.33
	0.095	6200	0.015	0.015	0.004	80.00	
	0.090	6200	0.015	0.015	0.004	80.00	
10.5	0.066	6200	0.011	0.011	0.002	54.00	56.00
	0.076	6200	0.012	0.012	0.003	60.00	
	0.068	6200	0.011	0.011	0.002	54.00	

2.7 References

1. P. K. Robinson, *Essays in Biochemistry*, 2015, **59**, 1-41.
2. N. R. Mohamad, N. H. C. Marzuki, N. A. Buang, F. Huyop and R. A. Wahab, *Biotechnology, Biotechnological Equipment*, 2015, **29**, 205-220.
3. <https://www.sigmaaldrich.com/life-science/core-bioreagents/biological-buffers/learning-center/buffer-reference-center.html> Accessed on, 1 Aug 2014
4. J. M. Bolivar, J. Rocha-Martín, C. Mateo and J. M. Guisan, *Process Biochemistry*, 2012, **47**, 679-686.
5. Y. Goto, L. J. Calciano and A. L. Fink, *Proceedings of the National Academy of Sciences*, 1990, **87**, 573-577.
6. R. Chandra and R. Rustgi, *Progress in Polymer Science*, 1998, **23**, 1273-1335.
7. J. L. Song and O. J. Rojas, *Nordic Pulp & Paper Research Journal*, 2013, **28**, 216-238.
8. I. Vroman and L. Tighzert, *Materials*, 2009, **2**, 307-344.
9. Q. Xing, S. R. Eadula and Y. M. Lvov, *Biomacromolecules*, 2007, **8**, 1987-1991.
10. A. Girelli, L. Salvagni and A. Tarola, *Journal of the Brazilian Chemical Society*, 2012, **23**, 585-592.
11. S. Yabuki, Y. Hirata, Y. Sato and S. Iijima, *Analytical Sciences*, 2012, **28**, 373-373.
12. X.J. Huang, P.C. Chen, F. Huang, Y. Ou, M.R. Chen and Z.-K. Xu, *Journal of Molecular Catalysis B: Enzymatic*, 2011, **70**, 95-100.
13. N. Isobe, D.-S. Lee, Y.-J. Kwon, S. Kimura, S. Kuga, M. Wada and U. J. Kim, *Cellulose*, 2011, **18**, 1251.
14. Z. Bilkova, M. Slovakova, A. n. Lycka, D. Horak, J. Lenfeld, J. Turkova and J. Churacek, *Journal of Chromatography B*, 2002, **770**, 25-34.
15. T. Nikolic, M. Kostic, J. Praskalo, B. Pejic, Z. Petronijevic and P. Skundric, *Carbohydrate Polymers*, 2010, **82**, 976-981.
16. I. J. Seabra and M. H. Gil, *Revista Brasileira de Ciencias Farmaceuticas*, 2007, **43**, 535-542.
17. J. V. Edwards, N. T. Prevost, B. Condon, A. French and Q. Wu, *Cellulose*, 2012, **19**, 495-506.
18. S. Arola, T. Tammelin, H. Setälä, A. Tullila and M. B. Linder, *Biomacromolecules*, 2012, **13**, 594-603.
19. H. Yildiz, E. Akyilmaz and E. Dinçkaya, *Artificial Cells, Blood Substitutes, and Biotechnology*, 2004, **32**, 443-452.
20. P. Kosaka, Y. Kawano, O. El Seoud and D. Petri, *Langmuir*, 2007, **23**, 12167-12173.
21. M. Yakup Arıca, *Polymer international*, 2000, **49**, 775-781.

22. H. Orelma, L.S. Johansson, I. Filpponen, O. J. Rojas and J. Laine, *Biomacromolecules*, 2012, **13**, 2802-2810.
23. X. Luo and L. Zhang, *Biomacromolecules*, 2010, **11**, 2896-2903.
24. V. Singh and S. Ahmad, *Cellulose*, 2012, **19**, 1759-1769.
25. Y. Kurokawa and H. Ohta, *Biotechnology techniques*, 1993, **7**, 5-8.
26. Y. Ikeda, Y. Kurokawa, K. Nakane and N. Ogata, *Cellulose*, 2002, **9**, 369-379.
27. M. Namdeo and S. Bajpai, *Journal of Molecular Catalysis B: Enzymatic*, 2009, **59**, 134-139.
28. F. Y. Mahlieli and S. A. Altinkaya, *Journal of Materials Science: Materials in Medicine*, 2009, **20**, 2167-2179.
29. Q. Wang, C. X. Li, X. Fan, P. Wang and L. Cui, *Biocatalysis and Biotransformation*, 2008, **26**, 437-443.
30. J. Rojas and E. Azevedo, *Functionalization and Crosslinking of Microcrystalline Cellulose in Aqueous Media: A Safe and Economic Approach*, 2011, **8**, 28-36.
31. J. V. Edwards, N. T. Prevost, B. Condon and A. French, *Cellulose*, 2011, **18**, 1239-1249.
32. H. T. Peng, C. Q. Yang, X. L. Wang and S. Y. Wang, *Industrial & Engineering Chemistry Research*, 2012, **51**, 11301-11311.
33. C. W. Chen, S. H. Hsieh, C. H. Cheng and T. T. Chang, *Cellulose Chemistry and Technology*, 2004, **38**, 431-444.
34. Y. Gao, T. Yen Bach, P. Cacioli, P. Butler and I. L. Kyratzis, *Enzyme and Microbial Technology*, 2014, **54**, 38-44.
35. J. A. Howarter and J. P. Youngblood, *Macromolecules*, 2007, **40**, 1128-1132.
36. Y. L. Liu, K. L. Ai and L. H. Lu, *Chemical Reviews*, 2014, **114**, 5057-5115.
37. H. Lee, S. M. Dellatore, W. M. Miller and P. B. Messersmith, *Science*, 2007, **318**, 426-430.
38. H. Lee, J. Rho and P. B. Messersmith, *Advanced Materials (Deerfield Beach, Fla.)*, 2009, **21**, 431-434.
39. L. Lu, Q.-L. Li, M. F. Maitz, J. L. Chen and N. Huang, *Journal of Biomedical Materials Research Part A*, 2012, **100A**, 2421-2430.
40. K. Kang, I. S. Choi and Y. Nam, *Biomaterials*, 2011, **32**, 6374-6380.
41. Q. Xu, Q. Kong, Z. Liu, J. Zhang, X. Wang, R. Liu, L. Yue and G. Cui, *The Royal Society of Chemistry, Advances*, 2014, **4**, 7845-7850.
42. C. Silva and A. Cavaco-Paulo, *Biocatalysis and Biotransformation*, 2004, **22**, 357-360.
43. A. De Maio, M. M. El Masry, M. Portaccio, N. Diano, S. Di Martino, A. Mattei, U. Bencivenga and D. G. Mita, *Journal of Molecular Catalysis B: Enzymatic*, 2003, **21**, 239-252.
44. M. Herrera-Alonso, T. J. McCarthy and X. Jia, *Langmuir*, 2006, **22**, 1646-1651.
45. B. Braun, E. Klein and J. L. Lopez, *Biotechnology and Bioengineering*, 1996, **51**, 327-341.
46. E. Fatarella, D. Spinelli, M. Ruzzante and R. Pogni, *Journal of Molecular Catalysis B: Enzymatic*, 2014, **102**, 41-47.

47. V. Vallejo-Becerra, J. Vasquez-Bahena, J. A. Santiago-Hernandez and M. E. Hidalgo-Lara, *Journal of Industrial Microbiology & Biotechnology*, 2008, **35**, 1289-1295.
48. C. Silva, C. J. Silva, A. Zille, G. M. Guebitz and A. Cavaco-Paulo, *Enzyme and Microbial Technology*, 2007, **41**, 867-875.
49. L. Amaya-Delgado, M. E. Hidalgo-Lara and M. C. Montes-Horcasitas, *Food Chemistry*, 2006, **99**, 299-304.
50. H. El Sherif, P. L. Martelli, R. Casadio, M. Portaccio, U. Bencivenga and D. G. Mita, *Journal of Molecular Catalysis B-Enzymatic*, 2001, **14**, 15-29.
51. M. J. Duenas and P. Estrada, *Biocatalysis and Biotransformation*, 1999, **17**, 139-161.
52. I. Alkorta, C. Garbisu, Maria, J. Llama and J. L. Serra, *Enzyme and Microbial Technology*, 1996, **18**, 141-146.
53. F. Pariente, C. LaRosa, F. Galan, L. Hernandez and E. Lorenzo, *Biosensors & Bioelectronics*, 1996, **11**, 1115-1128.
54. N. Bachinski, A. D. Panek and C. L. A. Paiva, *Brazilian Journal of Medical and Biological Research*, 1994, **27**, 1507-1516.
55. T. Asakura, M. Kitaguchi, M. Demura, H. Sakai and K. Komatsu, *Journal of Applied Polymer Science*, 1992, **46**, 49-53.
56. K. Moeschel, M. Nouaimi, C. Steinbrenner and H. Bisswanger, *Biotechnology and Bioengineering*, 2003, **82**, 190-199.
57. F. N. Onyezili and A. C. Onitiri, *Analytical Biochemistry*, 1981, **113**, 203-206.
58. S. Pahujani, S. S. Kanwar, G. Chauhan and R. Gupta, *Bioresource Technology*, 2008, **99**, 2566-2570.
59. M. Canella and G. Sodini, *European Journal of Biochemistry*, 1975, **59**, 119-125.
60. C. J. Dickenson and F. M. Dickinson, *Biochemical Journal*, 1975, **147**, 303-311.
61. H. Jornvall, H. Eklund and C. I. Branden, *Journal of Biological Chemistry*, 1978, **253**, 8414-8419.
62. Q. Feng, X. Q. Wang, A. F. Wei, Q. F. Wei, D. Y. Hou, W. Luo, X. H. Liu and Z. Q. Wang, *Fibers and Polymers*, 2011, **12**, 1025-1029.
63. O. Stoilova, N. Manolova, K. Gabrovska, I. Marinov, T. Godjevargova, D. G. Mita and I. Rashkov, *Journal of Bioactive and Compatible Polymers*, 2010, **25**, 40-57.
64. A. Hartwig, M. Mulder and C. A. Smolders, *Advances in Colloid and Interface Science*, 1994, **52**, 65-78.
65. E. Battistel, M. Morra and M. Marinetti, *Applied Surface Science*, 2001, **177**, 32-41.
66. H. Liu and Y.L. Hsieh, *Macromolecular Rapid Communications*, 2006, **27**, 142-145.
67. S. Mandal and V. G. Pangarkar, *Journal of Membrane Science*, 2002, **209**, 53-66.
68. T. C. Hung, C. C. Fu, C. H. Su, J. Y. Chen, W. T. Wu and Y. S. Lin, *Enzyme and Microbial Technology*, 2011, **49**, 30-37.

69. K. Gabrovska, T. Nedelcheva, T. Godjevargova, O. Stoilova, N. Manolova and I. Rashkov, *Journal of Molecular Catalysis B-Enzymatic*, 2008, **55**, 169-176.
70. G. H. Li, A. G. Nandgaonkar, K. Y. Lu, W. E. Krause, L. A. Lucia and Q. F. Wei, *Royal Society of Chemistry Advances*, 2016, **6**, 41420-41427.
71. J. Manuel, M. Kim, R. Dharela, G. S. Chauhan, D. Fapyane, S. J. Lee, I. S. Chang, S. H. Kang, S. W. Kim and J. H. Ahn, *Journal of Biomedical Nanotechnology*, 2015, **11**, 143-149.
72. F. Ishimura and H. Seijo, *Journal of Fermentation and Bioengineering*, 1991, **71**, 140-143.
73. Q. Feng, S. M. Bi, X. Q. Wang, Q. F. Wei, D. Y. Hou and X. H. Huang, in *Textile Bioengineering and Informatics Symposium Proceedings, Vols 1 and 2*, eds. Y. Li, M. Takatera, K. Kajiwara and J. S. Li, 2012, DOI: 10.3993/tbis2012015, pp. 114-119.
74. E. Lukowska, D. Pijanowska and A. Chwojnowski, *Polish Journal of Chemistry*, 2008, **82**, 1265-1272.
75. H. G. Hicke, P. Bohme, M. Becker, H. Schulze and M. Ulbricht, *Journal of Applied Polymer Science*, 1996, **60**, 1147-1161.
76. N. Rueda, J. C. S. d. Santos, C. Ortiz, O. Barbosa, R. Fernandez-Lafuente and R. Torres, *Catalysis Today*, 2016, **259**, 107-118.
77. J. Morales-Sanfrutos, J. Lopez-Jaramillo, M. Ortega-Munoz, A. Megia-Fernandez, F. Perez-Balderas, F. Hernandez-Mateo and F. Santoyo-Gonzalez, *Organic & Biomolecular Chemistry*, 2010, **8**, 667-675.
78. H. He, Y. Wei, H. Luo, X. Li, X. Wang, C. Liang, Y. Chang, H. Yu and Z. Shen, *Biotechnology Progress*, 2015, **31**, 387-395.
79. N. Rueda, J. C. S. dos Santos, C. Ortiz, R. Torres, O. Barbosa, R. C. Rodrigues, A. Berenguer-Murcia and R. Fernandez-Lafuente, *Chemical Record*, 2016, **16**, 1436-1455.
80. K. Nishimura and K. Tomioka, *Yakugaku Zasshi-Journal of the Pharmaceutical Society of Japan*, 2003, **123**, 9-18.
81. Q. A. Bui, T. H. H. Vu, V. K. T. Ngo, I. R. Kennedy, N. A. Lee and R. Allan, *Analytical and Bioanalytical Chemistry*, 2016, **408**, 6045-6052.
82. K. Opwis, D. Knittel and E. Schollmeyer, *Biotechnology Journal*, 2007, **2**, 347-352.
83. R. K. Singh, M. K. Tiwari, R. Singh and J. K. Lee, *International Journal of Molecular Sciences*, 2013, **14**, 1232-1277.
84. F. H. Isgrove, R. J. H. Williams, G. W. Niven and A. T. Andrews, *Enzyme and Microbial Technology*, 2001, **28**, 225-232.
85. P. K. Neghlani, M. Rafizadeh and F. A. Taromi, *Journal of Hazardous Materials*, 2011, **186**, 182-189.
86. M. H. El-Newehy, A. Alamri and S. S. Al-Deyab, *Arabian Journal of Chemistry*, 2014, **7**, 235-241.

87. D. H. Shin, Y. G. Ko, U. S. Choi and W. N. Kim, *Polymers for Advanced Technologies*, 2004, **15**, 459-466.
88. N. Horzum, T. Shahwan, O. Parlak and M. M. Demir, *Chemical Engineering Journal*, 2012, **213**, 41-49.

Chapter 3

Polyvinyl alcohol (PVA) fibre and fabric support for ADH immobilisation

This chapter describes the chemical modification of polyvinyl alcohol (PVA) fibre and fabric support for the immobilisation of ADH to increase its stability, prolong its activity and enhance its reusability. The strategy for immobilisation involved functionalisation of the PVA with chloropropionyl chloride followed by amination with ethylenediamine (EDA). Tethering of the ADH enzyme to the PVA scaffold was achieved by cross linking with glutaraldehyde (GA). The stability (pH, temperature, time) and recycling of the immobilised ADH construct was also investigated.

3.1 Introduction

A large number of enzymes have been successfully immobilised with very high activity yields on appropriate supports (Chapter 1, Table 1.4 and 1.5).¹⁻⁴ The type and texture of the support influences the immobilisation efficiency.⁵ Structured fibre supports in the form of fibre, fabric and textiles offer porosity and ultimately provide a way to overcome diffusion limits which are often experienced with beads and sphere supports.^{6,7}

In Chapter 3, PVA surface functionalisation of the fibre (yarn) and fabric (in knitted format) structure was investigated. Successfully functionalised PVA fibre and fabric (scaffolds) were exposed to ADH and immobilised PVA fibrous/fabric-ADH constructs were isolated and studied for stability (pH, temperature and storage). Listed below are the strategies that were utilized in this chapter for the construction of stable PVA fibrous/fabric ADH scaffolds:

- Chemical surface modification of PVA to generate scaffolds with various pendant functional groups. The detailed optimisation and characterisation of the modified PVA scaffolds were performed by spectroscopic and microscopic methods.
- Solution phase model reactions of the fibrous PVA phase were performed on 2,4-pentenediol.

- Successfully functionalised PVA scaffolds were subjected to immobilisation reactions and the enzyme activity of the immobilised ADH versus controls was measured.
- Stability studies, e.g. pH, temperature, storage and reusability, of a high activity PVA-ADH scaffold were performed.

Commercial synthesis of PVA is performed in a two-step process *via* the free-radical polymerization of vinyl acetate in an alcoholic solution, followed by the partial hydrolysis of the resultant polyvinyl acetate (PVA).⁷ By controlling the degree of hydrolysis, different grades of PVA polymer can be prepared.^{7,8} Baum *et al.*, in 1924, first reported the preparation of PVA from vinyl acetate. Since this time, PVA has been used in many applications aided by its properties such as biodegradability, excellent biocompatibility, low toxicity, film orientation characteristics, and adhesive properties.^{9, 10} A summary of some of the applications that use PVA are listed in Figure 3.1.

PVA properties can be modified *via* functionalisation of its hydroxyl groups.¹¹ Common crosslinking reagents of PVA (powder and gel forms) include glutaraldehyde, glyoxal,¹² maleic acid and acetic anhydride.¹³ Additionally, chloroacetylation¹⁴ and bromoacetylation¹⁵ with chloroacetic acid and bromopropionyl bromide provides branched PVA polymers (e.g. stars, combs, or dendrigrafts) with enhanced tensile strength. PVA has also been used as a support for enzyme immobilisation (Table 3.1)

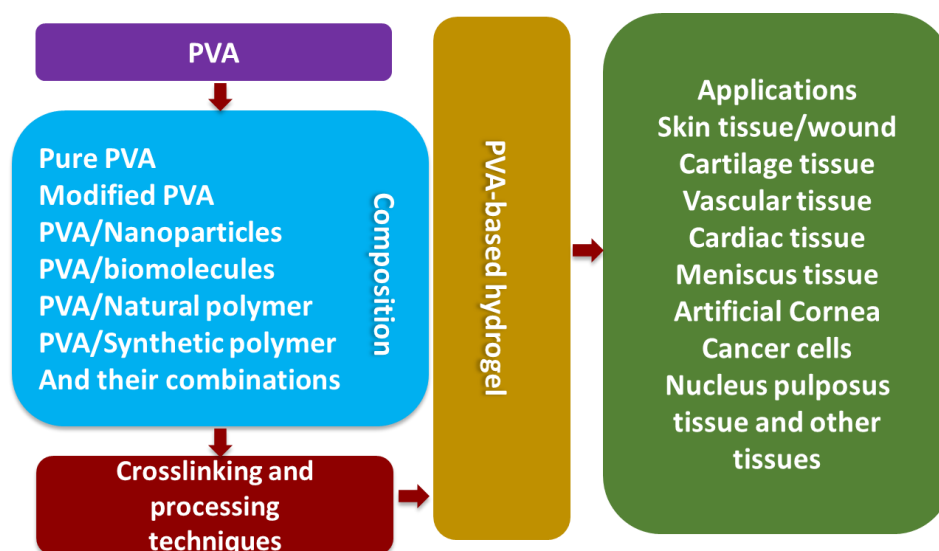
Figure 3.1. PVA various applications¹⁶

Table 3.1 PVA support used for various enzyme immobilisations

Support	Enzyme	Method of Immobilisation	Application	Ref.
Polyvinyl alcohol (PVA) hydrogel	Lactase	Entrapment	Biocatalyst	17
Polyvinyl alcohol-alginate beads	Manganese peroxidase (MnP)	Adsorption	Biocatalyst	18
Polyvinyl alcohol gel particles	<i>Escherichia coli</i> cells	-	Biocatalyst	19
PVA/alginate beads	Glucose oxidase (GOX) and catalase	Entrapment	Biocatalyst	20
Polyvinyl alcohol	Lipase	Covalent	Biocatalyst	21
Polyvinyl alcohol film	Glucose oxidase	Covalent	Biocatalyst	22
PVA-alginate beads	Invertase	Covalent	Biocatalyst	23
Polyvinyl alcohol hydrogel	Naringinase	Entrapment	Bioreactor	24
Polyvinyl alcohol capsules	Invertase	Entrapment	Bioreactor	25
Polyvinyl alcohol gel beads	Alcohol dehydrogenase from <i>Lactobacillus</i>	Entrapment	Bioreactor	26
Polyvinyl alcohol (PVA) membrane	Oxalate oxidase	-	Bioreactor	27
Polyvinyl alcohol	Lactase	Covalent	Biocatalyst	28
Table 3.1 Continued...				

Support	Enzyme	Method of Immobilisation	Application	Ref.
Polyvinyl alcohol cryogel	Beta-galactosidase	Covalent	Biocatalyst	29
Polyvinyl alcohol beads	Xanthine oxidase, alpha-amylase and amyloglucosidase	Covalent	Biocatalyst	30

In this work, PVA was investigated in fibre and knitted fabric form as a support for ADH immobilisation. The advantages of PVA include easy functionalisation of the hydroxyl group without activation or pre-treatment, and the availability of the fibre form, which can be readily converted into textiles. Literature examples of PVA modification mostly refer to the use of powder and gels.³¹⁻³³ There are no reports on the modification of fibrous PVA. PVA fibres can be made from dissolved PVA followed by spinning. PVA spun fibres can then be converted into fabrics *via* weaving and knitting fabrication methods (Chapter 1, Section 1.7.1). Known solution based PVA modification reactions involving alkylation, esterification, etherification and isocyanate formation were used for the surface modification of PVA fibre and fabric (see Table 3.2). Surface modification reactions were carried out with different bifunctional reagents such as epichlorohydrin, glutaraldehyde, dichloro and diisocyanate reagents. These reagents also served as spacers of different length. The functionalised PVA fibres and fabrics were primarily characterised by IR spectroscopy.

3.2 Surface modification of PVA fibre and fabric

3.2.1 Reactions with PVA fibre and fabric

Prior to functionalisation, the solubility of PVA was investigated in solvents such as ethanol, acetone, water and aqueous mixtures. Fibrous PVA was insoluble at RT in water, ethanol and acetone and became only slightly soluble upon heating at 60 °C in water, water: ethanol (1:1) and water: acetone (1:1) mixtures. At 90 °C and above, the PVA transformed to a gel form and eventually became soluble on further heating. Based on these observations, all reactions were carried out below 90 °C. This section provides a survey of PVA modification reactions; a range of methods have been applied and preliminarily assessed with IR spectroscopy as indicated in Table 3.2.

Table 3.2 Reactions of polyvinyl alcohol classified according to functional group interconversion

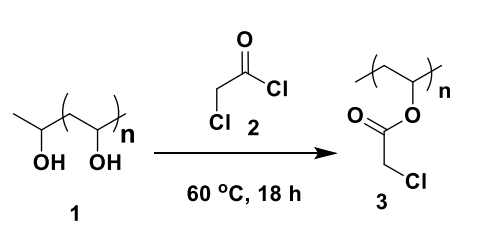
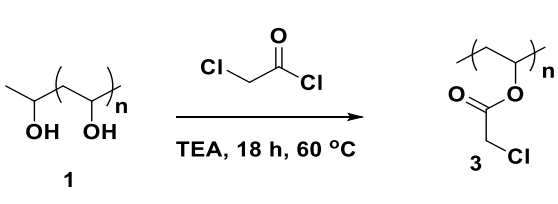
No	Reaction conditions	Results
Ester modification		
1	 <p style="text-align: center;"> $\text{PVA-OH} + \text{Cl-CH}_2\text{-CO-Cl} \xrightarrow{60\text{ }^\circ\text{C, 18 h}} \text{PVA-O-CO-CH}_2\text{-Cl}$ </p>	PVA fabric/fibre dissolved
2	 <p style="text-align: center;"> $\text{PVA-OH} + \text{Cl-CH}_2\text{-CO-Cl} \xrightarrow{\text{TEA, 18 h, 60 }^\circ\text{C}} \text{PVA-O-CO-CH}_2\text{-Cl}$ </p>	PVA fabric/fibre dissolved at RT

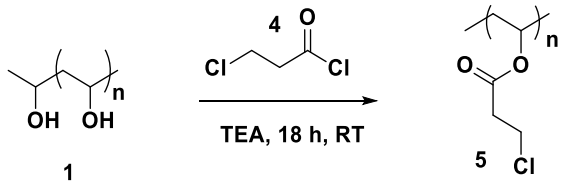
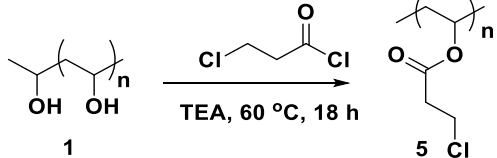
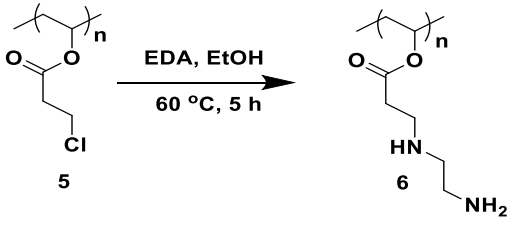
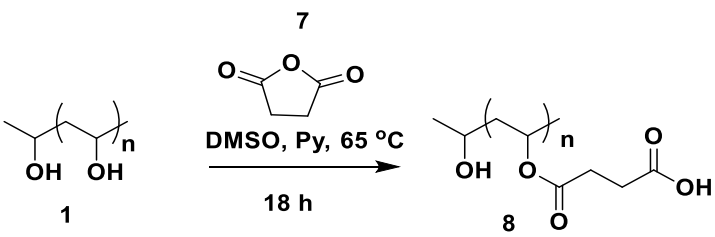
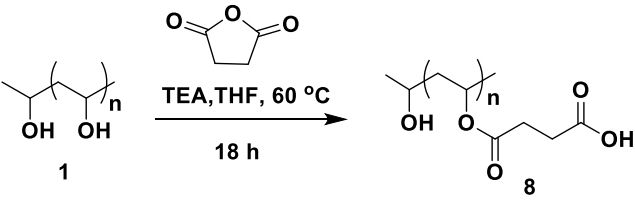
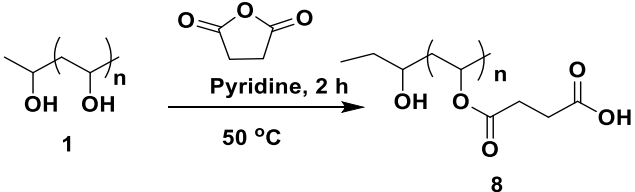
Table 3.2 Continued...		
No	Reaction Conditions	Results
3	 <p>1 + 4 $\xrightarrow{\text{TEA, 18 h, RT}}$ 5</p>	IR shows low absorption at 1734 cm^{-1} for ester-carbonyl formation
4	 <p>1 + 4 $\xrightarrow{\text{TEA, 60 }^\circ\text{C, 18 h}}$ 5</p>	IR shows strong absorption at 1744 cm^{-1} showing carbonyl ester. Further confirmed by ^{13}C -NMR spectroscopy. Reaction promising
5	 <p>5 $\xrightarrow{\text{EDA, EtOH, 60 }^\circ\text{C, 5 h}}$ 6</p>	IR shows strong absorption at 1744 cm^{-1} showing C=O stretch along with –NH bending at 1600 cm^{-1} . Reaction promising
6	 <p>1 + 7 $\xrightarrow{\text{DMSO, Py, 65 }^\circ\text{C, 18 h}}$ 8</p>	IR not consistent with predicted structure
7	 <p>1 + 7 $\xrightarrow{\text{TEA, THF, 60 }^\circ\text{C, 18 h}}$ 8</p>	IR not consistent with predicted structure
8	 <p>1 + 7 $\xrightarrow{\text{Pyridine, 2 h, 50 }^\circ\text{C}}$ 8</p>	IR not consistent with predicted structure

Table 3.2 Continued...

No	Reaction Conditions	Results
Carbamate modification		
1	<p>Step-1: DMSO</p> <p>Intermediate</p> <p>Step-2: THF</p> <p>Step-3: TFA:H₂O (95:5)</p> <p>NH₂.TFA</p>	Fibre dissolved in 5% TFA: H ₂ O and 2% TFA: H ₂ O
Ether modification		
1	<p>Step-1: (2.5 w/v), 2N NaOH</p> <p>Step-2: 25% NH₃</p>	IR not consistent with predicted structure
2	<p>Step-1: 19.2% NaOH (5N), 55-60 °C, 8 h</p> <p>Step-2: 30% NH₃</p>	IR not consistent with predicted structure
3	<p>Step-1: t-BuOK, THF, RT</p>	IR not consistent with predicted structure
4	<p>Step-1: 2.5% w/v, 0.05 M phosphate buffer pH 7, RT, 1 h</p>	IR not consistent with predicted structure

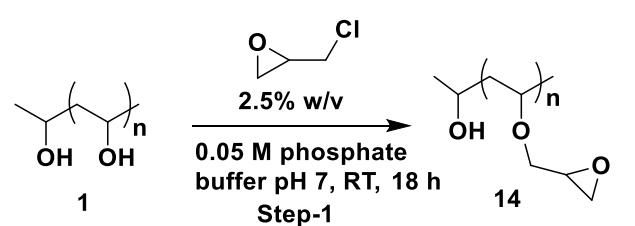
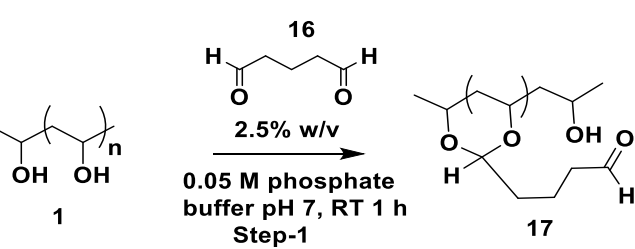
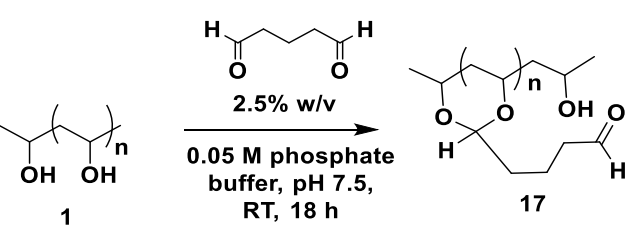
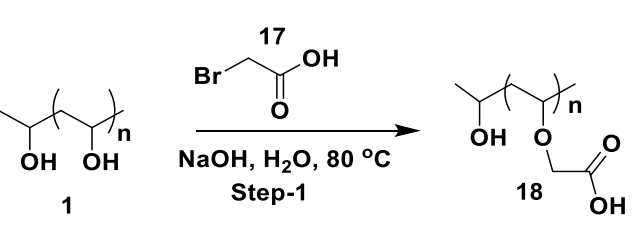
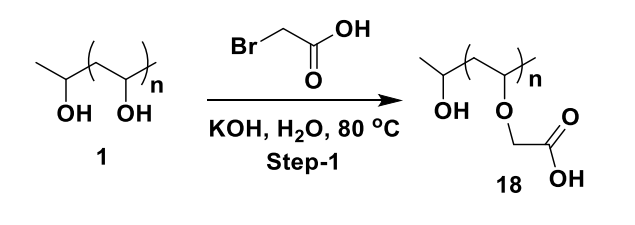
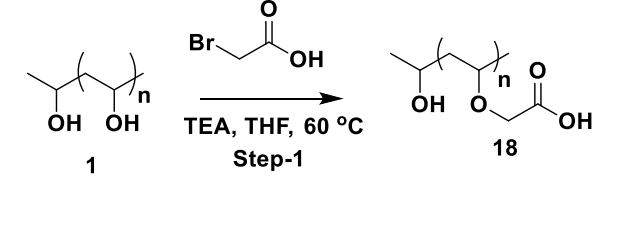
Table 3.2 Continued...		
No	Reaction Conditions	Results
5	 <p>2.5% w/v 0.05 M phosphate buffer pH 7, RT, 18 h Step-1</p>	IR not consistent with predicted structure
6	 <p>2.5% w/v 0.05 M phosphate buffer pH 7, RT 1 h Step-1</p>	IR not consistent with predicted structure
7	 <p>2.5% w/v 0.05 M phosphate buffer, pH 7.5, RT, 18 h Step-1</p>	IR not consistent with predicted structure
8	 <p>2.5% w/v NaOH, H₂O, 80 °C Step-1</p>	IR not consistent with predicted structure
9	 <p>2.5% w/v KOH, H₂O, 80 °C Step-1</p>	IR not consistent with predicted structure
10	 <p>2.5% w/v TEA, THF, 60 °C Step-1</p>	IR confirms C=O stretch at 1744 cm ⁻¹ . Further confirmed by ¹³ C NMR spectroscopy. Reaction promising

Table 3.2 Continued...

No	Reaction conditions	Results
11	<p>19 Cl-CH₂-CH₂-COOH NaOH, H₂O, 80 °C Step-1</p>	IR not consistent with predicted structure
12	<p>Cl-CH₂-CH₂-COOH TEA, THF 60 °C Step-1</p>	IR not consistent with predicted structure.
13	<p>Cl-CH₂-CH₂-COOH K⁺BuO⁻, THF, 60 °C Step-1</p>	IR not consistent with predicted structure
14	<p>21 Br-CH₂-CH₂-CH₂-N-CO-CH₂-CH₂-C(CH₃)₂-CH₃ TEA, THF RT Step-1</p>	IR not consistent with predicted structure
15	<p>1,4 Butanediol diglycidyl ether NaOH, RT, 18 h</p>	IR not consistent with predicted structure
16	<p>1,4 Butanediol diglycidyl ether 55 °C, 2 h PVA fibre as well as fabric dissolved</p>	PVA fibre/fabric dissolved on heating

Table 3.2 Continued...

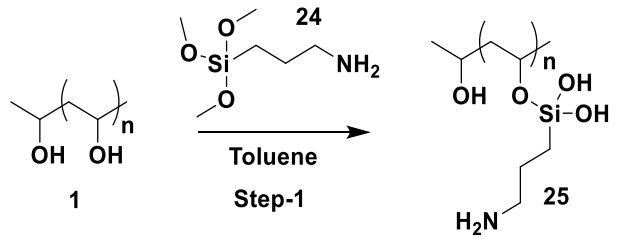
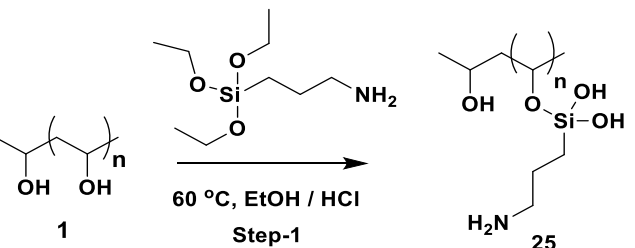
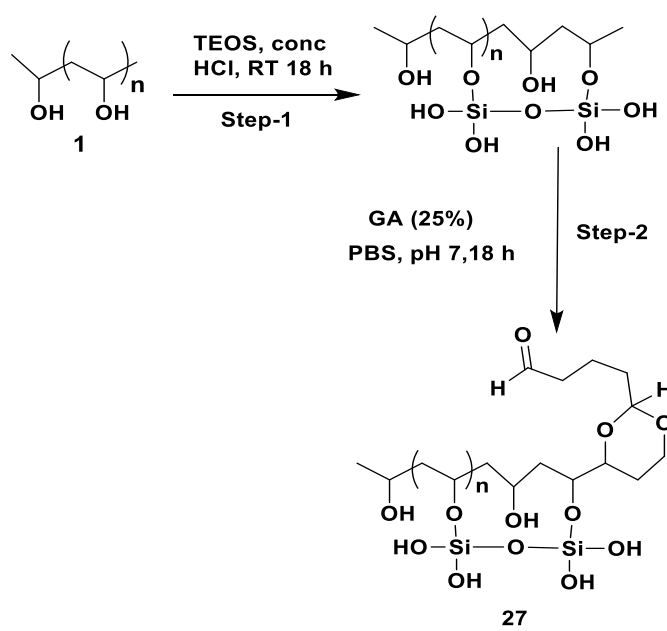
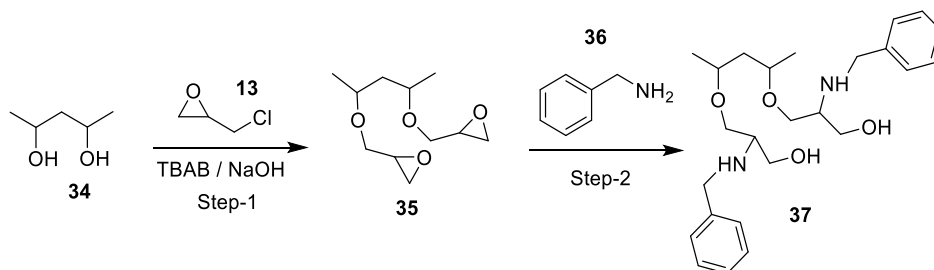
No	Reaction conditions	Results
Silane modification		
1	 <p style="text-align: center;">Step-1</p>	IR not consistent with predicted structure
2	 <p style="text-align: center;">Step-1</p>	Si-O-Si asymmetric stretch at 1069 cm ⁻¹ was seen but absorption for NH is not observed. EYOSIN dye colorimetric test was positive
3	 <p style="text-align: center;">Step-1</p> <p style="text-align: center;">Step-2</p> <p style="text-align: center;">27</p>	IR not consistent with predicted structure

Table 3.2 Continued...		
No	Reaction conditions	Results
4	<p>Step-1</p>	<p>IR showed small peak for NH bending at 1600 cm^{-1}.</p> <p>EYOSIN dye colorimetric test was positive</p>
Isocyanate formation		
1		<p>IR shows strong peak at 1744 cm^{-1} supporting carbamate formation</p>
Chlorotriazine modification		
1		<p>IR showed peak at $1600\text{-}1400\text{ cm}^{-1}$ for triazine along with PVA</p>

Table 3.2 summarises the surface modification of PVA fibre and fabric samples that are most promising *via* bromoacylation, chloroacylation, aminosilane, isocyanate and chlorotriazine formation. The other surface modification reactions were unsuccessful even after employing a range of reaction parameters including different reagent concentrations, temperatures, solvents and reaction times. In order to better understand the chemistry of PVA modification, the

reaction of 2,4-pentanediol (**34**) and epichlorohydrin (**13**) (Scheme 3.1) was conducted as a model of the solid state chemistry (Table 3.3, Section C, Reactions 1-5) described above.⁴⁵



Scheme 3.1. Model reaction for fibrous PVA

This reaction was clearly more complicated than anticipated and under a variety of experimental conditions, which included variation of the epichlorohydrin concentration, reaction temperature and time (Table 3.3), only complex reaction mixtures ensued (further experimental detail is provided in Section 3.6.4.1).

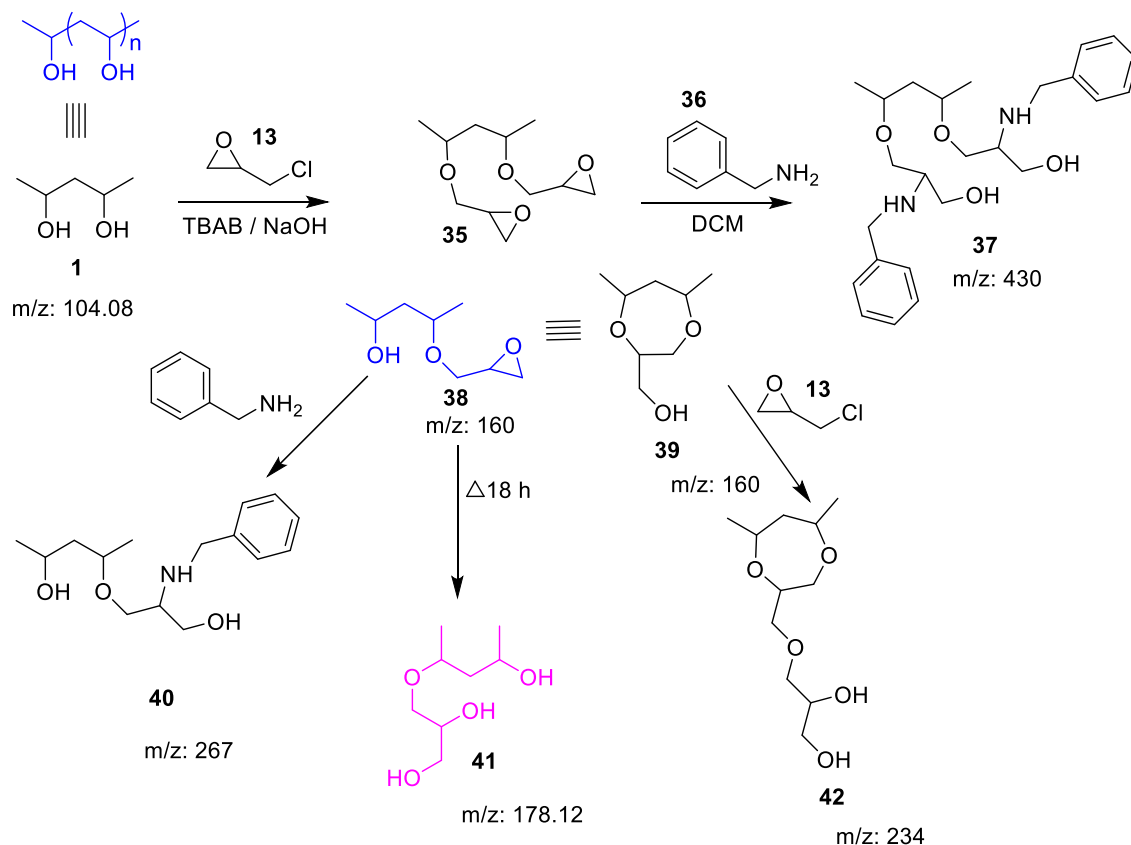
Table 3.3 Detailed reaction conditions and TLC analysis of the model reaction

No	Epichlorohydrin (Eq)	Tetra- <i>n</i> -butyl ammonium bromide (TBAB) (Eq)	Reaction Time/Temp	Benzyl amine (Eq)	TLC Results
1	4	0.05	1 h/RT	1.1/18h/RT	TLC showed a complex mixture comprised of four major spots in addition to starting material
2	4	0.05	2 h/RT	1.1/2h/RT	TLC showed a complex mixture comprised of three major spots in addition to starting material
3	4	0.05	4 h/RT	1.1/2h/RT	TLC showed a complex mixture with starting material
4	4	0.05	18 h/50 °C	1.1/4h	TLC showed a complex mixture with starting material

Table 3.3 Continued...					
No	Epichlorohydrin (Eq)	Tetra- <i>n</i> - butyl ammonium bromide (TBAB) (Eq)	Reaction Time/Temp	Benzyl amine (Eq)	TLC Results
5	4	0.05	1 h/50 °C	1.1/2h/RT	TLC complex mixture
6	8	0.05	18 min/RT	1.1/2h/RT	TLC complex mixture
7	4	0.05	15 min/RT	1.1 /2h/RT	TLC showed a complex mixture comprised of three major spots in addition to starting material

Mass spectral analysis of the reaction mixture after Step-1 revealed molecular ion peaks consistent with several plausible reaction products (Scheme 3.2). A peak observed at m/z 161 ($M+Na$)⁺ is consistent with the mono epoxy product (**38**) and cyclized alcohol (**39**), yet only (**38**) would be expected to react with benzylamine. A peak at m/z 178 ($M+Na$)⁺ is consistent with the polyol (**41**), arising from the hydrolysis of (**38**), and m/z 235 ($M+Na$)⁺ is consistent with diol (**42**). After reaction with benzylamine (Step-2), the mass spectrum of the crude reaction mixture showed no molecular ion for (**37**) and a low intensity molecular ion at m/z 268 ($M+H$)⁺ consistent with monobenzylated product (**40**) (Scheme 3.2). Changing the reaction conditions did not improve the outcome of this reaction and it became clear that a combination of inter- and intra-molecular reaction pathways were occurring post-epichlorohydrin functionalisation resulting in deactivation towards amine conjugation. Not surprisingly, attempts to immobilise ADH on the epoxy-modified fibrous PVA formed under the most promising reaction conditions described above (pH 8, PBS buffer, Reaction 7) resulted in poor enzyme immobilisation and a construct possessing low activity (0.170 ± 0.02 mmol/min/g fabric). In conclusion, this route to PVA modification was

abandoned in favour of other strategies providing well defined intermediates for enzyme attachment.



Scheme 3.2. Alternative reaction pathways post-epichlorhydrin attachment

Table 3.2 (Section 3.2.1) reveals that surface modification of PVA fibre and fabric was achieved *via* bromoacylation, chloroacylation, aminosilane, isocyanate and chlorotriazine formation. Other surface modification reactions failed even after exploring a range of reaction parameters such as reagent concentrations, temperatures, solvents and reaction times.

3.3 ADH immobilisation

In this section, ADH immobilisation was investigated on successfully modified PVA fabric scaffolds (Table 3.2) from Section 3.2.1. ADH immobilisation was performed on knitted PVA

fabric discs (13 mm diameter) to aid handling. After ADH immobilisation, the activity of the immobilised sample was measured and each experiment was conducted in triplicate. Fabric supports without any surface modification were treated with ADH under same conditions and used as controls. The PVA-ADH constructs with the highest activity were then assessed for stability under varying temperature, time and pH, and examined for reusability. Table 3.4 summarises ligation options between the surface modified PVA fabric and ADH enzyme.

Table 3.4 Covalent attachment of ADH and modified PVA fabric

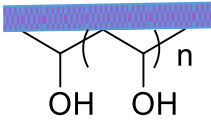
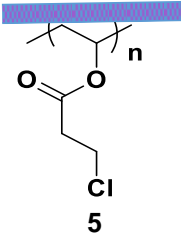
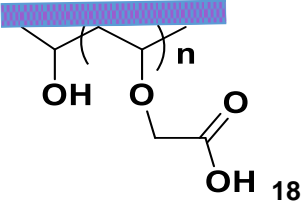
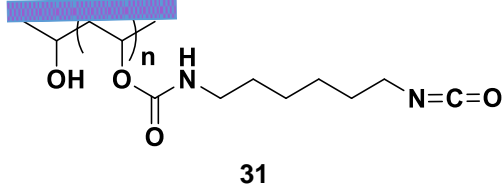
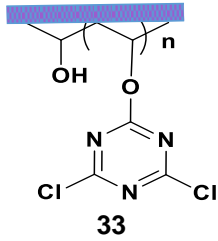
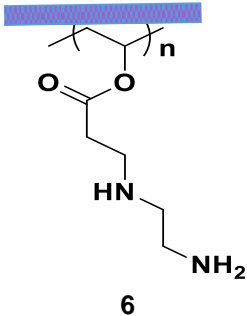
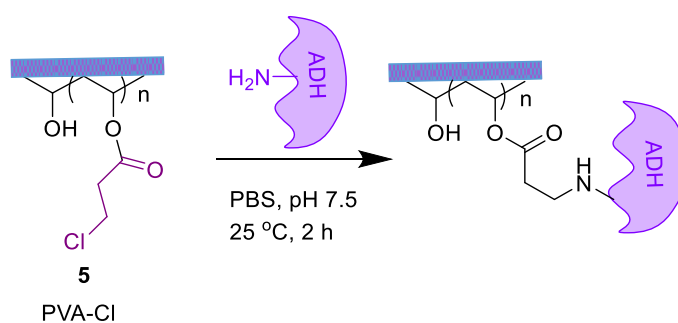
PVA modified support		Covalent Immobilisation
PVA fabric	 <p>The diagram shows a blue horizontal bar representing the fabric surface. Below it, a polymer chain is shown with two hydroxyl (-OH) groups attached to the backbone. The chain is labeled with 'n' to indicate it is a repeating unit.</p>	
PVA-Cl	 <p>The diagram shows a blue horizontal bar representing the fabric surface. Below it, a polymer chain is shown with a chloroethyl group (-CH₂CH₂Cl) attached to the backbone. The chain is labeled with 'n' to indicate it is a repeating unit. The number '5' is written below the chlorine atom.</p>	Chloride displacement by enzyme (-NH ₂)
PVA-COOH	 <p>The diagram shows a blue horizontal bar representing the fabric surface. Below it, a polymer chain is shown with a carboxylic acid group (-COOH) attached to the backbone. The chain is labeled with 'n' to indicate it is a repeating unit. The number '18' is written below the hydroxyl group of the carboxylic acid.</p>	Amide bond formation with enzyme (-NH ₂) upon activation

Table 3.4 Continued...		
PVA modified support		Covalent Immobilisation
PVA- isocyanate	 <p style="text-align: center;">31</p>	Carbamate formation
PVA-chlorotriazine	 <p style="text-align: center;">33</p>	Chloride displacement by enzyme (-NH ₂)
PVA-Cl-EDA	 <p style="text-align: center;">6</p>	Activation of amine with glutaraldehyde-Schiff base reaction with enzyme (-NH ₂)

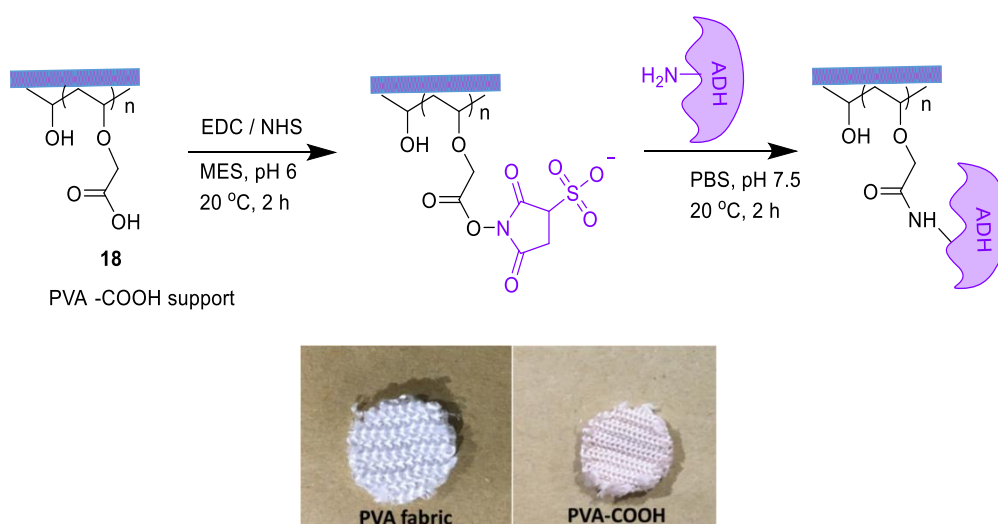
3.3.1 PVA-Cl immobilisation



Scheme 3.3. PVA-Cl support immobilisation with ADH

Fibrous PVA-Cl (**5**) from chloroacylation of PVA was used for ADH immobilisation as described in above Scheme 3.3. The ADH immobilisation procedure and activity assay were performed according to Sections 3.6.3.1.3 (1) and 3.7.2 respectively. The activity measured for the control discs was 0.036 ± 0.007 mmol/min/g fabric and for the treatment PVA fabric was 0.045 ± 0.012 mmol/min/g fabric. The activity values measured for both control and treatment discs were almost the same suggesting there was no covalent linkage between the PVA-Cl support and ADH. The recorded small amount of activity was presumably due to nonspecific interactions between the support and the enzyme. After an extended reaction time (4 h), no change in activity was observed (0.024 ± 0.02 mmol/min/g fabric). Efforts to increase ADH immobilisation were unsuccessful. Nucleophilic chloro displacement reactions usually require a strong unhindered base and higher temperature. The reaction conditions used for the enzyme bioconjugation were mild by comparison resulting in the lack of the desired conjugated product. Any increase in reaction temperature however would have deactivated the enzyme.

3.3.2 PVA-COOH immobilisation

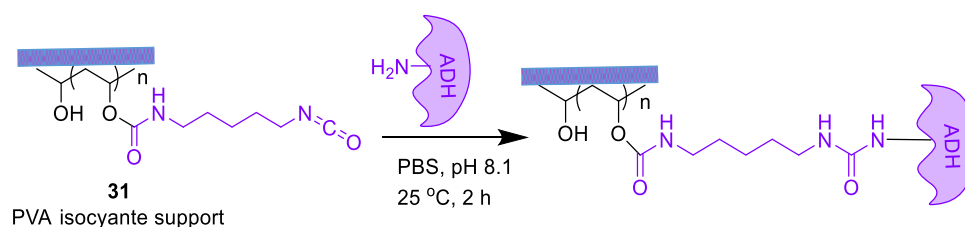


Scheme 3.4. EDC/NHS activation of PVA-COOH support and subsequent ADH immobilisation

Immobilisation of ADH on the PVA-COOH scaffold (**18**) involved a two step reaction: firstly, the activation of the acid groups of the PVA fabric with EDC/NHS, and secondly the covalent immobilisation of ADH (Scheme 3.4) The detailed experimental procedure for EDC/NHS activation and immobilisation is described in Experimental Section 3.6.3.2.7 (1).

ADH activity of the control and treatment (i.e. immobilised ADH on modified PVA acid) were 0.029 ± 0.006 mmol/min/g fabric and 0.039 ± 0.007 mmol/min/g fabric respectively. The activities of the two are not significantly different. The immobilisation procedure was also carried out at higher pH (pH 8.1) however no substantial difference in activity was observed (0.015 ± 0.02 mmol/min/g fabric). The low activity observed could be due to low immobilisation or conformational changes in the enzyme after immobilisation.

3.3.3 PVA-isocyanate immobilisation

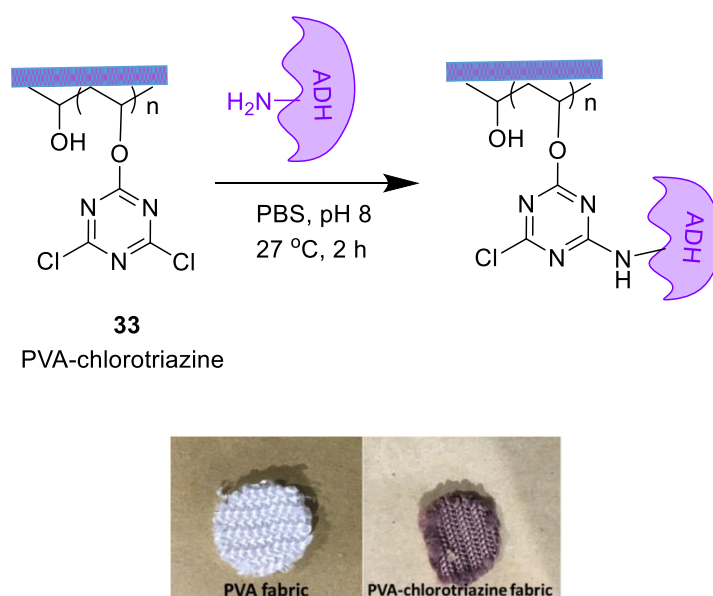


Scheme 3.5. ADH immobilisation on PVA isocyanate support

The objective of this functionalisation was to obtain isocyanate groups on the surface of fibrous PVA by means of a reaction with hexamethylene diisocyanate.³⁴ The reaction was run in such a way as to minimize the internal crosslinking by employing a large excess of hexamethylene diisocyanate to yield a pendent isocyanate with a six-carbon arm spacer linkage to the PVA surface. The advantages of the isocyanate functionality is its ability to undergo nucleophilic reaction with the enzyme without activation.

PVA isocyanate discs were exposed to ADH as shown in Scheme 3.5 and detailed immobilisation procedure is described in Experimental Section 3.6.3.4. The ADH activity for the isocyanate modified PVA was measured at 2.129 ± 0.028 mmol/min/g fabric while the control was measured at 2.758 ± 0.084 mmol/min/g fabric. Reasons for the poor activity are not known but could be due to the non-specific reaction of the catalytic functionality (e.g. active site cysteine and histidine residues) and/or deleterious conformational change.

3.3.4 PVA-chlorotriazine immobilisation

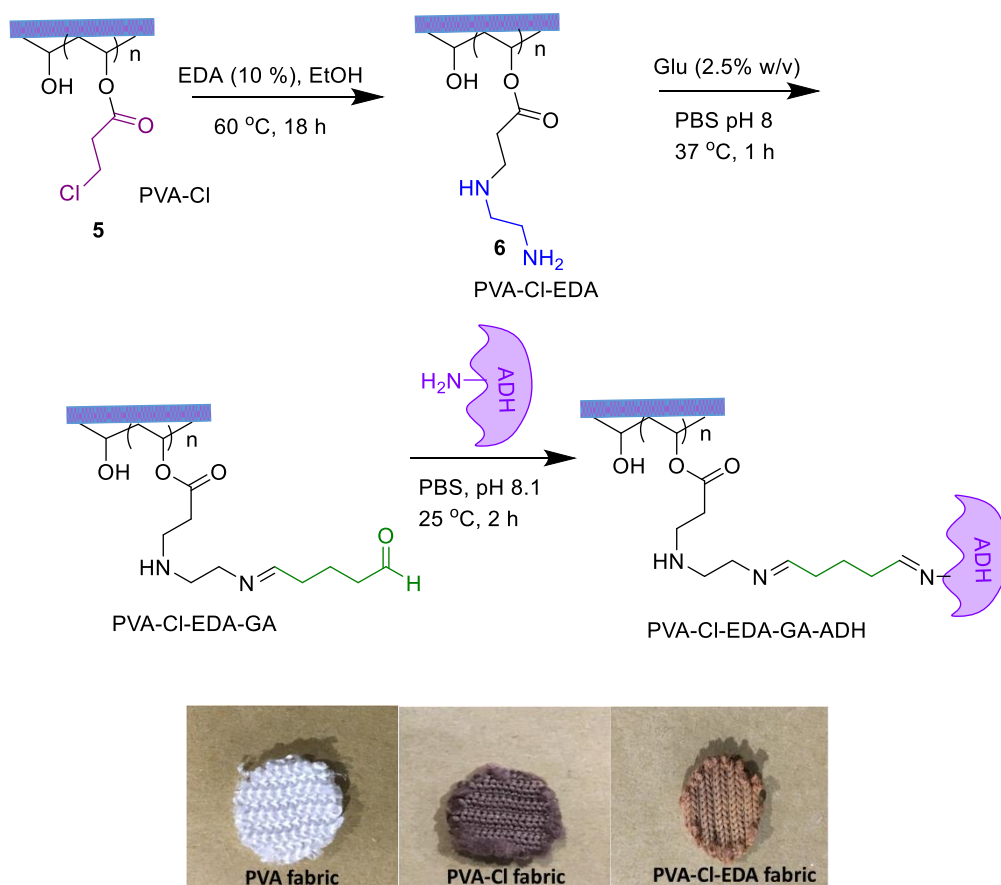


Scheme 3.6. ADH immobilisation using PVA-chlorotriazine support

The PVA chlorotriazine (**33**) scaffold was investigated for ADH immobilisation anticipating immobilisation through a chloro displacement reaction by side chain amine residues of ADH.³⁵ The chloro triazine modified PVA fabric supports were synthesised using TEA and NaHCO_3 bases and were subjected to ADH immobilisation separately. The ADH immobilisation on both chlorotriazine PVA fabrics (Scheme 3.6) was performed according to the procedure described in Experimental Section 3.6.3.5 (1). The activity of ADH when immobilised on chlorotriazine

PVA support synthesised with TEA base was 0.021 ± 0.001 mmol/min/g fabric and PVA-chlorotriazine generated with NaHCO_3 base showed the activity of 0.33 ± 0.0012 mmol/min/g fabric. The control PVA fabric (PVA fabric immobilised with ADH) showed an activity of 0.103 ± 0.007 mmol/min/g fabric under identical conditions. Reasons for the low activity of ADH are unclear but could be due to low immobilisation and/or deleterious enzyme conformation. This approach was subsequently abandoned.

3.3.5 PVA-Cl-EDA immobilisation



Scheme 3.7. ADH immobilisation on PVA-Cl-EDA-GA support

Low enzyme activity can also conceivably arise from steric effects imposed by ligation close to the support surface. Since immobilisation of ADH on PVA-Cl (see Section 3.3.1) resulted

only in low enzyme activity, the introduction of a spacer group, *via* reaction of ethylene diamine, was considered to increase the distance between the support surface and the enzyme using (EDA) (Scheme 3.7). Towards this end, Isgrove *et al.* reported enhanced activity of β -glucosidase and trypsin immobilised *via* a polyethyleneimine spacer arm compared with the corresponding support without an spacer arm.^{36,37} The PVA-Cl fibrous support was reacted with 10% EDA and subsequently crosslinked with GA (2.5% w/v in PBS) prior to exposure to ADH (Scheme 3.7). The PVA-Cl-EDA-GA fabric support immobilised with ADH and was measured for activity according to the procedure described in Experimental sections 3.6.3.1.4 and 3.7.2. The immobilised ADH showed an activity of 0.767 ± 0.037 mmol/min/g compared to the control PVA fabric of 0.187 ± 0.005 mmol/min/g fabric. Encouragingly, ADH immobilised *via* the EDA spacer showed approximately a sixfold excess in activity compared to the control. The activity observed from the above explorative ADH immobilisation is summarised below in Table 3.5.

Table 3.5 Activity data for immobilised ADH on modified PVA supports

No	PVA fabric supports	Immobilisation	Control (mmol/min/g)	Treatment (mmol/min/g)
1	PVA-Cl	pH 7.4, 25 °C, 2h	0.036 ± 0.004	0.045 ± 0.006
		pH 8.1, 25 °C, 4h	0.033 ± 0.071	0.0244 ± 0.002
2	PVA-COOH (EDC/NHS activation pH 6)	pH 7.5, 20 °C, 2h	0.029 ± 0.006	0.039 ± 0.014
		pH 8.1, 20 °C, 2h	0.0150 ± 0.022	0.0190 ± 0.07
3	PVA-isocyanate	pH 8.1, 25 °C, 2h	2.758 ± 0.008	2.129 ± 0.028
4	PVA-triazine(TEA)	pH 8.1, 27 °C, 2h	0.025 ± 0.006	0.0201 ± 0.001
5	PVA-triazine (NaHCO ₃)	pH 8.1, 27 °C, 2h	0.107 ± 0.13	0.033 ± 0.001
6	PVA-Cl-EDA-GA-activation	pH 8.1, 25 °C, 2h	0.187 ± 0.005	0.767 ± 0.037

Table 3.5 shows that ADH immobilised on PVA-Cl-EDA-GA fibrous scaffold showed the highest activity amongst all of the modified supports used for ADH immobilisation. The low activity observed by the other ADH constructs (1-5) could be due to one of the following reasons: i) low immobilisation, ii) loss of enzymatic activity during the immobilisation process, and/or iii) deleterious steric effects / conformational change imposed by immobilisation.

PVA-Cl-EDA-GA fibrous scaffold was consequently chosen as the lead PVA-ADH construct and further optimized *via* investigation of a) the PVA-Cl surface functionalization b) the spacer length and concentration, c) the PVA-Cl-EDA intermediate by IR spectroscopy, ¹³C-NMR spectrometry and microscopy. The PVA-Cl-EDA-GA-ADH construct was also assessed for stability (pH and thermal) and reusability. Complete stability studies of the PVA-Cl-EDA-GA-ADH are presented in publication format. The full citation for this work is provided below.

Immobilization and stabilization of alcohol dehydrogenase on polyvinyl alcohol fibre

Priydarshani Shinde, Mustafa Musameh, Yuan Gao, Andrea J. Robinson, and
Ilias (Louis) Kyrtzis

Biotechnology Reports, 2018, (19), e00260.

doi:[10.1016/j.btre.2018.e00260](https://doi.org/10.1016/j.btre.2018.e00260)



Immobilization and stabilization of alcohol dehydrogenase on polyvinyl alcohol fibre

Priyadarshani Shinde^{a,b}, Mustafa Musameh^a, Yuan Gao^a, Andrea J. Robinson^b, Ilias (Louis) Kyrtzsis^{a,*}

^a CSIRO Manufacturing, Clayton, VIC 3168, Australia

^b School of Chemistry, Monash University, Clayton, VIC 3800, Australia

ARTICLE INFO

Article history:

Received 11 December 2017

Received in revised form 12 May 2018

Accepted 24 May 2018

Available online xxx

Keywords:

Polyvinyl alcohol fibre

Alcohol dehydrogenase (ADH)

Enzyme immobilization

ABSTRACT

A polyvinyl alcohol (PVA) fibrous carrier has been chemically modified for the immobilization of yeast alcohol dehydrogenase (ADH) with an aim to increase its stability over a wide pH range, prolong its activity upon storage, and enhance its reusability. The strategy for immobilization involved functionalization of the fibrous carrier with chloropropionyl chloride followed by amination with ethylenediamine. Tethering of the ADH enzyme to the PVA scaffold was achieved with glutaraldehyde. The activity profile of the immobilized enzyme was compared to soluble enzyme as a function of pH, temperature and reusability. The immobilization of ADH on PVA fibrous carrier shifted the optimal reaction pH from 7 to 9, and improved the thermostability at 60 °C. Furthermore, the immobilized enzyme retained 60% of its original activity after eight cycles of reuse. These results demonstrate that PVA based textiles can serve as a flexible, reusable carrier for enzyme immobilization.

© 2018 Published by Elsevier B.V. This is an open access article under the CC BY-NC-ND license (<http://creativecommons.org/licenses/by-nc-nd/4.0/>).

1. Introduction

Alcohol dehydrogenase (ADH) has been widely used as a biocatalyst in synthetic chemistry. ADH catalyzes selective oxidation and reduction reactions and can be used for kinetic resolution, asymmetric synthesis [1–3], and drug preparation [4–6]. Its use in industrial transformations however, is limited by poor stability due to sensitivity to temperature and pH [7–9]. Under acidic conditions, ADH's multimeric subunits dissociate, and under alkaline conditions its tertiary structure gets distorted, both of which result in a loss of enzyme activity [10–12]. Attempts have been made to enhance the stability of ADHs via protein engineering [13,14], chemical modification and immobilization [15,16].

When immobilized on solid carriers, enzymes are generally more stable to denaturants and elevated temperature. Immobilized enzymes can be conveniently recovered from a process stream and recycled. This leads to simpler downstream processing and improved economics [17]. Various technologies have been developed for enzyme immobilization which comprise binding to a solid carrier, entrapment (encapsulation) and crosslinking [18,19]. Binding to a carrier can be via physical interaction (e.g. van der

Waals and hydrophobic interactions), and ionic and covalent bonding. Covalent immobilization provides a strong linkage between the enzyme and its carrier matrix to minimise enzyme leakage into the product stream, and therefore has been widely adopted by the chemical community [20–22].

ADH immobilization has been facilitated via several carriers including cellulose [23], epoxy functionalized nanoparticles [24], amino epoxy Sepabeads [25], agarose beads [26], and agarose activated carriers like MANAE-agarose, PEI-agarose, and glyoxyl agarose [27]. However, many of these protocols required toxic chemicals and/or expensive carrier materials such as synthetic mesoporous particles. Small particulate carriers can also result in slow reaction kinetics, and high back-pressure and blockage when used in packed columns and reactors [28–31].

Fibre and textile carriers have recently drawn considerable attention for enzyme immobilization due to their low price, large specific surface area, and ease of fabrication [32]. To date, common fibres such as cotton [33], silk [34], wool [28], polyester [35,36] and nylon [37–39] have been employed for enzyme immobilization mostly in non-woven form [14]. To the best of our knowledge, however, there are no reports on the use of polyvinyl alcohol (PVA) fibrous materials as carriers for enzyme immobilization despite its widespread utility in its hydrogel form [40,41].

PVA has been previously reported in the literature as a carrier for enzyme immobilization in various formats such as beads

* Corresponding author.

E-mail address: ily.kyrtzsis@csiro.au (I. Kyrtzsis).

[1,2], hydrogel particles [3–5], hybrid films [6,7] and electrospun nanofibrous mats [8]. The use of these formats of PVA in continuous flow reactors could adversely affect the flow parameters such as increasing backpressure and ultimately affecting the yield of the reaction. To the best of our knowledge, there are no reports on the use of polyvinyl alcohol (PVA) fabric materials as carriers for enzyme immobilization. The main advantage of fibres, including PVA fibres, is the ease of conversion into a fabric format with different “porosities” using traditional textile fabrication techniques such as weaving and knitting. Changing the porosity of the carrier can overcome flow issues related to back pressure etc. Further, PVA also possesses a functional group i.e. secondary hydroxyl capable of undergoing functionalization prior to enzyme immobilization. All of these features make PVA fabric a good candidate for the construction of a flexible carrier-enzyme construct suitable for continuous flow through processing.

Herein we report the immobilization of ADH onto PVA fibres in the form of knitted fabric discs. Carrier modification was facilitated by acylation of PVA with chloropropionyl chloride followed by the introduction of a spacer diamine. Subsequent reaction with glutaraldehyde and ADH then led to covalent attachment of the enzyme. The immobilized enzyme-carrier constructs were then analysed for reactivity, stability and recyclability and compared in performance to soluble ADH.

2. Materials and methods

2.1. Materials

3-Chloropropionylchloride (CPC-Cl), ethylenediamine (EDA), hexamethylenediamine (HMA), 1,12-dodecadiamine, glutaraldehyde (25 wt.% in water), alcohol dehydrogenase (ADH) from yeast (≥ 300 units/mg), nicotinamide adenine dinucleotide (NAD⁺), and Tris buffer were purchased from Sigma-Aldrich. Ethanol and tetrahydrofuran (THF) (analytical grade) were used as supplied from Merck. PVA yarn (250 dtex (i.e. mass in kg/1000 m length of yarn) 100 filaments, Solvron SHC) was purchased from Nitivy, Japan.

2.2. Methods

2.2.1. Characterisation

Infrared spectral analysis was carried out using a Nicolet 6700 ATR-FTIR (Thermo Scientific) in absorbance mode. Solid-state ¹³C cross-polarization (CP-MAS) NMR spectra were recorded on a Bruker AV500 MAS spectrometer. Morphology analysis was performed on a Scanning Electron Microscope (SEM, Philips XL30). The samples were imaged using a Zeiss Merlin FESEM after being coated with iridium under vacuum. Enzyme activity was measured using a Cary 300 Bio-UV visible spectrophotometer. Knitting was carried out using a flatbed Shima WG-14 (Japan).

2.2.2. Fabrication of knitted samples

PVA (Solvron SHC) yarn was knitted into a 2 × 1 rib with a loop length of 5.5 mm using a Shima WG-14 knitting machine. Discs of 13 mm in diameter were stamped from the knitted fabric, washed with deionised water, ethanol and dried in an oven at 50 °C before being subjected to further chemical modification.

2.2.3. PVA modification with chloropropionyl chloride (PVA-Cl)

PVA fabric discs (4.00 g, 0.0918 mol of available OH) were added into mixture of THF (80 mL) and triethylamine (28.8 mL, 0.211 mol) at room temperature in a three neck round bottom flask. 3-Chloropropionyl chloride (21.0 mL, 0.22 mol) was added dropwise at 0 °C over 30 min and then the reaction was heated at 60 °C for 18 h. The discs were then removed from the reaction mixture and washed with distilled water, ethanol and dried at 50 °C.

2.2.4. Spacer inclusion on PVA-Cl carrier

The introduction of a spacer involves two steps (A and B) as shown in Fig. 1.

2.2.4.1. Ethylenediamine modification (PVA-Cl-EDA). The PVA-Cl discs (1 g) were added to an EDA solution (30% (w/v) in ethanol, 10 mL) and heated at 60 °C for 5 h. After cooling, the aminated discs were washed with distilled water and then ethanol to remove residual diamine.

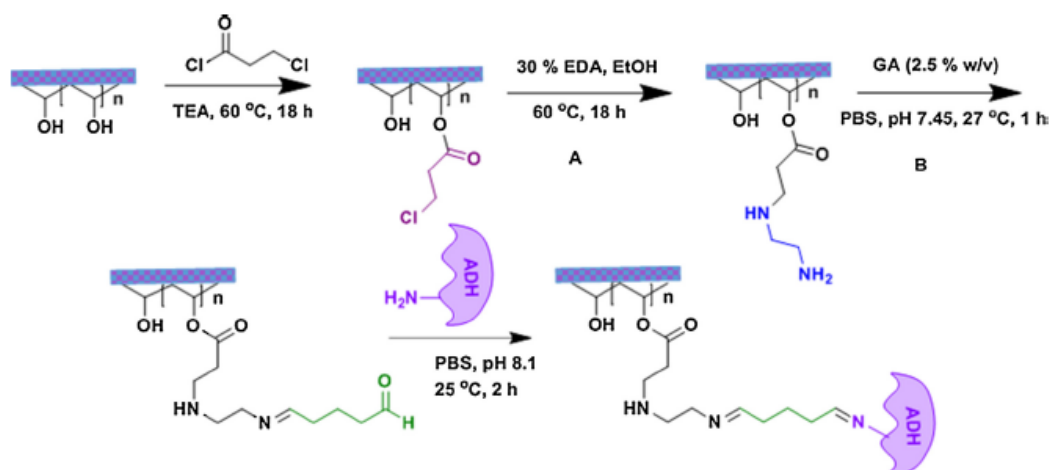


Fig. 1. Schematic representation of covalent immobilization of ADH on modified PVA fibrous carrier.

2.2.4.2. Cross-linking with glutaraldehyde (PVA-Cl-EDA-GA). The PVA-Cl-EDA fabric discs were activated with 2.5% (w/v) GA in phosphate buffer (PBS 0.05 M, pH 7.5) for 1 h at 27 °C in a sealed flask [42]. The carrier discs were thoroughly washed with distilled water over 30 min. to remove excess GA.

2.2.5. ADH immobilization

ADH (0.5 mg/mL) was dissolved in phosphate buffer (0.05 M, pH 8.1). The GA activated fabric discs (PVA-Cl-EDA-GA) were placed in a 12 well plate containing the ADH solution. After incubation for 2 h at 25 °C the carrier discs were washed with phosphate buffer (0.05 M, pH 8.1) four times over 30 min to remove unbound enzyme. PVA fabric without surface modification, PVA-Cl and PVA-Cl-EDA, were treated in an analogous way and subsequently used as controls.

2.2.6. ADH activity assay

ADH catalyses the oxidation of ethanol to acetaldehyde in the presence of nicotinamide adenine dinucleotide (NAD⁺).

The activity of ADH was determined spectrophotometrically by measuring the absorbance of NADH at 340 nm [43]. The activity of ADH immobilized on the carrier was assayed by immersing the carrier discs individually in Tris buffer (100 mM, pH 8.8), ethanol (20 mM), and NAD⁺ (1 mM) at 25 °C in 12 well plate. After shaking for 4 min at 100 rpm on an orbital shaker, 1 mL of the solution was withdrawn for absorbance measurement. The activity measurement experiments were performed in triplicate and the results were presented as averages \pm standard deviation.

The effect of pH on enzyme stability was measured in different buffer systems; for pH 6.5–8.0 sodium phosphate buffer (0.05 M)

and for pH 8.5–10.5, sodium carbonate/bicarbonate buffer (0.1 M) were used. The soluble ADH and immobilized ADH were incubated at 40 °C for 2 h in the various pH buffer solutions. The thermostability study was performed by incubating the soluble ADH (0.5 mg/mL) and the immobilized ADH for 2 h in phosphate buffer (0.05 M, pH 8.1) at various temperatures (20 °C, 40 °C, 60 °C, 80 °C) in a water bath. After each incubation, the enzyme was chilled in crushed ice for 5 min. The enzyme was then slowly brought to room temperature and activity was determined as described above.

Reusability of immobilized enzyme was measured by repetitive usage of the immobilized ADH to catalyse ethanol to acetaldehyde. After each use, the discs were washed with phosphate buffer (0.05 M, pH 7.5) in triplicate and the activity was remeasured using a fresh reaction mixture.

3. Results and discussion

3.1. Surface modification of PVA

Covalent attachment of an enzyme to a solid carrier can be achieved by carrier modification to generate reactive groups on the carrier. The electrophilic formyl groups introduced on the carrier will react with nucleophilic sites on the enzyme. In this paper we have used this approach to modify the PVA backbone to achieve enzyme immobilization.

Chloroacetylation [44] and bromoacetylation [45] of powdered PVA with chloroacetic acid and bromopropionyl bromide reagents have been used to synthesize branched polymers (e.g. stars, combs, or dendrigrafts) with higher tensile strength. In this

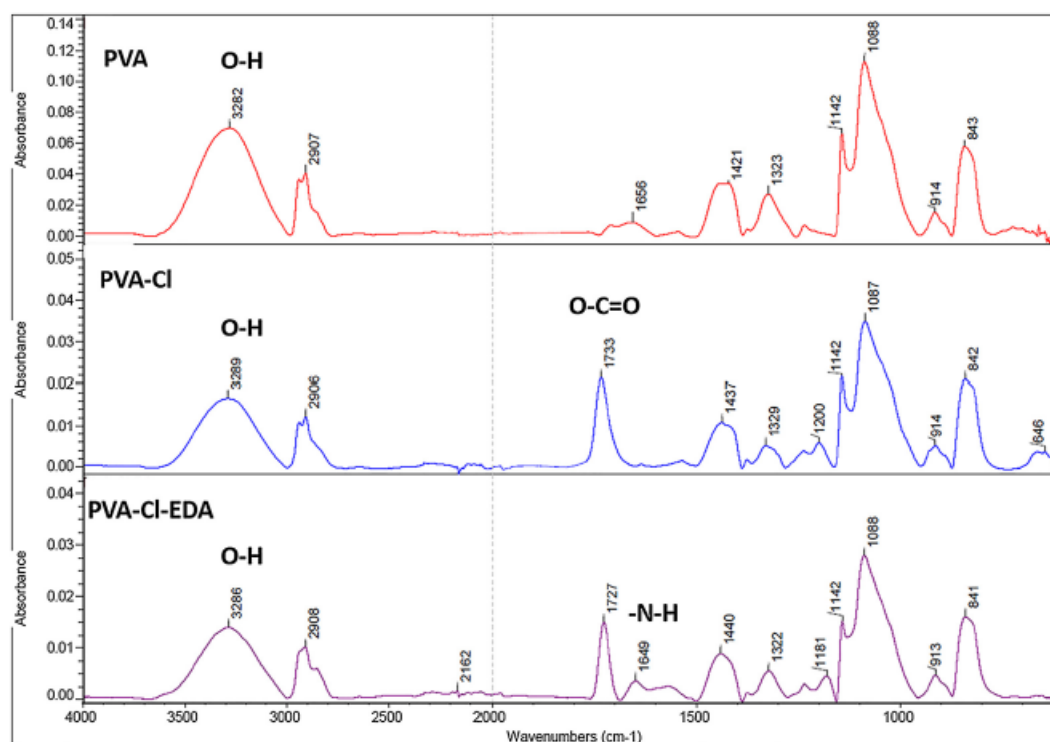


Fig. 2. ATR-FTIR spectra of PVA, PVC-Cl and PVA-Cl-EDA.

Table 1
ADH activity after immobilization on various modified PVA carriers.

PVA fibrous carriers	Activity (mmol/g min)
PVA-Cl-EDA-GA+ADH	0.765 ± 0.03
PVA-Cl-EDA+ADH	0.210 ± 0.02
PVA-Cl+ADH	0.170 ± 0.02
PVA+ADH	0.105 ± 0.07

study PVA fibres were functionalized by reaction with chloropropionyl chloride. In order to optimise the acylation process, the reaction was performed at different temperatures (20 °C, 40 °C, 60 °C, and 80 °C) and the resulting polymer was analysed by IR (data not shown). Optimal reaction was observed at 60 °C. Further increase in reaction temperature (85 °C) caused rapid disintegration of the PVA fabric resulting in the formation of a gel. In addition, the effect of reaction time (2 h, 6 h, 12 h, 18 h, and 24 h) was assessed and acylation was found to increase from 2 h to 18 h and plateau thereafter (data not shown). Hence, optimised acylation conditions were determined to be reaction at 60 °C for 18 h.

Several studies have reported the effect of spacer length and type of spacer between enzyme and carrier and its effect on the activity of the immobilized enzyme [38,46,47]. Higher activity is observed when a spacer is incorporated between the carrier and enzyme to reduce steric hindrance, promote conformational mobility, and reduce adverse surface interaction [18,19,48]. A spacer was introduced to the PVA-Cl discs by reaction with diamine in ethanol and resultant amine was reacted with glutaraldehyde [49,50].

3.1.1. Characterization of modified PVA carrier

The surface modification of PVA-Cl and PVA-Cl-EDA were confirmed by ATR-FTIR shown in Fig. 2. The spectra for PVA, PVA-Cl, and PVA-Cl-EDA fabrics show the change of chemical structure of the original and modified PVA fibrous carrier respectively. The PVA-Cl spectrum shows a distinct strong peak at 1733 cm^{-1} due to the ester group stretching vibration [44] and a peak at 646 cm^{-1} corresponding to the C—Cl stretching vibration of the PVA-Cl side chain. The PVA-Cl-EDA spectrum showed a new weak peak at 1649 cm^{-1} due to N—H bending vibration resulting from amino group present in PVA-Cl-EDA. Moreover the peak at 646 cm^{-1} disappears in the spectrum of the PVA-Cl-EDA. This supports successful nucleophilic substitution by ethylenediamine on the modified PVA-Cl-EDA construct. The presence of a broad peak at approximately 3286 cm^{-1} supports the presence of O—H and N—H stretching bands. Further characterisation with ^{13}C NMR was reported in Supplementary document (S.1).

The morphologies of PVA fibrous carriers with and without surface modification are shown in Fig. 3. Importantly, the integrity of the modified PVA fibrous carrier structure was maintained throughout the chemical modification process.

3.2. ADH immobilization

The immobilization of an enzyme onto carriers can take place either by adsorption or by the formation of covalent bonds between the nucleophilic amino acids of the enzyme and the functional group of the solid carrier. The binding forces of physical adsorption, such as van der Waals binding, hydrophobic or ionic interactions, are often too weak to keep the adsorbed enzymes

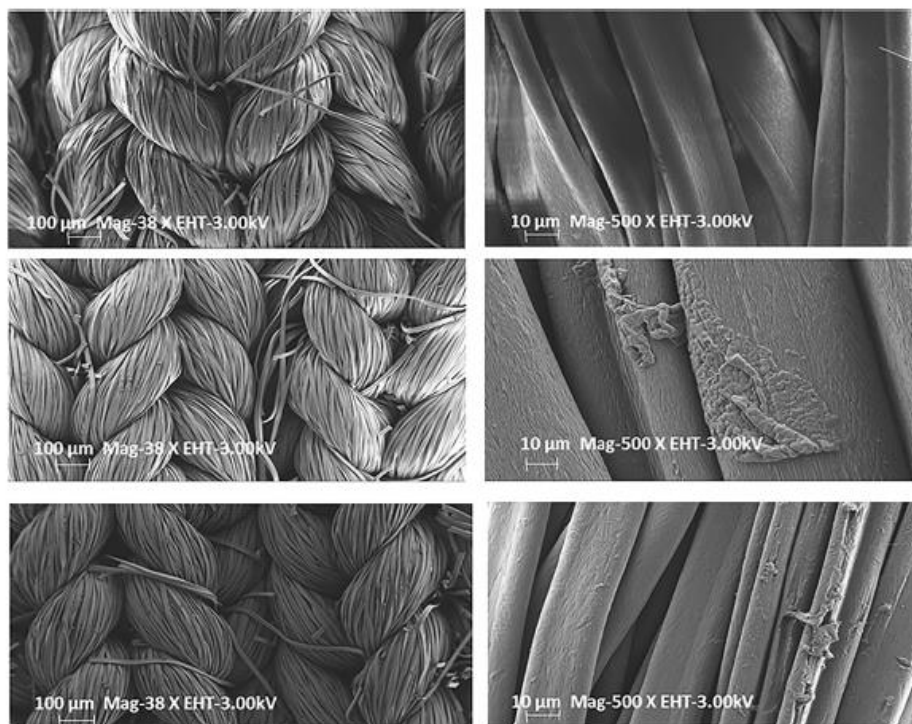


Fig. 3. SEM micrographs of PVA fibre surfaces (100 μm and 10 μm) after different chemical modifications: A) Before treatment; B) After treatment with chloropropionyl chloride; C) After treatment with chloropropionyl chloride, ethylenediamine and glutaraldehyde.

fixed to the carrier during use or washing. However, covalent attachment is strong and enables the enzyme molecules to be anchored to the carrier during use or repeated washing [18,19,51].

The measured activities for glutaraldehyde activated and non-activated immobilized carriers (i.e. PVA, PVA-Cl, PVA-Cl-EDA and PVA-Cl-EDA-GA) are shown in Table 1. There was a small amount of ADH activity recorded with PVA, PVA-Cl and PVA-Cl-EDA presumably due to nonspecific binding. When ADH was immobilized onto the PVA-Cl-EDA-GA fibrous carrier, a 7.3 fold increase in activity was observed compared to the PVA control (without chemical modification). This increase in activity supports successful ADH immobilization at pH 8.1.

The effect of spacer length on the activity of the immobilized ADH was investigated by incubating PVA-Cl discs in EDA, HMA and 1,12-dodecadiamine in ethanol (20% w/v) respectively at 60 °C for 5 h (diamine concentrations details were printed in Supporting document S_1). In the second step, the aminated PVA carriers were reacted with GA prior to enzyme attachment. Previous work suggested that branched amines such as PEI and polylysine would provide multiple binding sites for immobilization [52]. In this study this approach was further extended by producing spacer arms of defined length by using linear diamines of increasing carbon length (C2, C6 and C12). The experimental results on the effect of the spacer length on the activity of the immobilized ADH are presented in Table 2 and Supplement document).

Upon ADH immobilization, the highest activity was observed with EDA ($n=2$). When ADH was immobilized with the HMA spacer ($n=6$) a lower activity was recorded, and with the 1,12-dodecadiamine spacer ($n=12$) activity was greatly diminished. Loss of activity could be either due to aggregation of the saturated amines in the aqueous medium [53] or could also be the fact that longer diamines may be more prone to both ends reacting with the PVA-Cl surface, hence not as many options for ADH to immobilise. The EDA spacer provided the highest activity and hence was used in all subsequent work. The effect of EDA concentration was measured by reacting PVA-Cl fabric discs with EDA concentrations ranging from 10 to 40% (w/v) in ethanol. The EDA modified discs were immobilized with ADH after GA activation. Fig. 4 shows the effect different concentrations of EDA (10 to 30% w/v in ethanol) spacer on ADH activity. The activity of the ADH enzyme increased with increasing the concentration of EDA and the highest activity

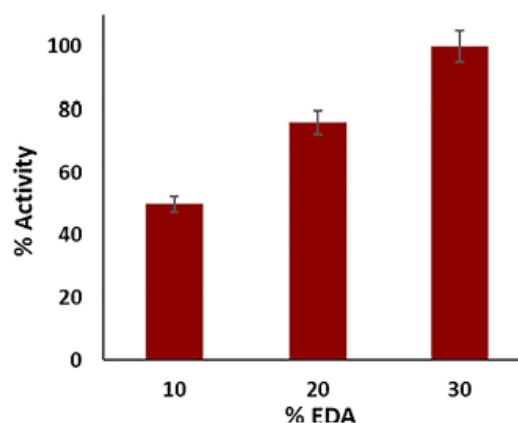


Fig. 4. The effect of EDA concentration on activity of immobilized ADH.

was observed with 30% EDA (0.785 ± 0.05 mmol/min g). Higher concentrations of EDA (above 30%) lead to disintegration of the PVA fabric.

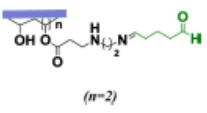
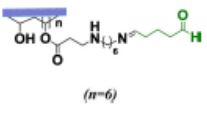
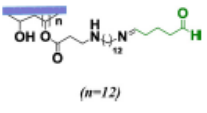
3.3. Stability of immobilized ADH

Immobilized enzymes are more easily recovered and recycled than soluble enzymes and can also possess higher stability over wider physical and chemical conditions [19]. Both of these features are essential for industrial applications where immobilized enzymes are required to sustain wider pH and temperature ranges to achieve optimal process.

3.3.1. pH stability

Enzyme stability is heavily dependent on the pH of the solution. The effect of pH on the enzyme stability was investigated by treating soluble ADH and immobilized ADH at 40 °C for 2 h at different pH values before their activities were measured (Fig. 5). The soluble enzyme showed good stability at pH 5–7. There was a

Table 2
Effect of diamine spacer length on immobilized ADH activity.

Diamine	Spacer	Activity (mmol/g min)
Ethylenediamine (EDA)	 ($n=2$)	0.512 ± 0.05
Hexamethylenediamine (HMA)	 ($n=6$)	0.283 ± 0.01
1,12-dodecadiamine	 ($n=12$)	0.063 ± 0.04

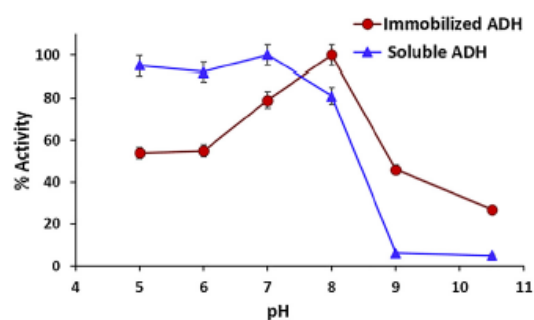


Fig. 5. Stability of soluble and immobilized ADH at different pHs. Both soluble ADH and immobilized ADH were incubated at 40 °C for 2 h in different pH buffered solutions.

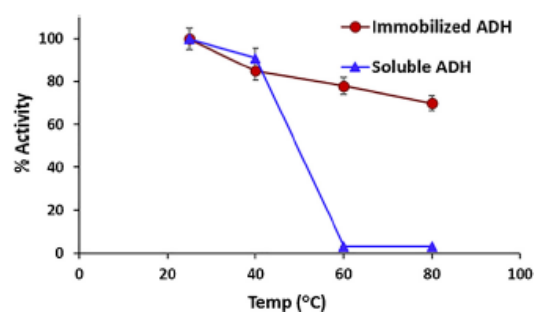


Fig. 6. Thermostability of soluble and immobilized ADH after being heated at different temperatures in phosphate buffer (0.05 M, pH 8.1) for 2 h.

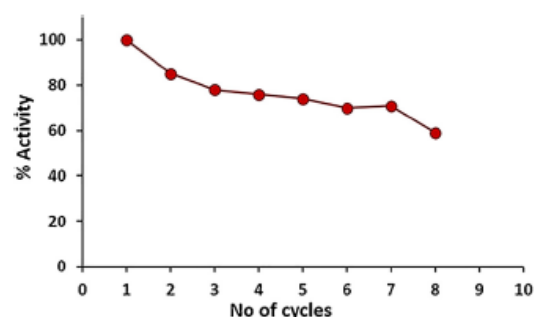


Fig. 7. Reusability of the immobilized ADH.

decrease in stability at pH 8 (with ~80% retention in activity) and complete loss of activity at pH 9 or higher. Immobilization of ADH changed its pH stability profile, with enzyme retaining 46% and 27% of its activity at pH 9 and 10.5, respectively. The optimal stability shifted to pH 8 compared to pH 5–7 for the soluble form. These findings show that covalent immobilization can provide enhanced pH stability with retention of enzyme activity over a broader pH range. Multipoint covalent attachment of the enzyme would reduce the conformational freedom of the enzyme and may be responsible for the enhanced stability profile. A similar

broadening of pH stability has been reported when ADH is immobilized on attapulgite nanofibers [54].

3.3.2. Thermostability

The thermostability of the immobilized and soluble ADH was assessed by treatment at different temperatures (20 °C–80 °C) for 2 h. Fig. 6 shows that there was a rapid thermal inactivation of soluble ADH at 60 °C and higher temperatures. Significantly, the immobilized ADH preserved 80% and 60% of its activity after being heated at 60 °C and 80 °C respectively.

Thermal denaturation of ADH at higher temperature (T_d 63 °C) is thought to arise from irreversible oxidation, aggregation and deamidation of the protein [9]. The observed increased thermal stability of the immobilized enzyme could also be due to multipoint attachment of the enzyme to the carrier (i.e. reduction in intermolecular reaction). Similar improvement in stability was observed when ADH was immobilized on glyoxyl agarose [55], magnetic graphene oxide nanocomposites [56], glass beads [12], and a cyanogen bromide-activated Sepharose system [57].

3.3.3. Reusability

An advantage of immobilized enzymes is their potential for reuse. To evaluate the reusability of the immobilized ADH, carrier discs with immobilized ADH were repeatedly suspended in a fresh reaction mixture for enzyme activity measurements. Between measurements the carrier discs were washed with phosphate buffer (0.05 M, pH 7.5).

Fig. 7 shows that the efficacy of the immobilized ADH declined slightly after each use, probably due to the change in conformation of immobilized enzyme after repeated washings or some enzyme detachment from the carrier (because of imine or ester hydrolysis). After eight consecutive runs, the immobilized ADH retained 60% of its original activity.

4. Conclusions

In summary, PVA textile fibrous carrier has been chemically modified and used for enzyme immobilization. It was found that ADH could be covalently immobilized on the modified PVA fibre to provide an immobilised form of the enzyme possessing good operational stability over a wider pH range and higher thermostability as compared to soluble ADH. Furthermore, the immobilized enzyme retained 60% of its original activity after eight reaction cycles making it attractive for industrial applications. These results indicate that PVA fibrous material can be used as an effective carrier material for enzyme immobilization.

Conflict of interest

None.

Funding

This work was supported by The Science and Industry Endowment Fund (SIEF) CSIRO Australia.

Acknowledgment

The authors greatly acknowledge Mr Peter Herwig from CSIRO for the knitting of PVA fabrics.

Appendix A. Supplementary data

Supplementary material related to this article can be found, in the online version, at doi:<https://doi.org/10.1016/j.btre.2018.e00260>.

References

- [1] J.C. Moore, et al., Advances in the enzymatic reduction of ketones, *Acc. Chem. Res.* 40 (12) (2007) 1412–1419.
- [2] S.M.A. De Wildeman, et al., Biocatalytic reductions: from lab curiosity to “first choice”, *Acc. Chem. Res.* 40 (12) (2007) 1260–1266.
- [3] T. Matsuda, R. Yamana, K. Nakamura, Recent progress in biocatalysis for asymmetric oxidation and reduction, *Tetrahedron: Asymmetry* 20 (5) (2009) 513–557.
- [4] Y. Huang, et al., Dehydrogenases/reductases for the synthesis of chiral pharmaceutical intermediates, *Curr. Org. Chem.* 14 (14) (2010) 1447–1460.
- [5] R.d.S. Pereira, The use of baker's yeast in the generation of asymmetric centers to produce chiral drugs and other compounds, *Crit. Rev. Biotechnol.* 18 (1) (1998) 25–64.
- [6] M. Breuer, et al., Industrial methods for the production of optically active intermediates, *Angew. Chem. Int. Ed.* 43 (7) (2004) 788–824.
- [7] V. Leskovic, S. Trivić, D. Pečin, The three zinc-containing alcohol dehydrogenases from baker's yeast, *Saccharomyces cerevisiae*, *FEMS Yeast Res.* 2 (4) (2002) 481–494.
- [8] S.B. Raj, S. Ramaswamy, B.V. Plapp, Yeast alcohol dehydrogenase structure and catalysis, *Biochemistry* 53 (36) (2014) 5791–5803.
- [9] K.A. Markossian, et al., Mechanism of thermal aggregation of yeast alcohol dehydrogenase I: role of intramolecular chaperone, *Biochim. Biophys. Acta (BBA)—Proteins Proteom.* 1784 (9) (2008) 1286–1293.
- [10] J.M. Bolivar, et al., Stabilization of a highly active but unstable alcohol dehydrogenase from yeast using immobilization and post-immobilization techniques, *Process Biochem.* 47 (5) (2012) 679–686.
- [11] O. De Smidt, J.C. Du Preez, J. Albertyn, The alcohol dehydrogenases of *Saccharomyces cerevisiae*: a comprehensive review, *FEMS Yeast Res.* 8 (7) (2008) 967–978.
- [12] Y. Yang, R. Chen, H.M. Zhou, Comparison of inactivation and conformational changes of native and apo yeast alcohol dehydrogenase during thermal denaturation, *Biochem. Mol. Biol. Int.* 45 (3) (1998) 475–487.
- [13] K.M. Polizzi, et al., Stability of biocatalysts, *Curr. Opin. Chem. Biol.* 11 (2) (2007) 220–225.
- [14] S.W. Chenevert, et al., Amino acids important in enzyme activity and dimer stability for *Drosophila* alcohol dehydrogenase, *Biochem. J.* 308 (Pt. 2) (1995) 419–423.
- [15] V. Stepankova, et al., Strategies for stabilization of enzymes in organic solvents, *ACS Catal.* 3 (12) (2013) 2823–2836.
- [16] Y. Zhang, J. Ge, Z. Liu, Enhanced activity of immobilized or chemically modified enzymes, *ACS Catal.* 5 (8) (2015) 4503–4513.
- [17] R.K. Singh, et al., From protein engineering to immobilization: promising strategies for the upgrade of industrial enzymes, *Int. J. Mol. Sci.* 14 (1) (2013) 1232–1277.
- [18] B. Brena, P. González-Pombo, F. Batista-Viera, Immobilization of enzymes: a literature survey, in: J.M. Guisan (Ed.), *Immobilization of Enzymes and Cells*, Humana Press, 2013, pp. 15–31.
- [19] S. Datta, L.R. Christena, Y.R.S. Rajaram, Enzyme immobilization: an overview on techniques and support materials, *3 Biotech* 3 (1) (2013) 1–9.
- [20] I. Es, J.D. Gonçalves Vieira, A.C. Amaral, Principles, techniques, and applications of biocatalyst immobilization for industrial application, *Appl. Microbiol. Biotechnol.* 99 (5) (2015) 2065–2082.
- [21] R.A. Sheldon, S. van Pelt, Enzyme immobilisation in biocatalysis: why, what and how, *Chem. Soc. Rev.* 42 (15) (2013) 6223–6235.
- [22] M.G. Roig, et al., Biotechnology and applied biology section: methods for immobilizing enzymes, *Biochem. Educ.* 14 (4) (1986) 180–185.
- [23] K.A. Pithawala, A. Bahadur, Studies on the immobilization of alcohol dehydrogenase and alkaline phosphatase onto cellulosic supports, *Cell. Chem. Technol.* 36 (3–4) (2002) 265–273.
- [24] X.-P. Jiang, et al., Immobilization of dehydrogenase onto epoxy-functionalized nanoparticles for synthesis of (*R*)-mandelic acid, *Int. J. Biol. Macromol.* 88 (2016) 9–17.
- [25] C. Mateo, et al., Epoxy-amino groups: a new tool for improved immobilization of proteins by the epoxy method, *Biomacromolecules* 4 (3) (2003) 772–777.
- [26] J.M. Guisan, Aldehyde-agarose gels as activated supports for immobilization-stabilization of enzymes, *Enzyme Microb. Technol.* 10 (6) (1988) 375–382.
- [27] C. Mateo, et al., Glyoxyl agarose: a fully inert and hydrophilic support for immobilization and high stabilization of proteins, *Enzyme Microb. Technol.* 39 (2) (2006) 274–280.
- [28] X.D. Feng, et al., Enabling the utilization of wool as an enzyme support: enhancing the activity and stability of lipase immobilized onto woolen cloth, *Colloids Surf. B: Biointerfaces* 102 (2013) 526–533.
- [29] P. Zucca, E. Sanjust, Inorganic materials as supports for covalent enzyme immobilization: methods and mechanisms, *Mol. Cell. Probes* 19 (9) (2014) 14139.
- [30] N.T.S. Phan, D.H. Brown, P. Styring, A facile method for catalyst immobilisation on silica: nickel-catalysed Kumada reactions in mini-continuous flow and batch reactors, *Green Chem.* 6 (10) (2004) 526–532.
- [31] S.J. Haswell, et al., The application of micro reactors to synthetic chemistry, *Chem. Commun.* (5) (2001) 391–398.
- [32] K. Kiehl, et al., Strategies for permanent immobilization of enzymes on textile carriers, *Eng. Life Sci.* 15 (6) (2015) 622–626.
- [33] J.V. Edwards, et al., Covalent attachment of lysozyme to cotton/cellulose materials: protein versus solid support activation, *Cellulose* 18 (5) (2011) 1239–1249.
- [34] S. Chatterjee, et al., Silk-fiber immobilized lipase-catalyzed hydrolysis of emulsified sunflower oil, *Appl. Biochem. Biotechnol.* 157 (3) (2009) 593–600.
- [35] Y. Gao, et al., Bioremediation of pesticide contaminated water using an organophosphate degrading enzyme immobilized on nonwoven polyester textiles, *Enzyme Microb. Technol.* 54 (2014) 38–44.
- [36] K. Opwis, D. Knüttel, E. Schollmeyer, Functionalization of catalase for a photochemical immobilization on poly(ethylene terephthalate), *Biotechnol. J.* 2 (3) (2007) 347–352.
- [37] A. Freeman, M. Sokolovsky, L. Goldstein, Chemically modified nylons as supports for enzyme immobilization, *J. Solid-Phase Biochem.* 1 (4) (1976) 261–274.
- [38] F.H. Isgrove, et al., Enzyme immobilization on nylon-optimization and the steps used to prevent enzyme leakage from the support, *Enzyme Microb. Technol.* 28 (2–3) (2001) 225–232.
- [39] S. Pahuji, et al., Glutaraldehyde activation of polymer Nylon-6 for lipase immobilization: enzyme characteristics and stability, *Bioresour. Technol.* 99 (7) (2008) 2566–2570.
- [40] M. Cereti, et al., Immobilisation of pectinases into PVA gel for fruit juice application, *Int. J. Food Sci. Technol.* 52 (2) (2017) 531–539.
- [41] M. Rebroš, et al., Hydrolysis of sucrose by invertase entrapped in polyvinyl alcohol hydrogel capsules, *Food Chem.* 102 (3) (2007) 784–787.
- [42] J.C. Santos, et al., *Pseudomonas fluorescens* lipase immobilization on polysiloxane-polyvinyl alcohol composite chemically modified with epichlorohydrin, *J. Mol. Catal. B: Enzym.* 52–53 (0) (2008) 49–57.
- [43] J.R.L. Walker, Spectrophotometric determination of enzyme activity: alcohol dehydrogenase (ADH), *Biochem. Educ.* 20 (1) (1992) 42–43.
- [44] B. Jin, et al., Synthesis, characterization, thermal stability and sensitivity properties of the new energetic polymer through the azidoacetylation of poly(vinyl alcohol), *Polym. Degrad. Stab.* 97 (4) (2012) 473–480.
- [45] J. Bernard, et al., Synthesis of poly(vinyl alcohol) combs via MADIX/RAFT polymerization, *Polymer* 47 (4) (2006) 1073–1080.
- [46] T. Cao, et al., Investigation of spacer length effect on immobilized *Escherichia coli* pili-antibody molecular recognition by AFM, *Biotechnol. Bioeng.* 98 (6) (2007) 1109–1122.
- [47] A. De Maio, et al., Influence of the spacer length on the activity of enzymes immobilised on nylon/polyGMA membranes: part 1. Isothermal conditions, *J. Mol. Catal. B: Enzym.* 21 (4–6) (2003) 239–252.
- [48] E.J. Shim, et al., Development of an enzyme-immobilized support using a polyester woven fabric, *Text. Res. J.* 87 (1) (2017) 3–14.
- [49] I. Migneault, et al., Glutaraldehyde: behavior in aqueous solution, reaction with proteins, and application to enzyme crosslinking, *Biotechniques* 37 (5) (2004) 790–802.
- [50] K.-J. Kim, S.-B. Lee, N.-W. Han, Kinetics of crosslinking reaction of PVA membrane with glutaraldehyde, *Korean J. Chem. Eng.* 11 (1) (1994) 41–47.
- [51] G. Peng, et al., Stabilized enzyme immobilization on micron-size PSt-GMA microspheres: different methods to improve the carriers' surface biocompatibility, *RSC Adv.* 6 (94) (2016) 91431–91439.
- [52] D. Kim, A.E. Herr, Protein immobilization techniques for microfluidic assays, *Biomicrofluidics* 7 (4) (2013) 041501.
- [53] B.S. Mahesh, *Biotechnology-3: including molecular biology biophysics*, *Biotechnology* 3 (2003) 227.
- [54] Q. Zhao, et al., Characterization of alcohol dehydrogenase from permeabilized brewer's yeast cells immobilized on the derived attapulgite nanofibers, *Appl. Biochem. Biotechnol.* 160 (8) (2010) 2287–2299.
- [55] J.M. Bolivar, et al., Improvement of the stability of alcohol dehydrogenase by covalent immobilization on glyoxyl-agarose, *J. Biotechnol.* 125 (1) (2006) 85–94.
- [56] M.-H. Liao, D.-H. Chen, Immobilization of yeast alcohol dehydrogenase on magnetic nanoparticles for improving its stability, *Biotechnol. Lett.* 23 (20) (2001) 1723–1727.
- [57] H. Görisch, M. Schneider, Stabilization of soluble and immobilized horse liver alcohol dehydrogenase by adenosine 5'-monophosphate, *Biotechnol. Bioeng.* 26 (8) (1984) 998–1002.

3.4 Storage stability of PVA-Cl-EDA-GA immobilised ADH

The PVA-Cl-EDA-GA-ADH construct was further investigated for storage stability and its suitability for use in a bioreactor or biosensor. Enzyme activity often declines over time due to autolysis or microbial growth however immobilisation has been shown to reduce both of these factors.³⁸ The storage stability of the soluble and immobilised ADH was evaluated at 4 °C in PBS buffer (0.05M, pH 7.45) for 30 days and activity measurements were taken at time zero, day 2, day 5, day 10, day 20 and day 25 using the standard assay method. Disappointingly, after two days, both the soluble and immobilised ADH showed a 35% and 30% loss in activity respectively (Figure 3.2).

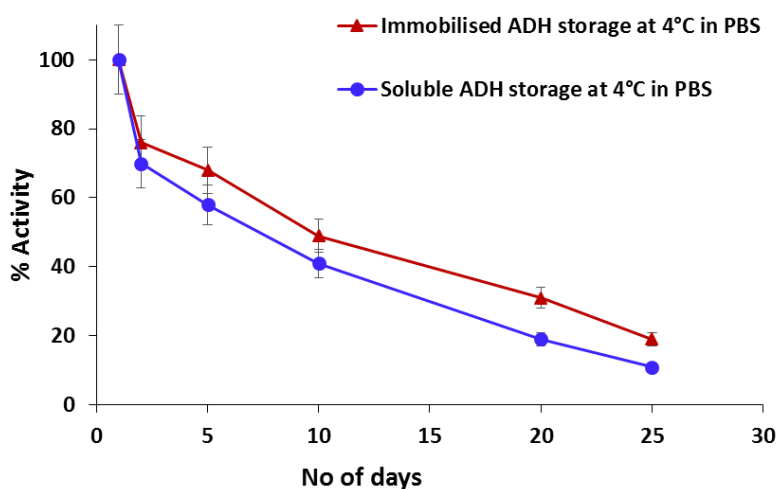


Figure 3.2. Storage stability of the immobilised ADH. The activity measurements were performed in triplicate and error bars present standard deviations. The highest activity was taken as 100 % and subsequent % activity was normalised against this value.

Thereafter there was a continuous decrease in activity for both soluble and immobilised ADH with denaturation of the immobilised ADH occurring slightly more slowly. Analogous results have been reported for ADH immobilised on cyanogen bromide-activated Sepharose.³⁹

3.5 Conclusion

Chapter 3 described functionalisation strategies investigated for the surface modification of solid fibrous PVA. A model reaction on 2,4-pentanediol revealed that the deceptively simple chemistry is in reality quite complex. This could account for the failure of many of the attempted PVA fibre and fabric polymer surface modification reactions.

Immobilisation of ADH on PVA-Cl-EDA-GA scaffold showed both higher activity and thermostability (at 60 to 80 °C), and also exhibited good operational stability over a wider pH range (pH 7-9). The construct also retained 60% of its original activity after eight reaction cycles making it attractive for industrial applications. These results indicate that PVA fibre based materials show promise as support materials for enzyme immobilisation.

Although denaturation of the immobilised ADH occurred at a slower rate to that of the soluble ADH, the PVA-Cl-EDA-GA-ADH construct retained only 18% activity over 25 days. This was disappointing since bioreactor applications require long-term stability. Its use in biosensors is also limited due to the lack of attachment mode for an electrode surface. With this knowledge in hand, we shifted attention to fibrous glass supports. In Chapter 4, ADH was successfully immobilised on the glass and assessed as a bioreactor and for amperometric detection of ethanol in a biosensor application.

3.6 Experimental Section

3.6.1 Solvents and reagents

Acetone, hydrochloric acid (concentrated HCl), dichloromethane (DCM), ethanol (EtOH), methanol (MeOH), tetrahydrofuran (THF), triethylamine (TEA), ethyl acetate (EtOAc), hexanes (light petroleum), pyridine, toluene, magnesium sulphate (MgSO₄), sodium chloride (NaCl), sodium hydroxide (NaOH), ammonia (30% in water), benzylamine and *N*-Boc-1, 2-diaminoethane were purchased from Merck and used without further purification.

Sodium bicarbonate (NaHCO₃), sodium carbonate (Na₂CO₃), potassium *t*-butoxide, ethylenediamine (EDA), hexamethylenediamine (HA), 1, 12-dodecadiamine, JEFFAMINE™ D-400, branched polyethyleneimine (PEI), 25% glutaraldehyde, epichlorohydrin, hexamethylene diisocyanate, succinic anhydride, 3-(trimethoxysilyl)propylamine, bromoacetic acid, chloroacetic acid, 3-chloropropanoic acid, *N*-(3-dimethylaminopropyl)-*N'*-ethylcarbodiimide hydrochloride (EDC), 2-(*N*-morpholino)ethane sulfonic acid (MES), 2,4-pentanediol, chlorotriazine, diglycidyl ether, tetraethoxysilane, 1,1'-carbonyldiimidazole, sodium borohydride (NaBH₄) powder, *N*-Boc-ethylenediamine and nicotinamide adenine dinucleotide (NAD⁺) were purchased from Sigma-Aldrich, Australia, and used without further purification.

Alcohol dehydrogenase (ADH) from yeast (500 units/mg) was purchased from Calzyme.

PVA yarn (250 dtex, 100 filaments, Solvron SHC) was purchased from Nitivy, Japan.

3.6.2 Instrumentation

Infrared spectra were collected using a Nicolet 6700 ATR-FTIR (Thermo Scientific) in absorbance mode. IR absorptions are reported in wavenumbers (cm^{-1}) with the relative intensities expressed as s (strong), m (medium), w (weak) or prefixed b (broad).

Solid-state ^{13}C cross-polarization (CP-MAS) NMR spectra were recorded on a Bruker AV500 MAS spectrometer. Chemical shifts (δ), measured in parts per million (ppm), are reported relative to TMS.

Low-resolution electrospray ionization (ESI) mass spectra were recorded on a Micromass Platform Electrospray mass spectrometer (QMS-quadrupole mass electrometry) as solutions in specified solvents. Spectra were recorded in positive and/or negative mode (ESI⁺/ ESI⁻).

Morphology analysis was performed on Scanning Electron Microscope (SEM, Philips XL30). The samples were imaged using a Zeiss Merlin FESEM after being coated with iridium under vacuum.

Enzyme activity was measured using a Cary 300 BioUV-visible spectrophotometer at 340 nm.

Analytical thin layer chromatography (TLC) was performed on plastic plates coated with 0.25 mm of silica gel (Polygram SIL G/UV254). Column chromatography was carried out using Merck silica gel 60, 0.063-0.200 mm (230 mesh). The compounds were visualised with ultraviolet irradiation at 254 nm or *via* the use of chemical stains such as ninhydrin, vanillin, or iodine, where necessary. Eluent mixtures are expressed as volume to volume ratios.

Knitting was carried out using a flatbed Shima WG-14 (Japan) using PVA (Solvron SHC) yarn. The fabric knitted was a 2 x 1 rib with a loop length of 5.5 mm producing a flat structure with little or no curling at the edges. Discs of 13 mm in diameter were stamped from the knitted

fabric, washed with deionized water and ethanol, and dried in an oven at 50 °C before being subjected to further chemical modification.

ADH Activity

Surface modification reactions were performed on fabric discs in bulk total mass (1-2 g) and enzyme immobilisation activity was measured on a single disc of known mass (170-180 mg) in triplicate according to the procedure described in Experimental Section 3.7.2. The activity was calculated from absorbance (Abs) using the following formula:

$$A = \epsilon \times c \times l,$$

$$c = A / \epsilon \times l$$

where A is the absorbance, ϵ is the extinction coefficient ($6220 \text{ M}^{-1} \text{ cm}^{-1}$), c is the concentration (M) and l is the path length (cm).

$$\text{Conc. mmol} = \text{Conc (mM)} / \text{Assay volume}$$

$$\text{Total activity} = \text{Conc. mmol} / \text{Time (i.e. assay time in min)}$$

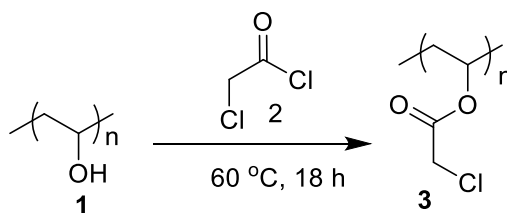
$$\text{Activity (Specific activity) of immobilised ADH} = \text{Conc. mmol} / \text{Time (min)} / \text{Weight of fabric disc (g)}$$

$$\text{Activity (Specific activity) of soluble ADH} = \text{Conc. mmol} / \text{Time (min)} / \text{Weight of ADH (g)}$$

3.6.3 PVA Surface modification procedures

3.6.3.1 Ester Modification

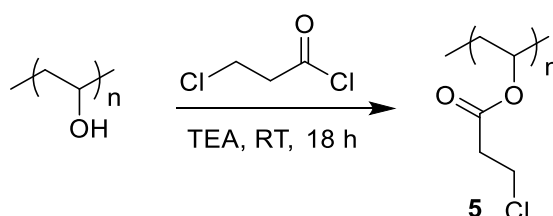
3.6.3.1.1 PVA-Chloroacetyl chloride reaction → (3)



PVA fabric discs (1.01 g, 0.022 moles –OH) were added into THF (20 mL) and stirred at R.T. To this mixture chloroacetic acid (3.6 mL, 0.045 mole) was added dropwise at 0 °C with constant stirring and then heated to 60 °C for 18 h. In this reaction fabric transformed into gel.

The PVA fibres were modified with acetic acid and synthesised according to the procedure outlined in Section 5.4.1 under the following conditions: PVA fibres (1g, 0.022 moles –OH), acetyl chloride (3.6 mL, 0.045 mole) and TEA (5 mL, 0.045 mol). This resulted in fibres into gel transformation.

3.6.3.1.2 PVA acylation with 3-chloropropinoyl chloride → (5)

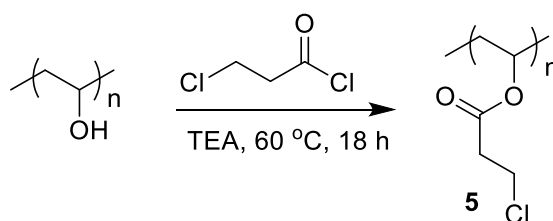


PVA acylation scaffold (5) was prepared according to a procedure described by J. Bernard.¹⁵

PVA fabric knitted discs (4 g, 0.091 mol –OH) were added to a solution of triethylamine

(28.8 mL, 0.211 mol) in THF (80 mL) at RT. To this mixture 3-chloropropionyl chloride (21.0 mL, 0.22 mol) was added dropwise at 0 °C over a 30 min and then the reaction mixture was stirred at RT for 18 h. At the end of the reaction, the fabric discs were then removed from the reaction solution and washed with distilled water (25 mL; 3 x 10 min), ethanol (25 mL; 3 x 10 min) and dried at 50 °C to obtain yellow coloured fabric. IR spectroscopic analysis was not consistent with the target product.

3.6.3.1.3 PVA acylation with 3-chloropropionyl chloride → (5)

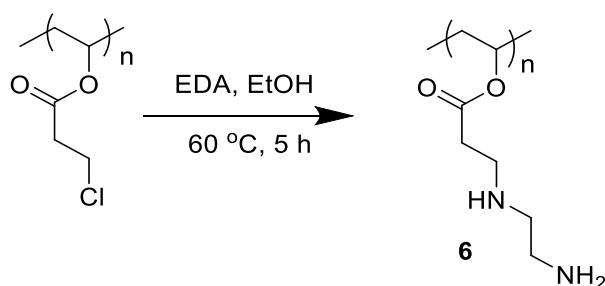


PVA scaffold (5) was carried out according to a procedure described by J. Bernard.¹⁵ PVA fabric knitted discs (4 g, 0.091 mol -OH) were added to a solution of triethylamine (28.8 mL, 0.211 mol) in THF (80 mL) at RT. To this mixture 3-chloropropionyl chloride (21.0 mL, 0.22 mol) was added dropwise at 0 °C over a 30 min and then the reaction mixture was heated to 60 °C for 18 h. At the end of the reaction, the fabric discs were then removed from the reaction solution and washed with distilled water (25 mL; 3 x 10 min), ethanol (25 mL; 3 x 10 min) and dried at 50 °C to obtain a red/brown coloured fabric. IR: 3289bs, 2908s, 1733s, 1437m, 1449s, 1329w, 1200w, 1142s, 1087bs, 914w, 841m, 646w cm^{-1} . ^{13}C NMR solid state (600 MHz): 38.7, 44.3, 64.6, 78.2, 78.2, 170.2 .

1) ADH immobilisation

ADH (0.5 mg/mL) was dissolved in PBS (0.05 M, pH 7.5). PVA-Cl fabric discs from above section were placed in a 12 well plate containing the ADH solution (1 mL). After incubation for 2 h at 25 °C the carrier discs were washed with phosphate buffer (0.05 M, pH 7.5, 25 mL; 4 x 30 min) to remove unbound enzyme. PVA fabric without surface modification were immobilised with ADH in an analogous way and subsequently used as controls. The activity of immobilised and soluble ADH was determined according to the procedure described in Section 3.7.2.

3.6.3.1.4 Ethylenediamine modification PVA-Cl-EDA → (6)



The PVA-Cl knitted fabric discs (1.01 g) were added to 10 % (w/v) ethylenediamine solution (10 mL in ethanol) and heated to 60 °C for 5 h under stirring. The reaction mixture was then cooled to RT and the modified discs were removed and washed with distilled water (25 mL; 3 x 10 min) and ethanol (25 mL; 3 x 10 min) respectively to remove residual diamine.

1) Spacer optimization procedure

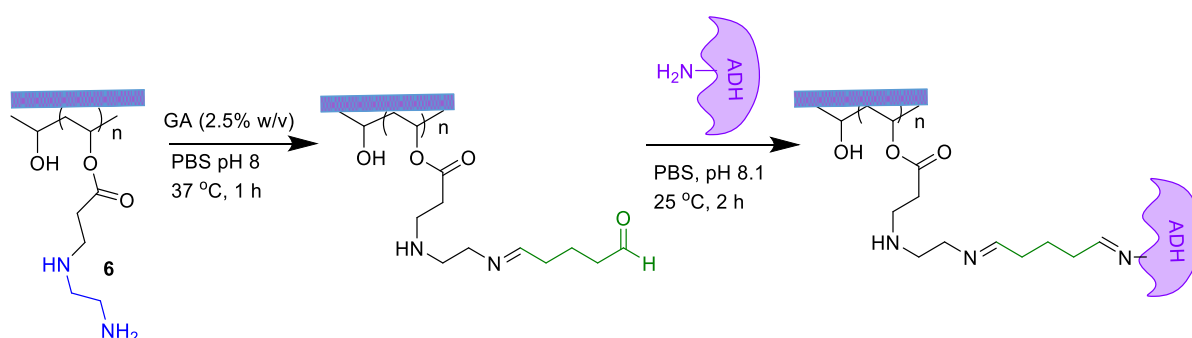
Spacer optimisation was investigated with ethylenediamine, hexamethylene diamine, and 1, 12-dodecamine 10% (w/v) in ethanol (10 mL) separately. Each reaction mixture was heated to 60°C for 5 h. The modified aminated discs were removed and subsequently washed with distilled water (25 mL; 3 x 10 min) and ethanol (25 mL; 3 x 10 min). The discs were then dried at 50 °C for 18 h.

2) EDA concentration optimisation procedure

The EDA concentration study was undertaken using 20%, 30% and 40% EDA in ethanol (10 mL). PVA-Cl discs (1.10 g) were added to each of the above EDA concentrations and treated according to the procedure described in above Section 3.6.3.1.4

The IR spectra for 30% EDA modified PVA-Cl fabric discs: 3286bs, 2908s, 2182w, 1727s, 1649w, 1440m, 1322m, 1181w, 1142s, 1087bs, 913w, 841m cm^{-1} . ^{13}C NMR solid state (600 MHz): 35.8, 44.5, 64.6, 78.2, 78.2, 172.4.

3) GA activation (PVA-Cl-EDA-GA)



GA activation was carried out according to the procedure described by J. C. Santos.³³ The PVA-Cl-EDA fabric discs (~0.985 g) were activated with 2.5% (w/v) GA (20 mL) in PBS

(0.05 M pH 7.5) for 1 h at 37 °C in a sealed flask. The support discs were removed from the solution and thoroughly washed with distilled water (25 mL; 3 x 30 min) to remove excess GA.

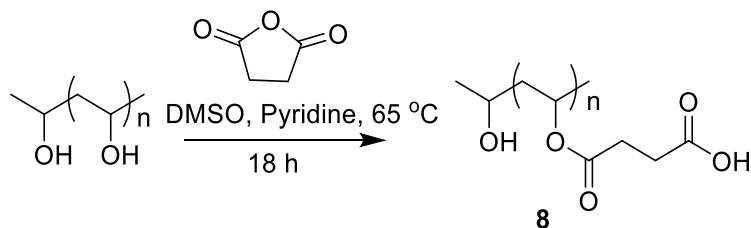
4) ADH immobilisation

ADH (0.5 mg/mL) was dissolved in PBS (0.05 M, pH 8.1). The GA activated fabric discs (PVA-Cl-EDA-GA) were placed in a 12 well plate containing the ADH solution. After incubation for 2 h at 25 °C the carrier discs were washed with phosphate buffer (0.05 M, pH 8.1) four times over 30 min to remove unbound enzyme. Control fabrics such as PVA fabric, PVA-Cl and PVA-Cl-EDA were immobilised in an analogous way and subsequently used as controls. The activity of the immobilised and soluble ADH was determined according to the procedure described in Section 3.7.2.

Table 3.6 Activity measurement: Effect of EDA concentration on immobilised ADH

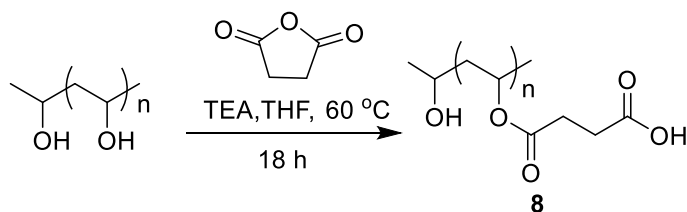
EDA Conc	Abs	NADH coefficient	Conc (mM)	Conc (mmol)*	Total activity mmol/min	Activity mmol/min/g	Average activity	% activity
10%	0.563	6200	0.091	0.182	0.045	0.378	0.366	55%
	0.564	6200	0.091	0.182	0.045	0.379		
	0.509	6200	0.082	0.164	0.041	0.342		
20%	0.864	6200	0.139	0.279	0.070	0.581	0.582	77%
	0.876	6200	0.141	0.283	0.071	0.589		
	0.86	6200	0.139	0.277	0.069	0.578		
30%	1.142	6200	0.184	0.368	0.092	0.767	0.763	100%
	1.126	6200	0.182	0.363	0.091	0.757		
	1.138	6200	0.184	0.367	0.092	0.765		
* Assay vol: 2 mL								

3.6.3.1.5 Succinic anhydride modification → (8)



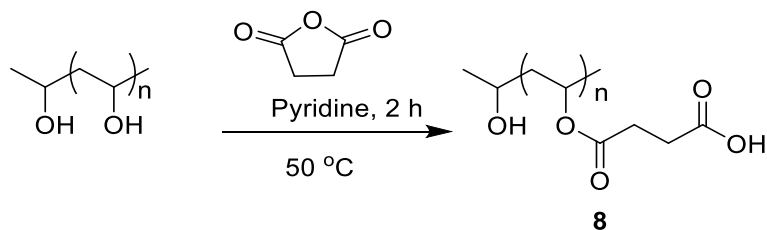
The succinic anhydride modification of PVA (**8**) was carried out according to a procedure described by V. Gimenez.⁴⁰ PVA fabric (1 g, 0.002 –OH moles) was added into the mixture of DMSO (10 mL) and pyridine (1.7 mL, 0.006 mol) and stirred at RT for 15 min. Succinic anhydride (0.5 g, 0.02 mol) was added into the above mixture and heated at 50 °C for 2 h. The discs were then removed from the reaction mixture and washed with distilled water (25 mL; 3 x 10 min), ethanol (25 mL; 3 x 10 min) and dried at 50 °C. IR spectroscopic analysis was not consistent with the target product.

3.6.3.1.6 Succinic anhydride modification → (8)



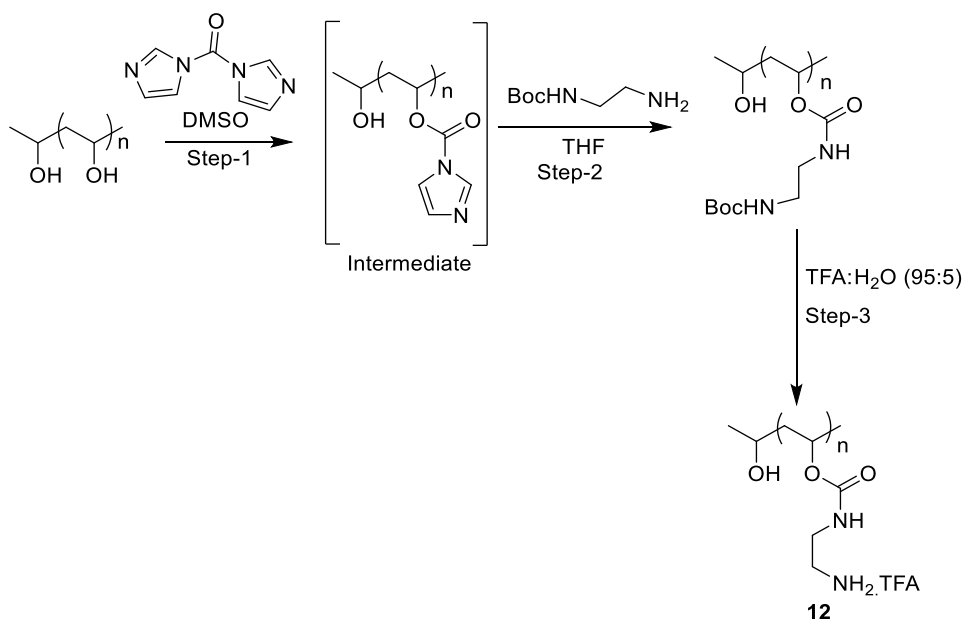
The PVA succinic anhydride scaffold (**8**) was prepared according to a procedure described by Optivas.¹¹ PVA fibre fabric (1.1 g, 0.002 –OH moles) was added to the mixture of THF (10 mL) and TEA (0.6 mL, 0.006 mol) and stirred at RT for 15 min. To this reaction mixture, succinic anhydride (0.5g, 0.005mol) was added and heated at 60 °C for 18 h. The discs were then removed from the reaction mixture and washed with distilled water (25 mL; 3 x 30 min), ethanol (25 mL; 3 x 30 min) and dried at 50 °C. IR spectroscopic analysis was not consistent with the target product.

3.6.3.1.7 Succinic anhydride modification → (8)



The succinic anhydride scaffold (**8**) was also prepared according to a procedure described by M. Zouhair Atassi.⁴¹ PVA fibre fabric (1.2 g, 0.002 –OH moles) was added into pyridine (5 mL) and stirred at RT for 15 min. Succinic anhydride (0.5 g, 0.005 mol) was added into the above reaction mixture and heated at 50 °C for 18 h. After cooling at RT, discs were removed from the reaction mixture and washed with distilled water (25 mL; 3 x 30 min), ethanol (25 mL; 3 x 30 min) and dried at 50 °C. IR spectroscopic analysis was not consistent with the target product.

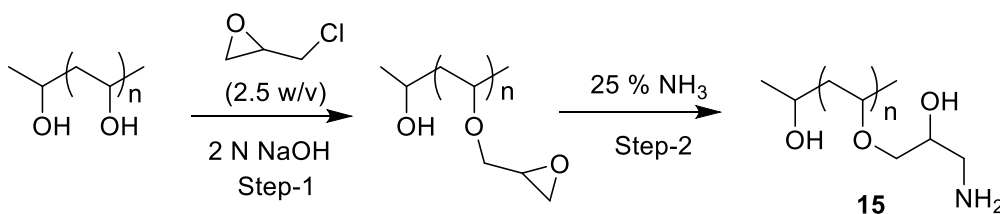
3.6.3.1.8 Carbamate formation → (12)



PVA carbamate scaffold (**12**) was synthesised according to the procedure described by D.Ossipov.⁴² PVA fabric discs (0.80 g, 18 mmol of OH groups) was added to dry DMSO (16 mL). CDI (1.56 g, 9 mmol) was added to the mixture in one portion at RT and the reaction was stirred under nitrogen for another 2.5 h. *N*-Boc-ethylenediamine (177.6 mg, 1.11 mmol) in DMSO (6 mL) was then added to the reaction solution, and the resulting mixture was stirred overnight at RT. Concentrated aqueous NH₃ (8 mL) was then added, and the mixture was stirred for a further 45 min at RT. Finally, the reaction mixture was diluted with distilled water (50 mL) and stirred for 2 h. The fabric was then removed from the reaction mixture and washed with distilled water (25 mL; 4 x 30 min), acetone (25 mL; 3 x 30 min) and dried at 50 °C. IR spectroscopic analysis was not consistent with the target product.

3.6.3.2 Ether modifications

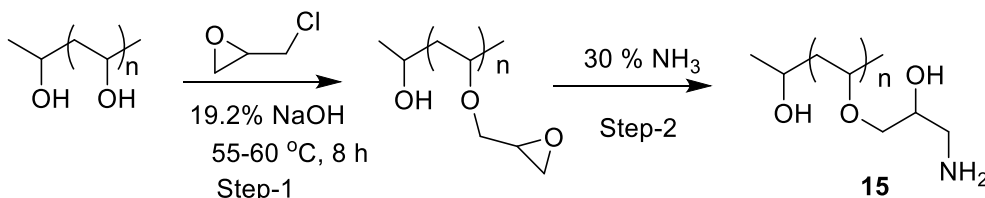
3.6.3.2.1 Epichlorohydrin modification → (**15**)



PVA epoxy scaffold was synthesised according to the procedure described by H.J.Xu.⁴³ PVA fabric discs (1.03 g, 0.022 moles –OH) were added into 2N NaOH (3 mL, 0.075 mol) in water at RT. Epichlorohydrin (5.8 mL, 0.075 mol) was added to the mixture and the reaction mixture was stirred at RT for 18 h. After 18 h, the fabric was removed from the reaction mixture and washed with distilled water (25 mL; 4 x 30 min) and dried at RT for 18 h. The PVA scaffold discs were then added to aqueous ammonia (10 mL) and stirred overnight at RT. The PVA

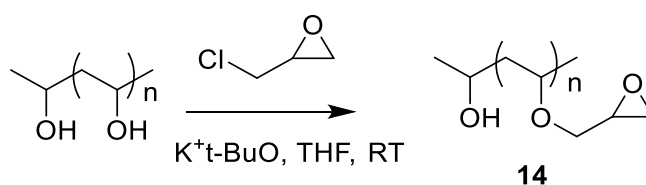
discs were then removed from the reaction and washed with distilled water (15 mL; 3 x 30 min) and dried at RT. IR spectroscopic analysis was not consistent with the target product.

3.6.3.2.2 Epichlorohydrin modification → (15)



The PVA epoxy scaffold was synthesised according to the procedure described by H.J.Xu.⁴³ PVA fabric discs (0.52 g, 0.011 moles –OH) were added into 5N NaOH (3 mL, 0.075 mol) in water. Epichlorohydrin (2.9 mL 0.037 mol) was added to the above mixture and heated to 55-60 °C for 8 h. After 8 h, the fabric was removed from the reaction mixture and washed with distilled water (25 mL; 4 x 30 min) and dried at RT for 18 h. Aqueous ammonia (10 mL) was then added and the mixture was stirred overnight at RT. The aminated PVA fabric discs were then washed with distilled water (25 mL; 4 x 30 min) and dried at RT. IR spectroscopic analysis was not consistent with the target product.

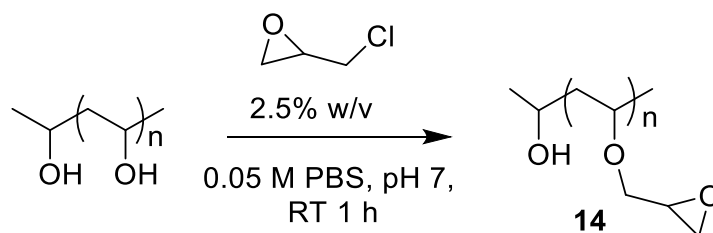
3.6.3.2.3 Epichlorohydrin modification → (14)



PVA fabric discs (1.0 g, 0.022 moles –OH) were added into the mixture of THF and potassium *t*-butoxide (0.6 g, 0.005 mol) at RT. Epichlorohydrin (2.8 mL, 0.066 mol) was added to the above mixture and stirred at RT. After 2 h, the fabric discs were removed from the reaction

mixture and washed with distilled water (15 mL; 3 x 30 min) and dried. IR spectroscopic analysis was not consistent with the target product.

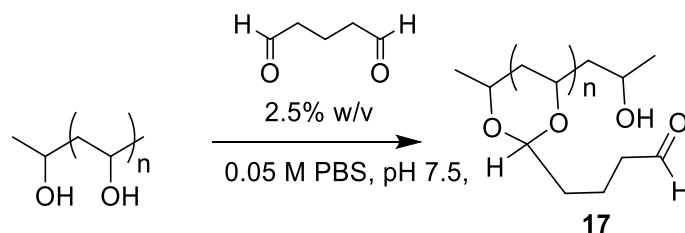
3.6.3.2.4 Epichlorohydrin modification → (14)



The PVA epoxy scaffold (**14**) was synthesised according to the procedure described by J.Santos.³³ The PVA fabric (1.02 g, 0.022 moles -OH) was allowed to react with 2.5% (w/v) epichlorohydrin in PBS buffer (10 mL, 0.05M, pH 7.0) for 1 h at RT. The PVA modified support was removed from the reaction mixture and washed with distilled water (15 mL; 3 x 30 min). IR spectroscopic analysis was not consistent with the target product.

The PVA epoxy scaffold (**14**) was synthesised analogously according to the procedure outlined in above Section 3.6.3.2.4 under the following conditions: PVA fabric (0.5 g, 0.011 moles -OH), 2.5% (w/v) epichlorohydrin (10 mL) in PBS. After 18 h the PVA modified support was removed from the reaction mixture and washed with distilled water (15 mL; 3 x 30 min). IR spectroscopic analysis was not consistent with the target product.

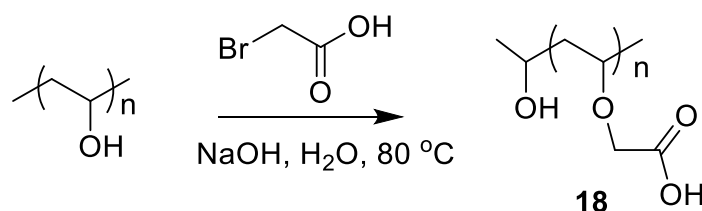
3.6.3.2.5 Glutaraldehyde activation → (17)



Preparation of the PVA acetal scaffold (**17**) was attempted using a procedure described by J.Santos.³³ The PVA fabric (0.51 g, 0.011 moles –OH) was reacted with GA 2.5% (w/v) in PBS (10 mL, 0.05 M, pH 7.4) at RT for 1 h. The GA exposed fabric discs were then washed with distilled water (20 mL; 3 x 30 min). IR spectroscopic analysis was not consistent with the target product.

Preparation of the PVA acetal scaffold (**17**) was also attempted under following conditions: PVA fabric discs (0.5 g), 2.5% (w/v) GA in PBS (10 mL, 0.05 M, pH 7.4), 18 h. IR spectroscopic analysis was not consistent with the target product.

3.6.3.2.6 PVA modification with bromoacetic acid → (18)



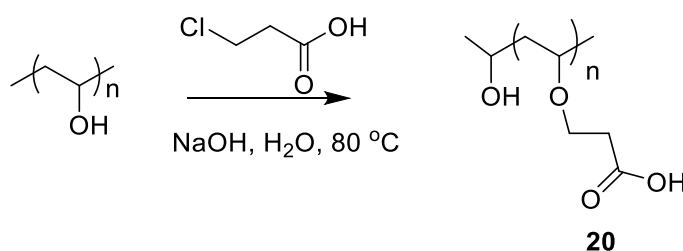
The PVA acid scaffold (**18**) was synthesised according to the procedure described by C.S.Yu.⁴⁴ To the PVA fabric (0.50 g, 0.011 mol –OH), sodium hydroxide (0.352 g, 0.08 mol) and distilled water (10 mL) were added. Bromoacetic acid (0.4858 g, 0.03 mol) was then added in one portion and the reaction mixture was stirred at 80 °C for 5 h. The reaction mixture was then cooled at RT and the pH of the mixture was adjusted to 6 with 1M hydrochloric acid.

(0.5 mg/mL) was dissolved in PBS (0.05 M, pH 8.1). The EDC activated fabric discs were placed in a 12 well plate containing the ADH solution. After incubation for 2 h at 25 °C the carrier discs were washed with PBS (0.05 M, pH 8.1 20 mL; 4 x 30 min) to remove any unbound enzyme. The PVA fabric samples without surface modification were treated in an analogous way and subsequently used as controls. The activity of both the immobilised and control fabric samples were determined according to the procedure described in Section 3.7.2.

Table 3.7 Activity measurement: ADH immobilised on PVA acid support

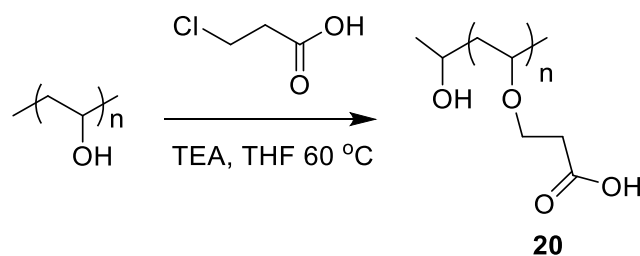
Abs	NADH coefficient	Conc (mM)	Conc (mmol)	Total activity mmol/min	Activity mmol/min/g	Average activity
Control- ADH immobilised on PVA fabric						
0.150	6200	0.024	0.024	0.006	0.040	0.039
0.094	6200	0.015	0.015	0.004	0.025	
0.146	6200	0.024	0.024	0.006	0.039	
0.190	6200	0.031	0.031	0.008	0.051	
Treatment- ADH immobilised on PVA acid fabric						
0.071	6200	0.011	0.011	0.003	0.019	0.029
0.114	6200	0.018	0.018	0.005	0.031	
0.167	6200	0.027	0.027	0.007	0.045	
0.087	6200	0.014	0.014	0.004	0.023	

3.6.3.2.8 PVA modification with chloropropionic acid → (20)



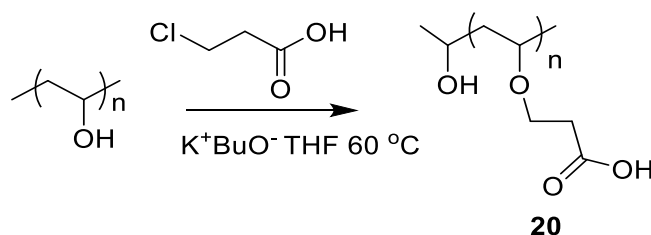
PVA scaffold (**20**) was synthesized according to the procedure described in Section 3.6.3.2.6 under the following conditions: PVA fabric discs (0.51 g, 0.011 mol –OH), chloropropionic acid (0.58 g, 0.03 mol), sodium hydroxide (0.352 g, 0.08 mol), 15 mL distilled water. IR spectroscopic analysis was not consistent with the target product.

3.6.3.2.9 PVA modification with chloropropionic acid → (20)



PVA carboxymethylation (**20**) was carried out according to a procedure described by J. Bernard.¹⁵ PVA fabric discs (1.12 g, 0.023 mol –OH) were added into a mixture of THF (20 mL) and TEA (5 mL, 0.045 mol) at RT. To this mixture 3-chloropropionic acid (4.8 g, 0.044 mol) was added and heated to 60 °C for 18 h. The reaction mixture was cooled to RT, then the discs were removed from the mixture and washed with distilled water (25 mL; 4 x 30 min), ethanol (25 mL; 4 x 30 min) and dried at 50 °C. IR spectroscopic analysis was not consistent with the target product.

3.6.3.2.10 PVA modification with chloropropionic acid → (20)

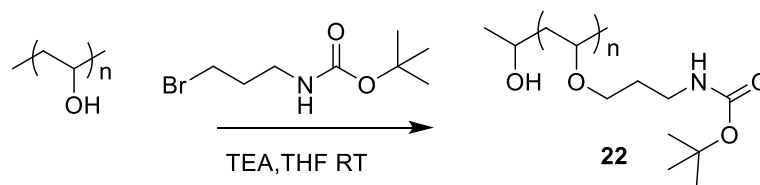


PVA fabric discs (1.01 g, 0.022 mol –OH) were added into a mixture of THF (20 mL) and potassium *t*-butoxide (6.4 g, 0.01 mol) at RT. 3-Chloropropionic acid (4.8 g, 0.04 mol) was added to the above mixture and heated at 60 °C for 18 h. The discs were then separated from the reaction mixture and washed with distilled water (25 mL; 4 x 30 min), ethanol

(25 mL; 4 x 30 min) and dried at 50 °C. IR spectroscopic analysis was not consistent with the target product.

3.6.3.2.11 *tert*-Butyl-*N*-(3-bromopropyl)carbamate reaction with

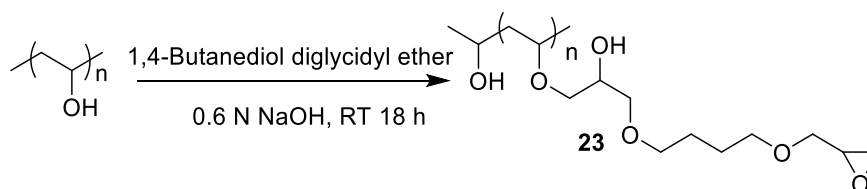
PVA → (22)



PVA fabric (1.10 g, 0.002 –OH moles) was added to a mixture of THF (20 mL) and TEA (0.8 mL, 0.008 mol). *tert*-Butyl-*N*-(3-bromopropyl)carbamate (1.1 g, 0.004 mol) was added to the above mixture which was then stirred at RT for 2 h. The fabric was then removed from the mixture and washed with ethanol (25 mL; 4 x 10 min) and acetone (25 mL; 4 x 10 min) and dried at 50 °C. IR spectroscopic analysis was not consistent with the target product.

3.6.3.2.12 PVA modification with butanediol diglycidyl ether →

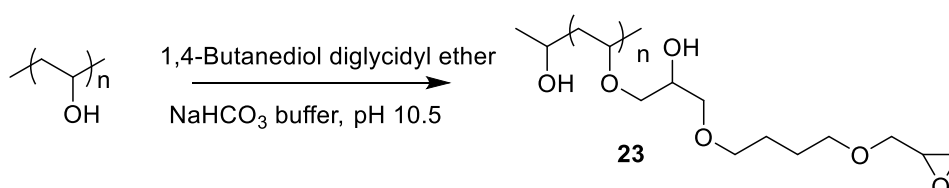
(23)



PVA carboxymethylation (23) was carried out according to a procedure described by R.A Sheldon.⁴⁵ A mixture of 1,4-Butanediol diglycidyl ether reagent (3 mL) and 0.6 N NaOH (3 mL) and sodium borohydride (2 mg) was prepared and cooled to 20 °C. The PVA fabric discs (1.02 g) were added to this turbid mixture and allowed to shake for 18 h at 150 rpm at

20 °C. After 18 h, the fabric was washed with 10%, 20%, 50% acetone in water (25 mL; 4 x 10 min) respectively and finally washed with distilled water (25 mL; 4 x 10 min). IR spectroscopic analysis was not consistent with the target product.

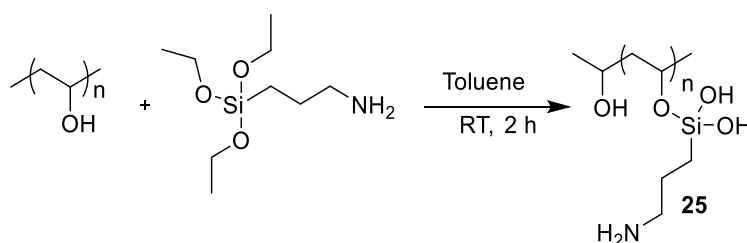
3.6.3.2.13 Butanediol-diglycidyl ether modification → (23)



PVA fabric (1.21 g, 0.002 -OH moles) was added into bicarbonate buffer solution (20 mL, pH 10.5). To this was added dropwise 1,4-butanediol diglycidyl ether (4.41 g, 0.024 mol). The mixture was stirred at RT for 3 h. The fabric was then removed from the mixture and washed with distilled water (25 mL; 4 x 10 min) and oven dried. IR spectroscopic analysis was not consistent with the target product.

3.6.3.3 Silane modifications

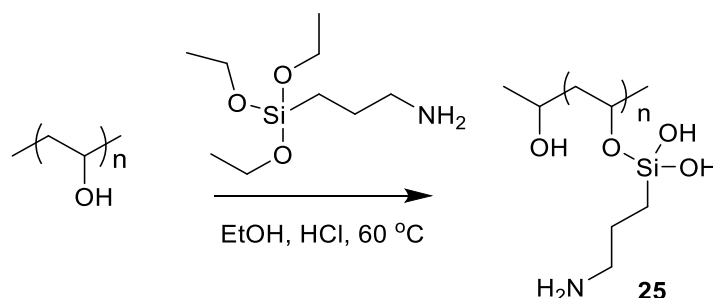
3.6.3.3.1 Silylation with APTMS → (25)



PVA fabric (250.1 mg) was added into a solution of 2.5 % APTMS in toluene (10 mL) and stirred at RT. After 2 h, the fabric was removed and washed with ethanol (25 mL; 4 x 30 min)

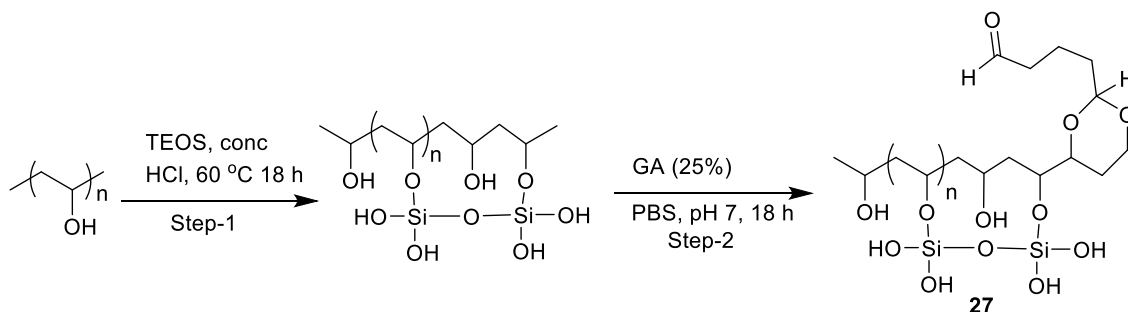
and cured at 100 °C for 10 min. IR spectroscopic analysis was not consistent with the target product.

3.6.3.3.2 Silylation with APTMS → (25)



The PVA silane amine modified scaffold (**25**) was synthesised according to the procedure described by J. A. Howarter.⁴⁶ PVA fabric (1.10 g, 0.002 –OH moles) was added into a mixture of ethanol and APTMS (1:1, 20 mL) at RT. This mixture heated to 60 °C for 10 min then three drops of conc HCl was added (pH 3) to catalyse the reaction. The reaction was heated for a further 40 min. before being cooled. The fibres/fabric was then removed from the solution and dried overnight at RT. IR spectroscopic analysis was not consistent with the target product.

3.6.3.3.3 Silylation with TEOS → (27)

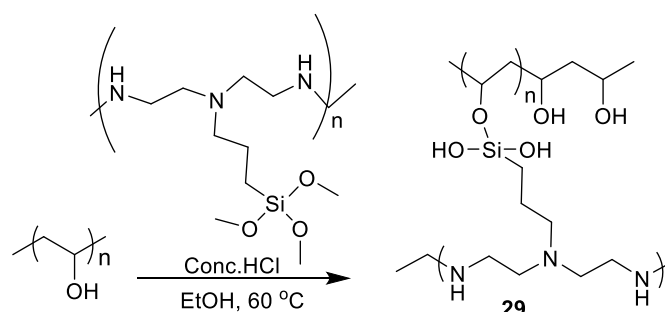


The PVA silane modified scaffold (**25**) was synthesised according to the procedure described by H. S. Mansur.⁴⁷ PVA fabric (1.21 g) was added into the ethanol and TEOS (1:1, 20 mL)

mixture at RT. The reaction mixture was heated initially at 60 °C for 10 min followed by the addition of conc HCl (3 drops) to catalyse the reaction. This reaction was heated for a further 40 min at the same temperature. The fibres/fabric were then removed from the solution and dried overnight at RT. IR spectroscopic analysis was not consistent with the target product.

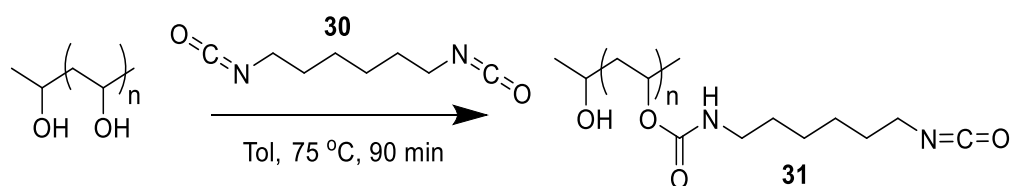
The PVA aldehyde scaffold was synthesised according to the procedure described by J.Santos.³³ The PVA silanized fabric (0.51 g) from above was reacted with 2.5% (w/v) GA (10 mL) at pH 7.4 for 18 h at R.T. After 18 h the fibres or fabric were removed and washed with distilled water (50 mL; 4 x 10 min). IR not consistent with the target structure.

3.6.3.3.4 Silylation with PEI silane → (29)



The PVA-PEI silane (29) was synthesized using trimethoxy-silyl propyl modified polyethyleneimine and ethanol (1:1, 20 mL) with 0.5 g of fibrous PVA according to the method described in above Section 3.6.3.3.2. IR spectroscopic analysis was not consistent with the target product and an eosin colorimetric dye test was positive.

3.6.3.4 Isocyanate modifications → (31)



The PVA isocyanate scaffold (**31**) was synthesised according to the procedure described by S. V. Caro.³⁴ The PVA fabric discs (0.81 g) were added into a solution of 10% hexamethylene diisocyanate (10 mL) in toluene at RT in a three neck round bottom flask. The reaction was stirred at 25 °C for 1.5 h. The fabric was then washed with acetone (25 mL; 4 x 10 min) and distilled water (20 mL; 2 x 10 min), and dried in the oven at 60 °C for 2 h. IR: 3261bs, 2907s, 2162w, 1962w, 1650m, 1417s, , 1318m, 1235w, 1142m, 1084bs, 914w, 828m cm⁻¹.

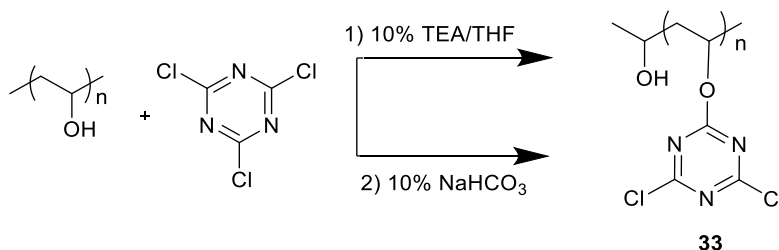
1) ADH immobilisation

PVA isocyanate discs from above section were immobilised with ADH (0.5 mg/mL, PBS) according to the procedure described in Section 3.7.1. The activity for control and immobilised ADH assayed according to the procedure described in Section 3.7.2 and detailed activity data is presented below in Table 3.8.

Table 3.8 Activity measurement: ADH immobilised on PVA-isocyanate support

PVA isocyanate	Abs	NADH coefficient	Conc (mM)	Conc (mmol)	Total activity mmol/min	Activity mmol/min/g	Average activity
Control	0.693	6200	0.112	0.112	0.028	2.794	2.758
	0.66	6200	0.106	0.106	0.027	2.661	
	0.699	6200	0.113	0.113	0.028	2.819	
PVA -isocyanate-ADH	0.531	6200	0.086	0.086	0.021	2.141	2.129
	0.533	6200	0.086	0.086	0.021	2.149	
	0.520	6200	0.084	0.084	0.021	2.097	

3.6.3.5 Chlorotriazine modifications → (**33**)



1) 10 % TEA

The PVA chlorotriazine scaffold (**33**) was synthesised according to the procedure described by S. Yrjölä and co-worker.⁵⁸ The PVA fabric (1.10 g, 0.002 –OH moles) was added into dry THF (9 mL) and TEA (1 mL, 0.03 mol) at RT. To this mixture, 2-chloro-4, 6-diamino-1,3,5-triazine (1.8 g, 0.8 mol) was added in portions at 25 °C over 10 min. and the reaction mixture was allowed to stir at 25 °C for 2 h. The fabric was then removed from the mixture and washed with acetone, distilled water (25 mL; 4 x 20 min) and dried in the oven at 60 °C for 18 h and analysed by IR spectroscopy: 3276bs, 2904s, 1715m, 1415s, 1320s, 1142m, 1087bs, 912w, 8233m cm⁻¹.

2) 10% NaHCO₃

The PVA chlorotriazine scaffold was synthesised according to the procedure described by C. Linder.³⁵ The PVA fibre or fabric (1.01 g, 0.002 –OH moles) was added into an aq.10 % NaHCO₃ solution (15 mL) at RT. 2-Chloro-4,6-diamino-1,3,5-triazine (1.8 g, 0.8 mol) was added in portions to the fibrous mixture and the mixture was stirred for 2h at RT. The fibre or fabric was then washed with distilled water and acetone (50 mL; 4 x 30 min) and then dried in an oven at 60 °C for 18 h. IR spectroscopy: 3248bs, 2904s, 1714s, 1413s, 1320s, 1329w, 1200w, 1142s, 1084bs, 912w, 821m, 756w cm⁻¹.

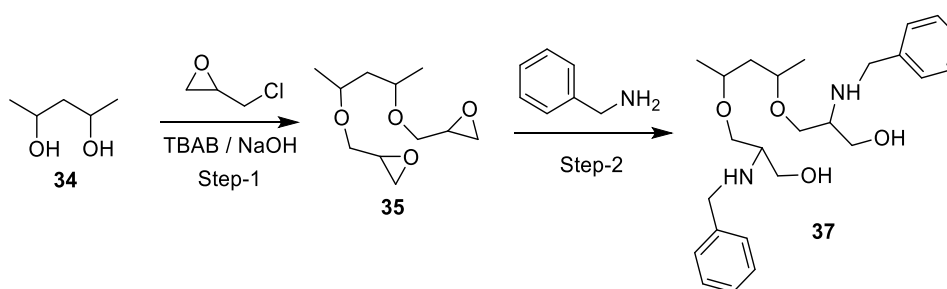
1) ADH immobilisation

ADH (0.5 mg/mL, PBS) was immobilised onto the PVA-chlorotriazine discs according to procedure according to the procedure described in Section 3.7.1. The activity for control and immobilised ADH was assayed according to the procedure described in Section 3.7.2 and detailed activity data is presented in Table 3.9.

Table 3.9 Activity measurement: ADH immobilised on PVA chlorotriazine support

	Abs	NADH coefficient	Conc (mM)	Conc (mmol)	Total activity mmol/min	Activity mmol/min/g	Average activity
ADH immobilised on PVA chlorotriazine support (2-NaHCO₃)							
Control (PVA fabric)	0.093	6200	0.015	0.015	0.004	0.025	0.103
	0.965	6200	0.156	0.156	0.039	0.259	
	0.098	6200	0.016	0.016	0.004	0.026	
Treatment	0.095	6200	0.015	0.015	0.004	0.025	0.033
	0.180	6200	0.029	0.029	0.007	0.048	
	0.094	6200	0.015	0.015	0.004	0.025	
ADH immobilised on PVA chlorotriazine support (1-TEA)							
	Abs	NADH coefficient	Conc (mM)	Conc (mmol)	Total activity mmol/min	Activity mmol/min/g	Average activity
Control (PVA fabric)	0.093	6200	0.015	0.015	0.004	0.025	0.026
	0.097	6200	0.016	0.016	0.004	0.026	
	0.098	6200	0.016	0.016	0.004	0.026	
Treatment	0.073	6200	0.012	0.012	0.003	0.02	0.021
	0.082	6200	0.013	0.013	0.003	0.022	
	0.076	6200	0.012	0.012	0.003	0.020	

3.6.4 Model reaction



3.6.4.1 Epoxy modification → (35)

The 2,4-pentanediol reaction was performed as per Deniz Güclü *et al.*⁴⁸ A mixture of 40% aq. NaOH (8 mL), epichlorohydrin (10 mL, 20 mmol) and tetra-*N*-butylammonium bromide (80 mg, 4 mmol) was stirred vigorously at 0 °C. To this mixture, 2,4-pentanediol

(0.5 g, 4.80 mmol) was added over 30 min at a controlled rate so that the temperature was maintained below RT. The reaction progress was monitored by TLC (SiO₂: plates with mobile phase of light petroleum: EtOAc: MeOH; 7:3:0.2). Upon completion, the mixture was diluted with water (10 mL) and extracted with ethyl acetate (3 x 25 mL). The combined ethyl acetate layer was washed with saturated brine solution (50 mL). The organic phase was then dried over NaSO₄, filtered and evaporated to give a colourless oil (0.435 g). Mass spectrometry of the mixture showed a complex mixture of products.

3.6.4.2 Benzylation reaction → (37)

Benylation was carried out on the above crude epoxide mixture (35). The crude epoxide (200 mg, 0.92 mmol) was added to benzylamine (0.2 mL, 1.8 mmol) in DCM (5 mL) and stirred at RT for 18 h. The reaction progress was monitored by TLC. Upon completion, the mixture was diluted with water (5 mL) and extracted with ethyl acetate (3 x 15 mL) and the combined organic extract washed with saturated brine solution (25 ml). The organic phase was then dried with NaSO₄, filtered, and evaporated to a colourless oil (0.274 g). The oil was purified by column chromatography using ethyl acetate: hexane (70:30) mobile phase. Mass spectrometry of the mixture showed a complex mixture of products.

3.7 ADH immobilisation and assay protocol

3.7.1 Immobilisation protocol

ADH (0.5 mg/mL) was dissolved in PBS (0.05 M, pH 8.1). The functionalised PVA fabric discs (treatment) were placed in a 12 well plate containing 1 mL ADH solution. After incubation for 2 h at 25°C, the PVA support discs were washed with PBS (0.05 M, pH 8.1)

with rotary shaking (25 mL x 3, 100 rpm for 10 min) to remove any unbound enzyme. The PVA fabric without surface modification, PVA-Cl and PVA-Cl-EDA, were exposed to ADH in an analogous way and subsequently assayed and used as controls.

3.7.2 ADH activity assay

The activity of the immobilised ADH on the support was assayed by immersing the support discs individually in tris buffer (100 mM pH 8.8), ethanol (20 mM) and NAD⁺ (1 mM) at 25 °C in 12 well plates. After shaking for 4 min at 100 rpm on an orbital shaker, 1 mL of the solution was extracted for absorbance measurement. The activity analyses were performed in triplicate for each sample (i.e. control and treatment PVA fabric supports).

3.7.3 Immobilised ADH pH stability

The effect of pH on ADH stability was measured in different buffer systems: for pH 6.5-8.0, sodium PBS (0.05 M) was used and for pH 8.5-10.5, sodium carbonate/bicarbonate buffer (0.1 M) was employed. The soluble ADH and immobilised ADH (i.e PVA-Cl-EDA-GA-ADH) were incubated at 40 °C for 2 h at the various pH buffer solutions. Table 3.10 shows the results of the detail activity data for soluble ADH and immobilised ADH for the various pH treatments.

Table 3.10 Activity measurement: pH stability of soluble and immobilised ADH

pH	Abs	Abs	Abs	Avg Abs	NADH coefficient	Conc (mM)	Conc mmol	Total activity mmol/min	Activity mmol/min/g
Effect of pH on soluble ADH activity									
5	1.233	1.299	1.249	1.250	6200	0.202	0.202	0.050	1008.1
6	1.19	1.219	1.222	1.222	6200	0.197	0.197	0.049	985.5
7	1.328	1.308	1.300	1.300	6200	0.210	0.210	0.052	1048.4
8	1.080	1.078	1.075	1.075	6200	0.173	0.173	0.043	866.9
9	0.086	0.071	0.088	0.088	6200	0.014	0.014	0.004	71.0
10.5	0.066	0.066	0.068	0.068	6200	0.011	0.011	0.003	55.0
Effect of pH on immobilised ADH (PVA-Cl-EDA-GA disc)									
5	0.213	0.212	0.226	0.217	6205	0.035	0.035	0.009	0.117
6	0.198	0.210	0.222	0.210	6205	0.034	0.034	0.008	0.113
7	0.310	0.308	0.291	0.303	6205	0.049	0.049	0.012	0.163
8	0.389	0.378	0.368	0.379	6205	0.061	0.061	0.015	0.203
9	0.189	0.189	0.179	0.186	6205	0.030	0.030	0.007	0.100
10.5	0.107	0.109	0.112	0.109	6205	0.018	0.018	0.004	0.059

3.7.4 Immobilised ADH thermal stability

The thermostability study was performed by incubating the soluble ADH (0.5 mg/mL) and the immobilised ADH (i.e PVA-Cl-EDA-GA-ADH) for 2 h in PBS (0.05 M, pH 8.1) at various temperatures (20 °C, 40 °C, 60 °C, 80 °C) in a water bath. After each incubation, the enzyme was quickly chilled in crushed ice for 5 min. The enzyme was brought to RT and the activity

determined as described in Section 3.7.2 Table 3.11 shows the detailed activity data for soluble ADH and immobilised ADH at various temperatures.

Table 3.11 Activity measurement: Thermal stability of soluble and immobilised ADH

Temp °C	Abs	NADH coefficient	Conc (mM)	Conc (mmol)	Total activity mmol/min	Activity mmol/min/g	Average activity
Effect of temp on soluble ADH activity							
25	2.075	6200	0.335	0.335	0.084	1675.00	167.58
	2.078	6200	0.335	0.335	0.084	1675.00	
	2.081	6200	0.336	0.336	0.084	1680.00	
40	1.891	6200	0.305	0.305	0.076	1525.00	153.28
	1.901	6200	0.307	0.307	0.077	1535.00	
	1.910	6200	0.308	0.308	0.077	1540.00	
60	0.063	6200	0.010	0.010	0.003	50.00	50.20
	0.060	6200	0.010	0.010	0.002	50.00	
	0.064	6200	0.010	0.010	0.003	50.00	
80	0.057	6200	0.009	0.009	0.002	45.00	45.90
	0.057	6200	0.009	0.009	0.002	45.00	
	0.057	6200	0.009	0.009	0.002	45.00	
Effect of temp on immobilised ADH activity (PVA-Cl-EDA-GA-ADH)							
25	0.544	6200	0.088	0.088	0.022	0.146	0.147
	0.548	6200	0.088	0.088	0.022	0.147	
	0.550	6200	0.089	0.089	0.022	0.148	
40	0.472	6200	0.076	0.076	0.019	0.127	0.127
	0.472	6200	0.076	0.076	0.019	0.127	
	0.472	6200	0.076	0.076	0.019	0.127	
60	0.433	6200	0.070	0.070	0.017	0.117	0.116
	0.432	6200	0.070	0.070	0.017	0.116	
	0.434	6200	0.070	0.070	0.018	0.117	
80	0.389	6200	0.063	0.063	0.016	0.105	0.105
	0.390	6200	0.063	0.063	0.016	0.105	
	0.390	6200	0.063	0.063	0.016	0.105	

3.7.5 Immobilised ADH recyclability

The reusability of the immobilised ADH on the PVA-Cl-EDA-GA supports was measured by repeat use of the immobilised ADH to catalyse ethanol to acetaldehyde. After each use, the discs were washed with PBS (0.05 M, pH 7.5) three times over 10 min and activity was

remeasured using a fresh reaction mixture. Table 3.12 presents detailed activity data for recycled immobilised ADH.

Table 3.12 Activity measurement: ADH immobilised on PVA-Cl-EDA-GA disc reusability

No of use	Abs	NADH coefficient	Conc (mM)	Conc (mmol)	Total activity mmol/min	Activity mmol/min/g	Average activity
1	1.051	6200	0.170	0.339	0.085	0.706	0.696
	1.021	6200	0.165	0.329	0.082	0.686	
	1.012	6200	0.163	0.326	0.082	0.680	
2	0.718	6200	0.116	0.232	0.058	0.483	0.480
	0.715	6200	0.115	0.231	0.058	0.481	
	0.711	6200	0.115	0.229	0.057	0.478	
3	0.539	6200	0.087	0.174	0.043	0.362	0.366
	0.544	6200	0.088	0.176	0.044	0.366	
	0.550	6200	0.089	0.177	0.044	0.370	
4	0.399	6200	0.064	0.129	0.032	0.268	0.261
	0.389	6200	0.063	0.125	0.031	0.261	
	0.376	6200	0.061	0.121	0.030	0.253	
5	0.198	6200	0.032	0.064	0.016	0.133	0.129
	0.190	6200	0.031	0.061	0.015	0.128	
	0.187	6200	0.030	0.06	0.015	0.126	
6	0.089	6200	0.014	0.029	0.007	0.060	0.060
	0.088	6200	0.014	0.028	0.007	0.059	

3.8 References

1. I. Es, J. D. Goncalves Vieira and A. C. Amaral, *Applied Microbiology and Biotechnology*, 2015, **99**, 2065-2082.
2. W. Tischer and F. Wedekind, in *Biocatalysis From Discovery to Application*, eds. W.D. Fessner, A. Archelas, D. C. Demirjian, R. Furstoss, H. Griengl, K. E. Jaeger, E. Moris-Varas, R. Ohrlein, M. T. Reetz, J. L. Reymond, M. Schmidt, S. Servi, P. C. Shah, W. Tischer and F. Wedekind, Springer Berlin Heidelberg, Berlin, Heidelberg, 1999, DOI: 10.1007/3-540-68116-7-4, pp. 95-126.
3. S. Datta, L. R. Christena and Y. R. S. Rajaram, *3 Biotechnology*, 2013, **3**, 1-9.
4. K. Kiehl, T. Straube, K. Opwis and J. S. Gutmann, *Engineering in Life Sciences*, 2015, **15**, 622-626.
5. C.W. Wu, J.G. Lee and W.C. Lee, *Biotechnology and Applied Biochemistry*, 1998, **27**, 225-230.
6. G. Pencreach and J. C. Baratti, *Applied Microbiology and Biotechnology*, 1997, **47**, 630-635.
7. L. Kiwi-Minsker, I. Yuranov, V. Holler and A. Renken, *Chemical Engineering Science*, 1999, **54**, 4785-4790.
8. A. Kumar and S. S. Han, *International Journal of Polymeric Materials and Polymeric Biomaterials*, 2017, **66**, 159-182.
9. C. E. Schildknecht, *Journal of Polymer Science: Polymer Letters Edition*, 1974, **12**, 105-106.
10. T. Miyata, T. Uragami and K. Nakamae, *Advanced Drug Delivery Reviews*, 2002, **54**, 79-98.
11. D. A. Ossipov and J. Hilborn, *Macromolecules*, 2006, **39**, 1709-1718.
12. R. Yamdej, K. Pangza, T. Srichana and P. Aramwit, *Journal of Bioactive and Compatible Polymers*, 2017, **32**, 32-44.
13. J. M. Gohil, A. Bhattacharya and P. Ray, *Journal of Polymer Research*, 2006, **13**, 161-169.
14. B. Jin, J. Shen, R. Peng, Y. Shu, B. Tan, S. Chu and H. Dong, *Polymer Degradation and Stability*, 2012, **97**, 473-480.
15. J. Bernard, A. Favier, T. P. Davis, C. Barner-Kowollik and M. H. Stenzel, *Polymer*, 2006, **47**, 1073-1080.
16. S. Moulay, *Polymer-Plastics Technology and Engineering*, 2015, **54**, 1289-1319.
17. K. Herkommerova, J. Zemancikova, H. Sychrova and Z. Antosova, *Biotechnology Letters*, 2018, **40**, 405-411.
18. M. Bilal and M. Asgher, *Chemistry Central Journal*, 2015, **9**, 2-14.
19. M. Rebros, L. Liptak, M. Rosenberg, M. Bucko and P. Gemeiner, *Letters in Applied Microbiology*, 2014, **58**, 556-563.

20. R. V. Garay-Flores, E. P. Segura-Ceniceros, R. De Leon-Gamez, C. Balvantín-García, J. L. Martínez-Hernández, R. Betancourt-Galindo, A. R. P. Ramírez, C. N. Aguilar and A. Ilyina, *Journal of General and Applied Microbiology*, 2014, **60**, 262-269.
21. F. Kartal, A. Akkaya and A. Kilinc, *Journal of Molecular Catalysis B-Enzymatic*, 2009, **57**, 55-61.
22. S. H. Zuo, Y. J. Teng, H. H. Yuan and M. B. Lan, *Sensors and Actuators B-Chemical*, 2008, **133**, 555-560.
23. A. Idris, N. A. M. Zain and M. S. Suhaimi, *Process Biochemistry*, 2008, **43**, 331-338.
24. M. D. Busto, V. Meza, N. Ortega and M. Perez-Mateos, *Food Chemistry*, 2007, **104**, 1177-1182.
25. M. Rebros, M. Rosenberg, Z. Mlichova and L. Kristofikova, *Food Chemistry*, 2007, **102**, 784-787.
26. D. M. De Temino, W. Hartmeier and M. B. Ansorge-Schumacher, *Enzyme and Microbial Technology*, 2005, **36**, 3-9.
27. G. Singh, Suman, D. N. Tanwar and C. S. Pundir, *Indian Journal of Biochemistry & Biophysics*, 2002, **39**, 397-400.
28. Y. H. Diao, Q. L. Wang and S. Y. Fu, *Letters in Applied Microbiology*, 2002, **35**, 451-456.
29. A. Rossi, A. Morana, I. Di Lernia, A. Ottombrino and M. De Rosa, *Italian Journal of Biochemistry*, 1999, **48**, 91-97.
30. A. M. Araujo, M. T. Neves, W. M. Azevedo, G. G. Oliveira, D. L. Ferreira, R. A. L. Coelho, E. A. P. Figueiredo and L. B. Carvalho, *Biotechnology Techniques*, 1997, **11**, 67-70.
31. B. Jin, J. Shen, R. F. Peng, Y. J. Shu, S. J. Chu and H. S. Dong, *Macromolecular Research*, 2014, **22**, 117-123.
32. M. Cerreti, K. Markosova, M. Esti, M. Rosenberg and M. Rebros, *International Journal of Food Science. Technology.*, 2017, **52**, 531-539.
33. J. C. Santos, A. V. Paula, G. F. M. Nunes and H. F. de Castro, *Journal of Molecular Catalysis B: Enzymatic*, 2008, **52-53**, 49-57.
34. S. V. Caro, C. S. P. Sung and E. W. Merrill, *Journal of Applied Polymer Science*, 1976, **20**, 3241-3246.
35. C. Linder, M. Nemas, M. Perry and R. Ketraro, *Journal*, 1993, **2**, 1-11.
36. D. H. Zhang, L. X. Yuwen and L. J. Peng, *Journal of Chemistry*, 2013, DOI: 10.1155/2013/946248.
37. F. H. Isgrove, R. J. H. Williams, G. W. Niven and A. T. Andrews, *Enzyme and Microbial Technology*, 2001, **28**, 225-232.
38. S. Soni, J. D. Desai and S. Devi, *Journal of Applied Polymer Science*, 2001, **82**, 1299-1305.
39. Q. Li, E. W. Grandmaison, M. F. A. Goosen and E. T. Dunn, *Journal of Bioactive and Compatible Polymers*, 1992, **7**, 370-397.

40. V. Gimenez, A. Mantecon, J. C. Ronda and V. Cadiz, *Journal of Applied Polymer Science*, 1997, **65**, 1643-1651.
41. M. Z. Atassi and T. Manshouri, *Journal of Protein Chemistry*, 1991, **10**, 623-627.
42. D. A. Ossipov and J. Hilborn, *Macromolecules*, 2006, **39**, 1709-1718.
43. H. J. Xu, D. D. Chen and Z. G. Cui, *Journal of Surfactants and Detergents*, 2011, **14**, 167-172.
44. C. S. Yu and B. Li, *Polymer Composites*, 2008, **29**, 998-1005.
45. R. A. Sheldon and S. van Pelt, *Chemical Society Reviews*, 2013, **42**, 6223-6235.
46. J. A. Howarter and J. P. Youngblood, *Macromolecules*, 2007, **40**, 1128-1132.
47. H. S. Mansur, R. L. Orefice and A. A. P. Mansur, *Polymer*, 2004, **45**, 7193-7202.
48. D. Guclu, M. Rale and W. D. Fessner, *European Journal of Organic Chemistry*, 2015, 2960-2964.

Chapter 4

Glass fibrous support for ADH immobilisation

This chapter describes surface modification and ADH immobilisation on both woven and non-woven glass fabric. ADH immobilised on non-woven glass fabric support was investigated for two applications: first for the fabrication of an electrode for biosensing, and secondly for the development of a continuous flow reactor. Chapter 4 represents a major component of this doctoral thesis and has resulted in one manuscript to date.

4.1 Introduction

In modern analytical practices, with help of enzyme selective recognition and conversion of target analytes into easily detected products can be obtained. These applications require high biocatalytic activity to provide the rapid conversion of an analyte into a product. Such processes typically involve continuous feed of the enzyme. From a practical point of view however, immobilised enzymes are preferred for biosensors and bioreactor applications.¹⁻³

The biosensors are categorised mainly into two types: one catalytic biosensor and another is affinity biosensors. The catalytic biosensor measure steady-state concentration of detectable species formed/lost due to a biocatalytic reaction.² The affinity biosensor binds to the proteins, lectins, receptors, nucleic acids, whole cells, or antibodies causing physicochemical change which can be detected.^{3,4} In a biosensor, the biomolecule layer is in intimate contact with the transducer resulting in an electrical signal in response to an analyte.^{5,8} The presenting biomolecule can be an enzyme, DNA, protein, whole cell, or an antibody.⁶ The sensing platform or transducer is usually a glassy carbon (GC) electrode and the site of the chemical reaction between the analyte and biomolecule.⁷ Biosensors are divided into different groups, for example electrochemical, optical, thermal and piezoelectric,⁸ based on the transducer (or signals transduced). Electrochemical biosensors generate an electrical signal on chemical reaction between the analyte and biomolecule. Optical biosensors analyze alteration in the

properties of light (e.g. fluorescence) when the analyte interacts with the biomolecule. Thermal biosensors respond to change in temperature and piezoelectric biosensors sense change in mass resulting from an interaction between analyte and biomolecule.⁹

Pharmaceutical, clinical, military, food and environmental disciplines show great interest in electrochemical biosensors due to the following advantages: they are simple, portable, possess short response time, sensitive, low cost, and display greater selectivity than optical, piezoelectric, and thermal biosensors. Moreover, they require less sample for analysis.¹⁰ In amperometric biosensors, a constant voltage is applied to the electrode to generate current flows in the system. Upon application of voltage, a redox reaction occurs on the electrode surface resulting in an electric current proportional to the concentration of the analyte. These biosensors show high sensitivity with low detection limits.¹¹ In this chapter, biosensor investigations were carried out using electrochemical techniques to facilitate the detection of ethanol.

Ethanol is a common chemical found in alcoholic beverages, medicine, mouthwash, household products and the degradation of food, and has been associated with adverse health risks.¹² Hence, there is considerable demand for simple, sensitive, and rapid assays for ethanol in food products and biological fluids.¹³ In alcohol biosensors, two enzymes have been extensively studied for the determination of alcohol, namely alcohol dehydrogenase (ADH) and alcohol oxidase (AOX). This is due to the ability of ADH and AOX to catalyse the reaction of alcohol and enhances the sensitivity of the analysis.¹² (Table 4.1)

Table 4.1 Examples of the analytical parameters and performance of some recently reported ADH based ethanol biosensors described in below table which is reproduced from literature^{14,15}

Electrode	Measurement Potential (mV)	Linear Range (mM)	Sensitivity (mA mM ⁻¹ cm ⁻¹)	NAD ⁺ (mM)
SPCE/MWCNTs/AuNPs/PNR/ADH	200 (vs SPR)	0.3–1 0	49	7
CPE/Fe ₃ O ₄ @Au/ADH	100 (vs Ag/AgCl)	100–2000	0.02	0.25
GC/ERGO-PTH/ADH	400 (vs SCE)	0.05–1.0	2.8	5
GC/SWCNTs-Polytyrosine (oxidized)/ADH/Naf	200 (vs Ag/AgCl)	0.01–0.15	5.8±0.1	2
ZnO/DPGP/ADH	5 (vs SCE)	0.01–0.65	7.6	5
Pt/PtNPs/PMDUS/ADH	250 (vs SCE)	1.4–10	0.26	1
PGE/SWCNTs/PCV/ADH	200 (vs SCE)	9.33 x 10 ⁻³ -0.32	1.94	5

Biosensors using ADH and cofactor nicotinamide adenine dinucleotide (NAD⁺) exhibit high selectivity and stability whereas those based on AOX show low storage stability.¹⁵ In the past mediators and signal promoters such as nanoparticles and redox polymers were used to improve the sensitivity.¹⁶⁻¹⁸ Immobilised ADH enzyme has been used with many different mediators including magnetic gold nanoparticles,¹⁹ cellulose acetate,²⁰ multi-wall carbon nanotubes²¹ and zirconium dioxide (ZrO₂) nanoparticles.²²

Immobilised enzyme reactors can be divided into several different categories including batch reactors, fixed-bed reactors, continuous stirred tank reactors, continuous flow reactors, and fluidized-bed reactors.²³ These reactor types can also be combined or modified. The biocatalytic reactions run in batch processes using immobilised enzymes can experience inhibition due to saturation of the reaction solution. In the enzymatic flow reactor, enzymes can be immobilised on high surface area functionalised supports and thus allow for a high density enzyme loading.²⁴ Furthermore, with an enzymatic flow reactor, the product is removed

continuously from the reaction mixture preventing enzyme inhibition. Furthermore, the enzyme remains stable in the reactor to facilitate recycling. Although immobilised enzymes have been used for chemical analysis for over a decade, their joint application with flow-injection analysis (FIA) dates from only 1982.²⁵⁻²⁷ Flow injection analysis method can allow the quantification of the species of interest using injection of defined liquid volume in a continuously flowing carrier stream. It is simple and offers many advantages over manual analytical methods such as flexibility, simplicity, selectivity, reproducibility, and higher sampling rate. FIA methods involving immobilised enzymes have been applied to a variety of analytes (e.g. ethanol, glucose and L-glutamine) where the most frequent technique for detection of this analyte has been amperometry, with enzymatic or non-enzymatic electrodes.²⁸ Immobilised ADH reactors were developed incorporating supports such as silica gel,²⁹ glass beads,³⁰ polyvinyl alcohol-hydrogel beads,³¹ controlled-pore glass,^{32, 33} and calcium alginate fibre,³⁴ and used in flow injection systems for the detection of ethanol. Amongst these various supports silica has been the predominant inorganic support material used as mesoporous silica,^{35, 36} silica nanoparticles,^{37, 38} chitosan-silica³⁹⁻⁴¹ and glass.^{42, 43} Irrespective of the type of biosensor, or flow reactor (bioreactor), a final analyte detection step at the solid-liquid interface or in the solution phase is required.⁴⁴ Therefore, the performance of biosensors and bioreactors greatly depends on the method of immobilisation and surface chemistry of the support.

Glass is commonly used as support for enzyme immobilisation because of its silicon dioxide (SiO₂) composition which is abundant in nature and thermally stable.⁴⁵ Glass substrates are also readily available, simple to handle, and possess high mechanical stability. Porous glass is a promising support where surface properties are mainly determined by the silanol groups and can be made in various geometrical forms, i.e. rods, beads, (hollow) fibres, plates or fabric.⁴⁶ Physical adsorption or physisorption is one of the simplest techniques used for DNA immobilisation on glass surfaces.⁴⁷ Glass surfaces can be modified by introducing different

functional groups on the surface for covalent bonding with an enzyme. Glass chips and beads have been modified to create amine functionality, *via* reaction with (3-aminopropyl) trimethoxysilane (APTMS), for reaction with GA (or other aldehydes).⁴⁸ Apart from silanisation, epoxylation is another commonly used approach for glass surface modification. One of the disadvantages of this approach is the need for a high pH (>9) which results in glass surface degradation and inconsistent results.⁴⁹ Furthermore, the high pH can also damage the native three-dimensional structure of enzymes resulting in decreased sensitivity and increased non-specific interactions.²⁴ The immobilisation effort can be further reduced by initially modifying the glass surface with bifunctional silane reagents, e.g. aldehydes (using 3-(trimethoxysilyl)propyl aldehyde),⁵⁰ and isocyanates (using 3-(trimethoxysilyl) propyl isocyanate).⁵¹ In these cases, no additional linker reactant is required for attaching an amine-functionalised enzyme because they readily form covalent bonds with the surface. However, in all the referenced procedures it is necessary to block non-specific binding after immobilisation.^{52, 53} Due to the variety of surface modification methods, glass as a support material has been extensively used for the immobilisation of enzymes for biocatalyst and biosensor applications.

Table 4.2 Glass supports used for the immobilisation of enzymes

Support	Enzyme	Method of Immobilisation	Application	Refs
Controlled pore glass	Glucose oxidase	Covalent	Biosensor	54
Amine functionalized glass beads	α -Amylase	Covalent	Biocatalyst	55
Controlled pore glass beads	Nitrite reductase	Covalent	Biosensor	56
Glass slide	Chicken immunoglobulin (IgG) was used as antigens	Covalent	Biocatalyst	57

Table 4.2 Continued...				
Support	Enzyme	Method of Immobilisation	Application	Refs
Glass beads	α -Amylase	Covalent	Biocatalyst	58
Glass beads	Chymotrypsin β -galactosidase	Covalent	Biocatalyst	59
Glass fibre	Alkaline phosphatase	Covalent	Biocatalyst	60
Controlled pore glass	Glucose dehydrogenase	Adsorption	Bioreactor	61
Glass beads	Chloroperoxidase	Covalent	Biocatalyst	43

In this chapter, woven glass fabric (E Glass, 55% Si-OH, diameter 76 mm) and non-woven glass fabric (glass microfiber filter, borosilicate glass, 80% Si-OH, diameter 47mm) were investigated as solid supports for ADH immobilisation. Both of these supports possess high porosity and surface area.⁶²⁻⁶⁴

The following approach was utilised in this chapter:

- Woven and non-woven glass fabric surfaces were functionalised with various silane reagents bearing different pendent functional groups to facilitate ADH covalent immobilisation.
- Surface modified glass fabric scaffolds were subjected to ADH immobilisation. ADH immobilisation protocols were performed at different pHs to optimise enzyme activity.
- ADH immobilised on surface modified glass fabric scaffolds was assayed for stability (pH, temperature and storage).
- The non-woven glass fabric-ADH construct possessing the highest activity was employed for the fabrication of an electrode for the indirect detection of ethanol. The performance of the electrode was evaluated across a range of ethanol concentrations.

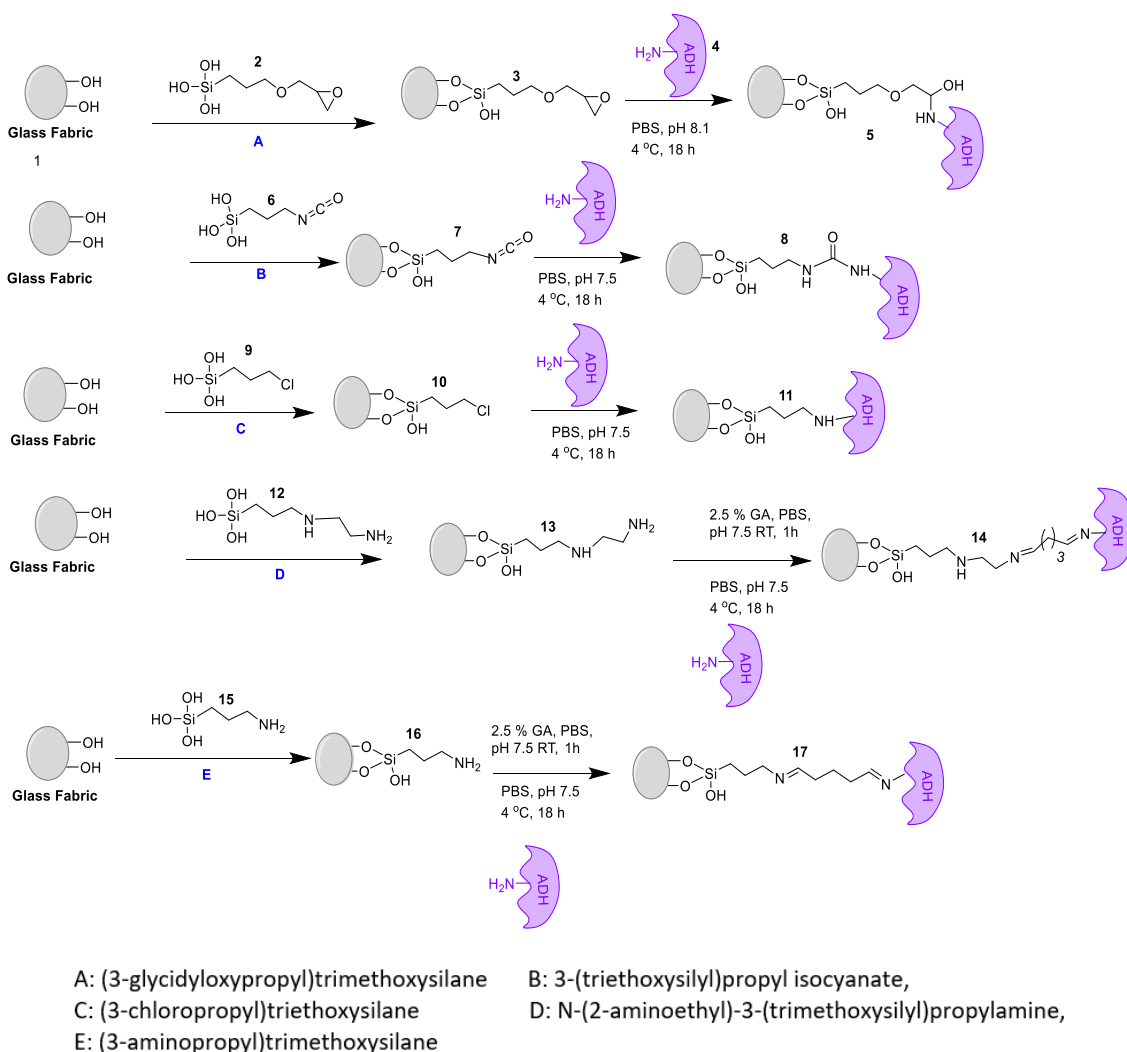
- The above mentioned non-woven glass fabric-ADH construct was also investigated in a continuous flow reactor, with a glassy carbon electrode, for the detection of ethanol.

4.2 Woven glass fabric

4.2.1 Surface modification and immobilisation

The woven glass fabric (E Glass, 55% Si-OH) were cut into discs (13 mm in diameter) and activated with 10 N HCl at different temperatures and times prior to the silanisation reactions. The activation process was optimised by varying the activation time (2 h, 4 h, and 8 h) and the temperature (50 °C, 60 °C, 85 °C). IR spectroscopy was used to monitor the activation process and the presence of free hydroxyl groups (3400-3200 cm^{-1}) which are not present in glass fabric. The optimum reaction time was found to be 85 °C for 2 h in 10 N HCl. The above mentioned activated glass fabric discs were silanised with silane reagents such as (3-glycidyloxypropyl)trimethoxysilane (A), 3-(triethoxysilyl)propyl isocyanate (B), (3-chloropropyl)triethoxysilane (C), *N*-(2-aminoethyl)-3-(trimethoxysilyl)propylamine (D), (3-aminopropyl)trimethoxysilane (E), each bearing reactive pendent functionality (Table 4.3). These immobilised silane reagents were then used for ADH immobilisation. To the best of our knowledge, these silane modified woven glass supports have not been used for covalent ADH immobilisation. Woven glass fabric supports after silanisation with 2.5% *N*-(2-aminoethyl)-3-(trimethoxysilyl)propylamine (D), (3-aminopropyl)trimethoxysilane (E) were activated with 2.5% GA prior to ADH immobilisation; other silane modified glass fabric samples were subjected to ADH immobilisation without GA activation (Scheme 4.1, A, B and C). Woven and non-woven glass surface modification with silane reagents such as (3-glycidyloxypropyl) trimethoxysilane (A) was initially analysed with FTIR.

After modification, the observed peak were $1,057\text{ cm}^{-1}$ and $1,037\text{ cm}^{-1}$ corresponding to the stretching vibration of Si-O-Si and 961 cm^{-1} broad band for Si-OH. However the required epoxy 915 cm^{-1} stretching vibration for C-O and 831 cm^{-1} stretching for C-O-C group were not observed due to their masking under broad peak of Si-OH backbone. Similar results were found for (3-chloropropyl) trimethoxysilane (C). Therefore, we assessed silane modification and subsequently immobilised enzyme activity via activity assay. Woven glass fabric supports without silane modification were exposed to ADH under identical conditions and enzyme activity was compared against the activity of immobilised ADH on silane modified supports (Table 4.3).



Scheme 4.1. Schematic representation of silane reactions with glass surfaces followed by ADH immobilisation

Table 4.3 Effect of various silane modifications on immobilised ADH activity

Silane reagent (2.5 % v/v in acetone)	ADH immobilisation conditions	Immobilised ADH activity on woven glass fabric (mmol/min/g)
(3-glycidyoxypropyl) trimethoxysilane (A)	PBS, pH 8.1, 18 h at 4 °C	0.420 ± 0.023
3-(triethoxysilyl)propyl isocyanate (B)	PBS, pH 7.5, 18 h at 4 °C	0.758 ± 0.088
(3-chloropropyl) triethoxysilane (C)	PBS, pH 7.5, 18 h at 4 °C	0.503 ± 0.039
<i>N</i> -(2-aminoethyl)- 3-(trimethoxysilyl)propyl amine (D)	PBS, pH 7.5, 18 h at 4 °C	1.037 ± 0.027
3-Triethoxysilylpropylamine (APTMS) (E)	PBS, pH 7.5, 18 h at 4 °C	2.778 ± 0.047

Table 4.3 presents measured ADH activity data for ADH immobilised on various silane woven glass fabric scaffolds. Woven glass fabric modified with epoxy silane (A) was reacted at higher pH (8.1) to aid immobilisation;⁴⁹ other silane modified glass fabric supports were immobilised at pH 7.5. APTMS modified glass fabric support exhibited the highest activity (2.778 ± 0.047 mmol/min/g). Hence, further investigation of APTMS modified glass fabric was performed *via* APTMS and GA concentration studies.

4.2.2 APTMS concentration effect on immobilised ADH activity

An APTMS concentration study was undertaken on woven glass fabric support to quantify the effect on ADH activity. The HCl activated glass fabric discs were allowed to react with different concentrations of APTMS ranging from 1 to 10 % (v/v) in acetone and the resultant construct was activated with GA prior to ADH immobilisation. The effect of APTMS

concentration on ADH activity is shown in Figure 4.1 and detailed activity data is presented in Table 4.8 in the Experimental Section 4.8.4.7.

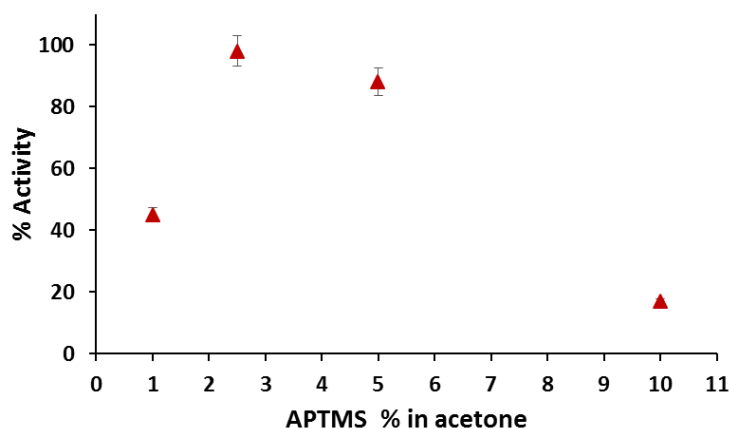


Figure 4.1. Effect of concentration of 3-trimethoxysilylpropylamine (APTMS) on ADH activity. The assay was performed in triplicate and error bars represent standard deviations (S.D.)

Figure 4.1 shows that use of the highest concentration of APTMS (10%) inhibited ADH activity. ADH immobilised on 5% APTMS modified glass fabric showed 85% activity and the highest enzyme activity was observed with 2.5% APTMS concentration. At the higher APTMS concentrations (5 and 10%) the lower activity observed could be due to polymerisation of APTMS reagent on the glass surface leading to deleterious GA cross-linking and poor ADH immobilisation.⁶⁵ Consequently, a 2.5% loading of APTMS reagent was used in subsequent immobilisation work.

4.2.3 GA concentration effect on immobilised ADH activity

The 2.5% APTMS modified glass fabric discs were incubated in varying concentrations of GA (1%, 2.5%, 5% and 10% w/v in PBS) solution and immobilised with ADH separately. Prior to the activity assay, GA activated APTMS-glass fabric discs were washed with excess PBS. The

effect of GA concentration on immobilised ADH activity is shown in Figure 4.2 (A). Detailed activity data is presented in Table 4.9 in the Experimental Section 4.8.4.8.

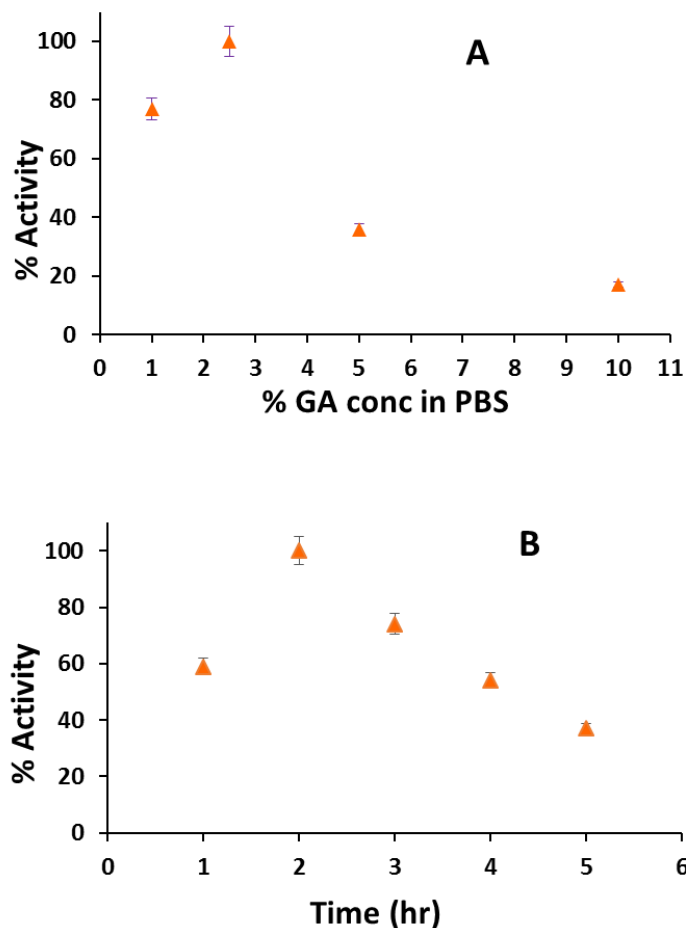


Figure 4.2 A. Effect of glutaraldehyde (GA) concentration on immobilised ADH activity. B. Effect of glutaraldehyde (GA) activation time on immobilised ADH activity. The ADH assay was performed on triplicate samples and error bars represent standard deviations. To display the data, the highest activity was taken as 100 % and subsequent activities were normalised accordingly

As shown in Figure 4.2 A, optimal GA concentration was found to be 2.5%. With increasing GA concentration, the amino groups of APTMS modified glass fabric support become modified and facilitate the immobilisation of the ADH enzyme. At higher GA concentration enzymatic activity is lower because of extensive crosslinking between support and enzyme. The excessive crosslinking can result in a distortion of enzyme structure (i.e. the active site)

which can affect accessibility and convenient arrangement of the substrate, and ultimately can affect the retention of the activity.⁶⁷

The effect of GA activation time on ADH activity was also investigated by treating APTMS modified glass fabric disc with 2.5% GA over different reaction times (0.5 h, 1 h, 2 h, 3 h, 4 h, 5 h) and results are presented in Figure 4.2 B. Enzyme activity reached a maximum when the reaction was performed over a 2 h period and thereafter declined rapidly. Hence, the GA solution concentration and cross-linking time had a significant effect on the immobilised ADH activity. In conclusion, immobilised ADH activity reached maximum (3.907 mmol/min/g) when the concentration of GA solution was 2.5% and had cross-linking time of 2 h. Further investigations such as the effect of pH, thermal stability and storage stability on glass woven fabric was performed utilising these optimised conditions.

4.2.4 Characterisation of APTMS-GA modified woven glass fabric

4.2.4.1 SEM

Electron microscopy was used to investigate changes in morphology after surface modification and immobilisation. After silanisation and curing, the glass fabric (Figure 4.3a) showed signs of thermal stress (cracks) (Figure 4.3b). After GA activation (Figure 4.3c) and ADH immobilisation (Figure 4.3d) the surface morphology had changed. However, during surface modification and ADH immobilisation glass fabric integrity was preserved and displayed 2.778 ± 0.047 mmol/min/g ADH activity.

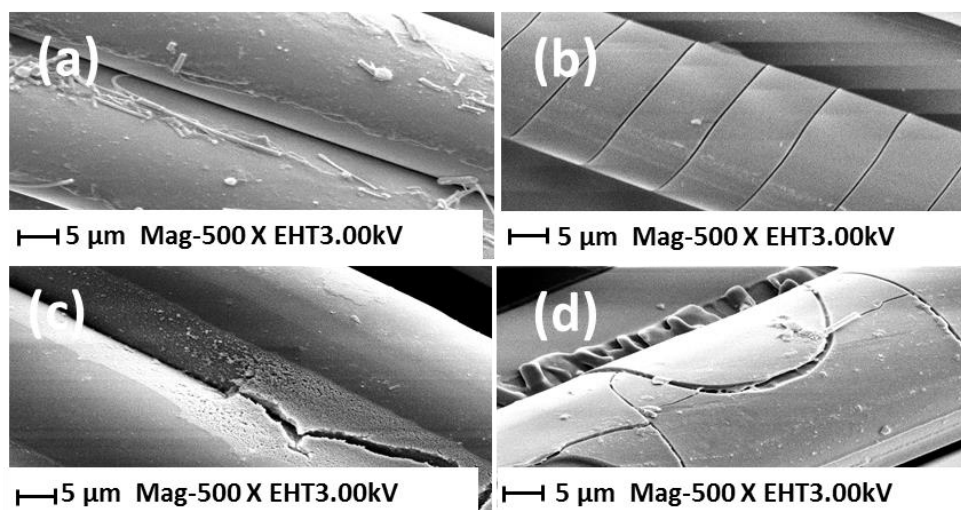


Figure 4.3. a) SEM images showing the morphology of woven glass fabric as received; b) HCl activated and APTMS treated c) GA crosslinked, and d) immobilised with ADH

4.2.4.2 XPS analysis

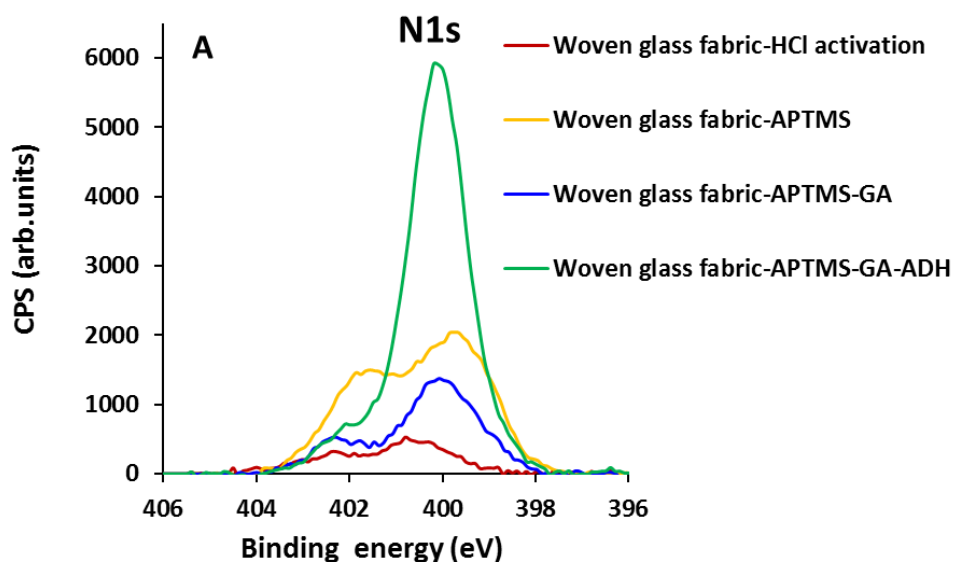
XPS was used to analyse for the presence of nitrogen on the glass fabric surfaces after APTMS and ADH immobilisation. The results for the main elements O, Si and N are described in Table 4.4.

Table 4.4 Elemental compositions expressed as atomic ratios X/C, i.e. the atomic concentration of element X relative to that of C

Element	Glass woven fabric HCl activated	Glass woven fabric HCl + APTMS	Glass woven fabric HCl + APTMS + GA	Glass woven fabric HCl + APTMS + GA + ADH
	Mean	Mean	Mean	Mean
O/C	1.169 ± 0.09	1.728 ± 0.05	1.586 ± 0.05	0.732 ± 0.01
Si/C	0.511 ± 0.03	0.832 ± 0.02	0.726 ± 0.04	0.301 ± 0.01
N/C	0.027 ± 0.003	0.134 ± 0.04	0.065 ± 0.01	0.134 ± 0.04

Table 4.4 shows that the O/C and Si/C ratios was increase along with N/C ratio indicating the presence of amino silane on the glass fabric support after APTMS modification.

The C1s spectrum for woven glass fabric supports (Figure 4.4) shows peaks at 285 eV (C–C) and 286.5 eV (C–O/C–N) which is consistent with silane modification. The increase in N/C ratio consists of two N1s peaks (Figure 4.4A, yellow line), one at 399–400 eV (amines), the other at approximately 402 eV (protonated amines, i.e. N⁺). This double peak is typically observed after APTMS surface modification. A further drop of O/C and Si/C with N/C ratio was observed after addition of GA; the C1s (Figure 4.4A, blue line) is very similar to silane modification glass fabric but with a slight increase at approximately 288 eV indicating the presence of aldehyde (GA). Upon ADH immobilisation, a further drop in O/C and Si/C with N/C ratio supports the presence of ADH. Here the C1s displays the characteristic peak shape of polypeptides/proteins (i.e. ADH) with a clearly resolved peak at >288 eV (due to peptide bonds) and a strong shoulder at 286.5 eV (due to various C–N and C–O based functional groups). The corresponding N1s (Figure 4.4B, green line) displays an additional strong peak at approx. 400 eV consistent with peptide bonds.



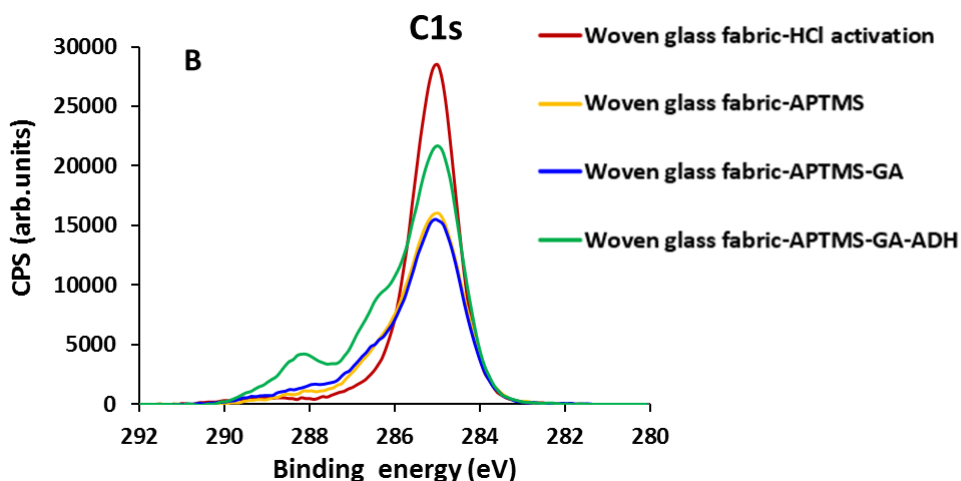


Figure 4.4. High-resolution XPS spectra C1s (A) and N1s (B) for woven glass fabric (red line), 2.5% APTMS modified glass fabric (yellow line), GA activation (blue line) and ADH immobilised glass fabric (green line)

Detailed characterisation of the woven glass fabric with SEM and XPS supported successful surface modification and ADH immobilisation. The glass fabric support modified with 2.5 % APTMS and GA reagent was further evaluated for stability across a pH range, varying temperature and storage half-life. These characteristics are important for industrial applications where immobilised enzymes are required to perform within variable pH and temperature ranges.

4.2.5 Immobilised ADH stability studies

4.2.5.1 pH stability

The activity of an enzyme is heavily dependent on the pH of the surrounding environment. Figure 4.5 shows the effect of pH on the activities of both the soluble and immobilised ADH (woven glass fabric support); detailed activity data is presented in Table 4.10, Section 4.8.5.1.

At pH 5 and 6, both soluble and immobilised ADH showed lower than optimal activity. The optimal pH of immobilised ADH was ~7 and identical to that of soluble ADH. The immobilised ADH retained 30% of its activity at pH 9 whereas soluble ADH showed complete loss of activity at pH 9 and above.

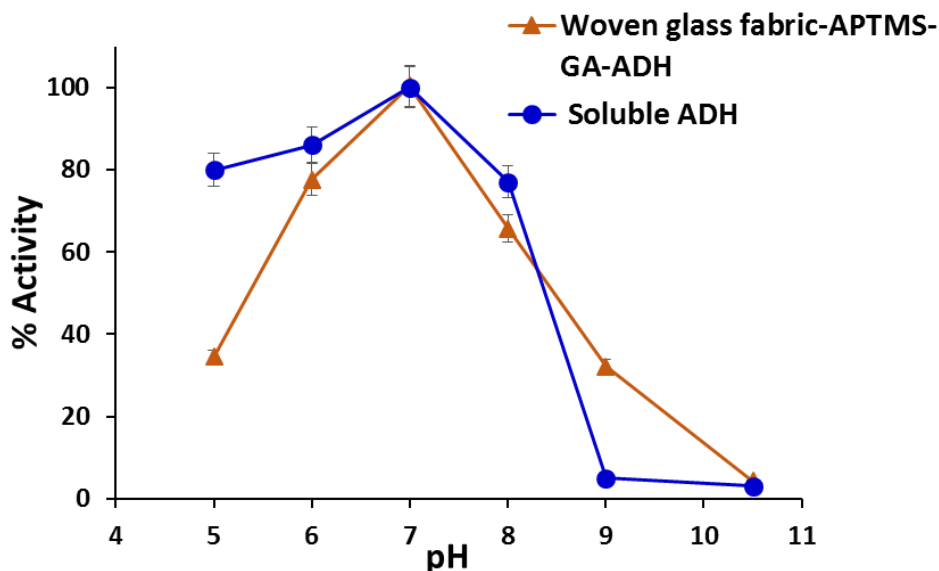


Figure 4.5. Effects of pH on the activities of the free and immobilised ADH. The ADH assay was performed on triplicate samples for each pH value and error bars represent standard deviations. To display the data, the highest activity was taken as 100 % and subsequent activities were normalised accordingly

It was found that APTMS modified glass fabric support could noticeably enhance the stability of ADH at higher pH values (i.e. > pH 8.5), as compared to the soluble enzyme. This implies that the APTMS modified glass fabric support could protect immobilised enzyme from inactivation in solutions higher than the optimum pH value. The enzymatic optimum pH value remained constant on immobilisation supporting the notion that the enzyme microenvironment did not significantly change.⁶⁸ Compared to soluble ADH, the immobilised ADH enhances the pH stability due to limited movement and multipoint linkage which leads to lower conformational change when the pH changes. Broadening of pH profiles by immobilisation

has been reported for numerous enzymes, such as acetylcholinesterase, chloroperoxidase, phospholipase A and lipase.⁶⁹

4.2.5.2 Thermal stability

To check the thermal stability of immobilised ADH, soluble and immobilised ADH were incubated at wide range of temperatures (20 to 80 °C) in PBS for 2 h and their residual activities were measured. The % activity data in Figure 4.6 shows that both free and immobilised ADH enzymes have significantly diminished relative activities above 40 °C. A detailed activity data table is presented in the Experimental Section 4.8.5.2, Table 4.11.

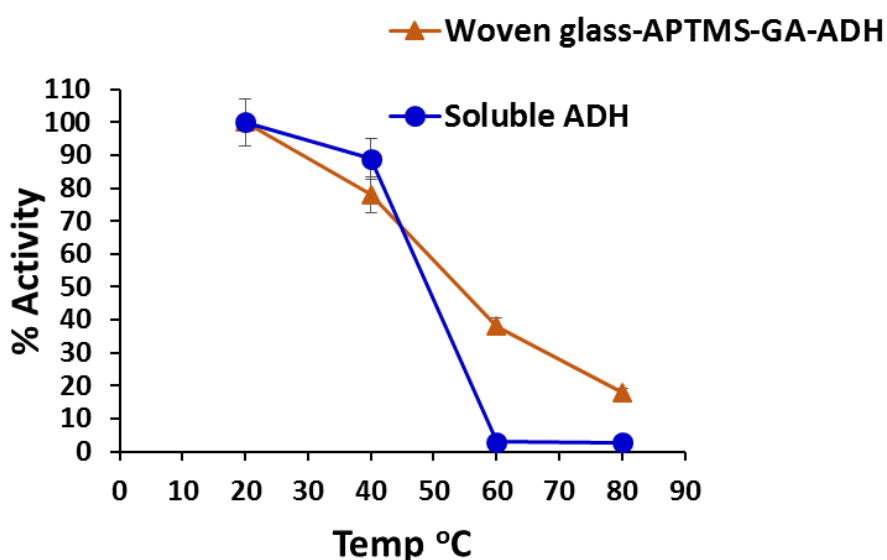


Figure 4.6. Effects of temperature on the activity of the soluble and immobilised ADH on woven glass fabric. The ADH assay was performed on triplicate samples for each temp value and error bars represent standard deviations. To display the data, the highest activity was taken as 100 % and subsequent activities were normalised accordingly

Figure 4.6 shows that soluble ADH had high enzyme activity below 50 °C, but less activity above 60 °C. ADH enzyme is tetrameric in nature, there could be possibility of negative effect on the subunits assembly of ADH due to the intense multiple interaction with the support, which reduced the immobilised enzyme stability at 40 °C. However, at 60 °C and above, the residual activity of the immobilised enzyme is higher than that of soluble enzyme.

Immobilised ADH on woven glass fabric retains 39 % activity at 60 °C, while soluble ADH retains less than ~2% above 60 °C. It has been observed that the thermal deactivation temperature (T_d) for ADH is 63 °C; at this temperature reversible thermo-induced thiol inactivation, aggregation and protein deamidation occur.⁷⁰ Significantly, the immobilised ADH retained activity (20%) at 80 °C. The similar observations were reported by Jiang *et al.*^{71, 72} The loss in ADH activity of the soluble form was observed due to denaturation of the enzyme at higher temperature. Thermal stability of ADH improved after immobilisation on glass fabric support, which is due to either the conformational limitation of the enzyme or low restriction to substrate diffusion at high temperature. The results indicate that ADH immobilised on glass fabric support has good thermal stability. Similar enhancement in stability was seen when ADH was immobilised on various supports like glyoxyl agarose,⁷³ magnetic graphene oxide nanocomposites, and glass beads.⁷⁴

4.2.5.3 Storage Stability

Storage stability of the immobilised ADH was investigated on glass fabric at 4 °C in PBS buffer (0.05 M, pH 7.4). Soluble ADH was stored under identical conditions and activity was measured and compared with the immobilised ADH. Detailed activity data is presented in Experimental Section 4.8.5.3, Table 4.12. Activity was measured on a 24 h cycle for the first 5 days and later tested at increasing time intervals. The soluble ADH showed 59% loss of activity after 10 days storage and total loss of activity after 60 days (Figure 4.7). Unfortunately, ADH immobilised on APTMS modified woven glass fabric support showed rapid loss of activity after 2 days of storage and complete loss of activity recorded after 30 days.

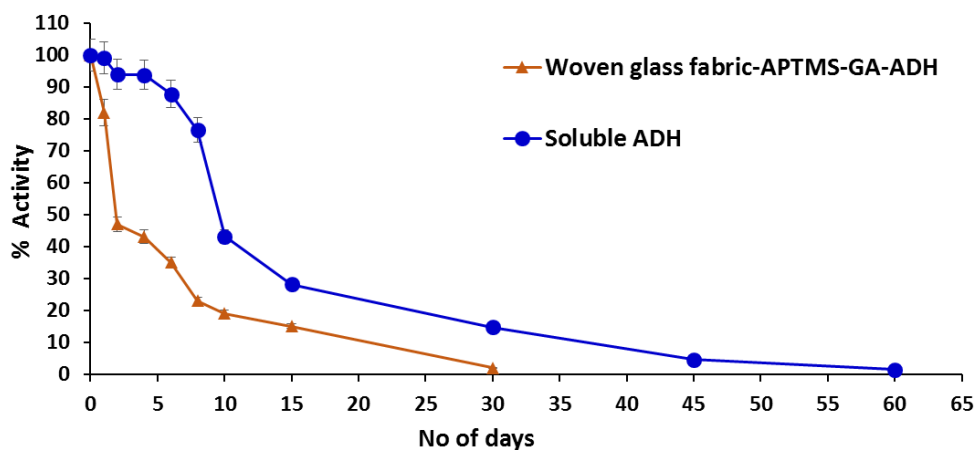


Figure 4.7. Storage stability of ADH immobilised on woven glass fabric and soluble ADH in PBS (0.05 M) at 4 °C. The ADH assay was performed on triplicate samples and error bars represent standard deviations. To display the data, the highest activity was taken as 100 % and subsequent activities were normalised accordingly

There could be following two reasons for the lower stability of immobilised ADH 1) The silane content of woven glass fabric was low (49-55%, Si-OH) which lead to less immobilisation and ultimately lower stability. 2) The immobilised ADH activity loss could be due to enzyme leakage from the support during the storage period from woven glass fabric. Figure 4.7 suggests that soluble ADH is more stable than immobilised ADH.

4.3 Non-woven glass fabric

In this section, non-woven glass fabric (borosilicate, 80% Si-OH) discs were investigated for surface modification and ADH immobilisation. Non-woven glass fabric surface modification was done with (3-Glycidyloxypropyl)trimethoxysilane (A), 3-(Triethoxysilyl)propyl isocyanate (B), (3-Chloropropyl)triethoxysilane(C), *N*-(2-Aminoethyl)-3-(trimethoxysilyl)propylamine(D), (3-Aminopropyl)trimethoxysilane (E), silane reagents as described for woven glass fabric (Section 4.2.1, Scheme 4.1). The modified non-woven glass fabrics were accessed for activity after ADH immobilisation. Higher activity silane modified

non-woven glass fabric supports were then subjected to the previously described stability studies (i.e. pH, temperature and storage).

4.3.1 Surface modification and ADH immobilisation

Prior to silanisation non-woven glass fabric were activated with 10 N HCl at 85 °C for 2 h. The activation process was optimised by varying the activation time (2h, 4h, and 8h) and the temperature (50 °C, 60 °C, 85 °C). IR spectroscopy was used to monitor the activation process (i.e. the presence of free hydroxyl groups 3400-3200 cm⁻¹). The optimum conditions for HCl activation were found to be similar to woven glass fabric HCl activation (85 °C for 4 h with 10 N HCl). The HCl activated non-woven glass fabric discs were then silanised with various silane reagents as per previously described for woven glass fabric (Section 4.2.1, Table 4.3, A to E). Silane reaction optimisation on non-woven glass fabric was performed at elevated temperature (110 °C) but resulted in the disintegration of the discs. Non-woven glass fabric supports, after silanisation with 2.5% *N*-(2-Aminoethyl)-3-(trimethoxysilyl)propyl amine (D) and triethoxysilylpropylamine amino propyl (E), were activated with 2.5% GA prior to ADH immobilisation; other silane modified glass fabric discs were subjected to ADH immobilisation without GA activation (Scheme 4.1). After surface modification and ADH immobilisation, the activities of the discs were compared against non-modified glass supports (control) (Table 4.5).

Table 4.5 Effect of various silane reagents on immobilised ADH activity

Silane reagent (2.5% v/v in acetone)	ADH immobilisation conditions	Immobilised ADH activity on non-woven fabric (mmol/min/g)
3-(Glycidyoxypropyl) trimethoxysilane (A)	PBS, pH 8.1, 18 h at 4 °C	0.603 ± 0.03
3-(Triethoxysilyl)propyl isocyanate (B)	PBS, pH 7.5, 18 h at 4 °C	0.758 ± 0.00

Silane reagent (2.5% v/v in acetone)	ADH immobilisation conditions	Immobilised ADH activity on non-woven fabric (mmol/min/g)
3-(Chloropropyl) triethoxysilane (C)	PBS, pH 7.5, 18 h at 4 °C	1.711 ± 0.03
<i>N</i> -(2-Aminoethyl)-3 (trimethoxysilyl)propyl amine (D)	PBS, pH 7.5, 18 h at 4 °C	2.855 ± 0.02
3-Triethoxysilylpropylamine (APTMS) (E)	PBS, pH 7.5, 18 h at 4 °C	5.645 ± 0.03

The above data reveals that ADH immobilised on amino propyl silane (APTMS) modified non-woven glass fabric exhibits the highest enzyme activity (5.645 ± 0.03 mmol/min/g). The activity is also presented in a graphical format (Figure 4.8).

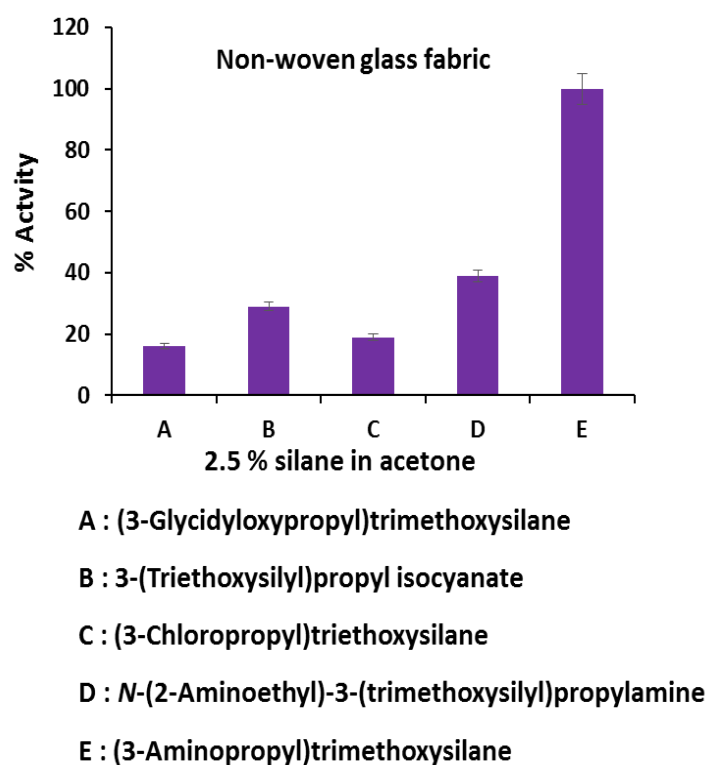


Figure 4.8. Effect of silane reagents on immobilised ADH activity. The ADH assay was performed on triplicate and error bars represent standard deviations. To display the data, the highest activity was taken as 100 % and subsequent activities were normalised accordingly

Figure 4.8 represents low activity for epoxy, isocyanate and chlorosilane modified non-woven glass fabric supports after immobilisation. The low activity for these silane supported enzymes could be due to the need for higher pH for immobilisation which can affect the bioactive conformation of the ADH (see pH stability studies, Chapter 2, Section 2.2, Figure 2.2). The APTMS modified non-woven glass fabric scaffold was further optimised in the following section.

4.3.1.1 Effect of APTMS concentration on ADH activity

APTMS concentration studies were undertaken on non-woven glass fabric supports to study the effect on ADH activity. The HCl activated non-woven glass fabric discs were allowed to react with various concentrations of APTMS (1 to 10 % (v/v)) and ADH was immobilised on these supports after GA activation. The effect of APTMS concentration on ADH activity is shown in Figure 4.9. Detailed activity data is presented in the Experimental Section 4.8.4.7, Table 4.8.

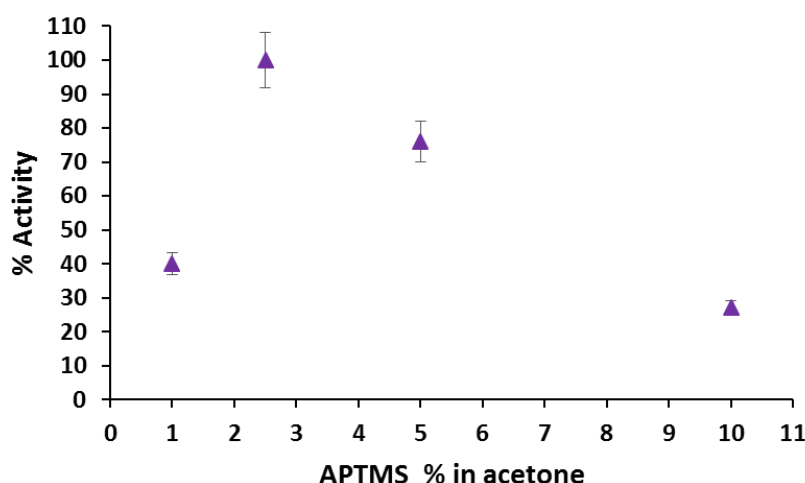


Figure 4.9. Effect of concentration of 3-trimethoxysilylpropylamine (APTMS) on ADH activity on non-woven glass fabric. The ADH assay was performed on triplicate samples and error bars represent standard deviations. To display the data, the highest activity was taken as 100 % and subsequent activities were normalised accordingly

Figure 4.9 reveals that ADH immobilised on 5% APTMS modified non-woven glass fabric support shows 77% activity; a higher concentration of APTMS (10%) led to significant reduction of ADH activity (22%). Similar results were observed with woven glass fabric where excess polymerization of silane reagent on the surface appears to impede enzyme immobilisation and/or activity.⁶⁵ The highest activity was recorded for the 2.5% loading of APTMS reagent (similar to woven glass fabric studies) and this concentration was used in subsequent work.

4.3.1.2 Effect of GA concentration on ADH activity

In this section the effect of GA concentration and activation time on the immobilised ADH activity were investigated on the APTMS-modified non-woven glass fabric discs. The silane modified discs were incubated in GA (1%, 2.5%, 5% and 10% w/v) in PBS solution and immobilised with ADH separately. The effect of GA concentration on the immobilised enzyme activity is shown in Figure 4.10. Detailed activity data is presented in the Experimental Section 4.8.4.8, Table 4.9.

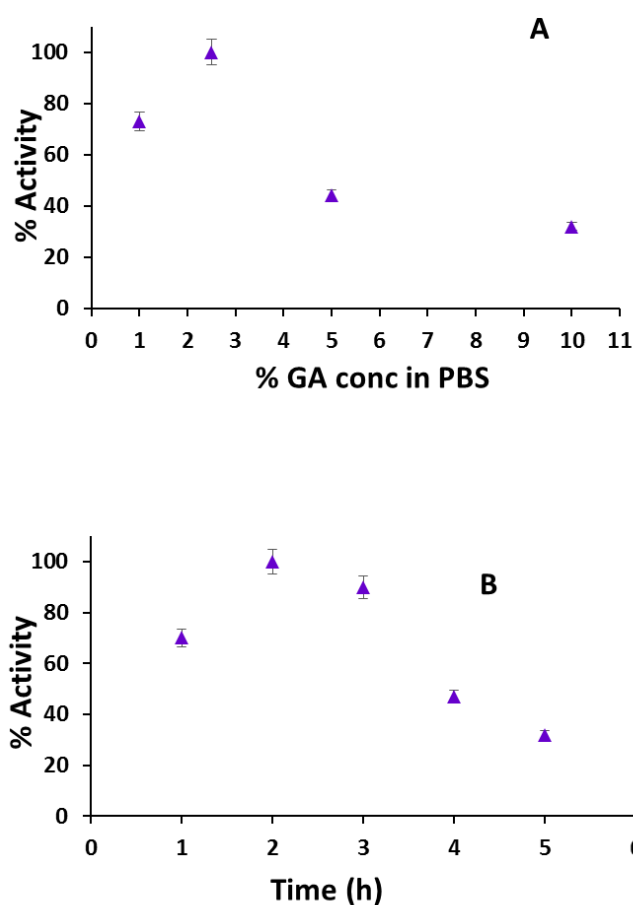


Figure 4.10. A. Effect of glutaraldehyde (GA) concentration on immobilised ADH activity. B. Effect of glutaraldehyde (GA) activation time on immobilised ADH activity. The ADH assay was performed on triplicate samples and error bars represent standard deviations. To display the data, the highest activity was taken as 100 % and subsequent activities were normalised accordingly

With an increase in the concentration of GA solution, the activity of the immobilised ADH also increased (Figure 4.10A). When GA concentration was 2.5%, the activity reached the maximum. Subsequently, as the GA solution concentration further increased, the immobilised enzyme activity decreased possibly due to extensive crosslinking resulting in distortion of the enzyme structure (i.e. the active site conformation)⁶⁶ and hence substrate accessibility and binding.⁶⁷

The effect of GA activation time on ADH activity was investigated by treating APTMS-modified non-woven glass fabric disc with 2.5% GA at different times (0.5 h, 1 h, 2 h, 3 h,

4 h, 5 h) (Figure 4.10B). The enzyme activity reached a maximum when crosslinked for 2 h. (4.407 mmol/min/g). GA activation over 3-4 h and cross-linking over 5 h both resulted in reduced enzyme activity.

4.3.2 Characterisation of APTMS modified non-woven glass fabric

4.3.2.1 SEM

The morphology of the surface modified non-woven glass fabric discs was investigated *via* electron microscopy. Upon silane treatment, agglomeration of the silane reagent was observed between the fibers (Figure 4.11B). Similar behavior has been reported by Sterman and Bradley.⁷⁵ After crosslinking with GA and immobilisation of the enzyme, the fibres showed isolated patches of extraneous material supporting the loading of cross linker and ADH (Figures 4.11C and 4.11D).

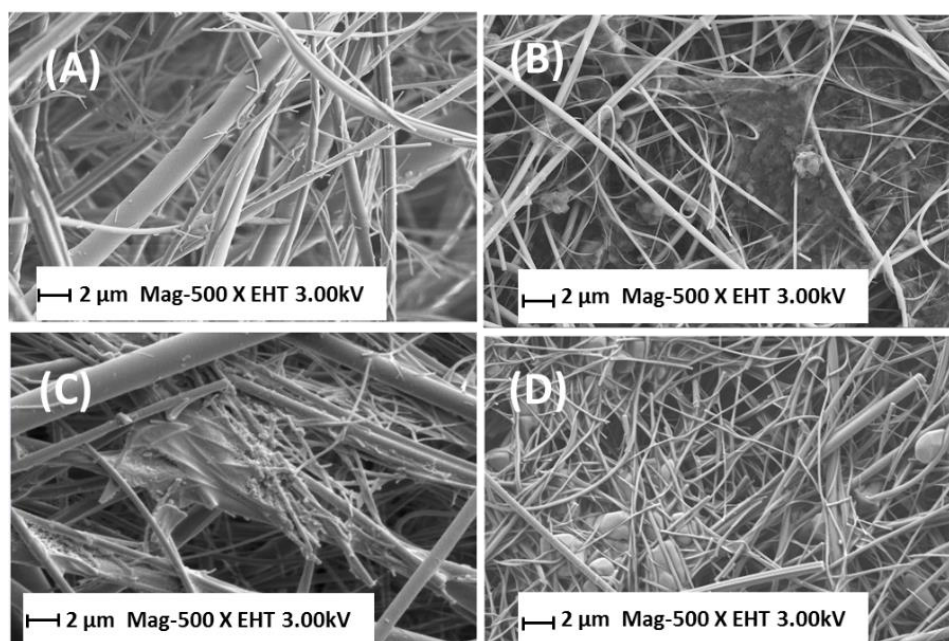


Figure 4.11. SEM images showing the morphology of non-woven glass fabric: as received (A); HCl activated and APTMS treated (B); GA crosslinked (C); and immobilised with ADH (D)

4.3.2.2 XPS analysis

Non-woven glass fabric after APTMS surface modification and ADH immobilisation was also analysed with XPS and the results for the elements C, O and N are described in Table 4.6.

Table 4.6 Elemental compositions expressed as atomic ratios X/C, i.e. the atomic concentration of element X relative to that of C. Listed are the mean values (\pm deviation) based on three analyses points

Element	Glass non- woven fabric HCl activated	Glass non- woven fabric HCl + APTMS	Glass non- woven fabric HCl + APTMS + GA	Glass non- woven fabric HCl + APTMS + GA + ADH
O/C	4.278 \pm 0.482	2.260 \pm 0.032	1.076 \pm 0.014	0.602 \pm 0.020
Si/C	1.860 \pm 0.251	1.059 \pm 0.017	0.443 \pm 0.006	0.240 \pm 0.011
N/C	0.019 \pm 0.003	0.138 \pm 0.004	0.074 \pm 0.005	0.151 \pm 0.005

Table 4.6 shows that the O/C and Si/C ratios drop significantly with increase in N/C ratio indicating the presence of amino silane on the non-woven glass fabric support after APTMS modification. The C1s spectrum for the non-woven glass fabric support (Figure 4.12B) shows peaks at 285 eV (C–C) and 286.5 eV (C–O/C–N) consistent with silane modification. An increase in the N/C ratio consists of two N1s peaks (Figure 4.12A, yellow line), one at 399–400 eV (amines), the other at approximately 402 eV (protonated amines, i.e. N⁺). This double peak is typically observed after APTMS surface modification. A further drop of O/C and Si/C with N/C ratio was observed after addition of GA; C1s (Figure 4.12B, blue line) is very similar to the silane modification but with a slight increase at approximately 288 eV indicating the presence of aldehyde (GA). C1s displays the characteristic peak shape of polypeptides/proteins (i.e. ADH) clearly resolved peak at >288 eV due to amide functionality and a strong shoulder at 286.5 eV due to various C–N and C–O based functional groups (Figure 4.12B, green line).

Additionally, N1s (Figure 4.12B, green line) displays an additional strong peak at approx. 400 eV consistent with amide functionality. The XPS results for non-woven glass fabric were identical to the results obtained for woven glass fabric support.

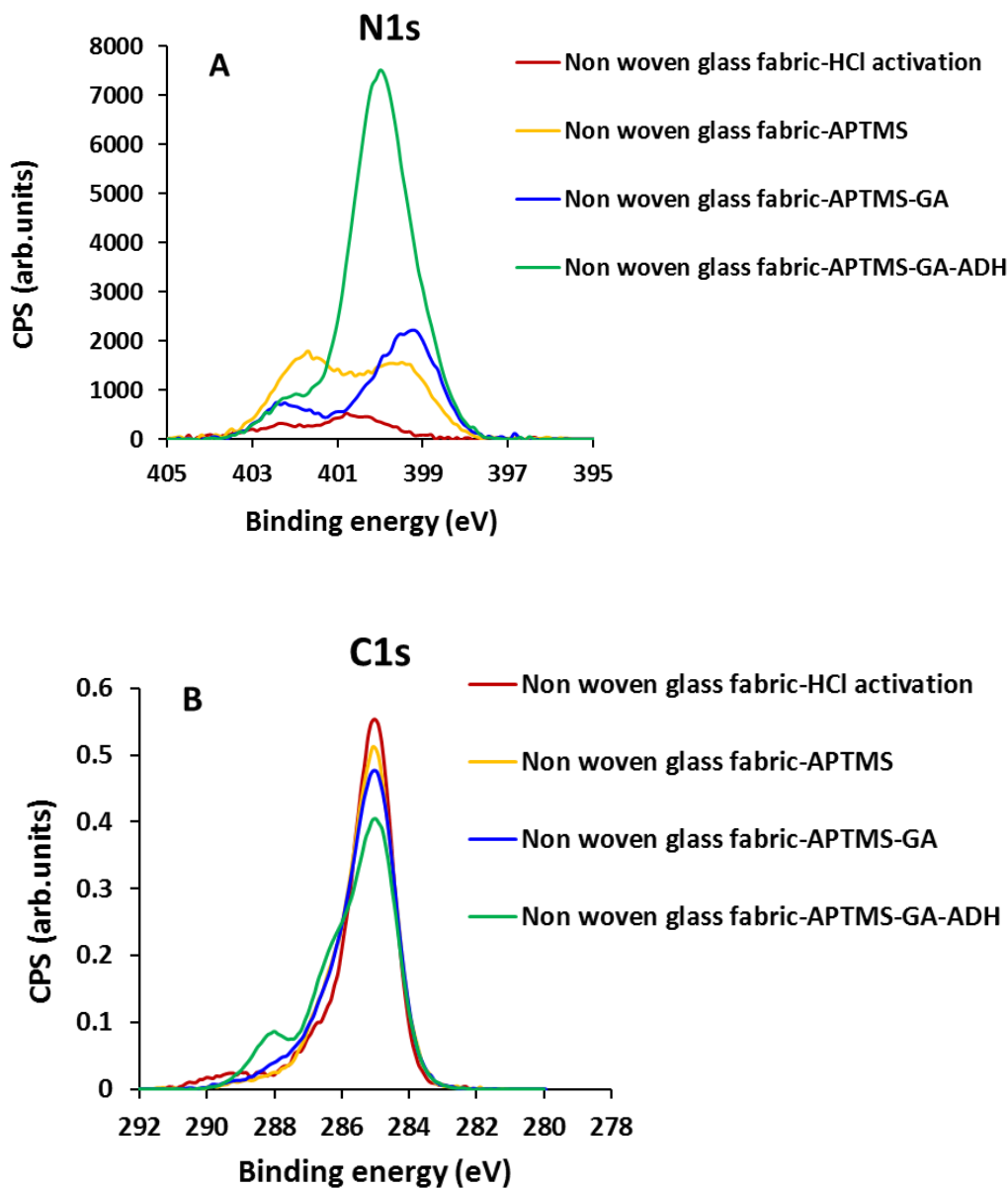


Figure 4.12. High-resolution XPS spectra N1s (A) and C1s (B) for non-woven glass fabric (red line), 2.5% APTMS modified glass fabric (yellow line), GA activation (blue line) and ADH immobilised non-woven glass fabric (green line)

4.3.3 Immobilised ADH stability studies

ADH immobilised on GA activated and APTMS modified non-woven glass support was subjected to stability studies as per the section below.

4.3.3.1 pH stability

The effect of pH on the activities of both the soluble and immobilised ADH (non-woven glass fabric support) are presented below (Figure 4.13) and detailed activity data is presented in the Experimental Section 4.8.5.1, Table 4.10. The results showed that the optimal pH for ADH immobilisation was at ~ pH 7, identical to that of soluble ADH. The immobilised ADH retained 43% of activity at pH 9 and at pH 10.5 showed 22% retention of activity; comparatively, soluble ADH showed almost complete loss of activity at pH 9 and above.

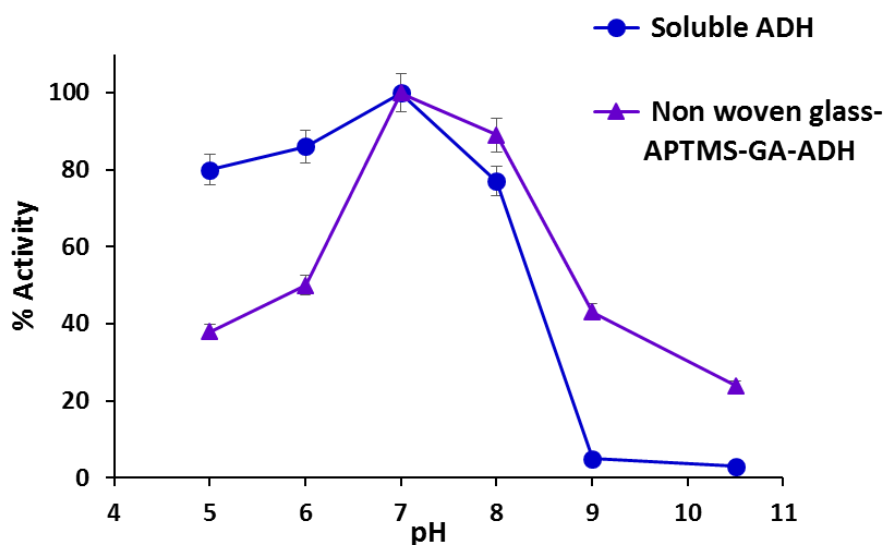


Figure 4.13. Effects of pH on the activities of the free and immobilised ADH. The ADH assay was performed on triplicate samples and error bars represent standard deviations. To display the data, the highest activity was taken as 100% and subsequent activities were normalised accordingly

Significantly, enzyme activity was retained over a broader pH range after immobilisation. The increased resistance of immobilised ADH against pH may be due to the buffering action of amino silane modified non-woven glass fabric support. Encouragingly, the configuration of ADH on the surface of the support was found to support the desired catalysis.⁶⁹

4.3.3.2 Thermal stability

In order to test the thermal stability of the immobilised ADH, soluble and immobilised ADH was incubated at different temperatures (20 to 80 °C) in PBS for 2 h and their residual activities were measured (Figure 4.14). Detailed activity data for this study is presented in the Experiential Section 4.8.5.2, Table 4.11.

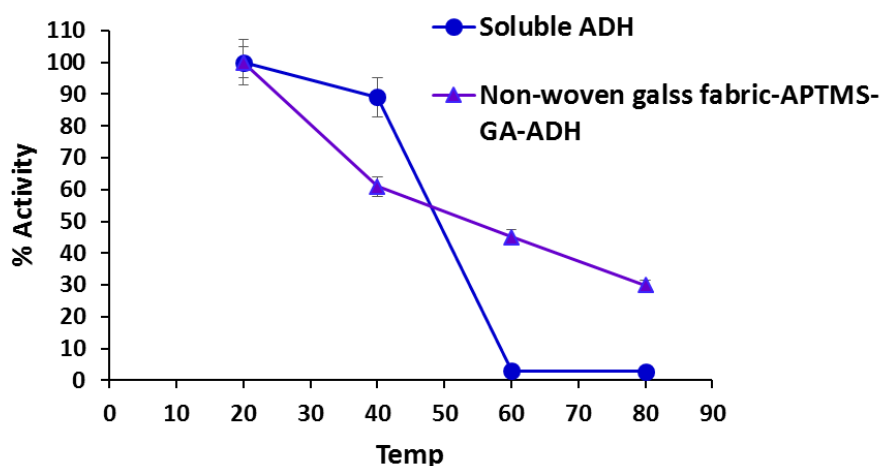


Figure 4.14. Effects of temperature on the activity of the soluble and immobilised ADH on glass fabric. The ADH assay was performed on triplicate samples and error bars represent standard deviations. To display the data, the highest activity was taken as 100% and subsequent activities were normalised accordingly

In Figure 4.14, the soluble ADH had more enzyme activity between 20 to 40 °C and less activity above 60 °C. When the incubation temperature is above 50 °C, the activity of the immobilised enzyme is consistently higher than that of soluble enzyme. Immobilised ADH on non-woven glass fabric showed 47% retention of activity at 60 °C, while soluble ADH holds less than 2% above 60 °C. Furthermore, the immobilised ADH showed 31% activity at 80 °C.

There is loss in the ADH activity of soluble form which was due to denaturation of the enzyme at high temp. Thermal stability of ADH improved after immobilisation on the non-woven glass fabric support probably arising from the conformational constraint of the enzyme. The results indicate that ADH immobilised on non-woven glass fabric support has good thermal stability.

4.3.3.3 Storage Stability

The storage stability of the immobilised ADH was investigated on APTMS modified non-woven glass fabric support at 4 °C in PBS buffer. Soluble ADH was stored under identical conditions and the activity was measured on a 24 h cycle for the first 6 days and assessed for a further 60 days. ADH immobilised on the non-woven glass fabric appeared to be stable for up to 60 days at 4 °C with retention of 49% of the initial activity (Figure 4.15). The soluble ADH showed 44% retention of activity after 10 days of storage and significant loss of activity after 45 days.

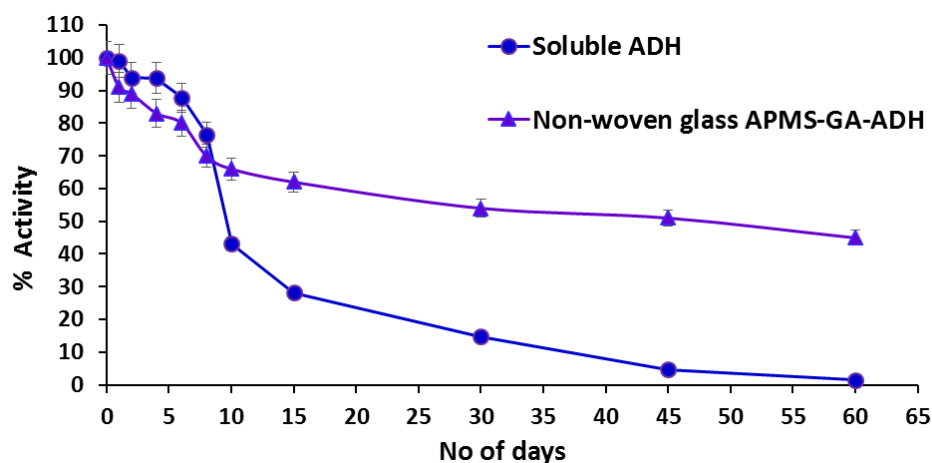


Figure 4.15. Storage stability of ADH immobilised on non-woven glass fabric and soluble ADH in PBS (0.05 M) at 4 °C. The ADH assay was performed on triplicate samples and error bars represent standard deviations. To display the data, the highest activity was taken as 100 % and subsequent activities were normalised accordingly

Gratifyingly, the ADH immobilised on glass fabric showed enhanced ADH storage stability compared to free ADH. The immobilised ADH stabilisation may be due to multipoint attachment of the enzyme to the support and hence decrease the propensity to unfold or denature.

4.4 Comparison of immobilised ADH activity

In this section, immobilised ADH activity obtained on both woven and non-woven glass fabric were compared to the activity obtained by physical adsorption. The non-woven glass fabric and modified (glass fabric-APTMS-GA) discs were immobilised with ADH separately according to the procedure described in the Experimental Section 4.8.4.2.1 and were assessed for enzyme activity. The non-modified, as well as APTMS modified woven and non-woven glass fabric discs, were immobilised with ADH under identical conditions and used as Control 1 and Control 2 respectively. For covalent immobilisation assessments, immobilised ADH activity was compared with Control 1 and Control 2 glass supports (Activity data is shown in Table 4.7).

Table 4.7 ADH activity after immobilisation after each modification of non-woven glass fabric and woven glass fabric (ADH was immobilised on these supports under identical protocols)

No.	Non-woven glass fabric	Activity (mmol/min/g)	Woven glass fabric	Activity (mmol/min/g)
Control 1	Glass fabric + ADH	0.489 ± 0.03	Glass fabric + ADH	0.447 ± 0.01
Control 2	Glass fabric-APTMS + ADH	1.020 ± 0.01	Glass fabric-APTMS + ADH	0.869 ± 0.03
Treatment	Glass fabric-APTMS-GA + ADH	5.403 ± 0.05	Glass fabric -APTMS-GA + ADH	2.290 ± 0.06

The measured activities for GA activated and non-activated woven and non-woven glass fabrics are shown in Table 4.7. There was a small amount of ADH activity recorded with both

non-modified glass fabrics (Control 1), and the APTMS modified glass fabrics (Control 2) presumably due to non-specific binding (Control-2). When ADH was immobilised onto the non-woven glass fabric-APTMS-GA treated support, an eleven-fold increase in activity (5.403 ± 0.05 mmol/min/g) was observed compared to the analogous Control-1 disc (0.489 ± 0.03 mmol/min/g). The modified woven glass fabric ADH immobilisation, returned a fivefold increase in activity (2.290 ± 0.06 mmol/min/g) compared to the control woven glass fabric.

The stability studies (i.e. pH, thermal and storage studies) previously conducted on the woven and non-woven glass fabric revealed that the APTMS modified woven glass fabric showed low stability compared to the APTMS modified non-woven glass fabric support. Notably, the woven glass fabric showed low activity and low stability when used as a support substrate for ADH. The lower activity for the woven fabric support is postulated to be due to: i) lower silane content on the woven glass support (E glass, ~55% Si-OH) compared to non-woven glass fabric (borosilicate glass, 65-78% Si-OH); ii) the reduced fibre diameter of the non-woven glass (47 mm) as compared to the woven glass fabric (74 mm) and; iii) the higher surface area available for the enzymatic reaction.

Since ADH immobilisation on the non-woven glass fabric-APTMS-GA support provided superior stability (pH, temp and storage) and the highest activity among all of the tested supports, this construct was employed in the development of a biosensor and flow reactor system. Hence, efforts towards the ultimate goal of this research are described in the sections below using non-woven glass fabric-APTMS-GA support. The electrode was fabricated using the non-woven glass fabric APTMS-GA support and then subjected to ADH immobilisation which was further used for the amperometric detection of ethanol. The non-woven glass fabric APTMS-GA support was also investigated in a continuous flow reactor designed for the amperometric detection of ethanol.

4.5 Non-woven glass fabric support use in the fabrication of a biosensor

In this work, the above described non-woven glass fabric support (i.e. glass fabric-APTMS-GA support) was fabricated into an electrode and used for the construction of an amperometric biosensor based on alcohol dehydrogenase (ADH) and Meldola's Blue (MB) mediator. The electro catalytic properties of MB to mediate the oxidation of NADH which was formed in the enzymatic reaction of ethanol with NAD^+ under catalysis controlled by ADH provides amperometric detections.

4.5.1 Fabrication of the electrode

ADH and NAD^+ can be use in ethanol oxidation process to generate acetaldehyde and NADH and this reaction utilises stoichiometric amounts of substrate and cofactor. One can measure concentration of ethanol (substrate) ameropmetrically by selecting potential whereby NADH can be observed and detected For the amperometric measurement, a glassy carbon working electrode (GC) was chosen because of its high over the potential for oxygen evolution and low over the potential for hydrogen evolution; these features increase the working potential window facilitating the use of the Meldola's blue ink mediator (MB). The fabrication process was carried out by polishing the GC electrode with alumina powder and then the MB ink was evenly cast onto the polished electrode surface. The glass fabric-APTMS-GA support disc was then placed on the electrode surface (Figure 4.16). ADH immobilisation was achieved by suspending the above cured electrode in ADH in PBS at 4 °C (as described in Section 4.8.4.2.1). Using this procedure, multiple modified electrode were prepared.

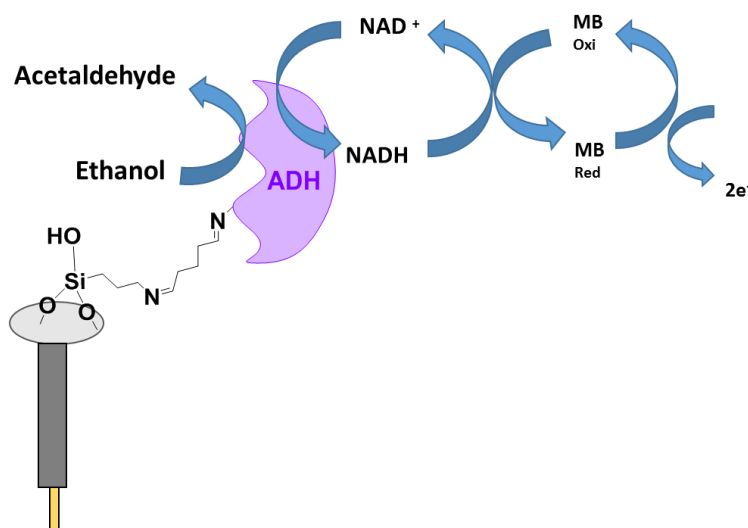


Figure 4.16. Mechanism of ethanol detection represented by the non-woven glass fabric-APTMS-GA-ADH biosensor. MB_{red} and MB_{oxi} represent the MB mediator reduced and oxidized, respectively

4.5.2 NADH oxidation

In order to evaluate the catalytic activity of the modified electrode (i.e. non-woven glass fabric-APTMS-GA-MB) towards electrochemical oxidation of NADH cyclic voltametric experiments were conducted in PBS containing (0.1 M) KCl and NADH. First, the non-woven glass fabric and APTMS modified non-woven glass fabric support were applied to the electrode surface with the MP mediator in the same buffer system without NADH. The electrochemical responses were measured for comparison. Next, the working electrode without APTMS-GA modification (i.e. glass fabric, as displayed in Figure 4.17a) was evaluated. In the absence of NADH, no Faradaic current was observed for either the glass fabric or glass fabric-APTMS-GA electrode as shown in Figures 4.17a and 4.17b respectively. The response to 2 mM NADH by the glass fabric-APTMS-GA electrode can be seen in Figure 4.17c; modification of the glass fabric electrode with APTMS and GA led to an increase in electrode capacitance which is clearly observed with an increase in the background current (Figure 4.17 b). Addition of NADH leads to a slight increase in current starting from ~ 0.05 V compared to the blank solution.

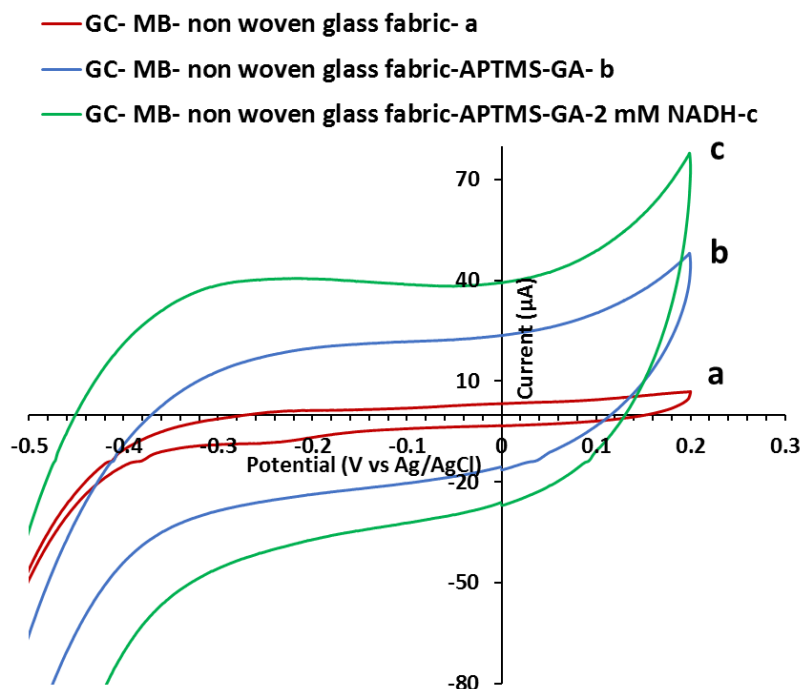


Figure 4.17. Cyclic voltammograms obtained using a GC electrode with non-woven glass fabric modification: (a) GC-MP-glass fabric in absence of NADH; (b) GC-MP-glass fabric-APTMS-GA electrode in the absence of NADH, and (c) GC-MP-glass fabric-APTMS-GA electrode in the presence of NADH. Scan rate 100 mVs^{-1} in PBS (0.05 M, pH 7.5) solution with 0.1 M KCl

4.5.3 Ethanol detection

The amperometric response of the non-woven glass fabric-APTMS-GA-MB-ADH electrode to ethanol was assessed at 0.6 V versus Ag/AgCl using a one enzyme electrode to cover the whole concentration range from 1 to 16 mM ethanol (Figure 4.18). The choice of potential was based on a compromise between sensitivity and stability where ADH is sensitive to potentials $> 0.7 \text{ V}$.¹⁴ After studying the results it shows that the response of the biosensor is non-linear between 1 mM and 14 mM which is in agreement with other electrodes employing ADH for ethanol detection.¹⁵

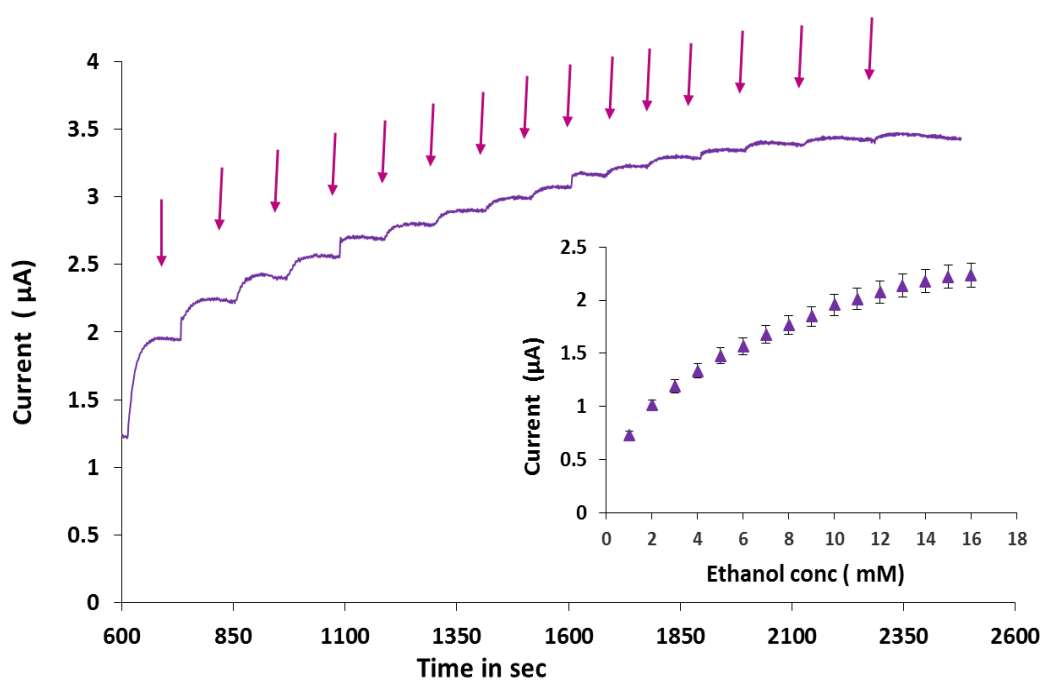


Figure 4.18. Amperometric response of the biosensor towards ethanol; 0.05 M PBS buffer (pH 7.5) and 1 mM NAD⁺; working potential 0.6 V, ethanol concentrations: 1 to 16 mM. (Inset) Calibration plot shows the response obtained upon increasing ethanol concentrations in PBS (0.05 M, pH 7.5) containing 1 mM NAD⁺ using modified GC electrodes at 0.60 V versus Ag/AgCl

A typical amperogram is depicted in Figure 4.18. It was observed that after inclusion of the dispersion of the analyte in the supporting electrolyte with a stirring rate of around 100 rpm, the response time is less than 5 s. The calibration curve shows a non-linear response shape which levels off at concentrations > 18 mM. This modified electrode provided a sensitivity of 0.75 µA/mM which is in agreement with other electrodes employing ADH for ethanol detection (Table 4.1).^{14, 15} Details of the electrode fabrication and measurement of ethanol are presented in the Experimental Section 4.8.6, Table 4.13.

4.6 Non-woven glass fabric supports in flow reactors

Finally, non-woven glass fabric supports were investigated with a GC electrode system in a continuous flow reactor. Amperometric ethanol determination was carried out by measuring the current produced upon oxidation of NADH at a constant potential (0.6V, versus Ag/AgCl). The following section describes a detailed investigation of amperometric analysis of various concentrations of ethanol and reproducibility studies of a continuous flow column bioreactor with immobilised ADH.

4.6.1 Flow-injection system

A schematic representation of the flow system is shown in Figure 4.19. Optimization of the flow injection system (FIA) system containing a column mini-bioreactor with immobilised ADH and electrochemical cell was made. The FIA system provided an on-line determination of NADH oxidation and amperometric determination of ethanol *via* a computerised Autlab instrument. The column mini-bioreactor (4.78 mm diameter, 1.8 cm length) was filled with ADH covalently immobilised on the modified non-woven glass fabric support (120 mg). Control of the flow rate was achieved *via* a peristaltic pump. The carrier solution (0.05 M PBS, pH 7.5) with NAD⁺ and 0.1 M KCl was passed through the column mini-bioreactor loaded with immobilized ADH and the electrochemical cell with a flow rate of 1.0 mL/min. The electrochemical cell consists of three different electrode types - Ag/AgCl electrode as the reference electrode, Pt wire as auxiliary electrode and GC electrode as a working electrode modified with MB. A potential of 0.6 V was applied to the working electrode and the electrochemical current was allowed to decay to a steady value. Ethanol in PBS (500 μ L) at

different concentrations was then injected into the system and passed through the column mini-bioreactor containing the immobilized ADH (Figure 4.19)

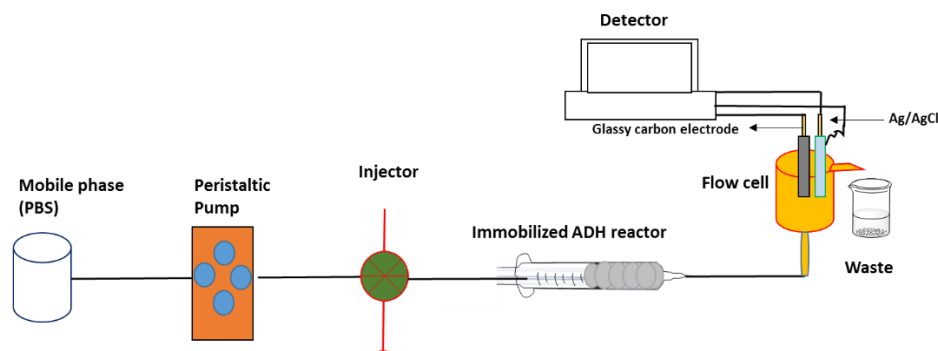


Figure 4.19. Schematic representation of FIA showing all the different components

4.6.2 Optimization of the flow-injection system

To evaluate the efficiency of the column mini-bioreactor which contains immobilised ADH on non-woven fabric support several studies were performed. These examined the effect of NAD^+ and ethanol concentration, and the reproducibility of the column mini-reactor. The amperometric signal was observed to increase when the volume of sample (ethanol) was increased. However this resulted in increase in time for each analysis since the cell washout process also required a longer time. A volume of $500\ \mu\text{l}$ was chosen as the optimum working volume in subsequent experiments. Furthermore, the effect of varying NAD^+ concentration (from $1\ \text{mM}$ to $8\ \text{mM}$) was also evaluated to assess the performance of the bioreactor. A concentration of $1\ \text{mM}$ NAD^+ provided reliable amperometric detection of ethanol.

Figure 4.20 displays the amperometric flow injection responses for NADH oxidation generated upon the addition of ethanol in the concentration range from 1 to $10\ \text{mM}$. Well defined and sharp peaks were generated as a result of ethanol addition with relatively fast response time and low level of noise.

To evaluate the analytical performance of this bioreactor towards ethanol, different concentrations from 1 to 10 mM were injected into the flow system as shown in Figure 4.20. The detailed electrochemical data for current vs concentration is presented in the Experimental Section 4.8.7.

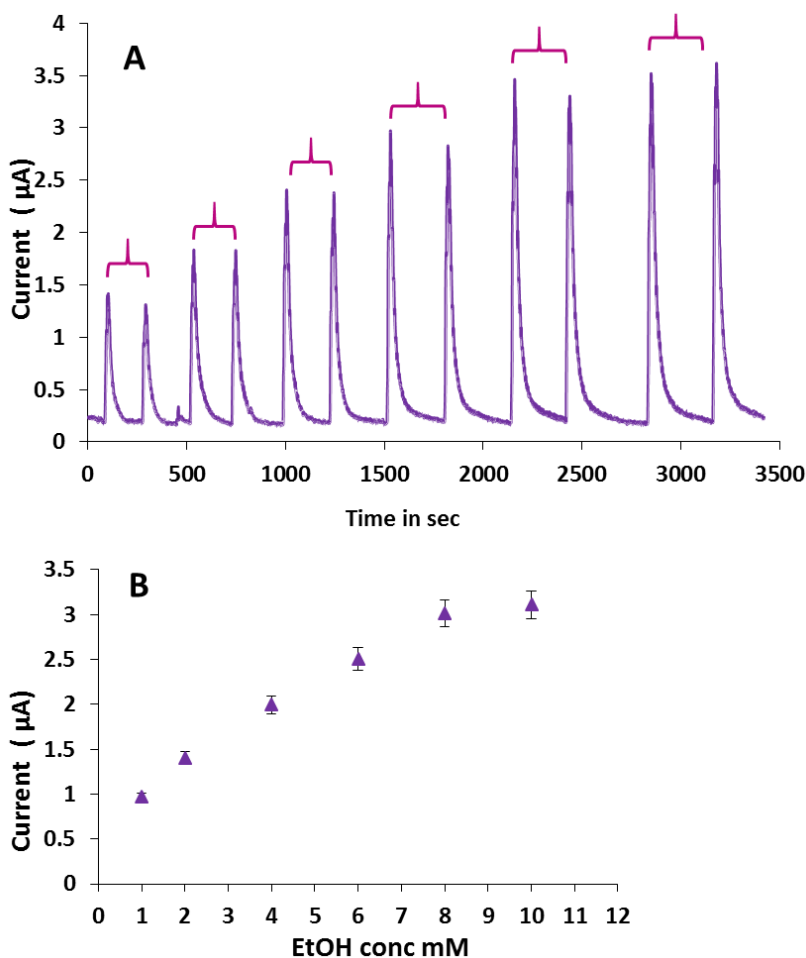


Figure 4.20. Flow injection amperometric responses of the GC-MP to increasing concentrations of ethanol (1mM to 10 mM) using PBS (0.05 M, pH 7.5) containing 1 mM NAD⁺ (mobile phase) when passed through the immobilised ADH bioreactor, flow rate 1 mL/min, working potential + 0.6 V(A); Calibration plot (B)

The resulting calibration plot shows (Figure 4.20 B) good linearity from 1 to 8 mM with a regression coefficient of 0.962. The reproducibility of the analytical performance of the immobilised ADH was evaluated based on eleven consecutive additions of 1 mM ethanol along with 1 mM NAD⁺. Figure 4.21 shows the amperometric flow injection responses to eleven injections of 1 mM ethanol where sharp and well-defined peaks with small current variations

were obtained. The results revealed that the bioreactor has good reproducibility with a relative standard deviation of 3.9% based on eleven measurements. The high observed reproducibility is resulting from the robust and stable covalent attachment between the enzyme and the modified non-woven glass fabric support.

The detailed electrochemical procedure for flow injection analysis for linearity and reproducibility studies is presented in the Experimental Section 4.8.7.2.

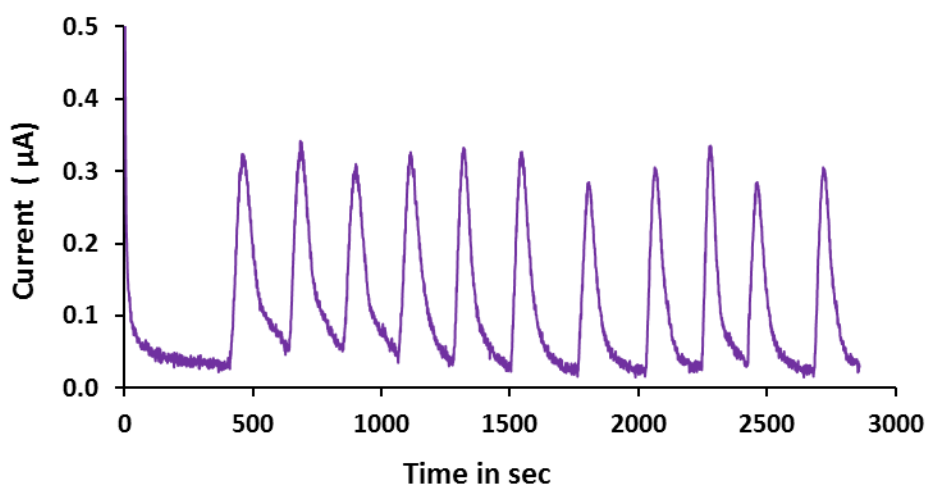


Figure 4.21. Flow injection amperometric responses of the GC/MB electrode with immobilised ADH supports eleven successive injections of 1 mM ethanol and 1 mM NAD⁺. The operating potential was + 0.6 V, flow rate 1 mL/min with mobile phase PBS (0.05 M, pH 7.5)

4.7 Conclusions

The above described research provides proof of principle that non-woven glass fabric APTMS- GA modified supports can be used for functional ADH immobilisation. This fibrous support combines high mechanical stability with the high surface area. The ADH enzyme was successfully immobilised on both woven and non-woven glass fabric supports. The non-woven support showed 5.403 ± 0.050 mmol/min/g higher activity than the woven fabric support. Significantly, the ADH immobilised on the non-woven glass support possessed enhanced thermal stability (31% retention of activity at 80 °C) and storage stability (49% retention after

60 days) over the non-immobilised soluble ADH. The immobilised ADH construct was used for ethanol biosensing and the developed prototype displayed a sensitivity of 0.789 $\mu\text{A}/\text{mM}$ with a response time of 5 seconds.

Additionally, the same immobilised ADH construct on non-woven glass support was successfully applied to a flow bioreactor in conjunction with a flow injection system. The flow bioreactor investigations showed good linearity in the current responses between 1 and 8 mM ethanol with a regression coefficient of 0.9622. Furthermore, with this flow reactor, high reproducibility was obtained with a RSD of 3.9% based on eleven consecutive measurements.

In conclusion, significant progress was made towards the development of biosensor and flow reactor systems building on the preliminary work which i) developed the APTMS modified non-woven glass fabric support for ADH immobilisation, and ii) examined the catalysis of ethanol to acetaldehyde.

4.8 Experimental Section

4.8.1 Instrumentation

Biosensor work: All electrochemical measurements were performed using a CHI1200A hand-held potentiostat (CH Instruments Inc., Texas, USA) with a three-electrode setup using a modified glassy carbon (3 mm diameter) working electrode, a platinum wire counter electrode and a Ag/AgCl reference electrode. All measurements were performed at RT (22 ± 2 °C) in PBS (0.05 M, pH 7.5 containing 0.1 M KCl) unless otherwise stated.

Flow injection bioreactor: All electrochemical experiments with were performed with computer controlled electrochemical workstation (Auto lab PGSTAT308) in conjunction with a three-electrode system: a glassy carbon electrode was used as a working electrode, a platinum wire was applied as a counter electrode and Ag/AgCl₃ as a reference electrode. All potentials were reported with respect to the reference electrode. Amperometric measurements were carried out under stirred conditions and the response current was recorded based on the difference in currents before and after addition of the substrate (NADH or ethanol). FIA system comprised an electrochemical cell, peristaltic pump, an injector for ethanol samples, support solution reservoir and 1 ml syringe used as a column mini-bioreactor (Figure 4.22).



Figure 4.22. The FIA used for electrochemical measurements

Infrared spectroscopy was carried out using a Nicolet 6700 ATR-FTIR (Thermo Fisher Scientific) in absorbance mode with absorptions reported in wavenumbers (cm^{-1}) and the relative intensities expressed as s (strong), m (medium), w (weak) or prefixed b (broad).

The elemental composition of the surface was analyzed using X-ray photoelectron spectroscopy (XPS) on an AXIS Nova spectrometer (Kratos Analytical Inc., UK) using a monochromated Al $K\alpha$ source at a power of 180W. Morphology analysis was performed on a Scanning Electron Microscope (SEM, Philips XL30). The samples were imaged using a Zeiss Merlin FESEM after coated with iridium under vacuum. Enzyme activity was measured using a Cary 300 Bio-UV visible spectrophotometer at 340 nm.

4.8.2 Solvents and reagents

Acetone, hydrochloric acid (concentrated HCl), ethanol (EtOH), methanol (MeOH), tetrahydrofuran (THF), triethylamine (TEA), sodium chloride (NaCl) and sodium hydroxide (NaOH) were purchased from Merck and used without further purification.

Sodium bicarbonate (NaHCO_3), sodium carbonate (Na_2CO_3), ethylenediamine (EDA), (3-glycidyloxypropyl)trimethoxysilane, 3-(triethoxysilyl)propylisocyanate, (3-chloropropyl)triethoxysilane, (3-aminopropyl)trimethoxysilane (APTMS), (3-chloropropyl)triethoxysilane, *N*-(2-aminoethyl)-3-aminopropyl trimethoxysilane, glutaraldehyde (25% solution), nicotinamide adenine dinucleotide (NAD^+), potassium chloride (KCl), phosphoric acid (H_3PO_4), Triton™ X-100, glass microfibres (Whatman® glass microfibre filters, diameter 47 mm circles, and ~ 0.7 μm diameter borosilicate glass) and aluminium oxide powder were purchased from Sigma-Aldrich Australia. β -Nicotinamide adenine dinucleotide, reduced disodium salt hydrate (NADH) was purchased from Alfa Aesar (Australia);

Alcohol dehydrogenase (ADH) from yeast (500 units/mg) was purchased from Calzyme. Glass fabric was a gift from Colan Australia. It was a Type E-glass, low alkali plain weave glass fabric, 205 g/m² (nominal weight), warp 42 end per inch and weft 126 picks per inch.

ADH Activity

Surface modification reactions were performed on fabric discs in bulk total mass (1-2 g) and enzyme immobilisation activity was measured on a single disc of known mass (80-100 mg) in triplicate according to the procedure described in Experimental Section 4.8.3. The activity was calculated from absorbance (Abs) using the following formula:

$$A = \epsilon \times c \times l,$$

$$c = A / \epsilon \times l$$

where A is the absorbance, ϵ is the extinction coefficient (6220 $\text{M}^{-1} \text{cm}^{-1}$), c is the concentration (M) and l is the path length (cm).

Conc.mmol = Conc (mM) / Assay volume

Total activity = Conc. mmol / Time (i.e. assay time in min)

Activity (Specific activity) of immobilised ADH = Conc. mmol/Time (min) / Weight of fabric disc (g)

Activity (Specific activity) of soluble ADH = Conc. mmol/Time (min) / Weight of ADH (g)

4.8.3 ADH assay

The activity of ADH was measured spectrophotometrically by measuring the absorbance of NADH at 340 nm. The activity of the ADH immobilised supports were assayed by immersing the support discs individually in Tris buffer (100 mM pH 8.8), ethanol (20 mM), and NAD⁺ (1 mM) at 25 °C in 12 well plate. After shaking for 4 min at 100 rpm on an orbital shaker, 1 mL of the solution was withdrawn and the absorbance measured at 340 nm immediately. The activity measurement experiments were performed in triplicate (or in doublet where specified).

4.8.4 Surface modification procedures woven and non-woven glass fabric

4.8.4.1 HCl Activation

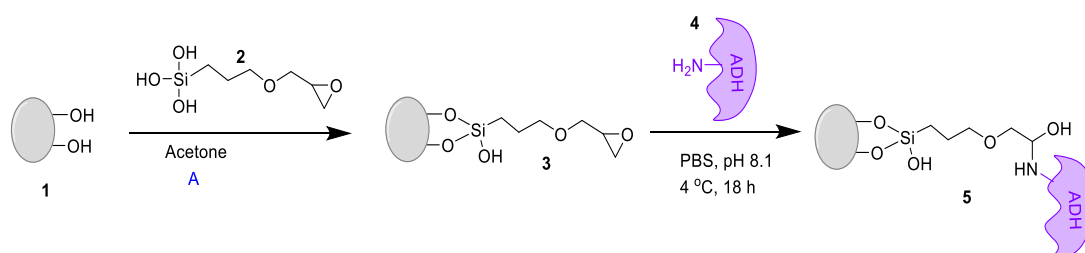
Glass woven fabric activation were carried out according to the modified procedure described by K. Sever *et al.*⁷⁶ The glass fabric discs (1 g, 13 mm diameter) were added to a 10 N HCl (25 mL) solution for 4 h at 85 °C. The HCl solution was cooled to RT. The glass fabric discs were removed from the solution and washed with distilled water 250 mL (50 mL; 3 x 20 min)

until the pH of the washes reached neutral. The discs were then dried at 110 °C for 3 h.

IR: 3374bs, 1631w, 1036bs, 937bs, 789m, 643w cm^{-1} .

Glass non-woven fabric discs were activated with HCl according to the procedure described for woven fabric under the following conditions: Glass fabric discs (1.01 g, 13 mm diameter), 10 N HCl (25 mL) solution for 4 h at 85 °C. IR: 3396bs, 2169w, 1633w, 1039bs, 941bs, 791m cm^{-1} . Detail FTIR spectra are presented in Appendix II (page 265).

4.8.4.2 Epoxy silane modification and immobilisation → (5)



Glycidoxyl propyl silane modification of woven glass fabric was carried out according to the modified procedure described by Gua.^{77,78} A solution of 2.5% glycidoxypopyl trimethoxysilane (10 mL, 2.5% v/v in acetone: water (95:5)) was allowed to stand at RT for 15 min. The HCl activated glass fabric discs (0.10 g) were added to the silane solution and stirred at RT for 1 h. The glass fabric discs were washed with distilled water (25 mL; 3 x 10 min) and methanol (25 mL; 3 x 10 min) and then cured at 110 °C for 30 min.

HCl activated non-woven glass fabric discs were allowed to react with glycidoxyl propyl silane according to the procedure described above for woven glass fabric under the following conditions: Glass fabric discs (0.15 g), glycidoxyl propyl silane (11 mL, 2.5% v/v in acetone: water (95:5)), incubation at RT for 15 min. Further fabric discs were washed with distilled

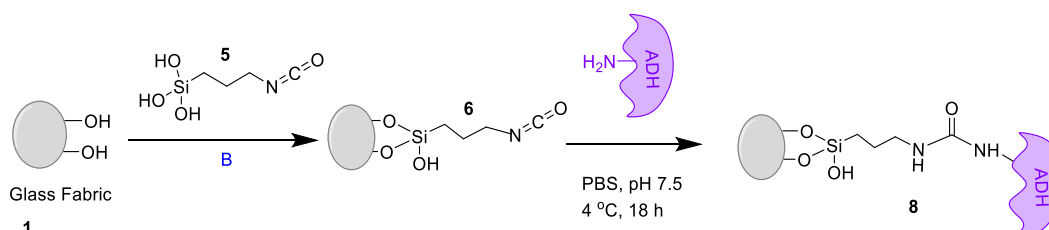
water (25 mL; 3 x 10 min) and methanol (25 mL; 3 x 10 min) and then cured at 110 °C for 30 min.

4.8.4.2.1 ADH immobilisation

The epoxy silane modified woven glass fabric supports (**3**) from the above section were allowed to react with ADH enzyme (10 mL, 0.5 mg/mL in PBS at pH 8.1) for 18 h at 4 °C. The glass fabric discs without silane modification were immobilised with ADH in an analogous fashion and were used as controls. Both these discs were washed with PBS buffer (pH 7.5) containing Triton-X (0.1 %) (20 mL; 3 x 20 min) to remove any unbound ADH enzyme and individually assayed according to the procedure described in Experimental Section 4.8.3.

Non-woven epoxy silane modified glass fabric was immobilised with ADH (10 mL, 0.5 mg/mL in 0.05 M PBS, pH 8.1) separately according to the procedure described for woven glass fabric ADH immobilisation in above section and assayed for activity according to the procedure described in Experimental Section 4.8.3.

4.8.4.3 Isocyanate silane modification and immobilisation → (8)



Isocyanate modification of woven and non-woven glass fabric was done according to the modified procedure described by Gua.^{77,78} A 2.5% solution of 3-isocyanatopropyl trimethoxysilane in acetone: water (95:5, 15 mL) was prepared and allowed to stand for 15 min

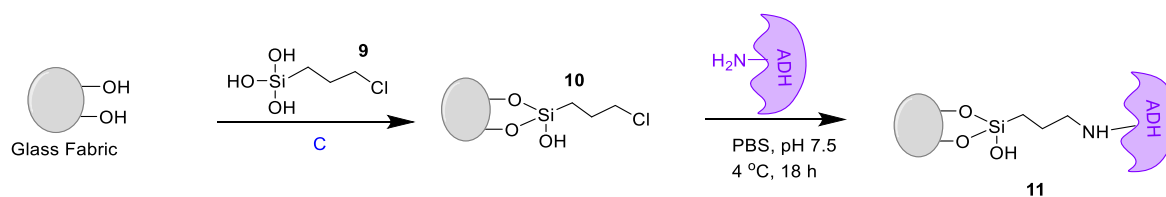
at RT. To this hydrolysed silane isocyanate solution HCl activated woven glass fabric discs (0.12 g) were added and the mixture was stirred for 1 h at RT. The discs were then washed with distilled water (20 mL; 3 x 20 min) and methanol (20 mL; 3 x 20 min) and cured at 110 °C for 30 min.

HCl activated non-woven glass fabric discs were allowed to react with 3-isocyanatopropyl silane according to the procedure described above for woven fabric under the following conditions: non-woven glass fabric discs (0.10 g), 2.5% solution of 3-isocyanatopropyl trimethoxysilane in acetone: water (95:5, 15 mL) at RT for 1 h.

4.8.4.3.1 ADH immobilisation

Isocyanate modified woven and non-woven glass fabric discs (**6**) were immobilised with ADH according to the procedure described in Section 4.8.4.2.1 under the following conditions: ADH (10 mL, 0.5 mg/mL, pH 7.5) was incubated at 4-8 °C for 19 h. All discs were then washed with PBS buffer (pH 7.5) containing Triton-X (0.1 %) (10 mL; 3 x 30 min) and individually assayed according to the procedure described in Experimental Section 4.8.3.

4.8.4.4 Chlorosilane silane modification and immobilisation → (11)



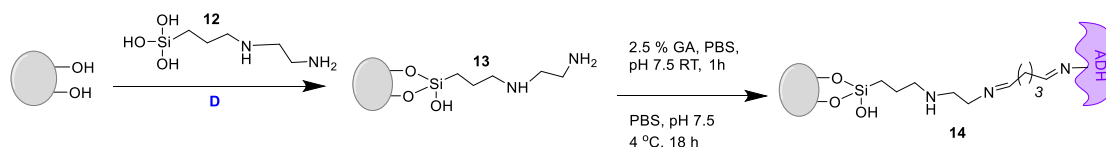
3-(Chloropropyl)trimethoxysilane (2.5% solution in acetone: water (95:5, 15 mL) was prepared and allowed to stand for 15 min at RT. The woven glass fabric discs (0.12 g) were added to the stirred hydrolysed silane isocyanate solution and incubated for 1 h at RT.⁷⁸ The glass discs were then washed with distilled water (20 mL; 3 x 20 min) and methanol (20 mL; 3 x 20 min) to neutral pH and then allowed to cure at 110 °C for 30 min.

HCl activated non-woven glass fabric discs were allowed to react with 3-chloropropylsilane according to the procedure described above for non-woven glass fabric under the following conditions: glass fabric discs (0.12 g), 3-chloropropyltrimethoxysilane (2.5% solution in acetone: water (95:5, 15 mL)) for 1 h at RT and analogously washed and cured at 110 °C for 30 min.

4.8.4.4.1 ADH immobilisation

The chlorosilane woven and non-woven glass fabric discs (**10**) from the above section were allowed to react with the ADH enzyme according to the procedure described in Section 4.8.4.2.1 under following conditions: ADH (10 mL, 0.5 mg/mL) incubated at 4-8 °C for 19 h. All discs were washed with PBS buffer (pH 7.5) containing Triton-X (0.1 %) (10 mL; 3 x 20 min) and individually assayed according to the procedure described in Experimental Section 4.8.3.

4.8.4.5 Aminoethyl silane modification and immobilisation → (14)



N-(2-Aminoethyl)-3-(trimethoxysilyl)propyl amine (2.5% solution in acetone: water (95:5, 15 mL) was allowed to stand for 15 min at RT. The acid activated woven glass fabric discs (0.18 g) were added to the hydrolysed amino ethyl silane and the mixture was stirred for 1 h at RT. The discs were then washed with distilled water (20 mL; 3 x 20 min) and methanol (20 mL; 3 x 20 min) and cured at 110 °C for 30 min.

HCl activated non-woven glass fabric discs were allowed to react with *N*-(2-Aminoethyl)-3-(trimethoxysilyl)propyl amine according to the procedure described above for woven glass fabric under the following conditions: Glass fabric discs (0.15 g), *N*-(2-Aminoethyl)-3-(trimethoxysilyl)propyl amine (2.5% solution in acetone: water (95:5, 12 mL) for 1 h at RT.

4.8.4.5.1 GA activation

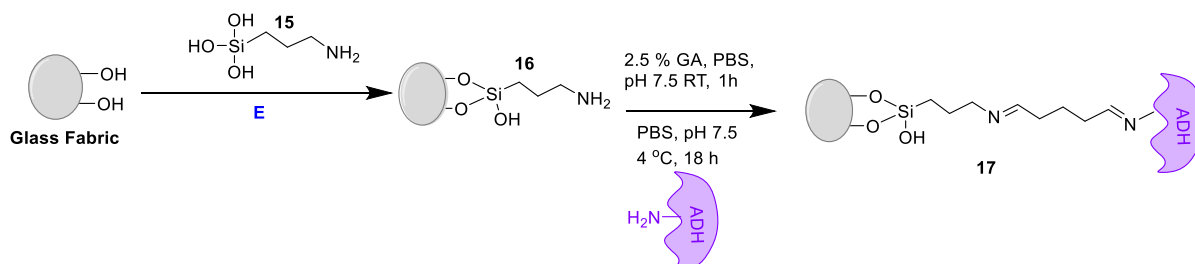
The woven glass diethyl amino silane fabric supports (13) were activated with GA according to the procedure described by Santosh.⁷⁹ Diethylamino silane modified woven glass fabric discs (0.05 g) were reacted with 2.5% GA (8 mL, w/v in 0.05 M PBS, pH 7.5) for 1 h at RT. The activated support was thoroughly washed with distilled water (20 mL; 3 x 20 min) to remove excess GA.

Non-woven glass fabric discs were allowed to react with GA according to the procedure described above for woven glass under the following conditions: glass fabric discs (0.14 g), 2.5% GA (10 mL, w/v in 0.05 M PBS, pH 7.5) for 1 h at RT.

4.8.4.5.2 ADH immobilisation

The silane diethylamine-GA modified glass woven and non-woven fabric supports (**13**) from the above section were exposed to the ADH enzyme according to the procedure described in Section 4.8.4.2.1 under the following conditions: ADH (10 mL, 0.5 mg/mL) incubated at 4 to 8 °C for 19 h. All discs were washed with PBS buffer (pH 7.5) containing Triton-X (0.1 %) (10 mL; 3 x 20 min) and individually assayed according to the procedure described in Experimental Section 4.8.3. Glass woven and non-woven discs without ethylamine-GA modification (control) were exposed to ADH and analogously used as controls

4.8.4.6 APTMS modification and ADH immobilisation → (17)



(3-Aminopropyl)trimethoxy-silane (APTMS) (2.5% solution in acetone: water (95:5, 15 mL)) was allowed to stand at RT for 15 min. HCl activated woven glass fabric discs (0.130 g) were then added to the hydrolysed silane solution and the mixture was stirred at RT for 1 h. The APTMS modified woven glass fabric discs were then washed with distilled water (20 mL x 3) and methanol (20 mL x 2) to neutral pH. The discs were then allowed to cure at 110 °C for 30 min. IR: 3246bs, 1057bs, 951bs, 792m cm^{-1} . XPS: Consistent with the target structure.

HCl activated non-woven glass fabric discs were allowed to react with APTMS according to the procedure described above for woven glass fabric under the following conditions: Glass

fabric discs (0.10 g), APTMS, (2.5% solution in acetone: water (95:5, 12 mL)) at RT for 1 h. IR: 3296bs, 2163w, 2105w 1980w, 1632w, 1039bs, 941bs, 791m cm^{-1} . XPS: Consistent with the target structure.

4.8.4.6.1 GA activation

The APTMS woven glass supports were activated with GA according to the procedure described by Santosh.⁷⁹ APTMS modified glass fabric discs (0.05 g) were reacted with 2.5% GA (8 mL, w/v in 0.05 M PBS, pH 7.5) for 1 h at RT. The activated support was thoroughly washed with distilled water (20 mL; 3 x 20 min) to remove excess GA. IR: 3296bs, 2163w, 2105w 1980w, 1632w, 1039bs, 941bs, 791m cm^{-1} . XPS: Consistent with the target structure.

APTMS modified non-woven glass fabric discs were allowed to react with GA according to the procedure described above for woven fabric under the following conditions: Glass fabric discs (0.14 g), 2.5% GA (10 mL, w/v in 0.05 M PBS, pH 7.5) for 1 h at RT. IR: 3327 bs, 2233w, 1634w, 1042bs, 792m, 699w cm^{-1} . XPS: Consistent with the target structure.

4.8.4.6.2 ADH immobilisation

The APTMS-GA modified woven and non-woven glass fabric supports from the above section were exposed to the ADH enzyme according to the procedure described in Section 4.8.4.2.1 under following conditions: ADH (15 mL, 0.5 mg/mL) incubated at 4-8 °C for 19 h. All discs were washed with PBS buffer (pH 7.5) containing Triton-X (0.1 %) (10 mL; 3 x 20 min) and individually assayed according to the procedure found in the Experimental Section 4.8.3. Glass woven and non-woven fabric discs without ethylamine-GA modification (control) were exposed to ADH analogously and used as controls.

4.8.4.7 Effect of APTMS concentration on ADH activity

(3-Aminopropyl)trimethoxysilane (APTMS) solution was prepared in various concentrations (1%, 2.5%, 5% and 10 %) in acetone and allowed to stand for 15 min at RT. Acid activated woven and non-woven fabric discs were added to the hydrolysed amino silane solution and allowed to stir for 1 h at RT. All discs were then washed with distilled water (20 mL; 3 x 20 min) and methanol (20 mL; 3 x 20 min) to neutral pH. The discs were then allowed to cure at 110 °C for 30 min.

4.8.4.7.1 GA activation and ADH immobilisation

The woven and non-woven glass fabric amino silane (APTMS) discs prepared above were activated with GA separately according to the procedure described by Santosh⁷⁹ under following conditions: Glass fabric discs (0.14 g), 2.5% GA (10 mL, w/v in 0.05 M PBS, pH 7.5) for 1 h at RT. The discs were then exposed to ADH (0.5 mg/mL, 0.05M PBS, pH 7.5) according to the procedure described in Section 4.8.2.1. ADH immobilisation on control and treatment glass fabric discs was done in four replicates and assayed to measure the immobilised ADH activity. The effect of APTMS concentration on ADH activity for both woven and non-woven glass fabric was then measured and is represented in below Table 4.8.

Table 4.8 Activity data measured for woven and non-woven glass fabric after various APTMS conc treatment

APTMS Conc % (acetone)	Abs	NADH coefficient	Conc (mM)	Conc (mmol)	Total activity mmol/min	Activity mmol/min/g	Average activity	% Activity
APTMS conc effect - ADH activity immobilised on woven glass fabric								
1% APTMS	0.236	6200	0.038	0.038	0.010	0.952	0.948	45%
	0.236	6200	0.038	0.038	0.010	0.951		

	0.234	6200	0.038	0.038	0.009	0.942		
2.5% APTMS	0.531	6200	0.086	0.086	0.021	2.141	2.120	100%
	0.526	6200	0.085	0.085	0.021	2.121		
	0.52	6200	0.084	0.084	0.021	2.097		
APTMS Conc % (acetone)	Abs	NADH coefficient	Conc (mM)	Conc (mmol)	Total activity mmol/min	Activity mmol/ min/g	Average activity	% Activity
5% APTMS	0.481	6200	0.078	0.078	0.019	1.940	1.989	94%
	0.500	6200	0.081	0.081	0.020	2.016		
	0.499	6200	0.08	0.081	0.020	2.012		
10% APTMS	0.119	6200	0.019	0.019	0.005	0.480	0.490	23%
	0.122	6200	0.02	0.020	0.005	0.493		
	0.124	6200	0.02	0.020	0.005	0.498		

APTMS Conc % (acetone)	Abs	NADH coefficient	Conc (mM)	Conc (mmol)	Total activity mmol/min	Activity mmol/ min/g	Average activity	% Activity
APTMS conc effect - ADH activity immobilised on non-woven glass fabric								
1% APTMS	0.531	6200	0.086	0.086	0.021	2.141	2.12	40%
	0.526	6200	0.085	0.085	0.021	2.121		
	0.520	6200	0.084	0.084	0.021	2.097		
2.5% APTMS	1.307	6200	0.211	0.211	0.053	5.270	5.25	100%
	1.300	6200	0.210	0.210	0.052	5.242		
	1.299	6200	0.210	0.210	0.052	5.238		
5% APTMS	1.013	6200	0.163	0.163	0.041	4.085	4.03	77%
	1.000	6200	0.161	0.161	0.040	4.032		
	0.989	6200	0.160	0.160	0.040	3.988		
10% APTMS	0.219	6200	0.035	0.035	0.009	0.883	0.91	22%
	0.222	6200	0.036	0.036	0.009	0.895		
	0.236	6200	0.038	0.038	0.01	0.952		

4.8.4.8 Effect of varying concentrations of GA

Aqueous 25% GA solution was diluted with PBS buffer (0.05 M, pH 7.5) to prepare 1% (w/v), 2.5 % (w/v), 5% (w/v) and 10% (w/v) GA solutions. Woven and non-woven glass fabric amino silane (APTMS) supports were reacted with the above GA solutions for 2 h at 25 °C as per the procedure described by Santosh.⁷⁹ After crosslinking with each GA concentration, the discs were exposed to ADH separately according to the procedure described in Section 4.8.4.2.1 and assayed to measure the immobilised ADH activity. The effect of GA concentration on ADH activity for both woven and non-woven glass fabric is recorded below in Table 4.9.

Table 4.9 Activity data measured for woven and non-woven glass fabric after varying GA concentrations

GA Conc	Abs	NADH coefficient	Conc (mM)	Conc (mmol)	Total activity mmol/min	Activity mmol/min/g	Average activity	% Activity
GA conc effect on ADH activity immobilised on non-woven glass fabric								
1% GA	1.013	6200	0.161	0.161	0.04	4.084	4.03	77%
	1.005	6200	0.159	0.159	0.039	4.032		
	0.989	6200	0.210	0.210	0.052	3.987		
2.5% GA	1.307	6200	0.209	0.209	0.052	5.27	5.25	100%
	1.300	6200	0.209	0.209	0.052	5.241		
	1.299	6200	0.085	0.085	0.021	5.237		
5% GA	0.531	6200	0.084	0.084	0.021	2.141	2.11	40.19%
	0.526	6200	0.083	0.083	0.021	2.121		
	0.52	6200	0.035	0.035	0.008	2.096		
10% GA	0.219	6200	0.035	0.035	0.009	0.883	0.9	17.14%
	0.222	6200	0.038	0.038	0.009	0.895		
	0.236	6200	0.038	0.038	0.009	0.951		
Control	0.256	6200	0.041	0.041	0.013	1.032		

Table 4.9 Continued....

GA Conc	Abs	NADH coefficient	Conc (mM)	Conc (mmol)	Total activity mmol/min	Activity mmol/min/g	Average activity	% Activity
GA conc effect on ADH activity immobilised on woven glass fabric								
1 % GA	0.710	6200	0.114	0.114	0.028	2.862	2.854	73%
	0.700	6200	0.112	0.112	0.028	2.822		
	0.416	6200	0.067	0.067	0.016	1.677		
2.5 % GA	0.960	6200	0.154	0.154	0.038	3.871	3.903	100%
	0.969	6200	0.156	0.156	0.039	3.907		
	0.714	6200	0.115	0.115	0.028	2.879		
5% GA	0.422	6200	0.068	0.068	0.017	1.701	1.701	44%
	0.428	6200	0.069	0.069	0.017	1.725		
	0.308	6200	0.049	0.049	0.012	1.241		
10% GA	0.219	6200	0.035	0.035	0.009	0.895	0.95	32%
	0.222	6200	0.038	0.038	0.009	0.951		
	0.236	6200	0.038	0.038	0.009	0.951		

4.8.5 Immobilised ADH Stability Studies

4.8.5.1 Effect of pH

The effect of pH on enzyme activity was measured in different buffer systems: for pH 6.5 to 8.0, sodium phosphate buffer (0.05 M Na₂HPO₄/0.05 M NaH₂PO₄) was used, and for pH 8.5 to 10.5, sodium carbonate/bicarbonate buffer (0.1M each) was used. The soluble ADH and immobilised ADH were incubated at 40 °C for 2 h in various pH buffer solutions. The pH at which the enzyme expressed the highest activity was taken as the control (100% activity) for the calculation of the remaining activity for both the soluble and immobilised ADH.

The effect of pH on ADH immobilised on both woven and non-woven glass fabric activity data is described in detail below in Table 4.10.

Table 4.10 Activity data for woven and non-woven glass fabric after various pH treatment

pH	Abs	NADH coefficient	Conc (mM)	Conc (mmol)	Total activity mmol/min	Activity mmol/min/g	Average activity	% Activity
Effect of pH on ADH activity immobilised on woven glass fabric								
5	0.100	6200	0.016	0.016	0.004	0.403	0.535	34%
	0.101	6200	0.016	0.016	0.004	0.407		
	0.104	6200	0.017	0.017	0.004	0.419		
6	0.226	6200	0.036	0.036	0.009	0.911	0.919	78%
	0.228	6200	0.037	0.037	0.009	0.919		
	0.230	6200	0.037	0.037	0.009	0.927		
7	0.293	6200	0.047	0.047	0.012	1.181	1.191	100%
	0.295	6200	0.048	0.048	0.012	1.190		
	0.298	6200	0.048	0.048	0.012	1.202		
8	0.195	6200	0.031	0.031	0.008	0.786	0.780	66%
	0.190	6200	0.031	0.031	0.008	0.766		
	0.195	6200	0.031	0.031	0.008	0.786		
9	0.095	6200	0.015	0.015	0.004	0.383	0.382	32%
	0.094	6200	0.015	0.015	0.004	0.379		
	0.095	6200	0.015	0.015	0.004	0.383		
10.5	0.011	6200	0.002	0.002	0.000	0.044	0.046	4%
	0.011	6200	0.002	0.002	0.000	0.044		
	0.012	6200	0.002	0.002	0.000	0.048		

pH	Abs	NADH coefficient	Conc (mM)	Conc (mmol)	Total activity mmol/min	Activity mmol/min/g	Average activity	% Activity
Effect of pH on soluble ADH								
5	1.681	6200	0.271	0.271	0.068	1356.00	1385.50	80%
	1.670	6200	0.269	0.269	0.067	1346.00		
	1.701	6200	0.274	0.274	0.069	1372.00		
6	1.820	6200	0.294	0.294	0.073	1468.00	1464.67	86%
	1.810	6200	0.292	0.292	0.073	1460.00		
	1.818	6200	0.293	0.293	0.073	1466.00		
7	2.096	6200	0.338	0.338	0.085	1690.00	1698.00	100%
	2.120	6200	0.342	0.342	0.086	1710.00		
	2.100	6200	0.339	0.339	0.085	1694.00		
8	1.635	6200	0.264	0.264	0.066	1318.00	1312.67	77%
	1.610	6200	0.260	0.260	0.065	1298.00		
	1.640	6200	0.265	0.265	0.066	1322.00		

Table 4.10 Continued...

pH	Abs	NADH coefficient	Conc (mM)	Conc (mmol)	Total activity mmol/min	Activity mmol/min/g	Average activity	% Activity
9	0.087	6200	0.014	0.014	0.004	70.00	72.67	43%
	0.095	6200	0.015	0.015	0.004	76.00		
	0.090	6200	0.015	0.015	0.004	72.00		
10.5	0.066	6200	0.011	0.011	0.003	54.00	56.67	33%
	0.076	6200	0.012	0.012	0.003	62.00		
	0.068	6200	0.011	0.011	0.003	54.00		

pH	Abs	NADH coefficient	Conc (mM)	Conc (mmol)	Total activity mmol/min	Activity mmol/min/g	Average activity	% Activity
Effect of pH on ADH activity immobilised on non-woven glass fabric								
5	0.344	6200	0.056	0.055	0.014	1.387	1.4	38%
	0.350	6200	0.057	0.056	0.014	1.411		
	0.348	6200	0.056	0.056	0.014	1.403		
6	0.451	6200	0.073	0.073	0.018	1.819	1.8	50%
	0.456	6200	0.074	0.074	0.018	1.839		
	0.460	6200	0.074	0.074	0.019	1.855		
7	0.901	6200	0.145	0.145	0.036	3.633	3.6	100%
	0.910	6200	0.147	0.147	0.037	3.669		
	0.914	6200	0.147	0.147	0.037	3.685		
8	0.804	6200	0.130	0.130	0.032	3.242	3.2	89%
	0.809	6200	0.131	0.130	0.033	3.262		
	0.800	6200	0.129	0.129	0.032	3.226		
9	0.389	6200	0.063	0.063	0.016	1.569	1.5	43%
	0.380	6200	0.061	0.061	0.015	1.532		
	0.390	6200	0.063	0.063	0.016	1.573		
10.5	0.216	6200	0.035	0.035	0.009	0.871	0.8	24%
	0.220	6200	0.036	0.035	0.009	0.887		
	0.230	6200	0.037	0.037	0.009	0.927		

4.8.5.2 Thermal stability

The thermostability studies were performed by incubating soluble ADH (0.5 mg/mL) and immobilised ADH for 2 h in PBS (0.05 M, pH 7.5) at variable temperature (20 °C, 40 °C, 60 °C, 80 °C) in a water bath. After each incubation, the enzyme was chilled in crushed ice for 5 min. The enzyme was then allowed to warm to RT and residual ADH activity was measured according to the procedure described in Experimental Section 4.8.4.2.1. Table 4.11 represents activity data observed for soluble ADH and immobilised ADH on both non-woven and woven glass fabric.

Table 4.11 Thermal stability activity data of soluble and immobilised ADH on both woven and non-woven glass fabric

pH	Abs	NADH coefficient	Conc (mM)	Conc (mmol)	Total activity mmol/min	Activity mmol/min/g	Average activity	% Activity
Thermal stability of immobilised ADH on non-woven glass fabric								
20	1.400	6200	0.226	0.226	0.056	5.645	5.635	100%
	1.395	6200	0.225	0.225	0.056	5.625		
40	0.853	6200	0.138	0.138	0.034	3.440	3.455	61%
	0.861	6200	0.139	0.139	0.035	3.471		
60	0.502	6200	0.081	0.081	0.020	2.024	2.018	50%
	0.499	6200	0.080	0.080	0.020	2.012		
80	0.292	6200	0.047	0.047	0.012	1.177	1.171	31%
	0.289	6200	0.047	0.047	0.012	1.165		

Table 4.11 Continued...

pH	Abs	NADH coefficient	Conc (mM)	Conc (mmol)	Total activity mmol/min	Activity mmol/min/g	Average activity	% Activity
Thermal stability of soluble ADH								
20	1.990	6200	0.321	0.321	0.080	1604.00	1608.00	100%
	2.000	6200	0.323	0.323	0.081	1612.00		
40	1.790	6200	0.289	0.289	0.072	1444.00	1443.00	90%
	1.789	6200	0.289	0.289	0.072	1442.00		
60	0.066	6200	0.011	0.011	0.003	54.00	52.00	3%
	0.062	6200	0.010	0.010	0.003	50.00		
80	0.056	6200	0.009	0.009	0.002	46.00	46.00	1%
	0.057	6200	0.009	0.009	0.002	46.00		

pH	Abs	NADH coefficient	Conc (mM)	Conc (mmol)	Total activity mmol/min	Activity mmol/min/g	Average activity	% Activity
Thermal stability of immobilised ADH on woven glass fabric								
20	0.502	6200	0.081	0.081	0.020	2.024	2.018	100%
	0.499	6200	0.080	0.080	0.020	2.012		
40	0.392	6200	0.063	0.063	0.016	1.581	1.575	78%
	0.389	6200	0.063	0.063	0.016	1.569		
60	0.192	6200	0.031	0.031	0.008	0.774	0.768	39%
	0.189	6200	0.030	0.030	0.008	0.762		
80	0.085	6200	0.014	0.014	0.003	0.343	0.348	20%
	0.088	6200	0.014	0.014	0.004	0.353		

4.8.5.3 Storage stability

ADH immobilised on both woven and non-woven glass fabric discs were stored in PBS (0.05 M, pH 7.5) buffer (0.05 M, pH 7.5) at 4 °C for 60 days and the ADH activity was assayed at defined time points using fresh discs taken from the buffered solution. The activity was assessed according to the procedure described in the ADH activity assay (Section 4.8.3).

Table 4.12 represents storage residual activity data observed for soluble and immobilised ADH on both non-woven and woven glass fabric.

Table 4.12 Storage stability activity data of soluble and immobilised ADH on both woven and non-woven glass fabric

No days	Abs	NADH coefficient	Conc (mM)	Conc (mmol)	Total activity mmol/min	Activity mmol/min/g	Average activity	% Activity
Storage stability of immobilised ADH on woven glass fabric at 4° C in PBS								
0	0.723	6200	0.117	0.117	0.029	2.915	2.910	100%
	0.720	6200	0.116	0.116	0.029	2.903		
1	0.569	6200	0.092	0.092	0.023	2.294	2.316	82%
	0.566	6200	0.091	0.091	0.023	2.282		
2	0.330	6200	0.053	0.053	0.013	1.331	1.304	47%
	0.310	6200	0.050	0.050	0.013	1.250		
4	0.299	6200	0.048	0.048	0.012	1.206	1.188	43%
	0.290	6200	0.047	0.047	0.012	1.170		
6	0.169	6200	0.027	0.027	0.007	0.681	0.677	15%
	0.165	6200	0.027	0.027	0.007	0.665		
8	0.159	6200	0.026	0.026	0.006	0.641	0.653	23%
	0.165	6200	0.027	0.027	0.007	0.665		
10	0.131	6200	0.021	0.021	0.005	0.528	0.530	19%
	0.132	6200	0.021	0.021	0.005	0.533		
15	0.101	6200	0.016	0.016	0.004	0.407	0.413	15%
	0.106	6200	0.017	0.017	0.004	0.427		
30	0.015	6200	0.002	0.002	0.001	0.060	0.060	2%
	0.013	6200	0.002	0.002	0.001	0.060		

Table 4.12. Continued...								
No days	Abs	NADH coefficient	Conc (mM)	Conc (mmol)	Total activity mmol/min	Activity mmol/min/g	Average activity	% Activity
Storage stability of soluble ADH at 4° C in PBS								
0	2.131	6200	0.344	0.344	0.086	1718.000	1715.00	100%
	2.123	6200	0.342	0.342	0.086	1712.000		
1	2.101	6200	0.339	0.339	0.085	1694.000	1702.00	99%
	2.120	6200	0.342	0.342	0.086	1710.000		
2	2.010	6200	0.324	0.324	0.081	1620.000	1612.00	95%
	1.989	6200	0.321	0.321	0.080	1604.000		
4	1.995	6200	0.322	0.322	0.080	1608.000	1611.00	94%
	2.001	6200	0.323	0.323	0.081	1614.000		
6	1.864	6200	0.301	0.301	0.075	1504.000	1509.00	88%
	1.877	6200	0.303	0.303	0.076	1514.000		
8	1.640	6200	0.265	0.265	0.066	1322.000	1313.00	77%
	1.618	6200	0.261	0.261	0.065	1304.000		
10	0.912	6200	0.147	0.147	0.037	736.000	741.00	43%
	0.926	6200	0.149	0.149	0.037	746.000		
15	0.599	6200	0.097	0.097	0.024	484.000	485.00	28%
	0.601	6200	0.097	0.097	0.024	486.000		
30	0.315	6200	0.051	0.051	0.013	254.000	252.00	15%
	0.311	6200	0.050	0.050	0.013	250.000		
45	0.101	6200	0.016	0.016	0.004	82.000	80.00	5%
	0.096	6200	0.016	0.016	0.004	78.000		
60	0.031	6200	0.005	0.005	0.001	26.000	26.00	1%
	0.032	6200	0.005	0.005	0.001	26.000		

Table 4.12 Continued...

No days	Abs	NADH coefficient	Conc (mM)	Conc (mmol)	Total activity mmol/min	Activity mmol/min/g	Average activity	% Activity
Storage stability of immobilised ADH on non-woven glass fabric at 4° C in PBS								
0	1.083	6200	0.175	0.175	0.044	4.365	4.394	100%
	1.097	6200	0.177	0.177	0.044	4.424		
1	1.002	6200	0.162	0.162	0.040	4.040	4.016	91%
	0.990	6200	0.160	0.160	0.040	3.992		
2	0.975	6200	0.157	0.157	0.039	3.932	3.913	89%
	0.966	6200	0.156	0.156	0.039	3.895		
4	0.899	6200	0.145	0.145	0.036	3.625	3.629	83%
	0.901	6200	0.145	0.145	0.036	3.633		
6	0.869	6200	0.140	0.140	0.035	3.504	3.521	80%
	0.878	6200	0.142	0.142	0.035	3.539		
8	0.758	6200	0.122	0.122	0.031	3.057	3.082	70%
	0.771	6200	0.124	0.124	0.031	3.109		
10	0.710	6200	0.115	0.115	0.029	2.863	2.885	66%
	0.721	6200	0.116	0.116	0.029	2.907		
15	0.681	6200	0.110	0.110	0.028	2.746	2.727	62%
	0.672	6200	0.108	0.108	0.027	2.709		
30	0.590	6200	0.095	0.095	0.024	2.379	2.364	54%
	0.583	6200	0.094	0.094	0.024	2.351		
45	0.553	6200	0.089	0.089	0.022	2.230	2.221	51%
	0.549	6200	0.089	0.089	0.022	2.214		
60	0.489	6200	0.079	0.079	0.020	1.972	1.975	45%
	0.491	6200	0.079	0.079	0.020	1.980		

4.8.6 Fabrication of glass fabric-APTMS-GA electrode

A glassy carbon electrode (GC) was carefully polished with 1 μm , 0.3 μm and 0.05 μm alumina oxide, rinsed with distilled water (20 mL) after each polish and sonicated in an ultrasonic bath in ethanol (10 mL). The electrode was finally rinsed with water before taking any measurements. MB ink mediator suspension (20 μL , 2 mg in DMF) was evenly cast onto the polished electrodes. GA activated amino propyl silane (APTMS) non-woven glass fabric support (glass-APTMS-GA) was placed firmly on the electrode surface (Figure 4.16). The electrode was cured at 65 °C for 2 h and then allowed to cool to RT. Cyclic voltammetric experiments were undertaken in PBS (0.05 M, pH 7.5) containing 0.1 M KCl, with and without 2 mM NADH, at a constant potential of 0.6 V versus Ag/AgCl without stirring at RT.

ADH immobilisation

For ethanol detection, the above fabricated electrode was incubated in ADH (2 mL, 0.5 mg/mL in 0.05 M PBS at pH 7.5) at 4 °C for 18 h as described in Section 4.8.4.21. Using this standard procedure, multiple replicates of the modified electrode were prepared. The glass APTMS-GA-ADH electrode was thoroughly washed with 20 mL PBS (0.05 M PBS pH 7.5) and then stored in PBS buffer (0.05 M, pH 7.5) prior to use. Electrochemical measurements were carried out in PBS (0.05 M, pH 7.5) containing 0.1 M KCl and 1 mM NAD⁺ at a constant potential of 0.6 V versus Ag/AgCl under stirring (100 rpm) conditions. Prior to the injection of ethanol (1 to 16 mM in PBS pH 7.5), the enzyme electrode was conditioned for 5 minutes at 0.6 V allowing the background current to stabilize. Ethanol, at a concentration of 1 mM, unless

otherwise stated, was then injected at 60 second intervals and the current response was recorded. All measurements were performed at RT (Table 4.13).

Table 4.13 Current measured at various concentrations of ethanol

Current (μA)	Current (μA) background subtract	Ethanol Conc (mM)
1.939	0.729	1.00
2.223	1.013	2.00
2.401	1.191	3.00
2.546	1.336	4.00
2.687	1.477	5.00
2.775	1.565	6.00
2.886	1.676	7.00
2.978	1.768	8.00
3.057	1.847	9.00
3.166	1.956	10.00
3.221	2.011	11.00
3.286	2.076	12.00
3.347	2.137	13.00
3.389	2.179	14.00
3.431	2.221	15.00
3.441	2.231	16.00

4.8.7 Flow-injection system

The FIA system was comprised of a GC electrode (working electrode), a Pt wire (auxiliary electrode) and an Ag/AgCl electrode (reference). The GC electrode was polished with 0.1 μm , 0.3 μm and 0.05 μm alumina oxide, rinsed with distilled water (20 mL) after each polish, sonicated in an ultrasonic bath in ethanol (10 mL) and finally rinsed with water before experimentation. MB ink mediator suspension (20 μL , 2 mg in DMF) was evenly cast onto the polished electrode and cured at 65 $^{\circ}\text{C}$ for 2 h and then the electrode was cooled to RT.

A 1 mL syringe column (1.5 mm of length) was packed with immobilised ADH on non-woven glass fabric support disc (120 mg) and a peristaltic pump was used to control the flow rate through the column. The carrier solution (0.05 M PBS, pH 7.5 containing cofactor (NAD⁺)) was allowed to flow through the bioreactor containing the immobilised ADH and the electrochemical cell at a flow rate of 1.0 ml/min. A potential of 0.6 V was applied to the working electrode and the electrochemical current was allowed to decay to a steady state. with Varying concentrations of ethanol (500 μ l) in PBS (0.05 M, pH 7.5) containing KCl (0.1 M) were injected into the system and allowed to pass through the syringe bioreactor containing immobilised ADH. All measurements were performed at RT (Table 4.14).

Table 4.14 Current measured at varying concentrations of ethanol

Ethanol conc (mM)	Current (μ A)	Current (μ A) background subtract	Average of two peaks	Std deviation
1	1.200	1.015	0.967	0.068
	1.104	0.919		
2	1.564	1.379	1.399	0.028
	1.604	1.419		
4	2.223	2.038	1.994	0.062
	2.135	1.950		
6	2.734	2.549	2.502	0.066
	2.640	2.455		
8	3.279	3.094	3.014	0.113
	3.119	2.934		
10	3.238	3.053	3.110	0.081
	3.352	3.167		
			Average	Average
			2.164	0.069
RSD = 3.188 (Avg. std deviation/Avg. of two peak x 100)				

4.8.7.1 NAD⁺ concentration study

Influence of NAD⁺ concentration was studied by injecting various concentrations of NAD⁺ solution (0.05 M PBS, pH 7.5) along with 1 mM ethanol (0.05 M PBS, pH 7.5). NAD⁺ solutions (1 mM to 8 mM) were prepared in PBS (0.05 M pH 7.5) and electrochemical responses were measured.

4.8.7.2 Reproducibility

The reproducibility of the analytical performance of the immobilised ADH in the continuous flow reactor was evaluated with eleven injections of ethanol (1mM in 0.05 M PBS, pH 7.5). At 5 min intervals, 0.5 mL of 1mM ethanol was injected along with cofactor NAD⁺ (100 µL, 1mM, 0.05 M PBS, pH 7.5). Electrochemical responses were then measured.

4.9 References

1. D. Vasic Racki, in *Industrial Biotransformations*, Wiley VCH Verlag GmbH & Co. KGaA, 2006, DOI: 10.1002/9783527608188.ch1, ch. 1, pp. 1-36.
2. A. P. F. Turner, *Chemical Society Reviews*, 2013, **42**, 3184-3196.
3. P. A. Paredes, J. Parellada, V. M. Fernandez, I. Katakis and E. Dominguez, *Biosensors and Bioelectronics*, 1997, **12**, 1233-1243.
4. K. Svensson, L. Bulow, D. Kriz and M. Krook, *Biosensors and Bioelectronics*, 2005, **21**, 705-711.
5. A. P. Brown and F. C. Anson, *Analytical Chemistry*, 1977, **49**, 1589-1595.
6. Y. X. Liu, X. C. Dong and P. Chen, *Chemical Society Reviews*, 2012, **41**, 2283-2307.
7. C. Parolo and A. Merkoci, *Chemical Society Reviews*, 2013, **42**, 450-457.
8. N. Bhalla, P. Jolly, N. Formisano and P. Estrela, *Essays in Biochemistry*, 2016, **60**, 1-8.
9. E. Howard, J. F. Cassidy and J. O'Gorman, *Electroanalysis: An International Journal Devoted to Fundamental and Practical Aspects of Electroanalysis*, 1998, **10**, 1208-1210.
10. J. Wang, G. Liu and M. R. Jan, *Journal of the American Chemical Society*, 2004, **126**, 3010-3011.
11. A. Pizzariello, M. Stredansky, S. Stredanská and S. Miertus, *Talanta*, 2001, **54**, 763-772.
12. T. Bhardwaj, Review on Biosensor Technologies, 2015, **32**, 1-10
13. M. Zachut, F. Shapiro and N. Silanikove, *Food Chemistry*, 2016, **201**, 270-274.
14. T. A. Wilson, M. Musameh, I. L. Kyratzis, J. Zhang, A. M. Bond and M. T. W. Hearn, *Electroanalysis*, 2017, **29**, 1985-1993.
15. C.X. Cai, K. H. Xue, Y. M. Zhou and H. Yang, *Talanta*, 1997, **44**, 339-347.
16. P. N. Bartlett, E. Simon and C. S. Toh, *Bioelectrochemistry*, 2002, **56**, 117-122.
17. M. M. Barsan and C. M. A. Brett, *Talanta*, 2008, **74**, 1505-1510.
18. J. Xie, X. Zhang, H. Wang, H. Zheng, Y. Huang and J. Xie, *Trends in Analytical Chemistry*, 2012, **39**, 114-129.
19. A. Samphao, K. Kunpatee, S. Prayoonpokarach, J. Wittayakun, L. Svorc, D. M. Stankovic, K. Zagar, M. Ceh and K. Kalcher, *Electroanalysis*, 2015, **27**, 2829-2837.
20. F. Jafari, A. Salimi and A. Navaee, *Electroanalysis*, 2014, **26**, 530-540.
21. A. S. Santos, A. C. Pereira, N. Duran and L. T. Kubota, *Electrochimica Acta*, 2006, **52**, 215-220.
22. F. Salimi, M. Negahdary, G. Mazaheri, H. Akbari-dastjerdi, Y. Ghanbari-kakavandi, S. Javadi and A. Sayad, *International. Journal of. Electrochemical. Science*, 2012, **7**, 7225-7234.

23. W. R. Vieth, K. Venkatasubramanian, A. Constantinides and B. Davidson, in *Applied Biochemistry and Bioengineering*, eds. L. B. Wingard, E. Katchalski-Katzir and L. Goldstein, Elsevier, 1976, vol. 1, pp. 221-327.
24. N. R. Mohamad, N. H. C. Marzuki, N. A. Buang, F. Huyop and R. A. Wahab, *Biotechnology, Biotechnological Equipment*, 2015, **29**, 205-220.
25. L. D. Bowers, *Trends in Analytical Chemistry*, 1982, **1**, 191-198.
26. S. K. Dahodwala, M. K. Weibel and A. E. Humphrey, *Biotechnology and Bioengineering*, 1976, **18**, 1679-1694.
27. J. Boudrant, J. L. Cuq and C. Cheftel, *Biotechnology and Bioengineering*, 1976, **18**, 1719-1734.
28. S. K. Dahodwala, A. E. Humphrey and M. K. Weibel, *Biotechnology and Bioengineering*, 1976, **18**, 987-1000.
29. A. Rangel and I. V. Toth, *American Journal of Enology and Viticulture*, 1999, **50**, 259-263.
30. E. Dominguez, G. Markovarga, B. Hahnagerdal and L. Gorton, *Analytica Chimica Acta*, 1991, **249**, 145-154.
31. M. A. A. Cunha, R. C. B. Rodrigues, J. C. Santos, A. Converti and S. S. da Silva, *Current Microbiology*, 2007, **54**, 91-96.
32. M. Hartmann and X. Kostrov, *Chemical Society Reviews*, 2013, **42**, 6277-6289.
33. J. Ruz, M. D. L. de Castro and M. Valcarcel, *Analyst*, 1987, **112**, 259-261.
34. E. Stevenson, P. G. Ibbotson and P. L. Spedding, *Biotechnology and Bioengineering*, 1993, **42**, 43-49.
35. C. T. Kresge, M. E. Leonowicz, W. J. Roth, J. C. Vartuli and J. S. Beck, *Nature*, 1992, **359**, 710.
36. D. Zhao, J. Feng, Q. Huo, N. Melosh, G. H. Fredrickson, B. F. Chmelka and G. D. Stucky, *Science*, 1998, **279**, 548.
37. H. Y. Chiu, H. Leonhardt and T. Bein, *Chemie Ingenieur Technik*, 2017, **89**, 876-886.
38. W. L. Xie and X. Z. Zang, *Food Chemistry*, 2017, **227**, 397-403.
39. S. L. Gilani, G. D. Najafpour, A. Moghadamnia and A. H. Kamaruddin, *Journal of Molecular Catalysis B-Enzymatic*, 2016, **133**, 144-153.
40. H. L. Ramirez, L. G. Brizuela, J. U. Iranzo, M. Arevalo-Villena and A. I. B. Perez, *Journal of Food Process Engineering*, 2016, **39**, 97-104.
41. L. T. Wu, S. S. Wu, Z. Xu, Y. B. Qiu, S. Li and H. Xu, *Biosensors & Bioelectronics*, 2016, **80**, 59-66.
42. A. Azevedo, V. Vojinovic, J. Cabral, T. Gibson and L. Fonseca, *Journal of Molecular Catalysis B: Enzymatic*, 2004, **28**, 121-128.
43. R. A. Sheldon and S. van Pelt, *Chemical Society Reviews*, 2013, **42**, 6223-6235.
44. F. Secundo, *Chemical Society Reviews*, 2013, **42**, 6250-6261.
45. H. H. Weetall, *Applied Biochemistry and Biotechnology*, 1993, **41**, 157-188.

46. A. Inayat, B. Reinhardt, H. Uhlig, W. D. Einicke and D. Enke, *Chemical Society Reviews*, 2013, **42**, 3753-3764.
47. Z. S. Lu, C. M. Li, Q. Zhou, Q. L. Bao and X. Q. Cui, *Journal of Colloid and Interface Science*, 2007, **314**, 80-88.
48. L. S. Jang and H. J. Liu, *Biomedical Microdevices*, 2009, **11**, 331-338.
49. M. C. Pirrung, J. D. Davis and A. L. Odenbaugh, *Langmuir*, 2000, **16**, 2185-2191.
50. F. Patolsky, G. Zheng and C. M. Lieber, *Nature Protocols*, 2006, **1**, 1711.
51. J. Escorihuela, M. J. Bañuls, J. G. Castello, V. Toccafondo, J. Garcia-Ruperez, R. Puchades and A. Maquieira, *Analytical and Bioanalytical Chemistry*, 2012, **404**, 2831-2840.
52. G. Zheng, F. Patolsky, Y. Cui, W. U. Wang and C. M. Lieber, *Nature Biotechnology*, 2005, **23**, 1294.
53. G. A. Blab, L. Cognet, S. Berciaud, I. Alexandre, D. Husar, J. Remacle and B. Lounis, *Biophysical Journal*, 2006, **90**, L13-L15.
54. V. R. Sarath Babu, M. A. Kumar, N. G. Karanth and M. S. Thakur, *Biosensors and Bioelectronics*, 2004, **19**, 1337-1341.
55. M. Kahraman, G. Bayramoglu, N. Kayaman-Apohan and A. Gungor, *International Journal of Chemical Reactor Engineering*, 2014, **2**, 587-596.
56. C. C. Rosa, H. J. Cruz, M. Vidal and A. G. Oliva, *Biosensors and Bioelectronics*, 2002, **17**, 45-52.
57. M. Qin, S. Hou, L. Wang, X. Feng, R. Wang, Y. Yang, C. Wang, L. Yu, B. Shao and M. Qiao, *Colloids and Surfaces B: Biointerfaces*, 2007, **60**, 243-249.
58. M. V. Kahraman, G. Bayramoglu, N. Kayaman-Apohan and A. Gungor, *Food Chemistry*, 2007, **104**, 1385-1392.
59. P. J. Robinson, P. Dunnill and M. D. Lilly, *Biochimica et Biophysica Acta (BBA) - Enzymology*, 1971, **242**, 659-661.
60. R. H. Taylor, S. M. Fournier, B. L. Simons, H. Kaplan and M. A. Hefford, *Journal of Biotechnology*, 2005, **118**, 265-269.
61. J. F. Liang, Y. T. Li and V. C. Yang, *Journal of Pharmaceutical Sciences*, 2000, **89**, 979-990.
62. K. M. de Lathouder, D. T. J. van Benthem, S. A. Wallin, C. Mateo, R. F. Lafuente, J. M. Guisan, F. Kapteijn and J. A. Moulijn, *Journal of Molecular Catalysis B: Enzymatic*, 2008, **50**, 20-27.
63. G. A. Kovalenko, O. V. Komova, A. V. Simakov, V. V. Khomov and N. A. Rudina, *Journal of Molecular Catalysis a Chemical*, 2002, **182**, 73-80.
64. R. Reshmi, G. Sanjay and S. Sugunan, *Catalysis Communications*, 2007, **8**, 393-399.
65. K. G. Marinova, D. Christova, S. Tcholakova, E. Efremov and N. D. Denkov, *Langmuir*, 2005, **21**, 11729-11737.
66. J. M. Bolivar, J. Rocha-Martin, C. Mateo and J. M. Guisan, *Process Biochemistry*, 2012, **47**, 679-686.

67. W. K. Chui and L. S. C. Wan, *Journal of Microencapsulation*, 1997, **14**, 51-61.
68. G. Peng, X. H. Hou, B. L. Liu, H. L. Chen and R. Luo, *The Royal Society of Chemistry Advances*, 2016, **6**, 91431-91439.
69. Y. Gao, T. Yen Bach, P. Cacioli, P. Butler and I. L. Kyratzis, *Enzyme and Microbial Technology*, 2014, **54**, 38-44.
70. K. A. Markossian, N. V. Golub, H. A. Khanova, D. I. Levitsky, N. B. Poliansky, K. O. Muranov and B. I. Kurganov, *Biochimica et Biophysica Acta (BBA)-Proteins and Proteomics*, 2008, **1784**, 1286-1293.
71. Y. Jiang, C. Guo, H. Xia, I. Mahmood, C. Liu and H. Liu, *Journal of Molecular Catalysis B: Enzymatic*, 2009, **58**, 103-109.
72. L. Lei, Y. Bai, Y. Li, L. Yi, Y. Yang and C. Xia, *Journal of Magnetism and Magnetic Materials*, 2009, **321**, 252-258.
73. J. M. Bolivar, L. Wilson, S. A. Ferrarotti, J. M. Guisan, R. Fernandez-Lafuente and C. Mateo, *Journal of Biotechnology*, 2006, **125**, 85-94.
74. F. Toldra, N. B. Jansen and G. T. Tsao, *Process Biochemistry*, 1992, **27**, 177-181.
75. S. Sterman and H. B. Bradley, *Polymer Engineering & Science*, 1961, **1**, 224-233.
76. K. Sever, Y. Seki, I. H. Tavman, G. Erkan and V. Cecen, *Polymer Composites*, 2009, **30**, 550-558.
77. Z. Guo, R. A. Guilfoyle, A. J. Thiel, R. F. Wang and L. M. Smith, *Nucleic Acids Research*, 1994, **22**, 5456-5465.
78. <http://www.bio.umass.edu/microscopy/silane.htm>, accessed on 10th Nov 2015
79. J. C. Santos, A. V. Paula, G. F. M. Nunes and H. F. de Castro, *Journal of Molecular Catalysis B-Enzymatic*, 2008, **52-53**, 49-57.

Chapter 5

Conclusion and future work

This Chapter summarises the thesis findings and outlines directions for future research.

5.1 Conclusion

This thesis describes efforts made towards the development of a redox enzyme based continuous flow reactor and biosensor which incorporates a redox based enzyme as the catalyst immobilised on a fibre based support. The concept is demonstrated using alcohol dehydrogenase (ADH), an enzyme which catalyses the oxidation of ethanol to acetaldehyde using NADH as the cofactor. The reaction was followed amperometrically by measuring the consumption of ethanol. The reaction was first undertaken in batch mode and then transferred to a continuous flow mode.

Efforts were made for ADH immobilisation on a number of different fibre based scaffolds including cotton, nylon, polyacrylonitrile (PAN), polyvinyl alcohol (PVA) and glass as shown in Chapter two, three and four. A number of different strategies and chemistries were investigated to fabricate the fibre based ADH adducts. Only benign chemistry could be used to fabricate the fabric-ADH adduct for fear of denaturing the enzyme. The stability (pH, temperature and storage time) of the various fibre based ADH adducts was measured against the free or soluble form of ADH. Additionally, the recyclability of the adduct was measured. Only the most stable adduct was used to fabricate the flow reactor and biosensor.

Further, both biosensor and flow reactor were assessed in the amperometric detection of ethanol in batch and continuous flow methods. ADH was chosen as a model enzyme for immobilisation because of its known high sensitivity, poor stability and its diverse industrial application.

The work described in this thesis demonstrates various methods/strategies for surface modification of fibrous solid supports such as cotton fabric, nylon fabric, PAN fibre, PVA

fabric, woven and non-woven glass fabric. These supports are readily available and their porosity can be controlled. Among the various immobilisation methods, covalent binding was investigated since it provides strong and stable enzyme attachment and minimises enzyme desorption and conformational changes ensuring higher activity when applied to industrial applications.

Chapter 2 described efforts made for ADH immobilisation with cotton fabric and nylon fabric as well as ADH modification with nylon monomers (C3 and C6), BMPS and AGE, which in turn can attach to a suitable modified fibrous carrier. Loss of activity after ADH modification was observed revealing that regioselective reactions are needed to avoid denaturation of the catalytic domain of ADH.

Chapter 3 focused on the surface modification of polyvinyl alcohol (PVA) fabric. PVA fibres were knitted into the fabric and the porosity could be controlled by the loop length. PVA fabric has a secondary hydroxyl group which can be functionalised without activation or pre-treatment and used for enzyme immobilisation. Various reactions including alkylation, esterification, and silyl ether formation were investigated on the fibrous PVA surfaces with bifunctional reagents. The highest activity and greater stability was obtained for the PVA-Cl-EDA-GA-ADH fabric adduct. The immobilisation method involved surface modification of PVA with chloropropionate followed by a spacer arm inclusion with EDA and GA. ADH was then immobilised by crosslinking to the fibrous support (PVA-Cl-DA-GA). This immobilisation enabled ADH to retain 50% enzymatic activity at pH 9 whereas soluble ADH became inactive (10% activity) at this pH. Additionally, thermal stability and recyclability were enhanced for this immobilized ADH construct. Although this work provided a significant step forward, the PVA fibre based support lacked long-term stability and functionality to achieve electrode surface attachment. Hence, its use for the fabrication of a biosensor was limited.

Chapter 4 investigated the use of silane chemistry for the functionalisation of glass fibre and fabric supports. An immobilised glass fibre-ADH construct possessing high activity and stability was used to develop a flow reactor and biosensor. The ADH immobilized on glass fibre-APTMS-GA discs showed 5.403 ± 0.050 mmol/g/min activity at 20 °C. Additionally, the immobilized ADH showed improvement in thermal stability (30% retention of activity at 80 °C) and storage stability (49% retention after 60 days storage) compared to the soluble ADH. The immobilized ADH was used for ethanol bio-sensing, displayed a sensitivity of 0.789 μ A, and possessed high reproducibility with a RSD of 4.9%.

The immobilized ADH was also successfully developed into a flow bioreactor using a flow-injection analysis system. The flow bioreactor showed linearity in the range between 1 to 8 mM and high reproducibility with a RSD of 3.99%. This work enabled the fabrication of a simple amperometric based biosensor suitable for translation into a bioreactor. The high reproducibility and stability of glass fibre support make this proposal an attractive proposition.

5.2 Future work

While this thesis has demonstrated the use of fibrous supports for the stabilisation of ADH and their application in biosensor and continuous flow reactors, there are several lines of research arising from this work which should be pursued:

1. Following from Chapter 3, it could be interesting to use stabilised PVA-Cl-EDA-GA-ADH constructs in flow reactors with varying fabric porosity to observe its effect on flow rate and ethanol conversion;
2. Different types of PVA fabric, such as woven and nonwoven, could be used for surface modification and subsequent ADH immobilisation. Further examination of fabricated PVA-ADH constructs in continuous flow applications would be of great interest particularly with a view to increasing conversion yield;
3. To extend the immobilisation studies to other enzymes, such as catalyse and glucose oxidase, to broaden the application of flow reactors in chemical synthesis;
4. To couple the immobilisation of a second enzyme, for example NADH oxidase, into the fabric-ADH system (Figure 5.1). ADH enzyme uses stoichiometric amounts of expensive cofactors (NAD^+). Regeneration of cofactors *in situ via* a second enzymatic process is a very attractive and challenging proposition. A method which enables the regeneration of the required cofactor (necessary oxidoreductase enzyme) within the same reactor would provide an industrially viable flow reactor system;

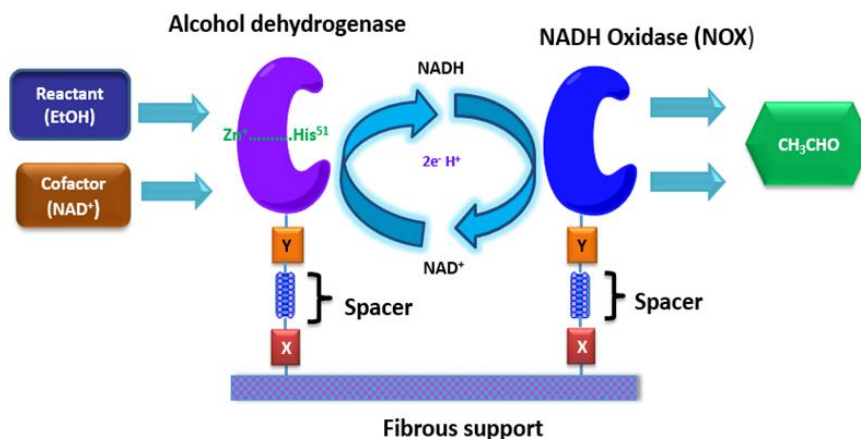


Figure 5.1. Proposed schematic of NAD⁺ regeneration by NADH oxidase with oxidation of alcohol when both enzymes immobilised on a fibrous support

5. The use of ADH immobilised on modified glass fabric could be investigated for use in flow reactors where flow parameters, such as flow rate, reaction time and amperometric response, can be easily studied; and finally,
6. The replacement of non-conductive polymers with conductive fibres (to replace NADH and recycling enzyme for NADH) could be examined.

Appendix-I

Chapter 4 work demonstrated non-woven glass fabric was a suitable support for immobilisation of ADH and provides high stability and activity. The draft manuscript below represents ADH immobilised on non-woven glass fabric application in amperometric detection of ethanol in a batch setup and in a continuous flow reactor with Flow injection analysis (FIA). Non-woven glass fabric is synonymously used as glass fibre in below manuscript.

Electrochemical detection of ethanol using glass fibre based biosensors and bioreactors

Abstract

Alcohol dehydrogenase (ADH) was covalently immobilized onto glass fibre membrane (Glass fibre) discs and utilized in the fabrication of an ethanol biosensor using a glassy carbon (GC) electrode and a continuous flow bioreactor after packing into a 1 ml syringe. The immobilisation process involved an amino silane surface modification of a glass support followed by crosslinking with glutaraldehyde (GA) and immobilisation of the ADH. The immobilized ADH showed enhanced thermal stability with 50% retention of activity at 60 °C and good improvement in storage stability with 49% retention in activity after 60 days storage in PBS buffer at 4 °C. The glass fibre membranes with immobilized ADH were used for amperometric detection of ethanol in a batch setup using a modified glassy carbon (GC) electrode and by Flow injection analysis (FIA) using a continuous flow reactor modified with glass fibre membrane discs. The present ethanol biosensor exhibited an increasing response towards ethanol in the range from 1 mM to 14 mM. In Flow Injection Analysis (FIA), a linear response was obtained from 1 mM to 8 mM ethanol ($r^2= 0.992$). The bioreactors showed good reproducibility with an RSD of 3.99% for 11 injections of 1 mM ethanol.

Keywords: Glass fibre, ADH immobilisation, ethanol detection, flow injection analysis (FIA), bioreactor

1 Introduction

Enzymes can be used in the chemical reaction to enhance reaction rate without changing their composition or utilizing themselves.¹⁻⁵ Enzymes are known to be unstable and hence their industrial application is often affected by a scarcity of long-term operational stability, recovery processes and reuse of the enzyme. When the enzyme is immobilized on solid supports, they are stable against denaturants and elevated temperature. Effective immobilisation depends on the selection of support and the conditions of the immobilisation process.⁶⁻⁸

Different support materials have been investigated to immobilize enzymes to improve reusability and stability.^{7, 9, 10} In many cases, it is found that glass as support material is being used for the immobilisation of enzymes as biocatalysts or biosensors. Porous glass, in particular, is a promising silica based support where surface properties are mainly determined by silanol groups. Another advantage of glass is that it can be made in diverse geometrical forms, i.e. rods, beads, fibres (hollow) or plates.¹¹ The porous glass can be easily modified using 3-(glycidoxypropyl)trimethoxysilane^{12, 13} and 3-(mercaptopropyl)triethoxysilane,^{14, 15} to generate epoxy groups or thiol groups, respectively on the glass surface. The most used approach for covalent immobilisation of enzyme on porous silica supports is modified with amino groups mainly using 3-(aminopropyl)triethoxysilane (APTES), followed by reaction with glutaraldehyde (GA) to provide a linker/spacer. The aldehyde groups on the surface can further react with the amino groups on the enzyme to form imine bindings.^{16, 17}

Among the various forms of glass, thick glass microfibres and woven fabric are worthy support materials for enzyme immobilisation as they have the ideal characteristics such as inherently large surface area with the porosity which, may allow greater interaction with enzyme compared to non-porous supports,¹⁸⁻²⁰ hence leading to higher loading and stability of biocatalysts.

The traditional conventional techniques such as chromatography, spectrophotometry are being used in industries but biosensors are found to be more useful and preferred analytical devices.^{21, 22} Biosensors are simple device that allow the easy of analysis in manufacturing industrial products, typically alcoholic beverages (beer, wines, and spirits) and relevant food industry. Numerous enzyme-based electrochemical devices have been developed for amperometric detection of ethanol where ADH with NAD⁺ cofactor immobilized with Meldola's Blue (MP),^{23, 24} Fe₃O₄/Au nanoparticles²⁵ and with carbon nanotubes composite matrix.²⁶ Despite their novelty, these systems require a high concentration of NAD⁺, involved complex fabrication process and also suffers from enzyme stability issues. The enzyme must be able to hold its activity for a prolong period to be useful. To address this problem, enzymes can be covalently immobilized onto a suitable supports such as Glass fibre and fabric support.^{17, 27}

In the present work, we show that commercial thick Glass fibre discs (47 mm diameter, borosilicate) upon treatment with 2.5% APTMS and GA activation served as an effective support for ADH immobilisation, whilst simultaneously enhancing NAD⁺ oxidation. The fabrication of electrode was performed with GA activated Glass fibre discs together with Meldola's Blue (MB) on glassy carbon (GC). MB acts as electron mediator as well as gluing agent for the modified glass fibre discs. In this work we also explored Glass fabric (E glass) as support for ADH immobilisation upon APTMS and GA treatment. ADH immobilized on both Glass fibre and fabric was investigated for stability study. Due to the more stability and high activity of ADH on Glass fibre support same was used in biosensor and continuous flow reactor application.

To the best of our knowledge, the present strategy of the fabrication of a biosensor has not been previously reported. However, the poly (phenothiazine) dyes are widely used in the construction of electrochemical sensors and biosensors.^{28, 29} The resulting ethanol biosensor

showed an enhanced response. Furthermore, when immobilized ADH used in a continuous flow reactor with FIA, demonstrated linearity with high reproducibility.

2 Experimental

2.1 Materials

Glass microfibres (Glass fibre) (47mm borosilicate glass, Whatman filter), Glass fabric (E glass, CSIRO), 3-aminopropyl trimethoxysilane (APTMS), glycidyl-3-(trimethoxysilyl) propyl ether, 3-chloropropyl triethoxysilane, *N*(2-aminoethyl,3-aminopropyl)trimethoxysilane, glutaraldehyde (25% aq solution) Tris buffer, sodium hydrogen phosphate (Na_2HPO_4), sodium dihydrogen phosphate (NaH_2PO_4), potassium chloride (KCl), and phosphoric acid (H_3PO_4) were purchased from Sigma Aldrich Australia., Meldola's Blue (MB), β -nicotinamide adenine dinucleotide sodium salt (NAD^+) were purchased from Sigma-Aldrich Australia. β -Nicotinamide adenine dinucleotide, reduced disodium salt hydrate (NADH) was purchased from Alfa Aesar (Australia); alcohol dehydrogenase (ADH) from yeast (500 units/mg) was purchased from Calzyme. HCl (37%), acetone ethanol and methanol were used as received from Merck without any further purification.

2.2 Characterisation

All electrochemical experiments were performed using Autolab PGSTAT308 in conjunction with a three-electrode system: a GC electrode modified with the Glass fibre-APTMS-GA-ADH as the working electrode, a platinum wire as the counter electrode while Ag/AgCl served as the reference electrode. The potentials were listed with respect to the reference electrode. All

amperometric measurements were carried out with stirred conditions and the response current was reported with the different value between the steady state and background current. The flow injection analysis (FIA) system comprising a wall-jet electrochemical cell with a GC electrode modified with MB, peristaltic pump, rhyodyne injector, support solution reservoir and 1 ml syringe used for reactor experiments.

Nicolet 6700 ATR-FTIR (Thermo Scientific) in the absorbance mode was used for infrared spectral analysis. SEM was used for morphology analysis using Scanning Electron Microscope (SEM, Philips XL30). The samples were imaged using a Zeiss Merlin FESEM after being coated with iridium under vacuum. The elemental composition of the surface was analyzed using X-ray photoelectron spectroscopy (XPS) on an AXIS Nova spectrometer (Kratos Analytical Inc., UK) using a monochromated Al K α source at a power of 180W. Enzyme activity was measured using a Cary 300 Bio U.V visible (Varin)

2.3 Methods

2.3.1 Modification of Glass Fibre and Fabric

HCl Treatment

Glass fibre and fabric both were stamped out as discs (~0.150 g, 13 mm diameter) and subjected to an activation pre-treatment with hydrochloric acid (10 N, 5 ml) for 4 h at 80 °C. After acid activation, G fibres and fabric discs were washed with distilled water (25 mL X 20) until pH of washing solution neutral (chloride-free) and then dried at 110 °C for 18 h.³⁰

Silane Modification

APTMS (2.5% in 15 mL acetone) solution was prepared and incubated for 15 min to hydrolyse silane methoxy. To this amino silane solution, the acid activated Glass fibre discs (0.120 g, 13 mm disc) were added and incubated for 1 h at RT under stirring. Silane treated discs were washed with distilled water (50 ml X 5) and methanol (20 ml X 3) until pH of washing solution reach to neutral and then cured at 110 °C for 1 h to drive the condensation of silanol groups on the surface. Similarly, Glass fabric discs (0.12 g) were also treated with APTMS reagent. The effect of various concentrations of APTMS on ADH activity was investigated with various % APTMS loadings (1%, 2.5%, 5% and 10%) in acetone and treated similarly as described above.

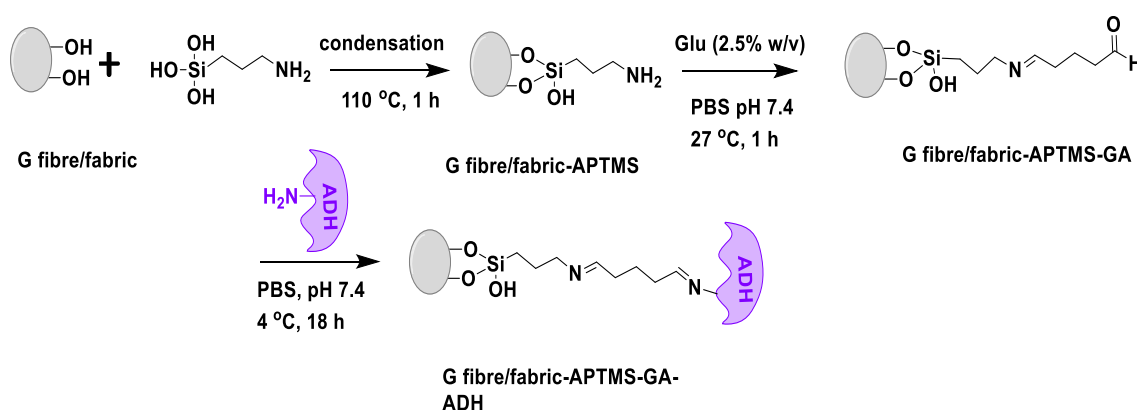


Figure 1. Schematic representation of Glass fibre and fabric surface modification and immobilisation with ADH

2.3.2 ADH Immobilisation and Assay

The Glass fibre and Glass fabric-APTMS support were modified with 2.5% (w/v) GA for 1h at 25 °C in PBS (0.05 M, pH 7.4).³¹ The GA activated support was thoroughly washed with distilled water to remove excess GA and incubated with 1 mL ADH (0.5 mg/mL) in PBS (0.05 M, pH 7.4) for 18 h at 4 °C (Figure 1). The immobilized discs were washed with 0.1%

Triton X in PBS (0.05M pH 7.4) over 30 min followed by PBS to remove any unbound ADH enzyme. ADH immobilized analogously with the Glass fibre and Glass fabric discs without any modification and with APTMS modified Glass fibre and fabric disc and used as control 1 and control 2 respectively. The activity of ADH immobilized on both control and treatment glass support was measured spectrophotometrically by submerging the discs individually in Tris buffer (100 mM pH 8.8), ethanol (20 mM), and NAD⁺ (1 mM) at 25 °C in 12 well plates for 4 min. After shaking for 4 min at 100 rpm on an orbital shaker, 1 mL of the solution was withdrawn and the absorbance measured at 340 nm immediately.³² The activity measurement experiments were performed in triplicates.

2.3.3 Stability Studies of Soluble and Immobilised ADH

In order to study effect of pH on enzyme activity, enzyme activity was measured in different buffer systems, such as for pH 6.5 to 8.0 sodium phosphate buffer (0.05 M Na₂HPO₄/0.05M NaH₂PO₄) was used and for pH 8.5 to 10.5 sodium carbonate/bicarbonate buffer (0.1M each) was used. The soluble ADH and immobilized ADH were incubated at 40 °C for 2 h in various pH buffer solutions. The pH at which the enzyme expressed the highest activity was taken as the control (100% activity) for the calculation of the remaining percent activity for both the soluble and immobilized ADH.

The thermal stability study was performed by incubating soluble ADH (0.5 mg/mL) and immobilized ADH for 2 h in PBS buffer (0.05 M, pH 7.5) at various temperatures (20 °C, 40 °C, 60 °C, 80 °C) using a water bath. After each incubation, both immobilized and soluble ADH were chilled in crushed ice for 5 min and then brought to RT to measure residual activity under standard assay conditions. For storage stability, soluble ADH and ADH immobilized

Glass fibre/fabric discs were stored in PBS buffer (0.05 M, pH 7.5) at 4 °C for 60 days before commencing activity assays as described above.

2.3.4 Fabrication of Biosensor

The working electrode (i.e. GC) was carefully polished with 1 μm , 0.3 μm and 0.05 μm alumina oxide powder, rinsed with distilled water after each polish sonicated in an ultrasonic bath in ethanol and finally rinsed again with water prior to amperometric measurements. The MB ink mediator suspension (20 μL , 2 mg in 1 mL DMF) was cast on the polished electrode evenly and the Glass fibre-APTMS-GA disc was placed firmly on the electrode surface (Figure 2). This assembly was cured at 65 °C for 2 h and then cooled at RT. ADH (2 ml, 0.5 mg/ml) was immobilized on this electrode surface as described in above section 2.3.2. The electrode (G fibre-APTMS-GA-MB-ADH) was then properly washed with excess water to remove any non-covalently bound enzyme. The enzyme electrode was stored in PBS (0.05 M, pH 7.4) prior to use.

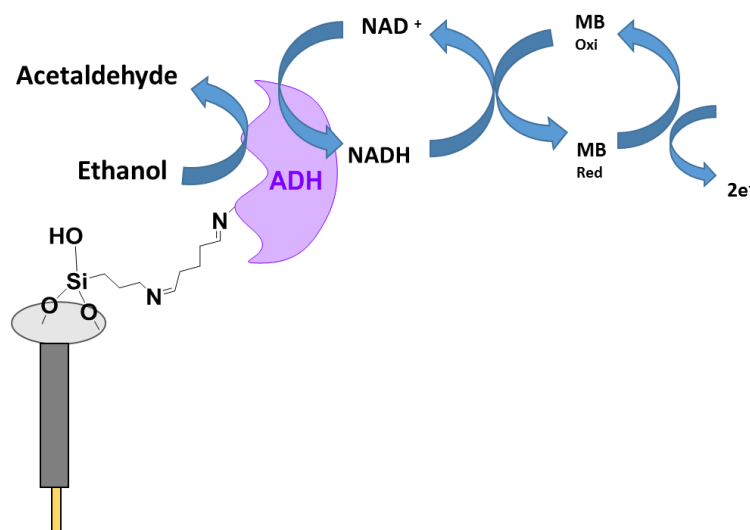


Figure 2. Mechanism of electrochemical detection for G fibre-APTMS-GA- MB-ADH biosensor. MB red and MB oxi represent the MB mediator reduced and oxidized, respectively.

Amperometric measurements were carried out in a phosphate buffer (0.05 M, pH 7.4), 1 mM NAD⁺ and ethanol in stirring conditions (100 rpm). A working potential of 0.6V was applied and transient currents were allowed to decay to a steady-state value. All measurements were performed at RT.

2.3.5 Continuous Flow-Injection System

A schematic representation of the flow injection system used for electrochemical measurements is depicted in Figure 3. The electrochemical cell contains the GC/MB working electrode, a Pt wire as an auxiliary electrode and an Ag/AgCl as the reference electrode. A 1 mL syringe (1.5 mm of length) was packed with G fibre-APTMS-GA-ADH support disc (120 mg). The flow rate 1.0 ml/min was controlled by a peristaltic pump. The mobile phase (0.05 M PBS, pH 7.5) was allowed to flow through the bioreactor containing the immobilized ADH and electrochemical cell at a flow rate of 1.0 ml/min with or without the cofactor (NAD⁺). A potential of 0.6 V was applied to the working electrode and the electrochemical current was allowed to decay to a steady state. Then a quantity of ethanol solutions (500 µl, 1mM) at different concentrations (1 to 16 mM in PBS pH 7.5) was injected into the system and allowed to pass through the syringe bioreactor with immobilized ADH.

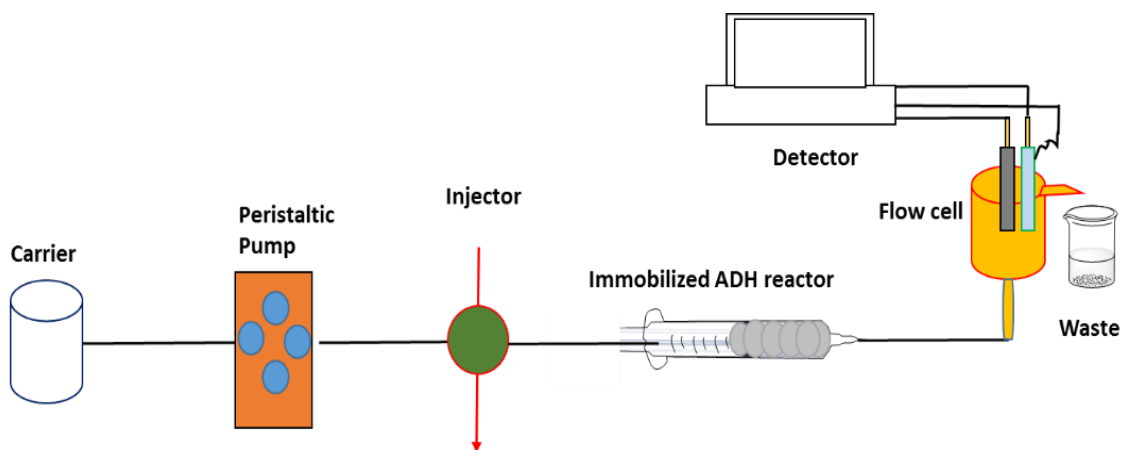


Figure 3. Schematic representation of FIA

3 Results and Discussion

3.1 Characterisation

The Glass fibre-APTMS-GA discs were characterized by SEM and XPS. Surface morphology of Glass fibre was studied by electron microscopy to study morphology changes on Glass fibre surface after each modification. After APTMS treatment, agglomerations of silane reagent was observed in Glass fibre cavities (Figure 4 B), which was consistent with findings of Sterman and Bradley.³³ After crosslinking and immobilisation of ADH on the G fibre, several island patches are observed which indicated GA activation and ADH immobilisation (Figure 4. C and D).

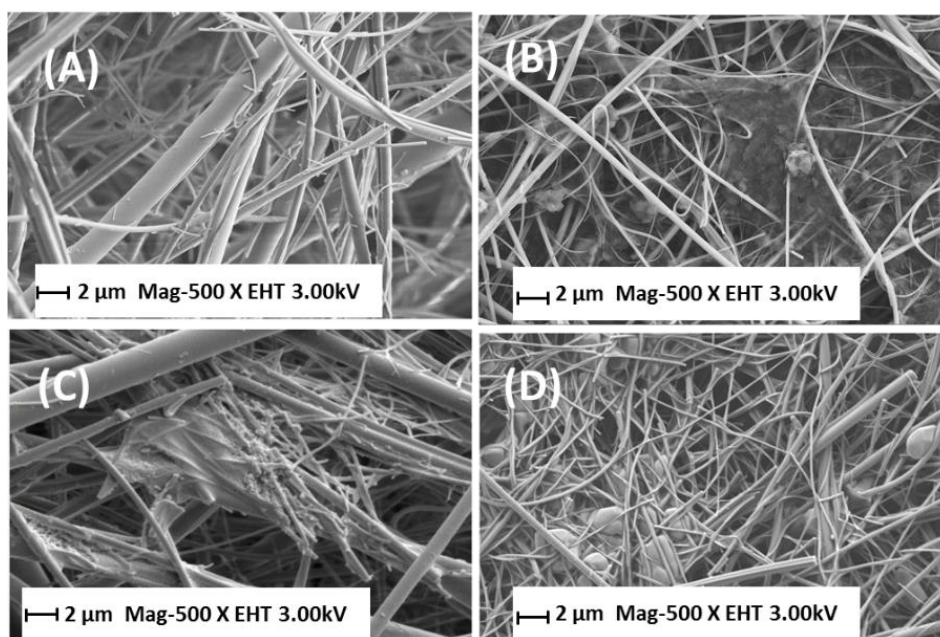


Figure 4. SEM images showing the surface morphology of G fibres as received (A), HCl activated and 2.5% APTMS treated (B), GA treatment and immobilized with ADH (D).

The surface modified Glass fibre disc was analysed by XPS to see the presence of amino groups. The results for the C, O and N are described in Table 1. As expected, after surface modification, the amount of oxygen and nitrogen increases.

Table 1 Elemental compositions expressed as atomic ratios X/C, i.e. atomic concentration of element X relative to that of C (mean value (+/- deviation) of two measurements at two different locations on each sample).

Sample	Glass fibre HCl treat		Glass fibre-APTMS		Glass fibre-APTMS-GA		Glass fibre-APTMS-GA-ADH	
	Mean	Dev.	Mean	Dev.	Mean	Dev.	Mean	Dev.
O/C	4.278	0.482	2.260	0.032	1.076	0.014	0.602	0.020
Si/C	1.860	0.251	1.059	0.017	0.443	0.006	0.240	0.011
N/C	0.019	0.003	0.138	0.004	0.074	0.005	0.151	0.005

After APTMS treatment, the O/C and Si/C ratio drops significantly with an increase in the N/C ratio compared to Glass fibre indicating the presence of amino groups. The C1s spectrum (Figure 6A, yellow line) shows peaks at 285 eV (C-C) and 286.5 eV (C-O/C-N) expected from the propylamine silane modification. The increase in N/C ratio consists of two N 1s peaks

(Figure 5B yellow line), one at 399-400 eV (amines), and the other at approx. 402 eV (protonated amines, i.e. N^+). This double peak is typically observed after aminopropyl silane surface modification. A further drop of O/C and Si/C and N/C ratios indicate the presence of reacted GA, C1s (Figure 5A blue line) very similar to sample silane modification (3) but slight increase at ca. 288 eV indicative of the presence of aldehydes (CHO). Upon ADH immobilisation further drop in O/C and Si/C with an increase in N/C ratio suggests the presence of ADH. C1s displays characteristic peak shape of polypeptides/proteins (i.e. ADH) clearly resolved peak at >288 eV due to amides (peptide bonds) and strong shoulder at 286.5 eV due to various C-N and C-O based functional groups. N 1s (Figure 5B green line) displays an additional strong peak at approx. 400 eV consistent with amides (peptide bonds).

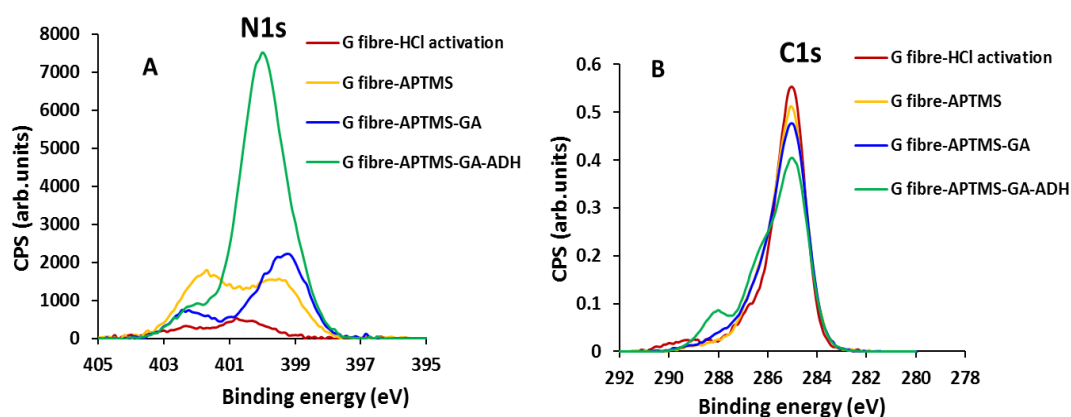


Figure 5. XPS spectra of Glass fibre HCl activated (red line), Glass fibre APTMS modification (yellow line), Glass fibre-APTMS-GA (blue line) and G fibre-APTMS-GA-ADH (green line)

To optimise the salinization reaction various silane reagents, bearing different pendent functional groups such as glycidoxypopyl silane, isocyanate silane, chloro-silane, ethanol diamine silane and APTMS were investigated. Each silane reagent was allowed to react with Glass fibre and fabric support individually in various concentration (2.5%, 5% and 10%) at RT. ADH immobilisation was done on above silane modified Glass fibre and fabric discs after GA activation and activity measured in Table 3. When the glass fibre discs were reacted with

glycidoxypropyl trimethoxysilane in toluene at a higher temperature (110 °C) the discs disintegrated and formed a gel which consistent with a previous report.³⁴ Table 2 summarises the activity of ADH when immobilized with different silane reagents (A to E) bearing various pendent functional groups.

Table 2 Effect of various silane reagents on immobilized ADH activity.

Silane reagents (in acetone 1 h RT)	Immobilisation conditions	Activity G- fabric (mmol/min/g)	Activity G-fibre (mmol/min/g)
2.5% epoxy propyl silane (A)	PBS, pH 8.1, 18 h at 4 °C	0.420±0.023	0.603±0.03
2.5% isocyanate propyl silane (B)	PBS, pH 7.5, 18 h at 4 °C	0.758±0.088	0.758±0.00
2.5% Cl trimethoxy propyl silane (C)	PBS, pH 7.5, 18 h at 4 °C	0.503±0.039	1.711±0.03
2.5% Ethanol diamine (D)	PBS, pH 7.5, 18 h at 4 °C	1.037±0.027	2.855±0.02
2.5% 3, amino propyl silane (E)	PBS, pH 7.5, 18 h at 4 °C	2.778±0.047	5.645±0.03
Soluble ADH	PBS, pH 8.1, 18 h at 4 °C	0.420±0.023	0.603±0.03

Table 2 reveals that immobilized ADH showed the highest activity with 2.5% APTMS modification among various silane modifications (A to E defined in Table.2) when immobilized on glass fibres.

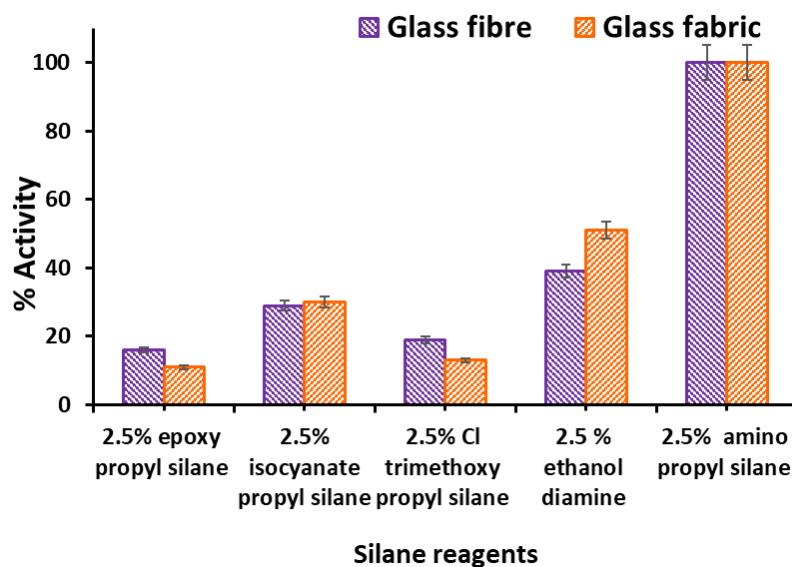


Figure 6. Comparison between glass fibre and fabric using various silane reagents effect on ADH activity. Activity assay was performed in triplicate and error bars represent standard deviations (S.D.)

Figure 6 shows a comparison between % activity data for Glass fibre and fabric when reacted with the various silane reagents (A to E). ADH immobilized on Glass fibre and fabric showed higher activity compared to other silane reagents.

Further, the effect of APTMS concentration on ADH activity was investigated on both Glass fibre and fabric as shown in Figure 7. Firstly HCl activated Glass fibre and fabric discs were allowed to react with 1% to 10% APTMS (in acetone) and then subjected to GA activation. The GA activated Glass fibre and fabric discs, further immobilized with ADH and assayed for activity.

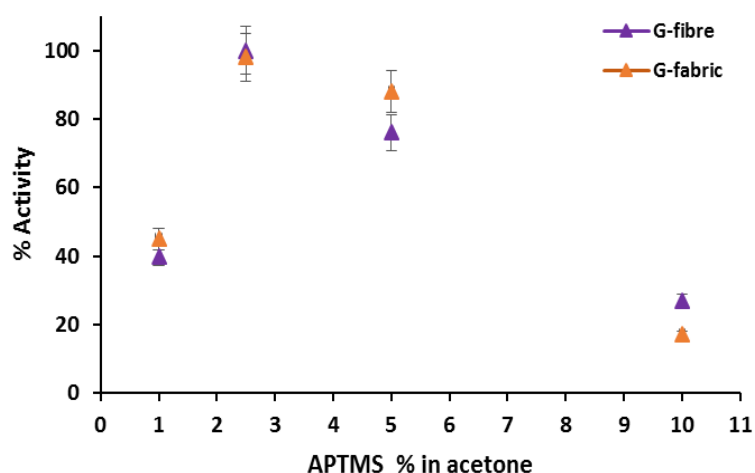


Figure 7. Effect showing various concentrations of APTMS on ADH activity. The assay was performed in triplicate and error bars represent standard deviations (S.D.)

Figure 7 indicated that higher concentrations of APTMS forbidden ADH activity. ADH when immobilized on 5% APTMS-GA support, showed 73% activity on the Glass fibre and 85% activity on G fabric. Further upon increasing APTMS concentration (10%) activity sharply decreased with both glass supports. The lower activity attributed due to the hydrophobization of the glass surface caused by the excess polymerization which could results in less functionalities on the surface for ADH immobilisation and ultimately affects ADH activity. The elevated activity was recorded with a 2.5% loading of APTMS and same was used in subsequent work.

3.2 ADH Covalent Immobilisation and Characterisation

Selection of the suitable immobilisation method is important part of the immobilisation process since it contributes in enzyme activity measurements. Basically, immobilisation techniques can be divided into two types: physical methods (i.e. weaker, monocovalent

interactions) and chemical method (i.e. formation of bonds through ether, thio-ether, amide or carbamate bonds between the enzyme and support).¹⁰ The covalent attachment of an enzyme results in more stable enzyme compared to immobilisation by physical adsorption.³⁵ Glass fibre and fabric support discs were immobilized with ADH after silane modification and GA activation and used as control-1 and control-2 respectively.

Table 3 ADH activity after immobilisation after each modification of Glass fibre and fabric (ADH was immobilized on these supports under identical protocols).

No.	G fibre	Activity (mmol/min/g)	G fabric	Activity (mmol/min/g)
Control-1	Glass fibre + ADH	0.489 ± 0.038	Glass fabric + ADH	0.447 ± 0.016
Control-2	Glass fibre -2.5% APTMS + ADH	1.020 ± 0.011	Glassfabric-2.5% APTMS + ADH	0.869 ± 0.031
Treatment	Glass fibre-2.5% APTMS - 2.5% GA + ADH	5.403 ± 0.050	Glass fabric-2.5% APTMS- 2.5% GA + ADH	2.290 ± 0.064

The measured activities for GA activated and non-activated Glass fibre and fabrics (i.e. control-1 and 2) are shown in Table 3. The small value of ADH activity recorded with the non-modified Glass fibre and fabric (Control-1), and APTMS modified Glass fibre and fabric (Control-2) mainly due to nonspecific binding. When ADH was immobilized onto the Glass fibre-2.5% APTMS-GA support (treatment), an 11 fold increase in activity was recorded compared to the Glass fibre Control-1 (i.e. without any modification).

The Glass fabric 2.5% APTMS-GA ADH immobilisation showed 5 fold increase in activity compared to the control-1 (i.e. without any modification Glass fabric). The lower activity observed for Glass fabric support after ADH immobilisation as compared to Glass fibre could

be mainly because of lower silane content of Glass fabric support (E glass, ~55% Si-OH) compared to Glass fibre (borosilicate, 80%) which mainly contain with higher amount of silane hydroxy than E glass. (55-68% Si-OH). The increase in ADH activity supports the successful ADH immobilisation at pH 7.4 on both modified Glass fibre and fabric supports.

Further immobilized ADH on both Glass fibre and fabric were investigated for stability studies such as pH, temperature and storage.

3.2.1 pH Study

The activity of an enzyme is mainly dependent on the pH of the surrounding environment. Figure 8 shows the effect of pH on the activities of both the soluble and immobilized ADH (both Glass fibre and fabric support). The optimal pH of immobilized ADH was in the range of 7 to 8, identical to that of soluble ADH. The immobilized ADH retained 43% and 30% of activity at pH 9 for the Glass fibre and Glass fabric respectively. At pH 10.5 ADH immobilized on Glass fibre, showed 22% retention of activity whereas soluble ADH showed complete loss of activity at pH 9 and above.

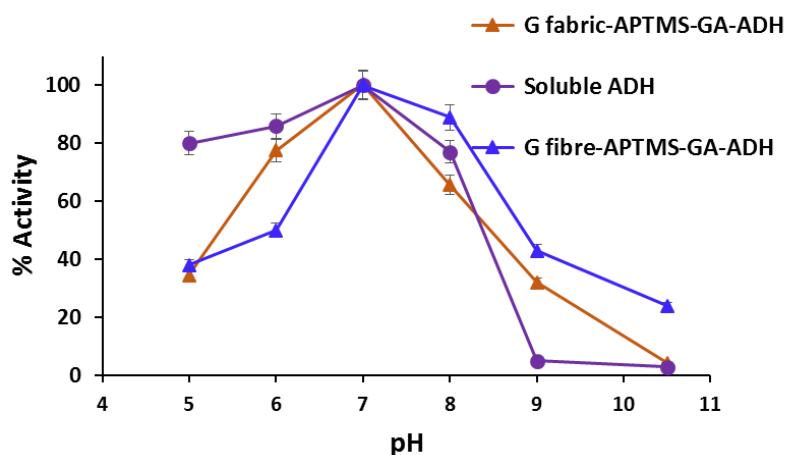


Figure 8. Effects of pH on the activities of the free and immobilized ADH (Glass fibre and fabric).

Reactions were performed in triplicate and error bars represent standard deviations (S.D.)

In summary, the enzyme activity was retained over a broader pH range after immobilisation on both glass supports. pH is very crucial for enzyme to work. The change in pH can affect the charges on the amino acid side chain groups which leads to unfolding and denaturation of proteins/enzyme and hence loss of activity. The increase in tolerance of immobilized ADH against change in pH could be due to the buffering action of amino silane modified Glass fibre support. It was believed that ADH immobilised on the surface of supports gave rise to an increase enzyme's tolerability to the pH changes in surroundings. A broadening pH profile by immobilisation has been reported for numerous enzymes, such as acetylcholinesterase, chloroperoxidase, phospholipase A and lipase.³⁶

3.2.2 Storage Stability

Storage stability of the immobilized ADH was investigated on both Glass fibre and fabric upon storage at 4 °C in PBS buffer (0.05M, pH 7.4) on each day. Soluble ADH was stored under identical condition and activity measured on each day to compare with immobilized ADH.

ADH immobilized on G fibres appeared to be stable up to 60 days at 4 °C with retention of 49% of initial activity (Figure 9). The soluble ADH showed 41% loss of activity after 10 days storage and total loss of activity after 45 days. The Glass fabric showed rapid loss of activity during storage with complete loss of activity recorded after 30 days.

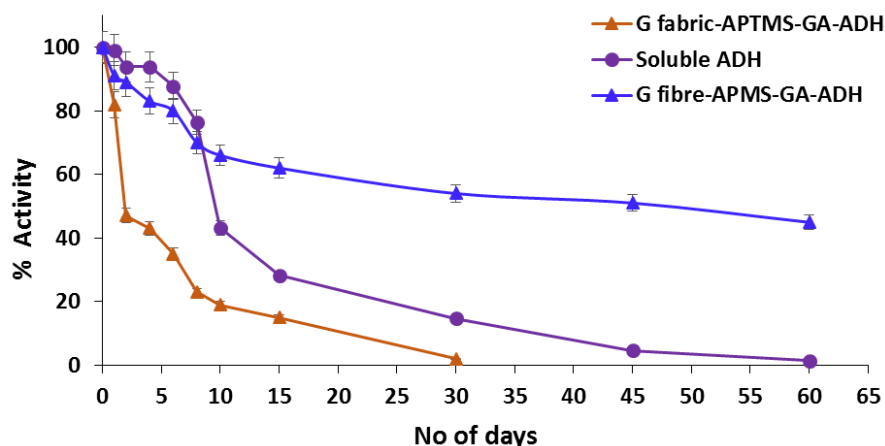


Figure 9. Storage stability of ADH immobilized on G fibres and Glass fabric and soluble ADH in PBS (0.05 M) at 4 °C

The ADH immobilised on G fibres shows enhanced ADH storage stability compared to free ADH and ADH glass fabric. The immobilized ADH stabilization may be due to multipoint attachment of the enzyme to the support and creating a more rigid environment for the enzyme molecule decreasing its likelihood of unfolding or denaturing during storage.

3.2.3 Thermal Stabilisation

In order to access the thermostability of immobilized ADH, soluble and immobilized ADH were incubated at distinct temperatures (20 to 80 °C) in PBS (0.05 M, pH 7.5) for 120 min and their residual activities were measured. The data in Figure 10 showed that both free and immobilized ADH enzymes had reduced relative activities from 40 to 80 °C

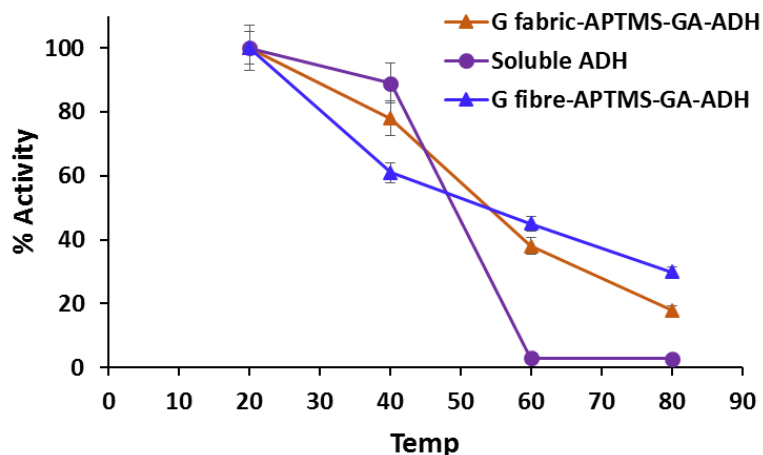


Figure 10. Effects of temperature on the activity of the soluble and immobilized ADH on Glass fibre and fabric

ADH thermal denaturation temperature T_d for is 63 °C due to the reversible thermo-inactivation of thiol, aggregation and deamidation of the enzyme.³⁷ Figure 10 describes, the soluble ADH had more enzyme activity below 50 °C, but less activity above 60 °C. Due to the multi-interaction between support and ADH enzyme (ADH tetrameric nature), it might have some interactions effect on the subunits structure, reducing the enzyme stability. Thus, from 40 to 50 °C, the activity of immobilized ADH decreased sharply than that of soluble ADH. When the incubation temperatures are above 60 °C, the residual activities of immobilized enzymes are consistently higher than that of soluble enzyme. Immobilized ADH on Glass fibre holds residual activity approximately 50 % and on Glass fabric 39 % at 70 °C, while soluble ADH holds less than 2 % at 65 °C and no activity at 70 °C. Furthermore, the immobilized ADH showed activity at stability even at 80 °C (31% retention for G fibre and 20 % for G fabric support). These observations were in accordance with the findings of some earlier investigators.^{38, 39} Due to denaturation of the enzyme at high temperatures, loss in activity was observed for the soluble form of ADH. Thermal stability of ADH improved after immobilisation on both Glass fibre and fabric support, which may be due to either enzyme

conformational limitation on enzyme movement or a low diffusion of the substrate at high temperature. The results indicate that ADH immobilized on both glass support had a good thermal stability. Such improvement in stability was reported when ADH was immobilized on various supports like glyoxyl agarose,⁴⁰ magnetic graphene oxide nanocomposites and glass beads.⁴¹

Since ADH immobilized on Glass fibre-APTMS-GA was more stable and possess higher activity same was employed in biosensor fabrication and in continuous flow reactor as a carrier for amperometric detection of ethanol.

3.3 Electrochemical Detection of Ethanol

3.3.1. Detection with Glass fibre-APTMS-GA-MB-ADH electrode

ADH and NAD^+ can be use in ethanol oxidation process to generate acetaldehyde and NADH and this reaction utilises stoichiometric amounts of substrate and cofactor. One can measure concentration of ethanol (substrate) amperometrically by selecting potential whereby NADH can be observed and detected A constant potential of 0.6 V versus Ag/AgCl was applied in a stirred solution of PBS containing 0.1 M KCl and 1 mM NAD for amperometric determination To stabilise the background current at 0.6 V the enzyme modified electrode was conditioned for 5 minutes before the addition of ethanol. 1 mM ethanol at ~60 second intervals was added , and then current response was recorded.

The modified electrode was used to measure ethanol in the concentration range from 1 to 16 mM. These results are displayed in Figure 12. It is observed from the detailed examination of the results that the new fabricated Glass fibre electrode had a non-linear

response over an ethanol concentration range from 1 to 14 mM in agreement with other electrodes employing ADH for ethanol detection.^{42, 43} This modified electrode presented a sensitivity $0.75 \mu\text{A}/\text{mM}$ and excellent reproducibility, with a relative S.D. of 4.1% for a series of five successive measurements of the 1mmol L^{-1} ethanol solution.

The wide concentration range of the biosensor is similar to most amperometric biosensors for ethanol described in the literature.⁴² Despite using thick modified glass fibres, the biosensor shows high porosity and wettability.

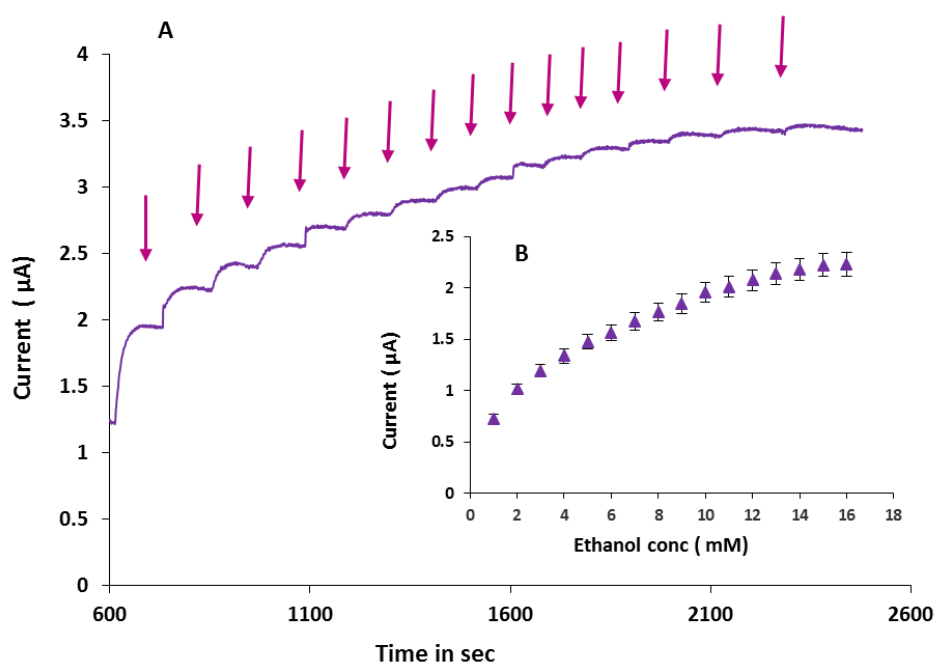


Figure 11. (A) Amperometric response of the biosensor towards ethanol; 0.5M phosphate buffer solution (pH 7.5) and 1 mM NAD^+ ; working potential: 0.6 V, ethanol concentrations: 1 to 16 mM (B) Calibration plot illustrating the response obtained upon increasing ethanol concentrations in PBS containing 1 mM NAD^+ using modified GC electrodes at 0.60 V versus Ag/AgCl

3.3.2 Detection using Glass fibre-APTMS-GA-ADH support in a continuous flow reactor

To examine the efficiency of a column mini reactor that contains Glass fibre-APTMS-GA-ADH, experiments involving consecutive injections of 1 mM ethanol were conducted. Glass fibre-APTMS-GA-ADH discs were packed into a 1 mL syringe used as mini reactor. The effect of parameters, such as sample volume and NAD^+ concentrations, were studied. Amperometric response for injections of 500 μL of 1 mM ethanol, as a function of the flow rate, was evaluated. 1.0 ml/min was chosen as the optimum rate since it showed good reproducibility and high throughput (data not shown). The amperometric signal was observed to increase when the volume of sample (ethanol) was increased. However, this resulted in increase in time for each analysis since the cell washout process also required a longer time. A volume of 500 μl was utilized as the optimal volume in subsequent experiments.

The effect of various concentration of NAD^+ from 1mM to 8 mM on the performance of the bioreactor was also evaluated and an optimum concentration of 1 mM was used based on reproducibility and sensitivity (data not shown).

3.3.3 Calibration Curve

The performance of the bioreactor (Figure.12) was evaluated by FIA coupled with amperometric detection using a GC electrode modified with MB. Below Figure 12 represents calibration plot of the amperometric response current to different ethanol concentrations

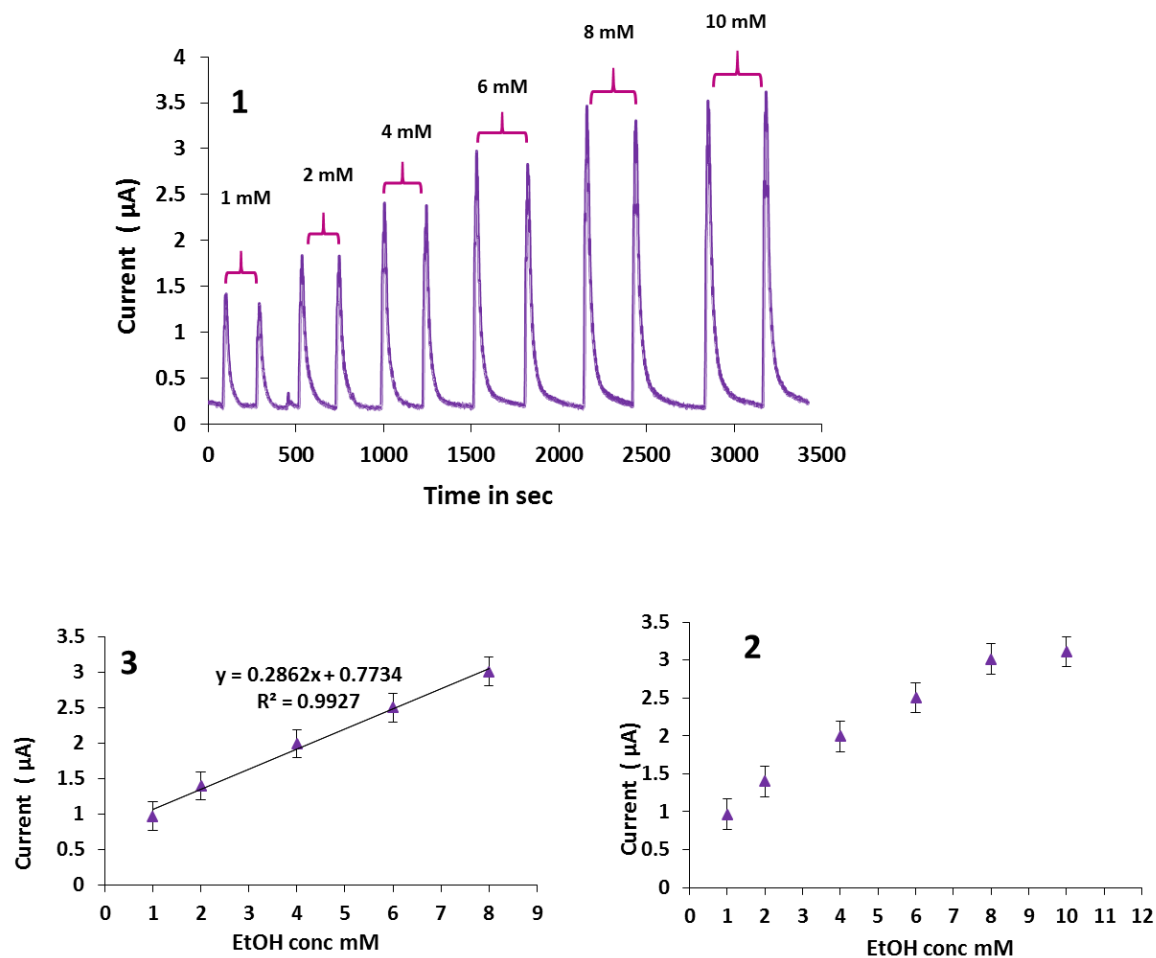


Figure 12. (1) Flow injection amperometric responses of the GC-MP to increasing concentrations of ethanol (1mM to 10 mM) in 0.05 M phosphate buffer (pH 7.5) and 1 mM NAD⁺ (mobile phase), flow rate 1 mL/min, working potential + 0.6 V, Calibration plot (2) and (3)

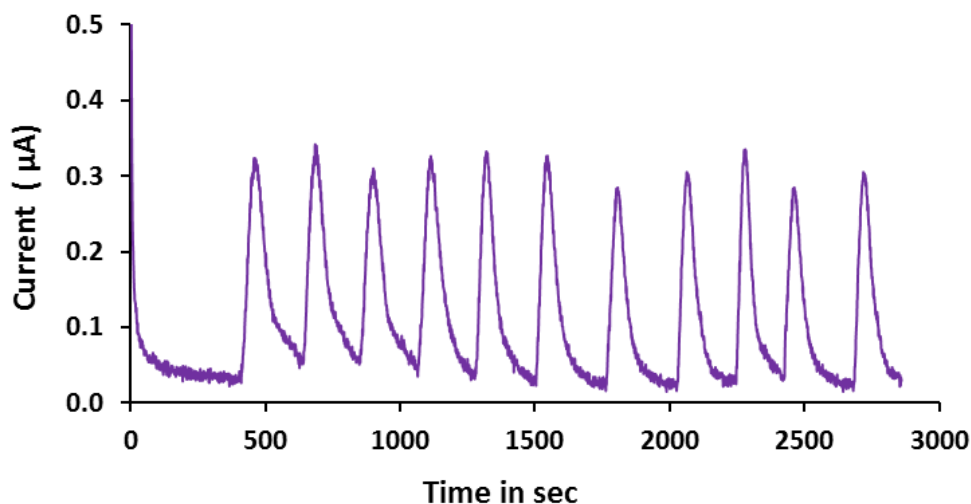


Figure 13. Flow injection amperometric responses of the Glass fibre-APTMS-GA-ADH electrode to 11 successive injections of 1 mM ethanol and 1 mM NAD⁺. Operating potential was + 0.6 V, flow rate 1 mL/min with 0.05 M phosphate buffer (pH 7.5) carrier

The reproducibility of the of the immobilized ADH towards repetitive injections of a fixed concentration of ethanol was evaluated using consecutive 11 additions of 1 mM ethanol with 1 mm NAD⁺ (Figure.13). The results revealed that the immobilised ADH shows good reproducibility with a relative standard deviation of 3.99%. The good reproducibility of the bioreactor is resulting from the enhanced stability of the immobilised ADH due to the strong interaction between ADH and the glass fibre support.

4 Conclusions

The present work has demonstrated the use of modified Glass fibre after modification with APTMS and GA, is a very suitable substrate for ADH immobilisation. This support combines advantages such as good mechanical stability, a high surface area for ADH immobilisation through amino groups on the enzyme and the modified Glass fibre surface. The ADH immobilized on Glass fibre-APTMS-GA discs, showed 5.403 ± 0.050 mmol/min/g activity at

20 °C. Further immobilized ADH showed improvement in thermal stability (30 % retention of activity at 80 °C) and storage stability (49 % retention of upon 60 days storage) compared to the soluble ADH which made it robust biocatalyst. The immobilized ADH was used for ethanol biosensing displayed a sensitivity of 0.789 μA .

Furthermore immobilized ADH was successfully used as a flow bioreactor using as part of a flow-injection analysis system. The flow bioreactor showed linearity in the range between 1 to 8 mM and high reproducibility with a RSD of 3.99%.

The work showed the fabrication of a very useful, simple and effective way to develop amperometric based biosensors sensitive to ethanol determination and in flow injection analysis format to form a bioreactor. The high reproducibility and stability of glass fibre support make this proposed method an attractive proposition.

5 Acknowledgement

Science and Industry Endowment Fund (SIEF) and CSIRO Manufacturing business unit granted the support for this work. The authors would like to thank Dr. Thomas Genenbach from CSIRO Manufacturing business unit for his help with XPS analysis.

6. References

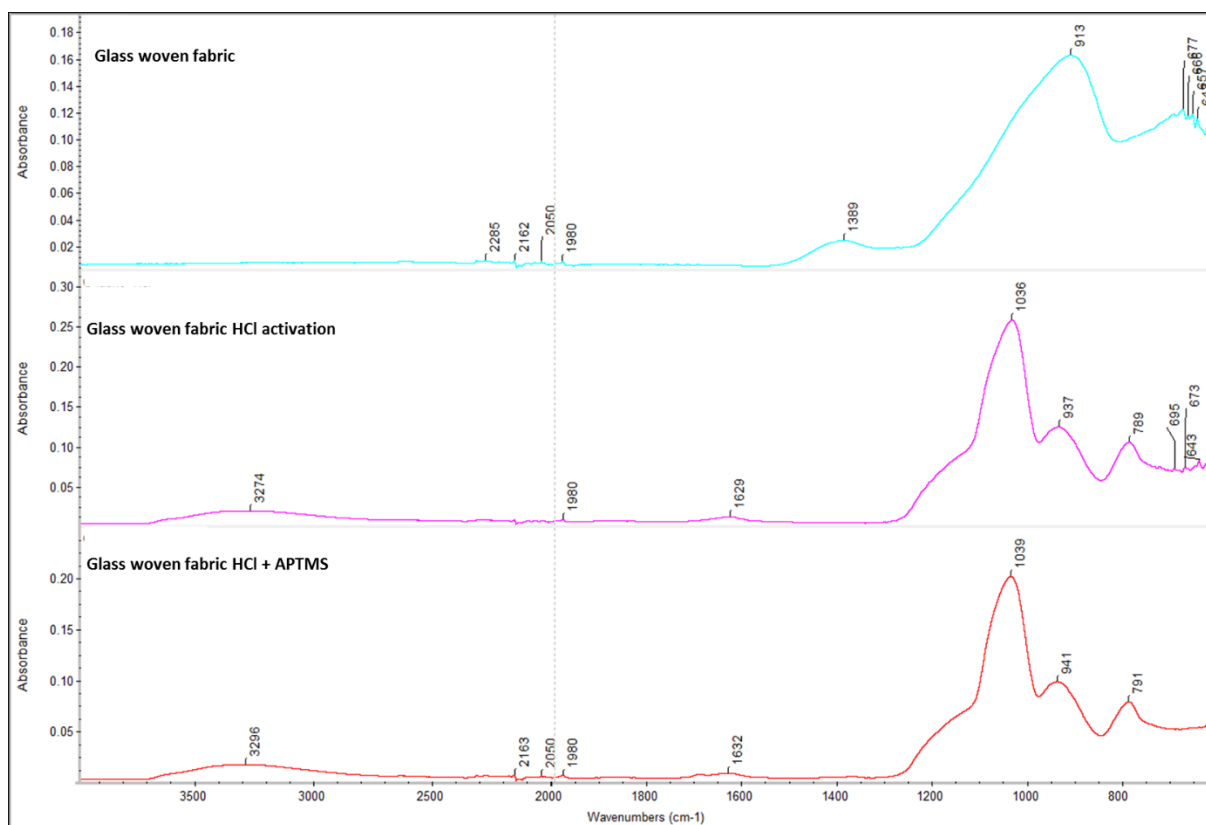
1. N. R. Mohamad, N. H. C. Marzuki, N. A. Buang, F. Huyop and R. A. Wahab, *Biotechnology & Biotechnological Equipment*, 2015, **29**, 205-220.
2. K. Faber and M. C. R. Franssen, *Trends in Biotechnology*, 1993, **11**, 461-470.
3. S. Sanchez and A. L. Demain, *Organic Process Research & Development*, 2011, **15**, 224-230.
4. K. M. Koeller and C.H. Wong, *Nature*, 2001, **409**, 232-240.
5. H. E. Schoemaker, D. Mink and M. G. Wubbolts, *Science*, 2003, **299**, 1694-1697.
6. Z. D. Knezevic-Jugovic, D. I. Bezbradica, D. Z. Mijin and M. G. Antov, in *Enzyme Stabilization and Immobilization: Methods and Protocols*, ed. S. D. Minter, Humana Press, Totowa, NJ, 2011, DOI: 10.1007/978-1-60761-895-9, pp. 99-111.
7. S. Datta, L. R. Christena and Y. R. S. Rajaram, *3 Biotech*, 2013, **3**, 1-9.
8. N. R. Mohamad, N. H. C. Marzuki, N. A. Buang, F. Huyop and R. A. Wahab, *Biotechnology, Biotechnological Equipment*, 2015, **29**, 205-220.
9. L. Cao, in *Carrier-bound Immobilized Enzymes*, Wiley-VCH Verlag GmbH & Co. KGaA, 2006, DOI: 10.1002/3527607668.ch1, pp. 1-52.
10. R. A. Sheldon and S. van Pelt, *Chemical Society Reviews*, 2013, **42**, 6223-6235.
11. A. Inayat, B. Reinhardt, H. Uhlig, W.D. Einicke and D. Enke, *Chemical Society Reviews*, 2013, **42**, 3753-3764.
12. D. Jung, C. Streb and M. Hartmann, *International Journal of Molecular Sciences*, 2010, **11**, 762.
13. P. Schonherr, A. Seifert, R. Lungwitz, F. Simon, N. Moszner, P. Burtscher and S. Spange, *Progress in Organic Coatings*, 2012, **75**, 335-343.
14. N. D. Meeks, S. Rankin and D. Bhattacharyya, *Industrial & Engineering Chemistry Research*, 2010, **49**, 4687-4693.
15. G. A. Petkova, K. Zaruba and V. Kral, *Biochimica et Biophysica Acta (BBA) - Proteins and Proteomics*, 2012, **1824**, 792-801.
16. F. Janowski, G. Fischer, W. Urbaniak, Z. Foltynowicz and B. Marciniak, *Journal of Chemical Technology & Biotechnology*, 1991, **51**, 263-272.
17. K. Kannan and R. V. Jasra, *Journal of Porous Materials*, 2011, **18**, 409-416.
18. K. M. de Lathouder, D. T. J. van Benthem, S. A. Wallin, C. Mateo, R. F. Lafuente, J. M. Guisan, F. Kapteijn and J. A. Moulijn, *Journal of Molecular Catalysis B: Enzymatic*, 2008, **50**, 20-27.
19. G. A. Kovalenko, O. V. Komova, A. V. Simakov, V. V. Khomov and N. A. Rudina, *Journal of Molecular Catalysis a-Chemical*, 2002, **182**, 73-80.
20. R. Reshmi, G. Sanjay and S. Sugunan, *Catalysis Communications*, 2007, **8**, 393-399.
21. P. A. Paredes, J. Parellada, V. M. Fernandez, I. Katakis and E. Dominguez, *Biosensors and Bioelectronics*, 1997, **12**, 1233-1243.

22. K. Svensson, L. Bulow, D. Kriz and M. Krook, *Biosensors and Bioelectronics*, 2005, **21**, 705-711.
23. A. S. Santos, R. S. Freire and L. T. Kubota, *Journal of Electroanalytical Chemistry*, 2003, **547**, 135-142.
24. E. Hua, L. Wang, X. Jing, C. Chen and G. Xie, *Talanta*, 2013, **111**, 163-169.
25. H. Teymourian, A. Salimi and R. Hallaj, *Biosensors and Bioelectronics*, 2012, **33**, 60-68.
26. C. A. Lee and Y.C. Tsai, *Sensors and Actuators B: Chemical*, 2009, **138**, 518-523.
27. T. Debeche, C. Marmet, L. Kiwi-Minsker, A. Renken and M.A. Juillerat, *Enzyme and Microbial Technology*, 2005, **36**, 911-916.
28. W. Wang, F. Wang, Y. Yao, S. Hu and K.K. Shiu, *Electrochimica Acta*, 2010, **55**, 7055-7060.
29. J. Zeng, W. Wei, L. Wu, X. Liu, K. Liu and Y. Li, *Journal of Electroanalytical Chemistry*, 2006, **595**, 152-160.
30. K. Sever, Y. Seki, I. H. Tavman, G. Erkan and V. Cecen, *Polymer Composites*, 2009, **30**, 550-558.
31. J. C. Santos, A. V. Paula, G. F. M. Nunes and H. F. de Castro, *Journal of Molecular Catalysis B-Enzymatic*, 2008, **52-53**, 49-57.
32. J. R. L. Walker, *Biochemical Education*, 1992, **20**, 42-43.
33. S. Sterman and H. B. Bradley, *Polymer Engineering & Science*, 1961, **1**, 224-233.
34. M.B. Stark and K. Holmberg, *Biotechnology and Bioengineering*, 1989, **34**, 942-950.
35. G. Peng, X. H. Hou, B. L. Liu, H. L. Chen and R. Luo, *Royal Society of Chemistry Advances*, 2016, **6**, 91431-91439.
36. Y. Gao, T. Yen Bach, P. Cacioli, P. Butler and I. L. Kyratzis, *Enzyme and Microbial Technology*, 2014, **54**, 38-44.
37. K. A. Markossian, N. V. Golub, H. A. Khanova, D. I. Levitsky, N. B. Poliansky, K. O. Muranov and B. I. Kurganov, *Biochimica et Biophysica Acta (BBA)-Proteins and Proteomics*, 2008, **1784**, 1286-1293.
38. Y. Jiang, C. Guo, H. Xia, I. Mahmood, C. Liu and H. Liu, *Journal of Molecular Catalysis B: Enzymatic*, 2009, **58**, 103-109.
39. L. Lei, Y. Bai, Y. Li, L. Yi, Y. Yang and C. Xia, *Journal of Magnetism and Magnetic Materials*, 2009, **321**, 252-258.
40. J. M. Bolivar, L. Wilson, S. A. Ferrarotti, J. M. Guisan, R. Fernandez-Lafuente and C. Mateo, *Journal of Biotechnology*, 2006, **125**, 85-94.
41. F. Toldra, N. B. Jansen and G. T. Tsao, *Process Biochemistry*, 1992, **27**, 177-181.
42. C.X. Cai, K.H. Xue, Y.M. Zhou and H. Yang, *Talanta*, 1997, **44**, 339-347.
43. A. Samphao, K. Kunpatee, S. Prayoonpokarach, J. Wittayakun, L. Svorc, D. M. Stankovic, K. Zagar, M. Ceh and K. Kalcher, *Electroanalysis*, 2015, **27**, 2829-2837.

Appendix - II

FTIR spectra for woven and non-woven glass fabric HCl activation (for page 204 -205 section 4.8.4.1)

Glass woven fabric



Glass non-woven fabric

